EPIGENETIC MODIFICATIONS IN COLORECTAL CANCER:

PREVENTION BY ASPIRIN AND CURCUMIN

By

YUE GUO

A dissertation submitted to the

Graduate School-New Brunswick

Rutgers, The State University of New Jersey

In partial fulfillment of the requirements

For the degree of

Doctor of Philosophy

Graduate Program in Pharmaceutical Science

Written under the direction of

Dr. Ah-Ng Tony Kong

And approved by

_____

_____

_____

_____

New Brunswick, New Jersey

October 2017

ABSTRACT OF THE DISSERTATION

Epigenetic Modifications in Colorectal Cancer: Prevention by Aspirin and Curcumin

By YUE GUO

Dissertation Director: Professor Ah-Ng Tony Kong

Colorectal cancer is the third most common cancer worldwide and remains the leading cause of cancer-related death in the world. Emerging evidence has suggested that epigenetic mechanisms play an important role in colorectal carcinogenesis. It is now recognized that the interplay of DNA methylation, post-translational histone modification, and non-coding RNAs can interact with genetic defects to drive tumorigenesis. The early onset, reversibility, and dynamic nature of such epigenetic modifications enable them to be developed as promising cancer biomarkers and preventive targets. Aspirin and curcumin are widely investigated chemopreventive candidates for colorectal cancer. However, the precise mechanisms of their action have not been fully understood. Therefore, this dissertation research aimed to identify novel epigenetic alterations in colorectal carcinogenesis and to elucidate the mechanisms of colorectal cancer prevention by aspirin and curcumin in epigenetic perspective. Genome-wide DNA methylation profiles indicated that adenomatous polyps from $Apc^{min/+}$ mice exhibited extensive aberrant DNA methylation that affected certain signaling pathways. Using human

colorectal cancer cell lines, we demonstrated that inhibitory effect of curcumin on anchorage-independent growth of HT29 cells involves, at least in part, the epigenetic demethylation and up-regulation of tumor suppressor gene *DLEC1*. Chronic inflammation appears to enhance the risk of colorectal cancer. Using an azoxymethane-initiated and dextran sulfate sodium-promoted inflammation associated colon cancer animal model, we demonstrated the chemopreventive effect of aspirin. Our results identified a novel epigenetic mechanism of aspirin in attenuating inflammation in colon cancer via the inhibition of histone deacetylases and the modification of H3K27ac marks that suppress iNos, Tnf-α, and iL6. By using the similar animal model, we provided the first evidence in support of the chemopreventive effect of a combination of low-dose aspirin and curcumin in colitis-accelerated colorectal cancer. The transcriptional profile obtained from RNA-seq in our study provides a framework for identifying the mechanisms under carcinogenesis process from normal colonic tissue to tumor development as well as the cancer inhibitory effects and potential molecular targets of aspirin and curcumin.

ACKNOWLEDGEMENTS

DEDICATION

To My Beloved Parents and Grandmother

TABLE OF CONTENTS

LIST OF TABLES

LIST OF FIGURES

1. CHAPTER ONE

Introduction: epigenetic modifications by dietary chemopreventive and herbal phytochemicals [1,2]

1.1 Introduction

Cancer is a disease involving dynamic changes in the genome. The activation of oncogenes and the loss of function of tumor suppressor genes due to genetic mutations have long been considered the driving force of neoplasia (1). However, the important contribution of epigenetic events to the malignant phenotype has been recognized with the help of significant advancements in the field of cancer epigenetics (2). The definition of "epigenetic" has evolved over time from the impact of chromatin structure on embryonic development to its implication in a wide variety of biological processes (3). Currently, the term "epigenetic" refers to the study of heritable alterations in gene expression without changes in the primary DNA sequence (4). These heritable alterations are primarily established and maintained through cell differentiation and division, enabling the cells with the same genetic information to have distinct identities. The major epigenetic mechanisms for regulating these heritable gene alterations are the methylation of cytosine bases in DNA, covalent modifications of histones, and post-transcriptional gene regulation by microRNAs (miRNAs) (2). The disruption of these epigenetic

---

[1] Part of this chapter has been published in Current Pharmacology Reports. 2015 Aug; 1(4):245-257

[2] **Key Words**: epigenetic; chemoprevention; phytochemicals

modifications is associated with abnormalities of various signaling pathways and can lead to the induction and maintenance of many disease states, including cancer (5).

It is now widely accepted that epigenetic abnormalities and genetic alterations in cancer cells may interact at all stages to initiate and promote cancer (6, 7). In contrast to genetic mutations, epigenetic modifications are potentially reversible. For example, genes with repressed transcriptional activity by epigenetic silencing can be reactivated through epigenetic interventions because the genes themselves are still intact, whereas genetic mutations are permanent. This fact may explain why increasing attention and effort had been focused on the discovery and development of epigenetic-targeted therapeutics to treat cancer in recent years. To date, several small-molecule epigenetic therapies targeting chromatin-modifying enzymes have been developed and approved for cancer treatment by the U.S. Food and Drug Administration (FDA). These drugs include DNA methyltransferase (DNMT) inhibitors (azacitidine and decitabine) and histone deacetylase (HDAC) inhibitors (vorinostat and romidepsin) (8). A number of clinical trials are also underway with these agents and many other newly developed epigenetic agents in a variety of cancer types. Moreover, the synergistic effects between epigenetic drugs and conventional antitumor therapies are quite promising (9). Other than these small-molecule agents, accumulating evidence suggests that the epigenetic landscape is largely influenced by dietary and environmental factors (10). With their relatively low toxicity, feasible long exposure, and promising effects observed *in vitro* and *in vivo* (11, 12), dietary phytochemicals may become potential chemopreventive agents by targeting epigenetic modifications.

In this chapter, we will discuss the current understanding of the epigenetic mechanisms that occur during carcinogenesis and highlight their potential roles in cancer chemoprevention. Studies published in the past five years regarding the impact of dietary chemopreventive phytochemicals in modulating epigenetic alterations will also be reviewed and discussed.

1.2 DNA methylation

DNA methylation, the addition of a methyl group by DNMTs to the cytosine bases located 5' to a guanosine in a CpG dinucleotide, is perhaps the most extensively investigated epigenetic modification in mammals (13). CpG dinucleotides are not evenly distributed across the entire genome but are clustered in short regions known as CpG islands that are 0.5-4 kb in length (13). These CpG islands are known to be preferentially located in the proximal promoter end of approximately 60% of genes in the genome and generally remain unmethylated in normal cells (14, 15), allowing access to transcription factors and chromatin-associated proteins for active transcription. In cancer, however, CpG islands in promoter regions become hypermethylated, and this event is believed to cause inappropriate transcriptional silencing of numerous tumor suppressors and other genes with important functions in carcinogenesis (Figure 1) (16). The recruitment of transcriptional proteins to DNA is reduced by hypermethylated CpG islands, thus resulting in gene silencing (17). Alternatively, methylated CpG islands provide binding sites for various methyl-binding proteins (MBDs), such as MBD1-MDB4 and methyl CpG binding protein 2 (MeCP2), which can mediate gene repression by interacting with

HDACs (18). Surprisingly, promoter CpG island hypermethylation-mediated gene silencing is at least as common as mutational alterations in the classic tumor-suppressor genes in human cancer (19). The list of cancer-related genes that are inactivated by CpG hypermethylation is ever-growing with advances in techniques. Examples of these genes include hMLH1 (human mutL homolog 1), MGMT (O^6-alkylguanine DNA alkyltransferase) (20, 21), p16^{INK4a}, p15^{INK4b} (22, 23), Bcl-2 (B-cell lymphoma), and DAPK (death-associated protein kinase 1) (24, 25). The studies conducted in our group demonstrated that Nrf2 [nuclear factor (erythroid-derived 2)-like 2] expression is down-regulated in TRAMP C1 cells and JB6 P+ cells due to promoter hypermethylation, and the expression of these genes can be restored by reducing the promoter methylation status with various phytochemical treatments (26-30). This effect will be further reviewed in Section 1.5. Other than the hypermethylation of promoter CpG islands, global DNA hypomethylation in tumor cells compared with normal cells has been reported repeatedly (Figure 1) (31, 32). Genome-wide hypomethylation is suggested to be associated with enhanced genomic instability and can thereby facilitate tumor progression (33). Thus, an imbalance of DNA methylation between genome-wide hypomethylation and regional hypermethylation may characterize human neoplasia (34).

The precise DNA methylation patterns in the mammalian genome are known to be regulated by DNMTs (Figure 1). DNMT3a and DNMT3b act cooperatively to establish de novo methylation independent of replication, whereas DNMT1 maintains methylation patterns during DNA replication by preferentially methylating hemimethylated DNA (35). A fourth member, DNMT-3L was first isolated in 2000 and had been shown to facilitate DNA methylation by interacting with DNMT3a and 3b (36, 37). Given that the DNMT

enzymes are modestly overexpressed in many types of tumor cells and that the inhibition of DNMTs has been found to reduce tumor formation in various mouse models (38, 39), the search for and studies of DNMT inhibitors has become extremely popular. Successful examples include FDA-approved anticancer drugs, potent DNMT inhibitors under clinical trials, and numerous dietary chemopreventive phytochemicals that have been identified in pre-clinical models. Although the enzymes that regulate DNA methylation have been well characterized, those that mediate methyl group removal are still elusive. A novel TET (ten-eleven translocation) enzyme family that is capable of modifying 5-methylcytosine to 5-hydroxymethylcytosine through oxidation has been discovered in recent years (Figure 1) (40, 41). We anticipate many more exciting discoveries regarding the mechanistic roles of TET in the dynamic regulation of DNA methylation to enhance our understanding of DNA methylation in tumorigenesis.

1.3 Histone modification

The covalent modification of histone proteins also plays a critical role in regulating gene expression, chromatin structure, cellular identity, and ultimately, carcinogenesis. Histone proteins (H3, H4, H2A, H2B and H1) are at the heart of chromatin structure and act as scaffolds to wrap ~146 bp of eukaryotic DNA into repeating nucleosomes, which are further folded into compact chromatin fibers (~30 nm) (42). The chromatin structure, which is closely involved in gene transcription, replication, and repair, is regulated by the "histone code", known as the language of histone modification (43). The two distinct chromatin structures, namely heterochromatin and

euchromatin, represent a tightly packed structure with repressed gene transcription or a loosely packed structure with active gene transcription, respectively (Figure 1) (44). While highly conserved, specific residues such as lysine, arginine, and serine, on the N-terminal tails of histones can undergo extensive post-translational modifications, including methylation, acetylation, phosphorylation, ubiquitination, sumoylation, and ADP ribosylation (45).

Histone modifications can lead to either gene activation or repression, depending on which residues are modified and what types of modifications are involved. Usually, lysine acetylation alters nucleosomal conformation by neutralizing the positive charge, thereby increasing the accessibility of transcriptional factors to chromatin and resulting in transcriptional activation (Figure 1) (46). Histone acetylation is dynamically catalyzed by enzymes that add (HATs, histone acetyltransferases) and remove (HDACs, histone deacetyltransferases) acetyl groups (Figure 1). To date, 18 HDACs and 25 HATs enzymes have been identified and classified into several families, and these enzymes are capable of controlling various physiological functions (47). The loss of acetyl groups in H4-lysine 16 and the overexpression of certain HDACs (1, 2, and 6) have been demonstrated in a number of cancers (48). Notably, two HDAC inhibitors have already been approved by the FDA, and more novel inhibitors are currently undergoing clinical investigations for the treatment of a broad range of cancers (8). It is exciting to note that some dietary phytochemicals may be involved in chromatin remodeling by targeting HDACs and HATs, highlighting their potential in cancer chemoprevention (49).

Unlike lysine acetylation, methylation at lysine residues appears to activate or repress transcription depending upon which residue is methylated and the degree of the

methylation. For example, methylated H3K4, H3K36, and H3K79 are generally associated with active genes in euchromatin, whereas the methylation at H3K9, H3K27, and H4K20 leads to gene repression (Figure 1) (50). Moreover, histone methylation has been suggested to cooperate with DNA methylation. For example, DNA methylation is associated with H3K9 methylation (51). Histone methyltransferases (HMTs) and histone demethylases (HDMs) dynamically regulate histone methylation (Figure 1). In contrast to HATs, HMTs specifically target certain lysine residues; for example, EZH2 (enhancer of zeste homolog 2) is primarily responsible for H3K27 methylation (52). Investigations in recent years have implicated hyperactive EZH2 in the development of prostate and breast cancer via its histone methylation-induced repression of tumor suppressors (53), making this enzyme a promising chemotherapeutic target.

1.4 microRNAs

MicroRNAs (miRNAs) are small non-coding RNAs approximately 22 nucleotides in length that are increasingly recognized as important players in epigenetic gene regulation in mammals. By specifically targeting mRNA degradation or translation inhibition, miRNAs can bind and interfere with a wide spectrum of transcripts and profoundly influence cancer-related processes, such as proliferation, apoptosis, differentiation, cell cycle, and migration (Figure 1) (54). Since the deregulation of miRNA in cancer was first documented in 2002 (55), the network of miRNAs identified in the cancer-related processes, their tissue distributions, and their potential targets have rapidly grown, elucidating their extensive roles in carcinogenesis and chemotherapy. For

example, miR-155 and miR-21 have been found to be overexpressed in many cancer types (56, 57), and the attenuated expression of miR-let7 was observed in human lung cancers (58). Interestingly, the expression of miRNAs can be controlled by epigenetic mechanisms, such as DNA methylation and histone modifications. Moreover, miRNAs can target key enzymes, such as DNMTs and EZH2, which mediate epigenetic mechanisms, thereby modulating the epigenetic landscape of cells (Figure 1) (59). Progress had been made in utilizing miRNAs in cancer prognosis and therapy. Notably, the first miRNA mimic entered the clinic for the treatment of liver cancer patients in 2013 (60). In addition, the interaction between dietary phytochemicals and miRNAs has been investigated in cancer cells. Hence, miRNAs might be a promising target for chemopreventive dietary phytochemicals.
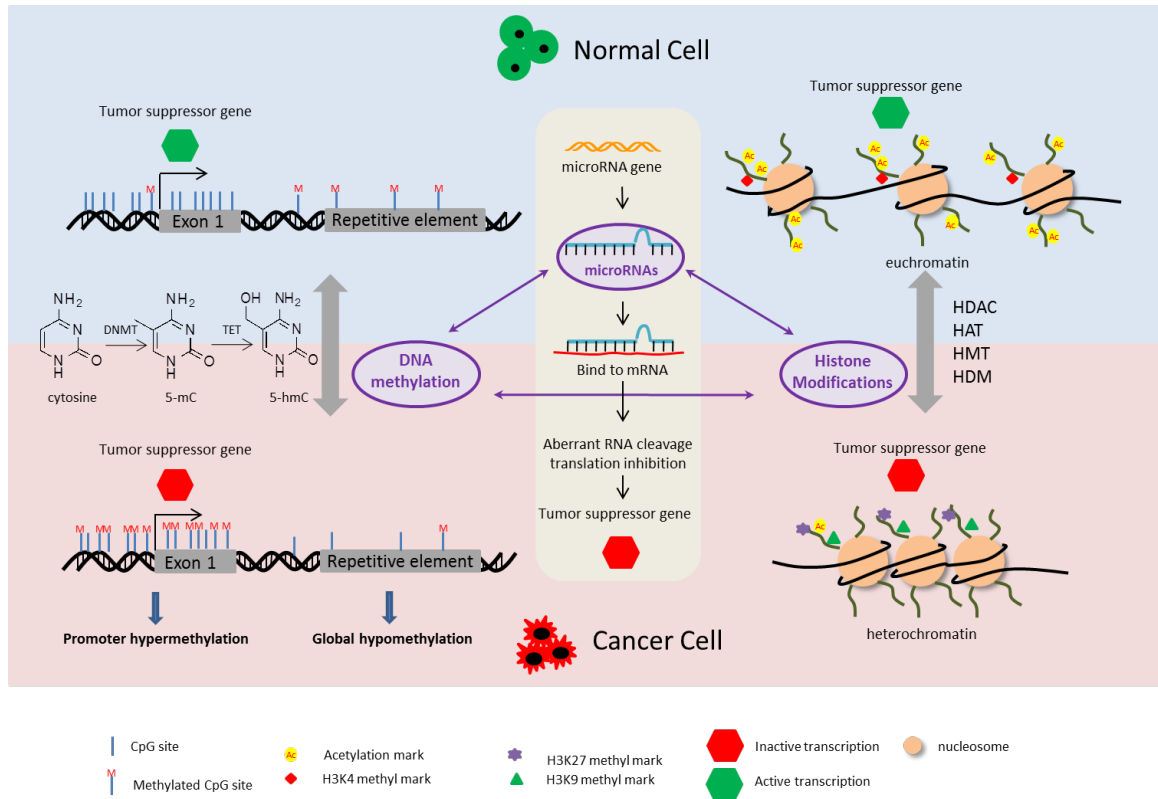
Figure 1: Schematic representation showing epigenetic modifications of tumor suppressor genes in normal cell and in cancer cell.

CpG island of promoter region remains hypomethylated to facilitate active transcription of tumor suppressor genes in normal cells. In cancer cells, however, promoter hypermethylation of tumor suppressor genes is frequently detected. In addition, genome-wide hypomethylation in cancer cells has been reported. The enzymes such as DNMT and TET dynamically regulate the DNA methylation. Acetylation and methylation on the histone tails influence the chromatin structure. For example, lysine acetylation and H3K4 methylation are associated with active transcription in euchromatin in normal cells. In cancer cells, loss of lysine acetylation and methylation at H3K9 and H3K27 leads to the

repression of some tumor suppressor genes. The enzymes such as HDAC, HAT, HDM, and HMT catalyze histone acetylation and methylation. miRNAs bind and interfere with mRNAs and specifically target mRNA degradation or translation inhibition of tumor suppressor genes in cancer cells. The interplay of epigenetic pathways is shown in the center of the figure.
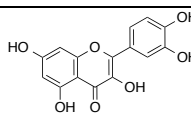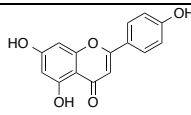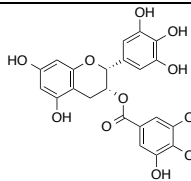
1.5 Dietary phytochemicals modulate epigenetic modifications
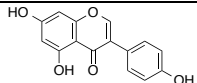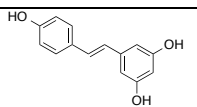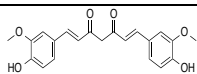
Environmental and dietary factors can influence the pathological progression of diseases, including cancer. Some naturally occurring phytochemicals that are common secondary metabolites in fruits and vegetables have been demonstrated to be beneficial for human health through various actions, including ameliorating oxidative stress, inducing detoxification enzymes, inhibiting nitrosamine formation, binding/diluting carcinogens in the digestive tract, altering hormone metabolism, and modulating carcinogenic cellular and signaling events (61). Recently, accumulating research has demonstrated that dietary phytochemicals can alter the epigenome and may help to prevent and treat human cancer. Here we review the most recent studies regarding the epigenetic role of dietary phytochemicals, including polyphenols [quercetin, apigenin, (−)-epigallocatechin-3-gallate (EGCG), genistein, resveratrol, and curcumin], organosulfur compounds [sulforaphane (SFN), phenethyl isothiocyanate (PEITC), diallyl disulfide (DADS)], and indoles [diindolylmethane (DIM)] in cancer chemoprevention and therapy. We also discussed the latest progress in the identification of chemopreventive phytochemicals from Chinese herbal medicine in modulating epigenetic
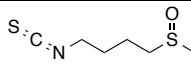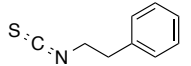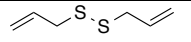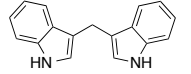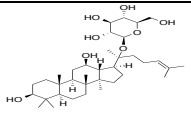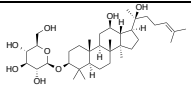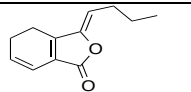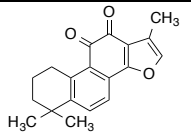
mechanisms. The epigenetic modifications regulated by phytochemicals are summarized in Table 1.
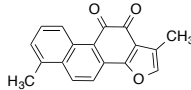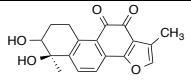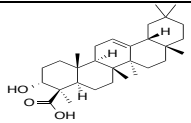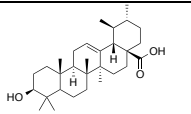
Table 1: Epigenetic modifications by phytochemicals

Category	Phytochemicals	Sources	Structure	Epigenetic modification(s)	Effect(s)	Citation
Polyphenols	Quercetin	Citrus fruits, onion, parsley, berries		Demethylated p16INK4a gene promoter, inhibited p300/HAT activity and HDACs, influenced miRNA expression (let-7, miR-146, miR-26, miR-17, miR-142-3p)	Suppressed the growth of colon cancer cells and pancereatic ductal adenocarcinoma cells, reduced COX-2 expression in breast cancer cells, induced apoptosis in human leukemia HL-60 cells, induced senescence in glioma cells	(62-67)
	Apigenin	Parsley, celery, chamomile tea		Demethylated Nrf2 promoter, reduced the expression of DNMTs and HDACs, increased global acetylation of histone H3 and H4, induced the expression of miR-138	Activated Nrf2 pathway in skin epidermal JB6 P+ cells, induced growth arrest and apoptosis in human prostate cancer cells and malignant neuroblastoma cells	(68-70)
	(−)-Epigallocatechin-3-gallate (EGCG)	Tea leaves		Demethylated WIF-1 promoter, inhibited the expression of HDAC1, MeCP2, and DNMT1, increased acetylation level of H3K9/14, H4K5/12/16, decreased methylation level of H3K9, decreased EZH2	Restored the expression of WIF-1 in lung cancer cells, reactivated ERα, PRB, TMS1, cyclin D2, and MGMT gene in MCF-7 cells, reactivated p16INK4a and Cip1/p21 in A431 cells, delayed breast cancer progression and	(71-76)

			localization and H3K27 trimethylation enrichment, increased histone H3K9/18 acetylation, induced the expression of miR-210, suppressed the expression of p53-targeted miRNAs (miR-25, miR-92, miR-141, miR-200)	invasion, reduced proliferation rate and anchorage-independent growth of lung cancer cells	
	Genistein	Soy beans	Suppressed global DNA methylation, DNMT activity, and DNMT1 expression, induced histone modifications (H3K9-me2, H3K9-me3, and H3K27-me3), down-regulated onco-miR-1260b and miR-27a	Increased expression of ATM, APC, PTEN, and SERPINB5 in breast cancer cells, activated sFRP1, Smad4, inhibited proliferation of prostate cancer cells, enhanced apoptosis of pancreatic cancer cells	(77-79)
	Resveratrol	Blueberries, cranberries, Grapes	Reduced DNA methylation of RASSF1A, suppressed DNMT3b, increased the expression of miR-129, -204, and -489, inhibited miR-21-mediated pathway, acted as a HDAC inhibitor	Inhibited prostate cancer growth and metastasis, promoted the apoptosis of pancreatic cancer cells	(80-84)
	Curcumin	Turmeric	Act as DNMT inhibitor, suppressed DNA methylation in Nrf2 and Neurog 1 promoter, inhibited HDAC and HAT activity, increased global level of	Restored the expression of Nrf2 and Neurog 1 in TRAMP C1 and LnCap cells, restored the expression of SOCS1 and SOCS3 in K562 and HEL cells, inhibited	(85-90)

				H3K18ac and H4K16ac, induced miRNA-9-mediated Akt/FOXO1 pathway, up-regulated miR-181b	cell proliferation of MCF-7 cells, induced apoptosis of SKOV3 cells, suppressed the expression of CXCL1 and CXCL2 in breast cancer cells	
Organosulfur compounds	Sulforaphane (SFN)	Broccoli, cabbage, brussels sprouts		Suppressed DNA methylation in Nrf2 promoter by inhibiting DNMTs and HDACs, epigenetically restored cyclin D2 expression, restored miR-140, up-regulated miR-200c	Restored Nrf2 expression, reduced breast tumor growth, inhibited proliferation of LnCap cells, inhibited EMT process in human bladder cancer T24 cells	(30, 91-94)
	Phenethyl isothiocyanate (PEITC)	Cruciferous vegetables		Demethylated GSTP1 promoter, modified the acetylation and methylation of H3, increased the expression of miR-17, decreased the expression of PCAF	Reactivated GSTP1 in LnCap cells, reduced inflammation-related genes in SW480 cells, inhibited prostate cancer cell growth	(95-97)
	Diallyl disulfide (DADS)	Garlic		Inhibited HDAC and increased the acetylation of H4, up-regulated miR-200b and miR-22	Enhanced apoptosis in human gastric cells and xenograft models.	(98, 99)
Indoles	3, 3'-Diindolylmethane (DIM)	Broccoli, cabbage, brussels		Altered the DNA methylation of cancer-associated gene promoters such as Nrf2, induced proteasome-mediated degradation of HDACs, influenced miR-21-mediated	Exerted chemopreventive effects in prostate tumorigenesis by up-regulating Nrf2, triggered cell cycle arrest and apoptosis in HT29 cells, inhibited cell proliferation in MCF-7 and	(29, 100-103)

		sprouts		Cdc25A degradation, up-regulated miR-let-7, down-regulated the expression of EZH2	MDA-MB-468 cells, attenuated prostate cancer aggressiveness	
Chinese herbal medicine	Compound K	Ginseng		Demethylated RUNX3 promoter	Reactivated RUNX3 and inhibited the proliferation of HT29 cells	(104)
	Ginsenoside Rh2	Ginseng		Regulated a network of miRNAs such as miR-128	Inhibited the proliferation of human glioma cells	(105, 106)
	Z-Ligustilide (Lig)	*Radix angelicae sinensis (*Danggui)		Hypomethylated the Nrf2 promoter	Restored Nrf2 expression in TRAMPC1 cells	(28)
	Tanshinone IIA	*Salvia miltiorrhiza,* (Danshen)		Reduced the methylation of Nrf2 promoter, suppressed DNMTs and HDACs, inhibited the over-expressed miR-155	Blocked TPA-mediated JB6 transformation through restoration of Nrf2 signaling, decreased inflammatory responses in LPS-induced macrophages	(107, 108)

	Tanshinone I	*Salvia miltiorrhiza,* (Danshen)		Reduced H3 acetylation levels in Aurora A promoter	Triggered cell cycle arrest in breast cancer cells	(109)
	Tanshindiols	*Salvia miltiorrhiza,* (Danshen)		Potential EZH2 inhibitor	Inhibited the growth of cancer cell lines	(110)
Other dietary phytochemicals	Boswellic acids	*Boswellia serrata*		Inhibited DNMT activity, induced genome-wide demethylation, up-regulated tumor-suppressive miRNAs such as let-7 and miR-200	Restored the expression of SAMD14 and SMPD3 in colon cancer cells, inhibited growth of colon cancer xenografts in nude mice	(111, 112)
	Ursolic acid	Apples, berries, Thyme, rosemary		Influenced miR-21 pathway	Suppressed proliferation of human glioma cell line	(113)

1.5.1 Polyphenols

Quercetin, a flavonol with yellow color, is widely found in fruits, vegetables and grains. Quercetin was shown to inhibit the recombinant prokaryotic SssI DNMT- and human DNMT1-mediated DNA methylation (114). Quercetin suppresses the growth of the human colon cancer cell line RKO via demethylation of the p16INK4a gene promoter (62). Quercetin has been found to block the binding of the transactivators CREB2 (cAMP-response element-binding protein 2), C-Jun, C/EBPβ (CCAAT-enhancer-binding protein beta), and NF-κB to the COX-2 promoter. In addition, quercetin suppresses COX-2 expression in breast cancer cells by attenuating p300/HAT-mediated signaling (63). Moreover, quercetin induces Fas ligand related apoptosis through the activation of the c-jun/AP-1 signaling pathway, the induction of HAT, and the inhibition of HDAC in HL-60 cells (64). Quercetin was also found to induce senescence in glioma cells via the inhibition of HDACs (65). A quercetin-rich diet has been reported to influence miRNA expression in human lung cancer tissues, including the tumor suppressor let-7 family and carcinogenesis-related miR-146, miR-26, and miR-17 (66). Quercetin also up-regulates miR-142-3p, a negative regulator of heat shock protein 70, which is related to the inhibition of the cell proliferation of pancreatic ductal adenocarcinoma cells (MIA PaCa-2, Capan-1, and S2-013) (67).

Apigenin is a yellow flavone compound in fruits and vegetables, especially in parsley, celery and chamomile tea. In our recent study, we found that apigenin effectively demethylated the Nrf2 promoter, resulting in an increase in the mRNA and protein expression of Nrf2 and the Nrf2 downstream target gene NQO1 (NAD[P]H:quinine oxidoreductase-1) in skin epidermal JB6 P+ cells. This effect was associated with the

reduced expression of epigenetic proteins, including DNMT1, DNMT3a, DNMT3b, and some HDACs (68). Apigenin also induces growth arrest and apoptosis in human prostate cancer cells through the up-regulation of global histone H3 and H4 acetylation and hyperacetylation of histone H3 on the p21/waf1 promoter in prostate cancer PC-3 and 22Rv1 cells. These effects may be caused by the inhibitive effect of apigenin on HDAC enzyme activity and the expression of HDAC1 and HDAC3 (69). The tumor suppressor miR-138 is correlated with telomerase activity in many human cancers, and apigenin-induced overexpression of miR-138 has been demonstrated to powerfully induce apoptosis of human malignant neuroblastoma in cell culture and animal models (70).

(−)-Epigallocatechin-3-gallate (EGCG) is one of the most abundant catechins in tea leaves and has been identified as a non-nucleoside DNMT inhibitor. The restoration of WIF-1 (Wnt inhibitory factor 1) expression by EGCG treatment, occurring via the demethylation of the WIF-1 promoter, has been found in lung cancer H460 and A549 cell lines (71). A recent study reported that EGCG treatment inhibits DNMT transcript levels and the protein expression of DNMT1, HDAC1, and MeCP2, effectively reactivating genes silenced by promoter methylation, such as ERα (estrogen receptor α), PRB (progesterone receptor B), TMS1 (target of methylation induced silencing-1), Cyclin D2 (G1/S-specific cyclin-D2), and MGMT in MCF-7 cells (72). EGCG treatment was found to reactivate the tumor suppressor gene p16INK4a and Cip1/p21 by reducing DNA methylation and increasing histone acetylation in human epidermoid carcinoma A431 cells (76). EGCG may delay breast cancer progression and invasion via the induction of tissue inhibitor of matrix metalloproteinase-3 (TIMP-3) expression. The proposed mechanism for this effect is that EGCG decreases EZH2 localization and H3K27

trimethylation enrichment at the TIMP-3 promoter, with a concomitant increase in histone H3K9/18 acetylation, in breast cancer cells (73). EGCG also induces the expression of miR-210, a major miRNA regulated by hypoxia-induced factor (HIF)-1α, in lung cancer cells, resulting in a reduced cell proliferation rate and anchorage-independent growth (74). EGCG can suppress the expression of p53-targeting miRNAs, including miR-25, miR-92, miR-141, and miR-200a, which are induced by the environmental carcinogen benzo[a]pyrene (BaP) in multiple myeloma, a common and deadly cancer of blood plasma cells (75).

Genistein, an isoflavone, is a major phytoestrogen compound in soy beans (Glycine max). Genistein has been demonstrated to suppress global DNA methylation, DNMT activity, and DNMT1 expression. These effects lead to promoter hypomethylation and increased mRNA expression of multiple tumor suppressor genes, including ataxia telangiectasia mutated (ATM), adenomatous polyposis coli (APC), phosphatase and tensin homolog (PTEN), and mammary serpin peptidase inhibitor (SERPINB5), in human breast cancer MCF-7 and MDA-MB-231 cells (77). Genistein induces the expression of two tumor suppressor genes, sFRP1 (secreted frizzled-related protein 1) and Smad4 (mothers against decapentaplegic homolog 4), via the demethylation of their promoter regions and histone modifications, such as H3K9-me2, H3K9-me3, and H3K27-me3, in prostate cancer cells (78). Genistein also down-regulates onco-miRNA-1260b in prostate cancer cells, resulting in the up-regulation of sFRP1 and Smad4 and the inhibition of cell proliferation and invasion (78). miR-27a down-regulation by genistein leads to enhanced apoptosis and reduced cell growth and invasion in pancreatic cancer cells (79).

Resveratrol is a stilbenoid, a type of natural polyphenol, and is found in blueberries, cranberries, and grapes. DNA methylation of the tumor suppressor gene RASSF1A (Ras association domain-containing protein 1) was reported to be reduced by resveratrol intake (twice daily for 12 weeks) in the breasts of women at high breast cancer risk (80). Resveratrol suppressed the increase in DNMT3b expression in estradiol-induced mammary tumor tissue in female ACI rats, an effect that may increase the expression of miRNA-129, -204, and -489 (81). The role of resveratrol as a HDAC inhibitor has also been demonstrated in glioma cells and human-derived hepatoblastoma cells (82). Recent studies suggested that resveratrol inhibits prostate cancer growth and metastasis and promotes the apoptosis of pancreatic cancer cells by inhibiting a miRNA-21-mediated pathway (83, 84).

Curcumin, a curcuminoid, is the primary component in the most popular Indian spice, turmeric (*Curcuma longa*). Growing evidence shows that curcumin harbors DNA demethylation potential in various cancer cell lines and might be a DNMT inhibitor (87, 89, 115, 116). For example, studies conducted in our laboratory suggested that curcumin restored the expression of Nrf2 and Neurog1 (Neurogenin-1) in murine prostate cancer Tramp C1 cells and human prostate cancer LnCap cells, respectively, by suppressing DNA methylation in the promoter region (87, 89). The hypomethylation effect of some novel synthetic curcumin analogs, such as EF31 and UBS109, has also been described to activate silenced genes, including p16, SPARC (secreted protein acidic and rich in cysteine), and E-cadherin (epithelial cadherin), in pancreatic cancer MiaPaCa-2 and PANC-1 cells (117). Curcumin has also been reported to modulate the activities of HDAC and HAT. Curcumin restored the expression of SOCS1 and SOCS3, suppressors

of cytokine signaling, via the inhibition of HDAC activity (especially HDAC8), resulting in increased histone acetylation in the SOCS1 and SOCS3 promoter regions of the myeloproliferative neoplasm cell lines K562 and HEL (85). In breast tumor MCF-7 cells, the inhibitory effects of curcumin in the activities of HAT have also been demonstrated, with increased global levels of acetylated H3K18 and H4K16, potentially leading to the arrest of cell proliferation (86). Curcumin may also induce apoptosis of ovarian cancer SKOV3 cells through inducing the miRNA-9-mediated Akt/FOXO1 (forkhead box protein O1) pathway (90). The up-regulation of miRNA-181b by curcumin was found to suppress the expression of the pro-inflammatory cytokines CXCL1 (chemokine [C-X-C motif] ligand 1) and CXCL2, leading to the diminished proliferation and invasion of breast cancer cells (88).

1.5.2 Organosulfur compounds

Sulforaphane (SFN) is a bioactive isothiocyanate, a group of organosulfur compounds, which are abundant in cruciferous vegetables, such as broccoli, cabbage, and brussels sprouts. According to our recent studies, SFN suppresses DNA methylation of the Nrf2 promoter in mouse skin JB6 and prostate Tramp C1 cells by down-regulating DNMTs and HDACs. These effects may contribute to its preventive potentials against TPA-induced skin transformation and prostate carcinogenesis, respectively (30, 93). SFN has also been demonstrated to exhibit anti-proliferative effects on LnCaP prostate cancer cells by epigenetically restoring the expression of cyclin D2 (91). The restoration of miR-140 by SFN, accompanied by the reduced expression of SOX9 and ALDH1 (aldehyde

dehydrogenases 1), has been reported to result in decreased breast tumor growth *in vivo* (94). SFN also inhibits the epithelial-to-mesenchymal transition (EMT) process in human bladder cancer T24 cells, and the up-regulation of miRNA-200c by SFN may be one of the mechanisms underlying this effect (92).

Phenethyl isothiocyanate (PEITC), another isothiocyanate, exists in some cruciferous vegetables. PEITC has been reported to be able to demethylate and reactivate GSTP1 (pi-class glutathione S-transferase). This protein is a frequently silenced detoxifying enzyme that is highly associated with prostate carcinogenesis through its regulation of the cross-talk between DNA and chromatin in LNCaP cells (97). PEITC was also observed to modify the acetylation and methylation of histone 3 in human colon cancer SW480 cells, leading to the down-regulation of some inflammation-related genes, such as CCL2 (chemokine ligand 2), CD40, CXCL10 (C-X-C motif chemokine 10), CSF2 (colony stimulating factor 2), IL-8 (interleukin 8), NF-kB, and TNFaip3 (tumor necrosis factor, alpha-induced protein 3) (96). PEITC treatment significantly increased the expression of miRNA-17 and decreased the expression of PCAF (p300/CBP-associated factor) in dihydrotestosterone-stimulated LNCaP cells, which might contribute to the inhibitory effect of PEITC against AR (androgen receptor) transcriptional activity and cell growth in prostate cancer (95)

Diallyl disulfide (DADS) is one of the principal sulfur compounds in Allium vegetables, such as garlic (*Allium sativum*). DADS has been found to exhibit an inhibitory effect on HDAC, resulting in hyperacetylation of histone 4 in the breast cancer MCF-7 cell line (99). In addition, DADS treatment has been demonstrated to impair proliferation and enhance apoptosis in both human gastric cell lines and xenograft models.

This effect occurred through the Wnt-1 signaling pathway and was mediated by the up-regulation of miRNA-200b and miRNA-22 (98).

1.5.3 Indoles

3, 3'-Diindolylmethane (DIM), an indole compound, is derived from glucosinolate indole-3-carbinol (I3C) in cruciferous vegetables, including broccoli, cabbage, cauliflower, and brussels sprouts. In addition to SFN, DIM can alter the DNA methylation status of many cancer-associated gene promoters in normal PrECs as well as in the prostate cancer cell lines LnCap and PC3 (103). Similarly, DIM exerts its chemopreventive effects in prostate tumorigenesis by epigenetically demethylating the Nrf2 promoter and up-regulating the expression of Nrf2 and its downstream gene NQO1 (29). The proteasome-mediated degradation of class I HDACs (HDAC1, HDAC2, HDAC3, and HDAC8) induced by DIM triggers cell cycle arrest and apoptosis in human colon cancer HT-29 cells and in tumor xenografts (102). DIM also inhibits cell proliferation in human breast cancer MCF-7 (estrogen-dependent) and MDA-MB-468 (estrogen receptor-negative, p53 mutant) cells via miRNA-21-mediated Cdc25A (cell division cycle 25 homolog A) degradation (101). A phase II clinical study in patients prior to radical prostatectomy suggested that formulated DIM intervention could attenuate prostate cancer aggressiveness via the up-regulation of miRNA let-7 and down-regulation of EZH2 expression in tissue specimens (100).

1.5.4 Phytochemicals from traditional chinese herbal medicine

During the last few decades, great progress had been made in the identification of chemopreventive agents and anticancer drugs in traditional Chinese herbal medicine. Recently, the potential of the components from Chinese herbs to influence epigenetic mechanisms in cancer prevention have been recognized. Ginseng is one of the most commonly used herbs in East Asia. Compound K (20-O-β-(D-glucopyranosyl)-20(S)-protopanaxadiol), the main metabolite of ginseng saponin, was found to inhibit the proliferation of human HT29 human colon cancer cells by demethylating and reactivating RUNX 3 (runt-related transcription factor 3), which is associated with reduced DNMT1 activity (104). Ginsenoside Rh2 is another biologically active triterpene saponin extracted from ginseng. The chemopreventive effect of Rh2 in inhibiting the proliferation of human glioma cells had been demonstrated to involve epigenetic modifications, such as the regulation of miRNAs. Specifically, the up-regulation of miR-128 by the treatment with Rh2 had been shown to trigger apoptosis-related signaling (106). Similarly, using miRNA microarray analysis, An et al. identified a network of miRNAs regulated by treatment with Rh2 in non-small cell lung cancer A549 cells, which may contribute to the anti-proliferative effect of Rh2 (105). A research study from our group demonstrated that the Chinese herb *Radix Angelicae Sinensis* (RAS; Danggui) and its bioactive component Z-Ligustilide (Lig) are able to hypomethylate the Nrf2 promoter, resulting in the restoration of Nrf2 and downstream targets such as NQO1, HO-1 (heme oxygenase 1), and UGT1A1 (UDP-glucuronosyltransferase 1 family, polypeptide A1) in murine prostate cancer TRAMP C1 cells (28). Another Chinese herb with great promise in altering epigenetic mechanisms is *Salvia miltiorrhiza,* also known as Danshen. We found

that tanshinone IIA, one of the main active components from Danshen, blocks TPA (12-O-tetradecanoylphorbol-13-acetate)-mediated JB6 transformation through epigenetic regulation of the Nrf2 signaling pathway (107). Treatment with tanshinone IIA reduced the methylation of the Nrf2 promoter, elevated the expression of Nrf2 and downstream targets, suppressed the protein levels of DNMT1, DNMT3a, DNMT3b, and HDAC3, and inhibited HDAC activity (107). Another study showed that tanshinone IIA decreases inflammatory responses in LPS-induced macrophages and inhibits the proliferation of inflammation-stimulated colon cancer cells by inhibiting the over-expressed miR-155 in macrophages (108). Tanshinone I, another main component derived from Danshen, has been shown to trigger cell cycle arrest in several breast cancer cells by down-regulating Aurora A gene expression via the reduction of H3 acetylation levels in the Aurora A promoter (109). In addition to tanshinones, the primary components, minor components, including tanshindiols, are currently under investigation for their potential antitumor ability by targeting epigenetic modifications. Using molecular docking and an enzyme kinetics approach, Woo et al. proposed that tanshindiols B and C are potential EZH2 inhibitors, resulting in the inhibition of the growth of several cancer cell lines (110).

1.5.5 Other dietary phytochemicals

In addition to above-mentioned dietary phytochemicals, various other natural compounds are currently under investigation regarding their cancer chemopreventive potential through epigenetic modifications. Boswellic acid, a pentacyclic triterpenoid derived from the plant *Boswellia serrata*, has long been used as anti-inflammatory and

cancer chemopreventive agents. Recently, Shen et al. demonstrated that boswellic acids inhibit DNMT activity and induce genome-wide demethylation, permitting the restoration of tumor suppressor genes, such as SAMD14 (sterile α motif domain containing 14) and SMPD3 (sphingomyelin phosphodiesterase 3) in colorectal cancer cells (112). In addition to modulating DNA methylation, boswellic acids were found to significantly up-regulate tumor-suppressive miRNAs, such as let-7 and miR-200, and to modulate the expression of downstream targets in several colon cancer cells and tumor xenografts in nude mice (111). Experimental evidence demonstrated that ursolic acid, another naturally occurring pentacyclic triterpene, suppresses proliferation and induces apoptosis in the human glioma cell line U251 by mediating the miR-21 pathway (113). A recent study proposed that the antitumor activity of rosemary extracts with high contents of phenolic diterpene carnosic acid and carnosol might involve the up-regulation of GCNT3 (glycosyltransferase 3) and down-regulation of miR-15b in colon and pancreatic cancer cells (118).

1.6 Conclusions and perspectives

Great accomplishments have been made in recent years in advancing our understanding of epigenetic alterations in the development of cancer. These epigenetic abnormalities are now believed to exist in all cancer types and drive tumor progression along with genetic defects. The reversible and dynamic nature of epigenetic modifications strongly encouraged clinicians and pharmaceutical industries to develop epigenetic biomarkers and therapeutic targets in cancer diagnosis and treatment. However,

the complexity of epigenetic pathways, including the interplay of the different epigenetic mechanisms in regulating gene transcription and the genetic mutations in epigenetic regulators, need to be addressed before we can fully apply our current understanding to the clinical field. For example, histone modification enzymes such as HDACs might be abnormally regulated by genetic or DNA methylation changes in cancer cells. Thus, further systematic studies may facilitate the development of epigenetic research in preventing and treating cancer.

The approval of several DNMT and HDAC inhibitors for clinical use has opened up a new avenue in cancer therapy. However, it could be reasonably argued that epigenetic interventions may be more effective in hematopoietic malignancies than solid malignancies. Factors such as the microenvironment, epigenetic landscape, drug exposure, and drug metabolism appear to be largely different in solid tumors than in hematopoietic malignances. However, more intensive studies regarding these cellular or epigenetic differences are urgently needed to successfully apply the concept of epigenetic therapy across a broader spectrum. Furthermore, adverse effects and a lack of selectivity have hindered the road towards effective epigenetic therapies. Investigations should be conducted regarding whether a selective subset or large numbers of genes will be influenced by the drugs or phytochemicals that target epigenetic modifications. Additionally, based on the crosstalk between genetic and epigenetic mechanisms, combining conventional antitumor drugs with epigenetic therapies or dietary phytochemicals that target epigenetic mechanisms might be a promising strategy for reducing toxicity and resistance.

Accumulating evidence indicates that some dietary phytochemicals can modulate epigenetic mechanisms. Here, we summarized and discussed the latest findings in the past five years. Together with numerous reports published more than five years ago, it is now clear that these natural compounds hold great promise in cancer prevention via acting on a variety of epigenetic targets. However, we should also notice that the success of epigenetic interventions elicited by phytochemicals was mostly limited in pre-clinical models. Thus, future studies should be carefully designed on the translation of these natural agents' effects to prevent human malignancies in clinical settings. Moreover, most phytochemicals have been reported to influence a wide range of epigenetic regulators. Therefore, understanding the global patterns of epigenetic modifications that are induced by phytochemicals will help to optimize strategies to prevent and treat cancer.

In summary, aberrant epigenetic modifications, such as DNA methylation, histone modifications, and miRNA, add another layer of complexity to the development of human cancer. The identification of dietary phytochemicals that modulate epigenetic modifications offers promising benefits in the management of human cancer. The primary goal of this graduate research is to identify the epigenetic modifications during the initiation and progression of colon carcinogenesis. This graduate research also aims to determine the effect of chemopreventive agents (such as NSAID aspirin, curcumin, and their combination) in colon cancer and to elucidate the mechanisms of such inhibition in epigenetic perspective.

2. CHAPTER TWO

Association of aberrant DNA methylation in Apc^{min/+} mice with the epithelial-mesenchymal transition and Wnt/β-catenin pathways: genome-wide analysis using MeDIP-seq [3,4]

2.1 Introduction

It is widely accepted that the accumulation of genetic and epigenetic alterations contributes to cancer initiation and progression. Genetic alterations refer to mutations in tumor suppressor genes and oncogenes, whereas epigenetic modifications involve changes in chromatin structure that result in altered gene expression without primary changes to the DNA sequence (119). The information conveyed by epigenetic modifications plays a vital role in regulating DNA-mediated processes, including transcription, DNA repair, and replication (52). Specifically, aberrant DNA methylation at the 5-carbon on cytosine residues (5mC) in CpG dinucleotides is perhaps the most extensively characterized epigenetic modification in cancer. DNA methylation affects the rate of gene transcription and therefore regulates various biological processes, such as proliferation, apoptosis, DNA repair, cancer initiation, and cancer progression (120). The genomic DNA methylation pattern is stably maintained in normal cells; however,

---

[3] Part of this chapter has been published in Cell & Bioscience, 2015 May 27; 5:24
[4] **Key Words**: DNA methylation; Epigenetic; Epithelial-mesenchymal transition pathway; MeDIP-seq; Wnt/β-catenin pathway

aberrant alterations in the epigenome have been identified in tumor cells (121). Evidence suggests that global hypomethylation and regional hypermethylation are characteristics of cancer cells (122). Global genome-wide loss of methylation has been associated with increased genomic instability and proto-oncogene activation, whereas DNA hypermethylation of CpG islands in promoter regions silences tumor suppressor genes (123). Unlike genetic mutations, the transcriptional repression of genes via epigenetic alterations can be reversed by further epigenetic modifications because these silenced genes remain genetically intact (124). Thus, it is very important to profile the global DNA methylation changes that occur in early tumorigenesis.

Colorectal cancer (CRC) is the second leading cause of cancer-related death in western countries (125), and more than 80% of CRC patients harbor a mutation in the adenomatous polyposis coli (APC) gene on chromosome 5q21 (126). APC is a tumor suppressor gene that down-regulates the pro-proliferative Wnt-signaling pathway by promoting the destruction of β-catenin. Deleterious mutations in APC stabilize β-catenin, increase its translocation into the nucleus, promote its binding to the transcription factor TCF4, and activate target genes such as C-MYC and CCND1 (127, 128). It has been suggested that the loss of APC function initiates tumorigenesis and that additional genetic and epigenetic events are involved in colon cancer progression (129). Numerous genes that are silenced by epigenetic mechanisms have been identified in colon cancer, including CDKN2A (130), DKK1 (131), DLEC1 (132, 133), UNC5C (134), and SFRP (135). However, the genome-wide profile of the aberrant methylation and the association of these methylation patterns with important signaling pathways and biological networks implicated in colon tumorigenesis remain unclear.

To address this issue, we examined the global DNA methylation profile in the well-established $Apc^{min/+}$ intestinal tumorigenesis mouse model using methylated DNA immunoprecipitation (MeDIP) and next-generation sequencing (MeDIP-seq). $Apc^{min/+}$ mice carry a heterozygous mutation in Apc and develop approximately 30 small intestinal adenomatous polyps following the somatic loss of functional Apc (136). This mouse model of intestinal tumorigenesis is commonly used because the phenotype resembles that of patients with familial adenomatous polyposis (FAP) (137). We analyzed adenomatous polyps from $Apc^{min/+}$ mice and not only identified genes with a modified methylation profile but also interpreted the data in the context of biological function, networks, and canonical signaling pathways associated with the methylation patterns.

2.2 Materials and Methods

2.2.1 Mouse strains

C57BL/6J male mice that are heterozygous for the Apc allele ($Apc^{min/+}$) and their wild type littermates ($Apc^{+/+}$) were originally obtained from Jackson Laboratories (Bar Harbor, ME, USA). The animals were housed in the Animal Care Facility at Rutgers University with a 12 h-light/12 h-dark cycle and were provided ad libitum access to food and water. The $Apc^{min/+}$ and control mice were sacrificed by CO_2 inhalation at 20 weeks of age. Polyp and intestine samples were collected as previously described (138). Briefly, after sacrificing the mice, the gastrointestinal tract was removed, opened longitudinally, and rinsed thoroughly with saline. Intestinal adenomatous polyps were excised from the

intestines carefully. The normal intestine tissue and polyps were snap frozen and stored at -80 °C for future use.

2.2.2 DNA extraction

Genomic DNA was isolated from adenomatous polyps from three $Apc^{min/+}$ mice and from normal intestinal tissue from three $Apc^{+/+}$ littermates using a DNeasy Kit (Qiagen, Valencia, CA, USA). Prior to fragmentation by Covaris (Covaris, Inc., Woburn, MA, USA), the quality of the extracted genomic DNA was confirmed by agarose gel electrophoresis and OD ratio. After fragmentation, the genomic DNA was further assessed for size distribution using an Agilent Bioanalyzer 2100 (Agilent Technologies, Santa Clara, CA, USA). The fragmented genomic DNA concentrations were measured with a Nanodrop spectrophotometer.

2.2.3 MeDIP-seq

MeDIP was performed using a MagMedIP kit (Diagenode, Denville, NJ, USA) as previously described (139). Briefly, immunoprecipitations were performed using a monoclonal antibody against 5-methylcytidine (Diagenode, Denville, NJ, USA) to separate the methylated DNA fragments from the unmethylated fragments. The captured DNA was used to create the Illumina libraries using NEBNext reagents (catalog# E6040; New England Biolabs, Ipswich, MA, USA). After the quality of the libraries was evaluated, the samples were sequenced using an Illumina HiSeq 2000 machine. The

results were analyzed for data quality and exon coverage using the platform provided by DNAnexus (DNAnexus, Inc., Mountain View, CA, USA). Subsequently, the samples were subjected to Illumina next-generation sequencing (Otogenetics Corporation, Norcross, GA, USA). After downloading the BAM files for analysis, MeDIP alignments were compared with control samples using Cuffdiff 2.0.2 as previously described (139, 140). To judge the quantitative enrichment in MeDIP samples versus control samples in Cuffdiff, the overlapping regions of sequence alignment common to the MeDIP and control samples were used. Significant peaks at a 5% false discovery rate (FDR) with a minimum of a 4-fold difference in R (Cummerbund package) were selected. The peaks were matched with adjacent annotated genes using ChIPpeakAnno as previously described (141).

2.2.4 Ingenuity Pathway Analysis (IPA)

To investigate the significance of the altered methylation observed by MeDIP-seq, we analyzed genes that exhibited greater than a 2-fold change ($\log_2$) in methylation (Apc$^{min/+}$ polyps vs. control) using IPA (IPA 4.0, Ingenuity Systems, www.ingenuity.com). IPA utilized gene symbols that were identified as neighboring enriched methylation peaks by ChIPpeakAnno for all of the analyses. IPA mapped the input genes to its knowledge bases and identified the most relevant biological functions, networks, and canonical pathways related to the altered methylation profiles in the Apc mutant polyps.

2.3 Results

2.3.1 MeDIP-seq results

To identify changes in DNA methylation patterns during the progression of mouse intestinal polyps, whole-genome DNA methylation analysis was performed using the described MeDIP-seq method. The global differences in the DNA methylation profile between adenomatous polyps from Apc[min/+] mice and intestinal tissue from control mice are described in Figure 2. We identified 12,761,009 mapped peaks and 2,868,549 non-mapped peaks from a total of 15,629,558 peaks in control mice and 11,470,541 mapped peaks and 2,262,073 non-mapped peaks from a total of 13,732,614 peaks in Apc[min/+] mice (Figure 2). A total of 17,265 differentially methylated regions (DMRs) had a $\geq$ 2-fold change ($\log_2$) in methylation in Apc[min/+] mice compared with control mice, of which 9,078 DMRs (52.6%) exhibited increased methylation, and 8,187 (47.4%) DMRs exhibited decreased methylation (Figure 2).
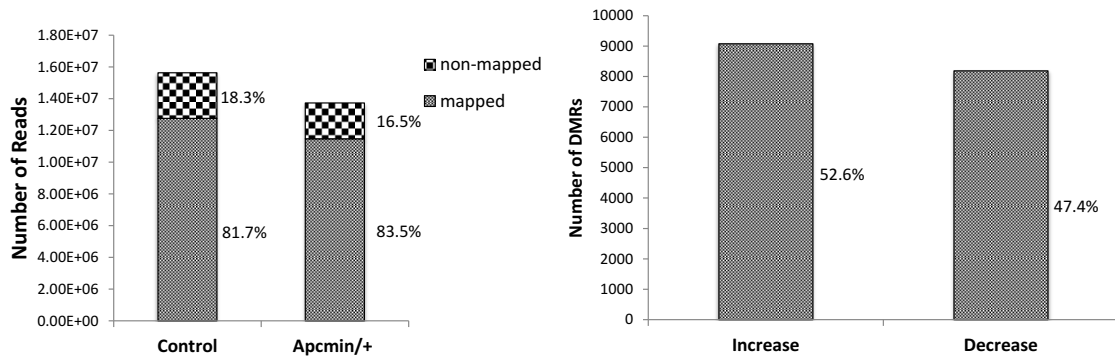
Figure 2: Global changes in the DNA methylation profile between Apc mutant adenomatous polyps and control tissue.

Left: Total number of peaks generated by MeDIP-seq. Right: Number of DMRs with significantly increased or decreased changes in methylation (≥ 2-fold in log2) in polyps from Apcmin/+ mice.

2.3.2 Functional and pathway analysis by IPA

To identify the biological function, networks, and canonical pathways that were affected by the differentially methylated genes, we performed Ingenuity Pathway Analysis (IPA) after the MeDIP-seq analysis. In the analysis of genes with altered methylation (≥ 2-fold in $\log_2$) in $Apc^{min/+}$ mice compared with control mice as determined by MeDIP-seq, IPA mapped 5,464 unique genes that were associated with its knowledge base. The top 50 genes with increased and decreased methylation levels based on $\log_2$ fold change are listed in Table 2 and Table 3. The molecules with methylation changes were mainly categorized into 38 disease and biological functions. The five highest IPA-rated disease and biological functions were as follows: cancer, gastrointestinal disease, organismal injury and abnormalities, cellular growth and proliferation, and reproductive system disease (Figure 3). Among the IPA-mapped genes with differential methylation patterns in polyps from $Apc^{min/+}$ mice, 3,299 were associated with cancer, and 1,668 were associated with gastrointestinal diseases. To examine the interaction networks that were affected by DNA methylation in Apc mutant polyps, IPA identified 25 networks with up to 35 focus molecules in each network. The five most affected gene networks as determined by IPA are shown in Table 4, and the detailed interactions in the most significant networks (cancer, cell cycle, and molecular transport) are presented in Figure

4. In accordance with the most relevant biological functions as determined by IPA, genes with different methylation patterns predominantly mapped to the networks associated with cancer and gastrointestinal diseases. Taken together, these results suggested an important role for the altered methylation of genes associated with the development of cancer and gut disease in $Apc^{min/+}$ mice.
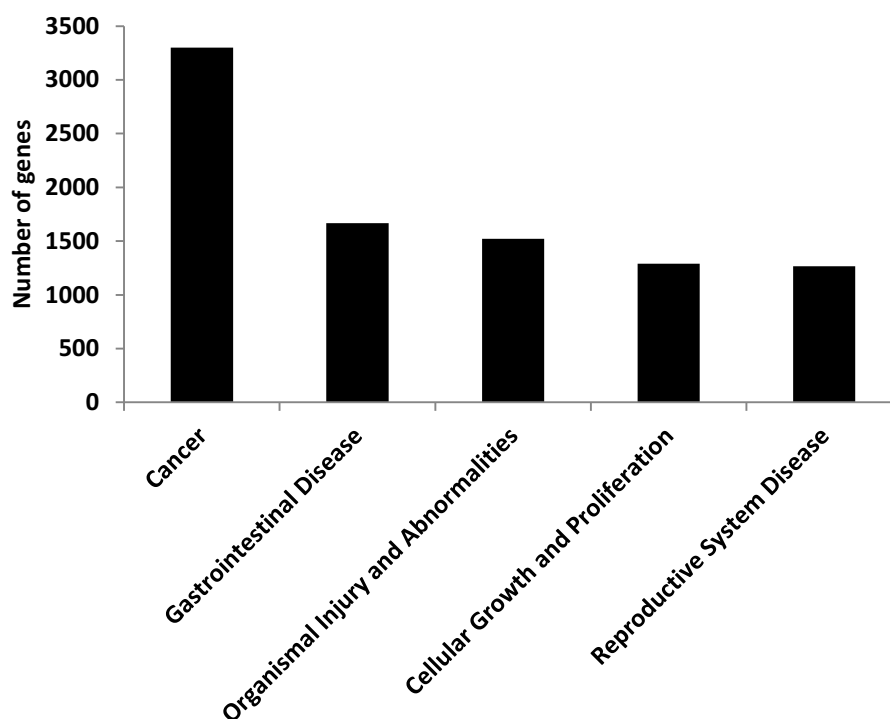
Figure 3: The 5 most significant biological functions and diseases related to changes in the methylation patterns.

The number of molecules in the dataset associated with a known function was determined by IPA functional analysis.
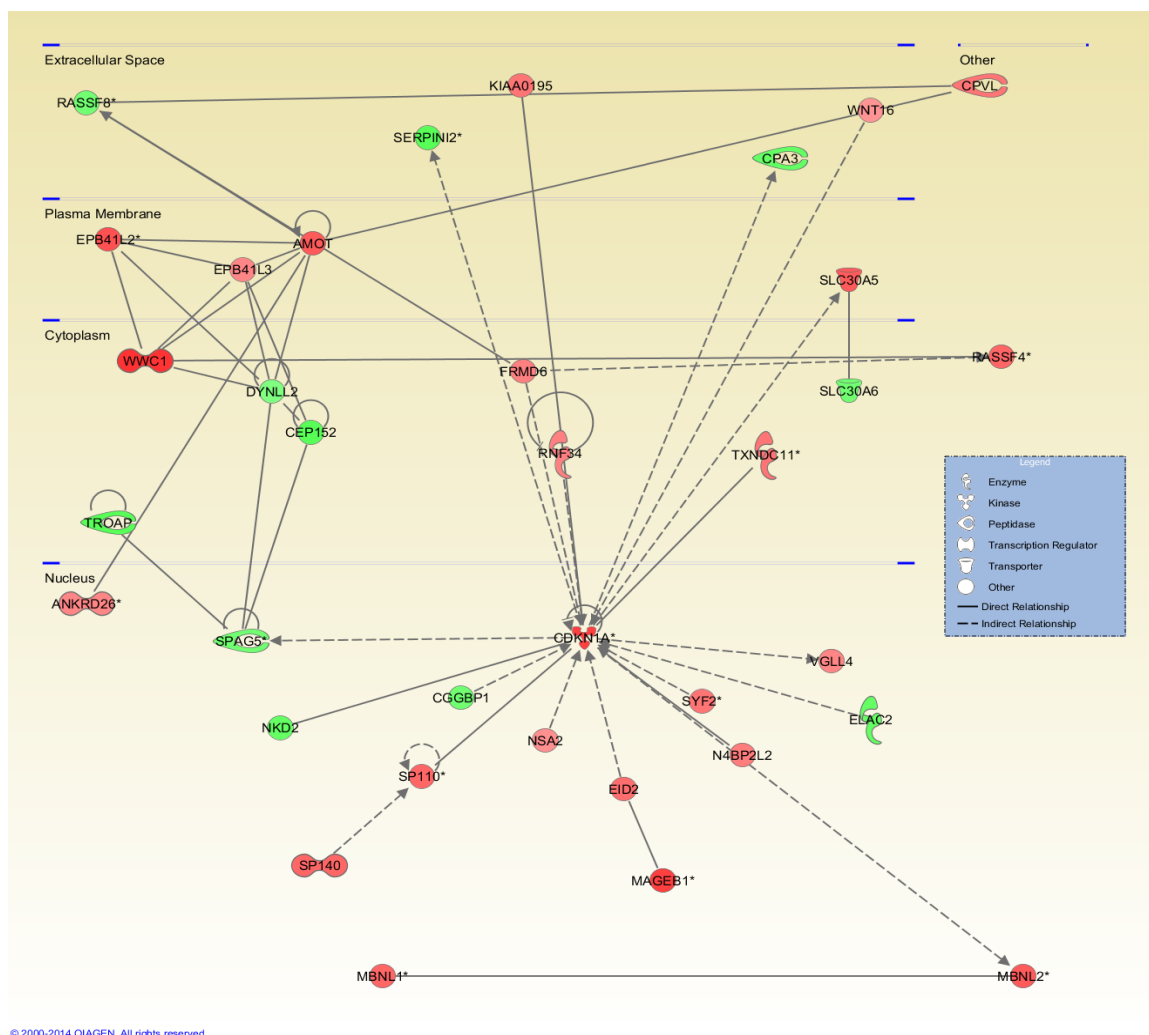
Figure 4: The most significant networks determined by IPA: cancer, cell cycle, and molecular transport.

The IPA network analysis was conducted using the genes that were differentially methylated and their close relationships. IPA used triangle connectivity based on 30 focus genes and built the network according to the number of interactions between a single gene and others in the existing network. Red, increased methylation; green, decreased methylation.

Table 2: Top 50 annotated genes with increased methylation

Rank	Symbol	Gene Name	log2 Fold Change	Location	Type(s)
1	ZNF330	zinc finger protein 330	4.614	Nucleus	other
2	ACTR3B	ARP3 actin-related protein 3 homolog B (yeast)	4.540	Other	other
3	CAV3	caveolin 3	4.292	Plasma Membrane	enzyme
4	NKX2-3	NK2 homeobox 3	4.199	Nucleus	transcription regulator
5	TLN2	talin 2	4.199	Nucleus	other
6	CPD	carboxypeptidase D	4.100	Extracellular Space	peptidase
7	CTNNBL1	catenin, beta like 1	4.100	Nucleus	other
8	Vmn2r1	vomeronasal 2, receptor 1	4.100	Plasma Membrane	other
9	Cmtm2a	CKLF-like MARVEL transmembrane domain containing 2A	3.993	Cytoplasm	transcription regulator
10	HPS6	Hermansky-Pudlak syndrome 6	3.993	Cytoplasm	other
11	KANK1	KN motif and ankyrin repeat domains 1	3.993	Nucleus	transcription regulator
12	RRP1	ribosomal RNA processing 1	3.993	Nucleus	other
13	SNX10	sorting nexin 10	3.993	Cytoplasm	transporter
14	UNC93A	unc-93 homolog A (C. elegans)	3.993	Plasma Membrane	other
15	Zfp932	zinc finger protein 932	3.993	Nucleus	other
16	ANKRD13D	ankyrin repeat domain 13 family, member D	3.877	Plasma Membrane	other
17	DACT1	dishevelled-binding antagonist of beta-catenin 1	3.877	Cytoplasm	other

18	DMRT2	doublesex and mab-3 related transcription factor 2	3.877	Nucleus	other
19	DSC3	desmocollin 3	3.877	Plasma Membrane	other
20	LDOC1	leucine zipper, down-regulated in cancer 1	3.877	Nucleus	other
21	LRRC8B	leucine rich repeat containing 8 family, member B	3.877	Other	other
22	SEPP1	selenoprotein P, plasma, 1	3.877	Extracellular Space	other
23	SMAD3	SMAD family member 3	3.877	Nucleus	transcription regulator
24	Smok2a	sperm motility kinase 2B	3.877	Other	other
25	TCEAL3	transcription elongation factor A (SII)-like 3	3.877	Other	other
26	TNS1	tensin 1	3.877	Plasma Membrane	other
27	TRHR	thyrotropin-releasing hormone receptor	3.877	Plasma Membrane	G-protein coupled receptor
28	WWC1	WW and C2 domain containing 1	3.877	Cytoplasm	transcription regulator
29	PER2	period circadian clock 2	3.853	Nucleus	other
30	BHLHE23	basic helix-loop-helix family, member e23	3.752	Nucleus	transcription regulator
31	GALNT13	UDP-N-acetyl-alpha-D-galactosamine:polypeptide N-acetylgalactosaminyltransferase 13 (GalNAc-T13)	3.752	Cytoplasm	enzyme
32	KCNF1	potassium voltage-gated channel, subfamily F, member 1	3.752	Plasma Membrane	ion channel
33	MPP1	membrane protein, palmitoylated 1, 55kDa	3.752	Plasma Membrane	kinase

34	OPA1	optic atrophy 1 (autosomal dominant)	3.752	Cytoplasm	enzyme
35	PTP4A1	protein tyrosine phosphatase type IVA, member 1	3.752	Cytoplasm	phosphatase
36	SGCZ	sarcoglycan, zeta	3.752	Plasma Membrane	other
37	ADCY7	adenylate cyclase 7	3.614	Plasma Membrane	enzyme
38	ALCAM	activated leukocyte cell adhesion molecule	3.614	Plasma Membrane	other
39	AR	androgen receptor	3.614	Nucleus	ligand-dependent nuclear receptor
40	C4orf33	chromosome 4 open reading frame 33	3.614	Other	other
41	CCNH	cyclin H	3.614	Nucleus	transcription regulator
42	CDKN1A	cyclin-dependent kinase inhibitor 1A (p21, Cip1)	3.614	Nucleus	kinase
43	CDV3	CDV3 homolog (mouse)	3.614	Cytoplasm	other
44	COMT	catechol-O-methyltransferase	3.614	Cytoplasm	enzyme
45	CRYGC	crystallin, gamma C	3.614	Cytoplasm	other
46	FAM13A	family with sequence similarity 13, member A	3.614	Cytoplasm	other
47	IGF1R	insulin-like growth factor 1 receptor	3.614	Plasma Membrane	transmembrane receptor
48	IYD	iodotyrosine deiodinase	3.614	Plasma Membrane	enzyme
49	JAG1	jagged 1	3.614	Extracellular Space	growth factor
50	KCNMA1	potassium large conductance calcium-activated channel, subfamily M, alpha member 1	3.614	Plasma Membrane	ion channel

Table 3: Top 50 annotated genes with decreased methylation

Rank	Symbol	Gene Name	log2 Fold Change	Location	Type(s)
1	IRX1	iroquois homeobox 1	-5.897	Nucleus	transcription regulator
2	OSBP2	oxysterol binding protein 2	-5.408	Cytoplasm	other
3	CAPN5	calpain 5	-5.231	Cytoplasm	peptidase
4	INTS9	integrator complex subunit 9	-4.837	Nucleus	other
5	TRIML1	tripartite motif family-like 1	-4.837	Other	other
6	CSMD1	CUB and Sushi multiple domains 1	-4.614	Plasma Membrane	other
7	NCOR2	nuclear receptor corepressor 2	-4.272	Nucleus	transcription regulator
8	C6orf89	chromosome 6 open reading frame 89	-4.167	Other	other
9	TMEM242	transmembrane protein 242	-4.167	Other	other
10	DCLRE1A	DNA cross-link repair 1A	-4.100	Nucleus	other
11	EDNRA	endothelin receptor type A	-3.877	Plasma Membrane	transmembrane receptor
12	GALNT11	UDP-N-acetyl-alpha-D-galactosamine:polypeptide N-acetylgalactosaminyltransferase 11 (GalNAc-T11)	-3.877	Cytoplasm	enzyme
13	PTPN11	protein tyrosine phosphatase, non-receptor type 11	-3.877	Cytoplasm	phosphatase
14	AGPAT9	1-acylglycerol-3-phosphate O-acyltransferase 9	-3.795	Cytoplasm	enzyme
15	IER5	immediate early response 5	-3.795	Other	other
16	PPM1D	protein phosphatase, Mg2+/Mn2+ dependent, 1D	-3.708	Cytoplasm	phosphatase
17	RBBP6	retinoblastoma binding protein 6	-3.708	Nucleus	enzyme

18	BLOC1S2	biogenesis of lysosomal organelles complex-1, subunit 2	-3.614	Cytoplasm	other
19	CPEB2	cytoplasmic polyadenylation element binding protein 2	-3.614	Cytoplasm	other
20	ECI2	enoyl-CoA delta isomerase 2	-3.614	Cytoplasm	enzyme
21	MMGT1	membrane magnesium transporter 1	-3.614	Cytoplasm	transporter
22	NALCN	sodium leak channel, non-selective	-3.614	Plasma Membrane	ion channel
23	RETNLB	resistin like beta	-3.614	Extracellular Space	other
24	AMD1	adenosylmethionine decarboxylase 1	-3.515	Cytoplasm	enzyme
25	C1orf198	chromosome 1 open reading frame 198	-3.515	Other	other
26	DGKI	diacylglycerol kinase, iota	-3.515	Cytoplasm	kinase
27	DYNLT3	dynein, light chain, Tctex-type 3	-3.515	Cytoplasm	other
28	EPHA6	EPH receptor A6	-3.515	Plasma Membrane	kinase
29	GABRA6	gamma-aminobutyric acid (GABA) A receptor, alpha 6	-3.515	Plasma Membrane	ion channel
30	Gk2	glycerol kinase 2	-3.515	Cytoplasm	other
31	GLT1D1	glycosyltransferase 1 domain containing 1	-3.515	Extracellular Space	enzyme
32	HMGN2	high mobility group nucleosomal binding domain 2	-3.515	Nucleus	other
33	KLHL17	kelch-like family member 17	-3.515	Cytoplasm	other
34	Olfr266	olfactory receptor 266	-3.515	Plasma Membrane	G-protein coupled receptor
35	Ott	ovary testis transcribed	-3.515	Other	other
36	P2RX7	purinergic receptor P2X, ligand-gated ion channel, 7	-3.515	Plasma Membrane	ion channel
37	PTER	phosphotriesterase	-3.515	Other	enzyme

		related			
38	Rnf213	ring finger protein 213	-3.515	Cytoplasm	enzyme
39	SERPINC1	serpin peptidase inhibitor, clade C (antithrombin), member 1	-3.515	Extracellular Space	enzyme
40	TPD52L1	tumor protein D52-like 1	-3.515	Cytoplasm	other
41	ZMAT4	zinc finger, matrin-type 4	-3.515	Nucleus	other
42	RBM20	RNA binding motif protein 20	-3.462	Nucleus	other
43	BEGAIN	brain-enriched guanylate kinase-associated	-3.408	Nucleus	other
44	CHSY3	chondroitin sulfate synthase 3	-3.408	Cytoplasm	enzyme
45	CKAP4	cytoskeleton-associated protein 4	-3.408	Cytoplasm	other
46	DPF3	D4, zinc and double PHD fingers, family 3	-3.408	Other	other
47	Ear2	eosinophil-associated, ribonuclease A family, member 2	-3.408	Cytoplasm	enzyme
48	FAM135B	family with sequence similarity 135, member B	-3.408	Other	enzyme
49	POT1	protection of telomeres 1	-3.408	Nucleus	other
50	POU6F1	POU class 6 homeobox 1	-3.408	Nucleus	transcription regulator

Table 4: Ingenuity Pathway Analysis of gene networks

Rank	Molecules in network	Score	Focus molecules	Top function
1	↑AMOT,↑ANKRD26,↑CDKN1A,↓CEP152,↓CGGBP1,↓CPA3,↑CPVL, ↓DYNLL2, ↑EID2, ↓ELAC2, ↑EPB41L2,	30	35	Cancer, Cell Cycle, Molecular

	↑EPB41L3, ↑FRMD6, ↑KIAA0195, ↑MAGEB1, ↑MBNL1, ↑MBNL2, ↑N4BP2L2, ↓NKD2, ↑NSA2, ↑RASSF4, ↓RASSF8, ↑RNF34, ↓SERPINI2, ↑SLC30A5, ↓SLC30A6, ↑SP110, ↑SP140, ↓SPAG5, ↑SYF2, ↓TROAP, ↑TXNDC11, ↑VGLL4, ↑WNT16, ↑WWC1			Transport
2	↑ACACA, ↓ATRNL1, ↓BHMT, ↑CYP2A13, ↓Cyp2c70, ↑CYP3A43, ↓DCLRE1A, ↑E330013P04Rik, ↓FASN, ↑GPC6, ↑GSTP1, ↓HNMT, ↓IVNS1ABP, ↓Keg1, ↓Lcn4, ↑LRTM1, ↓MC4R, ↓Mill1, ↑MRGPRX3, ↑MT1E, ↑MTF1, ↑NR1H4, ↑RORA, ↑SLC13A1, ↑SLC16A7, ↓SLC29A4, ↓SLC30A1, ↓SLC38A4, ↑SULT1C3, ↓TMC6, ↓UCP1, ↑UPP2, ↓Xlr3c (includes others), ↑ZNF275, ↓ZNF292	30	35	Renal Damage, Renal Tubule Injury, Molecular Transport
3	↑ABTB2, ↑ALKBH8, ↑ALPK1, ↓BCKDHB, ↑BTBD7, ↑C11orf70, ↑C20orf194, ↑CAMKV, ↓CCDC39, ↑CUL2, ↓CUL3, ↑DCLK2, ↑EGFLAM, ↑FAM98A, ↓FARS2, ↑FBXO10, ↑FBXO34, ↑G2E3, ↓G3BP2, ↑HSP90AA1, ↓KCNG1, ↓KCNS3, ↓KCTD8, ↑KLHL10, ↓KLHL14, ↑KLHL29, ↑KLHL32, ↑KLHL36, ↑KRR1, ↑QDPR, ↑RCBTB1, ↓SEPHS1, ↓UST, ↓YWHAE, ↑ZBED4	30	35	Hereditary Disorder, Respiratory Disease, Metabolic Disease
4	↓ABCA6, ↓ABLIM3, ↓ABRA, ↑AIF1L, ↓AMBRA1, ↓ARAP2, ↓ARL6, ↓ATL2, ↓CAPN5, ↑CAPN6, ↓CASP12,CD80/CD86, ↑CLEC2D, ↑CLEC6A, ↑CRTAM, ↑GBP5, ↑Gbp8,Gbp6 (includes others), ↑GFM1, ↑GIMAP1-GIMAP5, ↑Gvin1 (includes others), ↑HERC6, ↑IFNG, ↓KIAA0226, ↓KIF16B,↑KLRB1, ↓KMO, ↓KY, ↑LAMP3, ↑LIX1, ↓Neurl3, ↑PCDH17, ↑Phb, ↑PILRB, ↓PMP2	28	34	Endocrine System Disorders, Gastrointestinal Disease, Immunological Disease

5	↑AFF2, ↑AP4S1, ↑ASAP2, ↓C21orf91, ↑C2orf88, ↑DLGAP1, ↑Eif2s3x, ↓FAM110A, ↑GNS, ↑GRB2, ↑HDGFRP3, ↓KCNH7, ↓KIRREL, ↑KRT83, ↑LRFN4, ↑MEPE, ↑NCK1, ↑NCKAP5, ↓PANX2, ↑PHACTR2, ↑RALGAPA2, ↓RALGPS1, ↑SEPN1, ↑SH2D4A, ↑SHANK2, ↓SHROOM2, ↓SLCO2A1, ↑SNX8, ↑SNX12, ↑SNX18, ↓SPRY, ↑TJAP1, ↑TTYH2, ↑WDR44, ↑ZNF32	28	34	Cellular Assembly and Organization, Tissue Development, Cellular Function and Maintenance

Canonical pathways associated with methylation changes in Apc mutant polyps were analyzed based on the ratio of the number of input genes to the total number of reference genes in the corresponding pathways in the IPA knowledge bases. Fisher's exact test was employed to calculate the P values to determine whether the associations between the differentially methylated genes and the canonical pathways were significant or random. Using a cutoff value of $P < 0.05$, IPA identified 84 significant signaling pathways that contained genes with increased or decreased methylation. The 15 most significant pathways that correlated with methylation changes in polyps are presented in Figure 5. Notably, regulation of the epithelial-mesenchymal transition (EMT) pathway was mapped by IPA and ranked as the 4th most significant canonical pathway associated with altered methylation. According to the IPA knowledge bases, the regulation of the EMT pathway includes 196 molecules. Among these molecules, 62 displayed greater than a 2 fold change ($\log_2$) in methylation in the polyps from Apc[min/+] mice by MeDIP-seq. The abnormal methylation changes in the EMT pathway included alterations in the methylation profiles of kinases, peptidases, phosphatases, transcription regulators, transmembrane receptors, and microRNAs. Table 5 and Table 6 list the genes involved in

the EMT pathway that exhibited altered methylation (37 genes with increased methylation in Table 5; 25 genes with decreased methylation in Table 6). Signaling pathways, such as the Wnt/β-catenin, TGF-β, NOTCH, and receptor tyrosine kinase (RTK) pathways, can initiate an EMT program alone or in combination (142). Although the genes that were determined to have differential methylation patterns in polyps by MeDIP-seq were not significantly associated with the TGF-β, NOTCH, and RTK signaling pathways, the Wnt/β-catenin pathway was identified as one of the most significant canonical pathways implicated based on methylation changes in the polyps (ranked 11th). Specifically, 53 out of 175 molecules in this pathway showed methylation changes of greater than 2-fold (log$_2$) in polyps from Apc$^{min/+}$ mice; these molecules are listed in Table 7 and Table 8 (30 genes with increased methylation in Table 7; 23 genes with decreased methylation in Table 8). Additionally, we found many shared genes in the EMT and Wnt/β-catenin pathways with altered methylation levels; these genes are shown in bold in Tables 5 to 8. To understand the role of DNA methylation in the crosstalk between the EMT and Wnt/β-catenin pathways in Apc$^{min/+}$ mice, IPA was utilized to predict the direct interaction of the differentially methylated genes in these two pathways based on the publication database (Figure 6). The pathway analysis of the MeDIP-seq data suggested that cellular changes mediated via the EMT and Wnt/β-catenin pathways may be significantly associated with altered DNA methylation in polyps from Apc$^{min/+}$ mice.
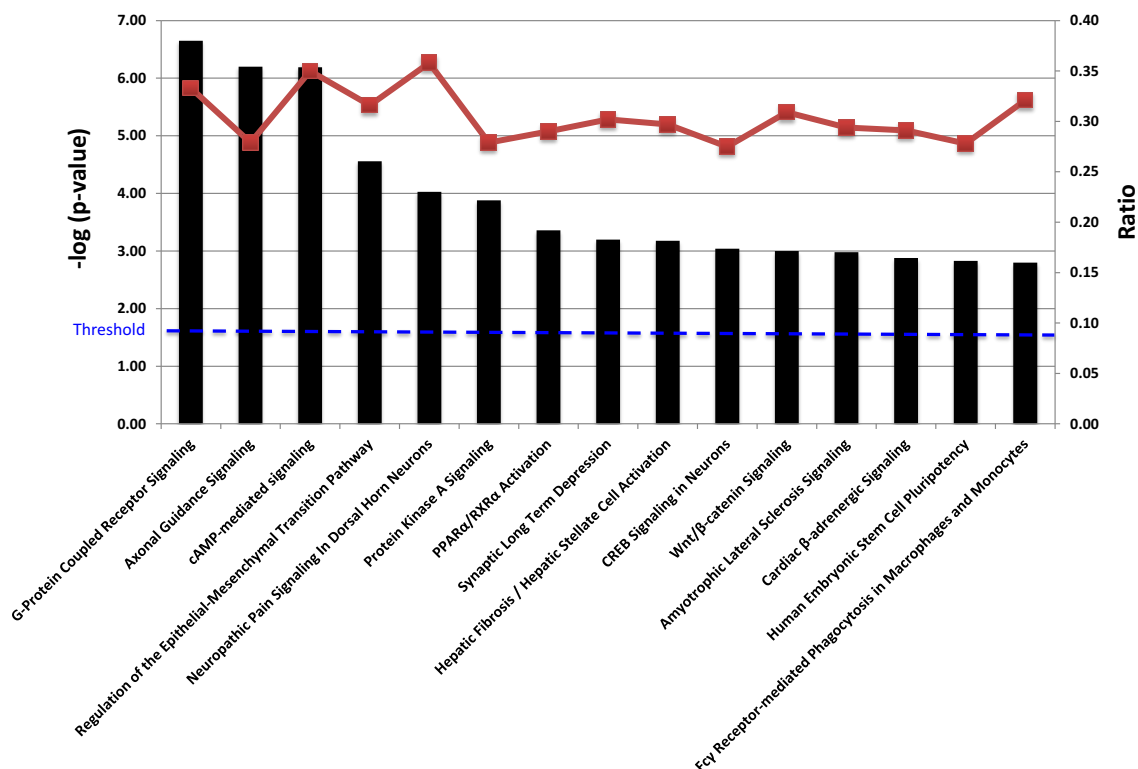
Figure 5: The 15 most significant canonical pathways related to changes in the methylation patterns.

The left y-axis (bar graph) presents the data as the log (p-value) of each pathway using Fisher's exact test. The right y-axis (line graph) corresponds to the ratio data for each pathway. The ratios were calculated as the number of input molecules mapped to a specific pathway divided by the total number of molecules in the given pathway.
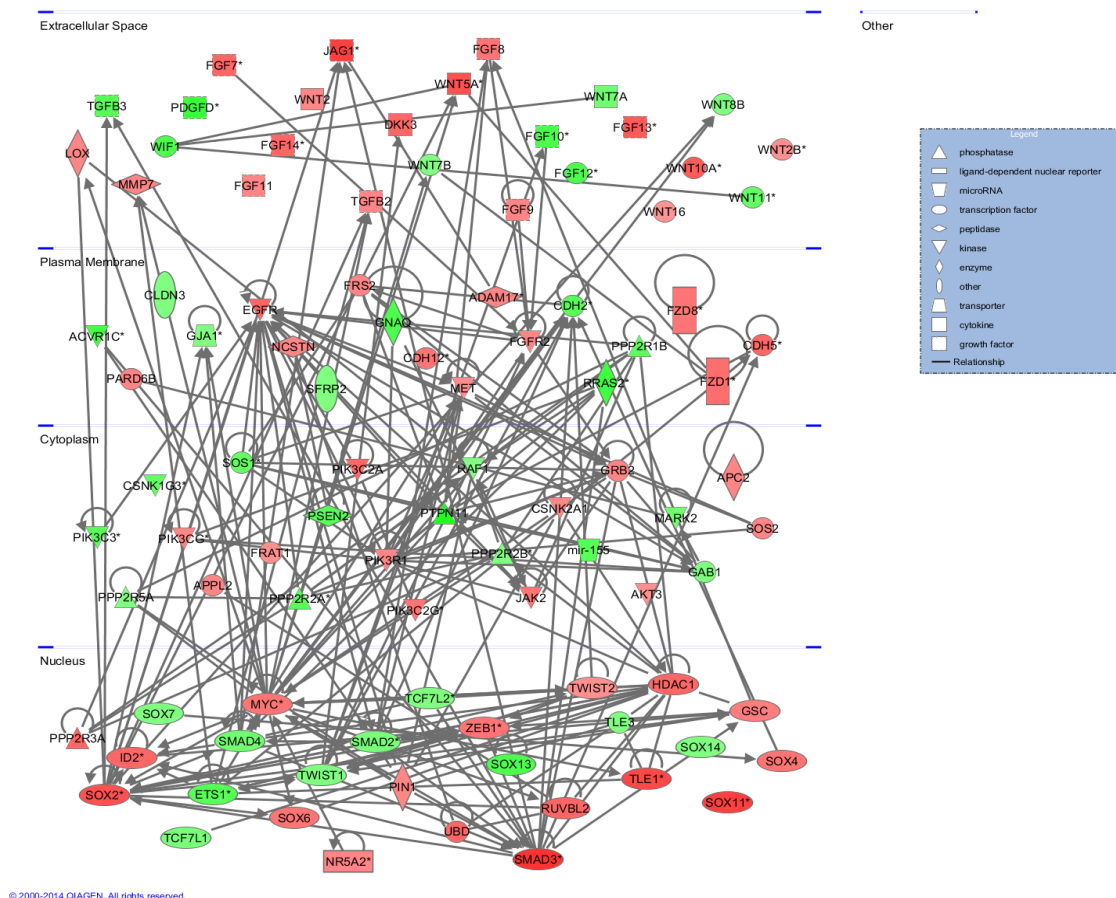
Figure 6: Predicted interactions between molecules with altered methylation that mapped to the EMT and Wnt/β-catenin pathways.

IPA predicted direct interaction of the genes with altered methylation patterns in the EMT and Wnt/β-catenin pathways based on the publication database. Red, increased methylation; green, decreased methylation.

Table 5: Genes with increased methylation that mapped to the regulation of the EMT pathway by IPA

Symbol	Gene Name	$\log_2$ Fold Change	Location	Type(s)

SMAD3	SMAD family member 3	3.877	Nucleus	transcription regulator
JAG1	jagged 1	3.614	Extracellular Space	growth factor
WNT5A	**wingless-type MMTV integration site family, member 5A**	**3.292**	**Extracellular Space**	**cytokine**
FGF13	fibroblast growth factor 13	3.100	Extracellular Space	growth factor
WNT10 A	**wingless-type MMTV integration site family, member 10A**	**3.100**	**Extracellular Space**	**other**
EGFR	epidermal growth factor receptor	2.877	Plasma Membrane	kinase
FGF7	fibroblast growth factor 7	2.877	Extracellular Space	growth factor
FGF14	fibroblast growth factor 14	2.877	Extracellular Space	growth factor
ID2	inhibitor of DNA binding 2, dominant negative helix-loop-helix protein	2.877	Nucleus	transcription regulator
PIK3C2 A	phosphatidylinositol-4-phosphate 3-kinase, catalytic subunit type 2 alpha	2.877	Cytoplasm	kinase
FZD1	**frizzled class receptor 1**	**2.752**	**Plasma Membrane**	**G-protein coupled receptor**
CDH12	**cadherin 12, type 2 (N-cadherin 2)**	**2.614**	**Plasma Membrane**	**other**
FGF8	fibroblast growth factor 8 (androgen-induced)	2.614	Extracellular Space	growth factor
FZD8	**frizzled class receptor 8**	**2.614**	**Plasma Membrane**	**G-protein coupled receptor**
JAK2	Janus kinase 2	2.614	Cytoplasm	kinase
PIK3C2 G	phosphatidylinositol-4-phosphate 3-kinase, catalytic subunit type 2 gamma	2.614	Cytoplasm	kinase
ZEB1	zinc finger E-box binding homeobox 1	2.614	Nucleus	transcription regulator
GSC	goosecoid homeobox	2.462	Nucleus	transcription regulator
ADAM1 7	ADAM metallopeptidase domain 17	2.292	Plasma Membrane	peptidase
FGF9	fibroblast growth factor 9	2.292	Extracellular Space	growth factor

FGF11	fibroblast growth factor 11	2.292	Extracellular Space	growth factor
FGFR2	fibroblast growth factor receptor 2	2.292	Plasma Membrane	kinase
FRS2	fibroblast growth factor receptor substrate 2	2.292	Plasma Membrane	other
GRB2	growth factor receptor-bound protein 2	2.292	Cytoplasm	other
LOX	lysyl oxidase	2.292	Extracellular Space	enzyme
NCSTN	nicastrin	2.292	Plasma Membrane	peptidase
PARD6B	par-6 family cell polarity regulator beta	2.292	Plasma Membrane	other
PIK3CG	phosphatidylinositol-4,5-bisphosphate 3-kinase, catalytic subunit gamma	2.292	Cytoplasm	kinase
PIK3R1	phosphoinositide-3-kinase, regulatory subunit 1 (alpha)	2.292	Cytoplasm	kinase
SOS2	son of sevenless homolog 2 (Drosophila)	2.292	Cytoplasm	other
TGFB2	**transforming growth factor, beta 2**	**2.292**	**Extracellular Space**	**growth factor**
WNT2	**wingless-type MMTV integration site family member 2**	**2.292**	**Extracellular Space**	**cytokine**
MET	MET proto-oncogene, receptor tyrosine kinase	2.180	Plasma Membrane	kinase
AKT3	**v-akt murine thymoma viral oncogene homolog 3**	**2.100**	**Cytoplasm**	**kinase**
TWIST2	twist family bHLH transcription factor 2	2.100	Nucleus	transcription regulator
WNT2B	**wingless-type MMTV integration site family, member 2B**	**2.100**	**Extracellular Space**	**other**
WNT16	**wingless-type MMTV integration site family, member 16**	**2.029**	**Extracellular Space**	**other**

Table 6: Genes with decreased methylation that mapped to the regulation of the EMT pathway by IPA

Symbol	Gene Name	log$_2$ Fold Change	Location	Type(s)
PTPN11	protein tyrosine phosphatase, non-receptor type 11	-3.877	Cytoplasm	phosphatase
PDGFD	platelet derived growth factor D	-3.167	Extracellular Space	growth factor
RRAS2	related RAS viral (r-ras) oncogene homolog 2	-3.090	Plasma Membrane	enzyme
FGF10	fibroblast growth factor 10	-2.877	Extracellular Space	growth factor
FGF12	fibroblast growth factor 12	-2.877	Extracellular Space	other
CDH2	**cadherin 2, type 1, N-cadherin (neuronal)**	**-2.708**	**Plasma Membrane**	**other**
ETS1	v-ets avian erythroblastosis virus E26 oncogene homolog 1	-2.708	Nucleus	transcription regulator
mir-155	microRNA 155	-2.708	Cytoplasm	microRNA
PIK3C3	phosphatidylinositol 3-kinase, catalytic subunit type 3	-2.708	Cytoplasm	growth factor
PSEN2	presenilin 2	-2.708	Cytoplasm	peptidase
TGFB3	**transforming growth factor, beta 3**	**-2.708**	**Extracellular Space**	**growth factor**
SOS1	son of sevenless homolog 1 (Drosophila)	-2.515	Cytoplasm	other
WNT11	**wingless-type MMTV integration site family, member 11**	**-2.515**	**Extracellular Space**	**other**
SMAD4	SMAD family member 4	-2.292	Nucleus	transcription regulator
WNT7A	**wingless-type MMTV integration site family, member 7A**	**-2.292**	**Extracellular Space**	**cytokine**
SMAD2	SMAD family member 2	-2.167	Nucleus	transcription regulator
TCF7L1	**transcription factor 7-like 1 (T-cell specific, HMG-box)**	**-2.167**	**Nucleus**	**transcription regulator**
CLDN3	claudin 3	-2.029	Plasma Membrane	transmembrane receptor

GAB1	GRB2-associated binding protein 1	-2.029	Cytoplasm	other
HMGA2	--	-2.029	Other	other
RAF1	Raf-1 proto-oncogene, serine/threonine kinase	-2.029	Cytoplasm	kinase
TCF7L2	**transcription factor 7-like 2 (T-cell specific, HMG-box)**	**-2.029**	**Nucleus**	**transcription regulator**
TWIST1	twist family bHLH transcription factor 1	-2.029	Nucleus	transcription regulator
WNT7B	**wingless-type MMTV integration site family, member 7B**	**-2.029**	**Extracellular Space**	**other**
WNT8B	**wingless-type MMTV integration site family, member 8B**	**-2.029**	**Extracellular Space**	**other**

Table 7: Genes with increased methylation that mapped to the Wnt/β-catenin pathway by IPA

Symbol	Gene Name	$\log_2$ Fold Change	Location	Type(s)
SOX11	SRY (sex determining region Y)-box 11	3.614	Nucleus	transcription regulator
TLE1	transducin-like enhancer of split 1 (E(sp1) homolog, Drosophila)	3.462	Nucleus	transcription regulator
SOX2	SRY (sex determining region Y)-box 2	3.292	Nucleus	transcription regulator
WNT5A	**wingless-type MMTV integration site family, member 5A**	**3.292**	**Extracellular Space**	**cytokine**
WNT10A	**wingless-type MMTV integration site family, member 10A**	**3.100**	**Extracellular Space**	**other**
CDH5	cadherin 5, type 2 (vascular endothelium)	2.877	Plasma Membrane	other
DKK3	dickkopf WNT signaling pathway inhibitor 3	2.877	Extracellular Space	cytokine
HDAC1	histone deacetylase 1	2.877	Nucleus	transcription regulator
PPP2R3	protein phosphatase 2,	2.877	Nucleus	phosphatase

A	regulatory subunit B'', alpha			
RUVBL2	RuvB-like AAA ATPase 2	2.877	Nucleus	transcription regulator
UBD	ubiquitin D	2.877	Nucleus	other
FZD1	**frizzled class receptor 1**	**2.752**	**Plasma Membrane**	**G-protein coupled receptor**
CDH12	**cadherin 12, type 2 (N-cadherin 2)**	**2.614**	**Plasma Membrane**	**other**
FZD8	**frizzled class receptor 8**	**2.614**	**Plasma Membrane**	**G-protein coupled receptor**
MYC	v-myc avian myelocytomatosis viral oncogene homolog	2.614	Nucleus	transcription regulator
SOX4	SRY (sex determining region Y)-box 4	2.614	Nucleus	transcription regulator
SOX6	SRY (sex determining region Y)-box 6	2.614	Nucleus	transcription regulator
APC2	adenomatosis polyposis coli 2	2.292	Cytoplasm	enzyme
APPL2	adaptor protein, phosphotyrosine interaction, PH domain and leucine zipper containing 2	2.292	Cytoplasm	other
CSNK2A1	casein kinase 2, alpha 1 polypeptide	2.292	Cytoplasm	kinase
MMP7	matrix metallopeptidase 7 (matrilysin, uterine)	2.292	Extracellular Space	peptidase
NR5A2	nuclear receptor subfamily 5, group A, member 2	2.292	Nucleus	ligand-dependent nuclear receptor
PIN1	peptidylprolyl cis/trans isomerase, NIMA-interacting 1	2.292	Nucleus	enzyme
TGFB2	transforming growth factor, beta 2	2.292	Extracellular Space	growth factor
WNT2	**wingless-type MMTV integration site family member 2**	**2.292**	**Extracellular Space**	**cytokine**
AKT3	**v-akt murine thymoma viral oncogene homolog 3**	**2.100**	**Cytoplasm**	**kinase**
FRAT1	frequently rearranged in advanced T-cell lymphomas	2.100	Cytoplasm	other
WNT2B	**wingless-type MMTV**	**2.100**	**Extracellular**	**other**

	integration site family, member 2B		Space	
WNT16	**wingless-type MMTV integration site family, member 16**	**2.029**	**Extracellular Space**	**other**

Table 8: Genes with decreased methylation that mapped to the Wnt/β-catenin pathway by IPA

Symbol	Gene Name	$\log_2$ Fold Change	Location	Type(s)
ACVR1C	activin A receptor, type IC	-3.029	Plasma Membrane	kinase
GNAQ	guanine nucleotide binding protein (G protein), q polypeptide	-2.877	Plasma Membrane	enzyme
SOX13	SRY (sex determining region Y)-box 13	-2.877	Nucleus	transcription regulator
WIF1	WNT inhibitory factor 1	-2.877	Extracellular Space	other
CDH2	**cadherin 2, type 1, N-cadherin (neuronal)**	**-2.708**	**Plasma Membrane**	**other**
PPP2R2A	protein phosphatase 2, regulatory subunit B, alpha	-2.708	Cytoplasm	phosphatase
TGFB3	**transforming growth factor, beta 3**	**-2.708**	**Extracellular Space**	**growth factor**
PPP2R1B	protein phosphatase 2, regulatory subunit A, beta	-2.614	Plasma Membrane	phosphatase
CSNK1G3	casein kinase 1, gamma 3	-2.515	Cytoplasm	kinase
WNT11	**wingless-type MMTV integration site family, member 11**	**-2.515**	**Extracellular Space**	**other**
MARK2	MAP/microtubule affinity-regulating kinase 2	-2.292	Cytoplasm	kinase
WNT7A	**wingless-type MMTV integration site family, member 7A**	**-2.292**	**Extracellular Space**	**cytokine**
TCF7L1	**transcription factor 7-like 1 (T-cell specific, HMG-box)**	**-2.167**	**Nucleus**	**transcription regulator**

GJA1	gap junction protein, alpha 1, 43kDa	-2.029	Plasma Membrane	transporter
PPP2R2 B	protein phosphatase 2, regulatory subunit B, beta	-2.029	Cytoplasm	phosphatase
PPP2R5 A	protein phosphatase 2, regulatory subunit B', alpha	-2.029	Cytoplasm	phosphatase
SFRP2	secreted frizzled-related protein 2	-2.029	Plasma Membrane	transmembran e receptor
SOX7	SRY (sex determining region Y)-box 7	-2.029	Nucleus	transcription regulator
SOX14	SRY (sex determining region Y)-box 14	-2.029	Nucleus	transcription regulator
TCF7L2	**transcription factor 7-like 2 (T-cell specific, HMG-box)**	**-2.029**	**Nucleus**	**transcription regulator**
TLE3	transducin-like enhancer of split 3	-2.029	Nucleus	other
WNT7B	**wingless-type MMTV integration site family, member 7B**	**-2.029**	**Extracellular Space**	**other**
WNT8B	**wingless-type MMTV integration site family, member 8B**	**-2.029**	**Extracellular Space**	**other**

2.4 Discussion

Global hypomethylation and hypermethylation of CpG islands in tumor suppressor genes occurs in human colon cancer cell lines and primary colon adenomatous tissues (129). However, the global genomic distribution of aberrant methylation and the association of these methylation signatures with pivotal signaling pathways and biological networks in colon cancer remain unclear, mainly due to the limitations of the existing techniques for analyzing DNA methylation at specific sequences (143). Recently, the development of the MeDIP-based approach has enabled the rapid and comprehensive

identification of multiple CpG sites. MeDIP in conjunction with high-throughput sequence (MeDIP-seq) provides a genome-wide mapping technique that has been successfully used to profile the global DNA methylation patterns of many cancer models (144-147). Notably, Grimm et al. used MeDIP-seq to identify a large number of DMRs with distinct methylation patterns in Apc mutant adenomas, that are partially conserved between intestinal adenomas in Apc$^{min/+}$ mice and human colon cancer (148). In the present study, we used pathway analysis after MeDIP-seq to screen the global genomic methylation profile to identify genomic loci with aberrant methylation patterns in adenomatous polyps from Apc$^{min/+}$ mice and to determine the biological function, networks, and canonical pathways that were affected by the DNA methylation in Apc mutant adenomas.

The top-ranked genes with increased and decreased methylation may provide information to facilitate the discovery of key genes, therapeutic targets, and biomarkers for the development, diagnosis, prognosis, and prevention of colon cancer. For example, CTNNBL1 [catenin (cadherin-associated protein) b-like 1] exhibited increased methylation in adenomatous polyp tissue (log$_2$ fold change = 4.1, Table 2), as evidenced by MeDIP-seq. The CTNNBL1 gene is associated with obesity, a known risk factor for the development of CRC (149). Recently, CTNNBL1 was reported to be a putative regulator of the canonical Wnt signaling pathway, and the dysregulation of this pathway are involved in CRC (150). However, the potential epigenetic regulation of CTNNBL1 in colon cancer remains to be elucidated. To the best of our knowledge, this is the first report to suggest that CTNNBL1 might by aberrantly methylated in Apc mutant mice. Further experiments are necessary to investigate the epigenetic regulation of CTNNBL1

in colon cancer cells and patient specimens. CDKN1A (cyclin-dependent kinase inhibitor 1A, p21) showed increased methylation ($\log_2$ fold change = 3.6, Table 2) in adenomatous polyp tissue compared with control tissue. CDKN1A is a cyclin-dependent kinase inhibitor that plays a key role in regulating the cell cycle, especially the G1/S checkpoint, and its expression is lost in most cases of colon cancer. By analyzing 737 CRC samples, Ogino et al. concluded that the down-regulation of p21 inversely correlates with microsatellite instability and the CpG island methylator phenotype in colon cancer (151). Here, we provided additional evidence by demonstrating potentially increased p21 methylation in Apc$^{min/+}$ polyps.

It is commonly believed that promoter hypermethylation is associated with silencing of tumor suppressor genes in carcinogenesis (152). One study observed a significant increase in DNA methylation in primary colon adenocarcinoma samples relative to normal colon tissue by analyzing the DNA methylation data from Cancer Genome Atlas (TCGA) and found an inverse correlation between DNA methylation and gene expression: genes with cancer-specific DNA methylation showed decreased transcription activity in colon adenocarcinoma (153). However, Grimm et al. reported that the correlation of gene expression and DNA methylation applies only to a small set of genes by analyzing the results from MeDIP-seq and RNA-seq in normal intestine tissues and Apc mutant adenomas. In addition, they analyzed the mRNA expression of 31 selected tumor suppressors, only 2 were found both promoter hypermethylated and transcriptionally silenced. Surprisingly, the majority of tumor suppressors examined in their study didn't exhibit a decreased transcription activity in adenoma compared to normal intestine samples (148). These results suggested that silencing of tumor

suppressor genes by aberrant methylation might not be common events during early polyposis of Apc mutant mice. Nevertheless, it is possible that epigenetic changes mediated gene silencing arises during progression of adenoma to carcinoma (154). Furthermore, it was reported that instead of directly intervene active promoters, DNA methylation affects genes that are already silent by other mechanisms such as histone modification (13). Thus, further studies are needed to elucidate the dynamic changes of DNA methylation, histone modifications, and gene transcription in different stages, such as initiation, progression, and metastasis during colon carcinogenesis.

This study aimed to discover functions and pathways associated with epigenomic alterations in colon cancer in addition to the individual affected molecules. We utilized IPA to interpret the MeDIP-seq data in the context of molecular interactions, networks, and canonical pathways. IPA revealed that the genes with altered methylation patterns in adenomatous tissues predominantly occupied the cancer and cell cycle networks (Table 4) and the cancer and gastrointestinal disease functional categories (Figure 3). This information suggested that dynamic epigenetic modifications might occur in genes associated with cancer, cell cycle regulation, and gut disease development in Apc$^{min/+}$ mice.

Biological changes that lead to the switch from an epithelial to a mesenchymal cell phenotype, defined as EMT, play an important role in embryonic development and carcinogenesis (155). In the context of tumorigenesis-associated EMT, neoplastic cells lose epithelial characteristics, such as cell-cell adhesion, cell polarity, and lack of motility, and acquire mesenchymal features, such as migratory ability, invasiveness, plasticity, and resistance to apoptosis (142). The morphological alterations that occur during EMT

enable neoplastic cells to escape from the basement membrane, migrate to neighboring lymph nodes, and eventually enter the circulation to establish secondary colonies at distant sites (156). Thus, EMT program activation is considered a critical step in tumor growth, angiogenesis, and metastasis (157). Chen et al. reported elevated expression of the mesenchymal marker vimentin in intestinal adenomas from Apc$^{min/+}$ mice and suggested that molecular alterations in the initial steps of EMT are involved in early tumorigenesis in Apc$^{min/+}$ mice; the early stages of intestinal tumorigenesis lack signs of invasion and metastasis (158). These interesting observations highlighted the necessity to study the EMT process during early tumorigenesis. Although the molecular and biochemical mechanisms involved in the initiation and regulation of EMT in carcinogenesis are not yet fully understood, they appear to be associated with growth factor receptors (for example, RTKs), signaling pathways (for example, the Wnt/β-catenin, NOTCH, and TGF-β pathways), and stimuli (for example, oxidative stress) (159). The involvement of epigenetic events in regulating the EMT proteome during carcinogenesis was recently demonstrated (160). Using ChIP-seq (chromatin immunoprecipitation followed by sequencing) assays, Cieslik et al. showed that EMT is driven by the chromatin-mediated activation of transcription factors (161). The current study identified many genes with increased or decreased methylation in the EMT pathway (Figure 5, Table 5, and Table 6), suggesting that aberrant DNA methylation may be associated with the activation of EMT during tissue remodeling in early tumorigenesis in Apc$^{min/+}$ mice. The present study also provided useful information regarding important molecules in the EMT pathway that undergo alterations in their methylation pattern during polyposis in Apc$^{min/+}$ mice. For example, SMAD3 (mothers against

decapentaplegic homolog 3), a molecule that plays an essential role in TGF-β pathway-mediated EMT, was one of the genes that exhibited increased methylation ($\log_2$ fold change = 3.9, Table 5) in adenomas in Apc$^{min/+}$ mice. Interestingly, SMAD3 deficiency promotes tumor formation in the distal colon of Apc$^{min/+}$ mice (162). EGFR (epidermal growth factor receptor), another important molecule that exhibited increased methylation, has been implicated in EMT in adenomas ($\log_2$ fold change = 2.9, Table 5). EGFR can induce EMT in cancer cells by up-regulating Twist (163), and promoter methylation of EGFR has been detected in metastatic tumors from patients with CRC (164). The results of the current study indicated that aberrant methylation of EGFR may occur during early tumorigenesis in Apc$^{min/+}$ mice. Important transcription factors in the EMT pathway, including ZEB 1 and TWIST 2, also exhibited increased methylation in adenomas from Apc$^{min/+}$ mice (Table 5). Although the contribution of TWIST 2 to promoting EMT in breast cancer progression was recently reported (165), there is limited knowledge of the role of TWIST 2 in colon cancer; however, one study proposed that TWIST 2 is a potential prognostic biomarker for colon cancer (166). Notably, aberrant methylation of TWIST 2 has been demonstrated in chronic lymphocytic leukemia (167) and acute lymphoblastic leukemia (168). The present study is the first to suggest that methylation of the TWIST 2 gene may be involved in tumorigenesis in Apc$^{min/+}$ mice. Further studies are necessary to elucidate the role of DNA methylation in EMT pathway regulation in early tumorigenesis in Apc$^{min/+}$ mice.

Apc$^{min/+}$ mice are thought to have a hyperactive Wnt/β-catenin pathway (127), but the epigenetic modifications of the Wnt/β-catenin pathway are still not fully understood. IPA identified the Wnt/β-catenin pathway as one of the most significant canonical

pathways that contained genes with increased or decreased methylation, suggesting an important role for epigenetic alterations in the Wnt/β-catenin pathway in tumorigenesis. Some of the molecules with increased or decreased methylation patterns that were mapped to this pathway in the present study are consistent with the findings of previous publications. For example, Dhir et al. analyzed tissue samples from inflammatory bowel disease (IBD) and colon cancer patients and demonstrated that aberrant methylation of Wnt/β-catenin signaling genes is an early event in IBD-associated colon cancer. Aberrant methylation of APC2 (adenomatousis polyposis coli 2), SFRP1 (secreted frizzled-related protein 1), and SFRP2 (secreted frizzled-related protein 2) is associated with the progression from colitis to neoplasia (169). In the current study, we observed increased methylation of APC2 and decreased methylation of SFRP2 in adenomas in Apc$^{min/+}$ mice (Table 7 and Table 8). Wang et al. demonstrated that black raspberries can prevent colonic ulceration in a DSS-induced model and in interleukin-10 knockout mice by epigenetically modifying genes with hypermethylated promoters in the Wnt/β-catenin pathway, such as DKK3 (dickkopf-related protein 3), APC, SFRP1, and SOX17 [SRY (sex determining region Y)-box 17] (170, 171). In the present study, DKK3 consistently displayed increased methylation (log$_2$ fold change = 2.9, Table 7) in adenomas from Apc$^{min/+}$ mice compared with normal tissue. Furthermore, we provided additional information regarding the genes with altered methylation in the Wnt/β-catenin pathway in polyps from Apc$^{min/+}$ mice, potentially facilitating future research on the involvement of aberrantly methylated Wnt/β-catenin pathway components in colon cancer development and on potential targets for epigenetic modification for the prevention of colon cancer. Intestinal adenoma in mouse originated from intestinal stem cells (ISC), a small fraction

of cells in proliferative crypts (172). Interestingly, Grimm and co-workers demonstrated that the adenoma-specific methylation signatures are not acquired from ISC by showing that the methylation patterns were similar in ISC, proliferative crypt cells, and differentiated villus cells, but are distinct in adenoma tissue (148). Since ISC are responsive to Wnt signaling and we identified Wnt/β-catenin pathway as one of the most significant pathways associated with DNA methylation in polyps from Apc$^{min/+}$ mice, it would be important to understand the mechanisms underlying the acquisition of aberrant DNA methylation patterns in Wnt/β-catenin pathway in adenoma and how the hypermethylated genes involved in Wnt/β-catenin pathway influence the neoplastic transformation from ISC to adenoma. Furthermore, the Wnt/β-catenin pathway is intimately associated with EMT pathway (173). The present study provided valuable information regarding the potential crosstalk between the EMT and Wnt/β-catenin pathways, which are both affected by DNA methylation in Apc$^{min/+}$ mice. Further studies are needed to understand the role of the complex crosstalk between multiple signaling pathways in the progression of colon cancer. In addition to DNA methylation, histone modification and non-coding RNA are major epigenetic mechanisms that regulate gene transcription in carcinogenesis (2). It is currently accepted that these epigenetic modifications are linked to one another in the modulation of the epigenome landscape (174, 175). For example, these epigenetic modifications may work in combination in carcinogenesis (176). It was found that DNA hypermethylation in Apc mutant adenomas preferentially target the polycomb repressive complex 1/2 (PRC 1/2) target genes, suggesting an interplay of DNA methylation and histone modification in Apc$^{min/+}$ mice (148). On the other hand, different epigenetic mechanisms may cross-regulate each other

in the regulation of cellular activity. For instance, the expression of certain microRNAs is potentially controlled by DNA methylation or histone modification. However, some microRNAs can target epigenetic-modifying enzymes, such as DNMTs (DNA methyltransferases) and EZH2 (enhancer of zeste homolog 2) (59). Furthermore, Tahara, et al. found that 74 chromatin regulatory genes are mutated more frequently in CpG island methylator phenotype - high CRC in the TCGA dataset (177). Changes in the methylation patterns of several genes encoding microRNAs, histone modification enzymes, and proteins that function in chromatin remodeling were identified using MeDIP-seq. For example, we discovered decreased methylation of microRNA-155 ($\log_2$ fold change = -2.7, Table 6), which mapped to the EMT pathway; microRNA-155 expression promotes the migration and invasion of several CRC cell lines (178). Moreover, HDAC1 (histone deacetylase 1) was mapped to the Wnt/β-catenin pathway with a 2.9-fold ($\log_2$) increase in methylation in Apc mutant polyps (Table 7). In addition, we observed an increased methylation in the gene coding for chromodomain-helicase-DNA-binding protein 1 (CHD1) in Apc mutant polyps (data not shown). CHD1 protein is known to be involved in transcription-related chromatin remodeling (179). Taken together, our data indicated that epigenetic alterations may be complex and may occur at multiple levels during tumorigenesis in Apc$^{min/+}$ mice.

2.5 Conclusion

In conclusion, polyps from Apc$^{min/+}$ mice exhibited extensive, aberrant DNA methylation. The methylation changes in the genes detected using the MeDIP-seq assay

were mainly attributed to functions and networks in cancer, the cell cycle, and gastrointestinal diseases. These differentially methylated genes were situated in several canonical pathways that are important in colon cancer, such as the EMT and Wnt/β-catenin signaling pathways.

3. CHAPTER THREE

Curcumin inhibits anchorage-independent growth of HT29 human colon cancer cells by targeting epigenetic restoration of the tumor suppressor gene *DLEC1* [5,6]

3.1 Introduction

Colorectal cancer is one of the leading causes of cancer-related morbidity and mortality worldwide. As one of the most well-studied malignancies, colorectal cancer is now considered a complex disease that results from the accumulation of genetic and epigenetic alterations (180). Extensive studies of colorectal cancer have identified several significant genetic mutations implicated in proliferation, differentiation, adhesion, apoptosis, cell cycle, and DNA repair (181). In recent years, emerging evidence has suggested that the aberrant epigenetic landscape (heritable alterations in gene expression without changes in DNA sequence) may add an additional layer of complexity to the initiation and progression of colorectal cancer. The reversible and dynamic nature of these epigenetic alterations has enabled their development as potential biomarkers for diagnostic, prognostic, and therapeutic targets in colorectal cancer (182). Among epigenetic mechanisms, DNA methylation is perhaps the most extensively studied

epigenetic alteration in colorectal cancer. Importantly, inactivation of tumor suppressor genes by promoter CpG island hypermethylation has been recognized as one of the hallmarks of cancer (122) and is frequently detected even in the early stages in colorectal cancer patients (183, 184). Multiple genes, including *MLH1*, *p16*, *RASSF1A*, and *APC*, are frequently silenced in colorectal cancer by promoter hypermethylation (185). Enhanced understanding of the aberrant methylation patterns in colorectal cancer has shed light on the development of agents that target enzymes responsible for reactivating epigenetically silenced genes. For example, several epigenetic therapeutics have been approved for cancer treatment by the U.S. Food and Drug Administration (FDA), such as DNA methyltransferase (DNMT) inhibitors and histone deacetylase (HDAC) inhibitors (8). However, adverse effects after chronic exposure have hindered their use in chemoprevention (186). By contrast, multiple lines of evidence have suggested that dietary and environmental factors may be important contributors to cancer development by dynamically modifying the epigenetic landscape (10). Therefore, great effort has been applied to evaluate the capacity of chemopreventive nutritional phytochemicals to alter the profile of adverse epigenetic marks in cancer cells to attenuate tumor growth.

Curcumin (CUR) is the major active component in the golden spice *Curcuma longa* (also known as turmeric). Turmeric has been used as a common food spice for millennia. According to epidemiological reports, the consumption of *Curcuma longa* is associated with lower cancer incidence (187). Accumulating evidence has indicated that CUR may be a potent chemopreventive agent by targeting various molecular signaling pathways involved in carcinogenesis (188). Despite the high safety and tolerability of oral CUR as evidenced in phase I studies, CUR was also found to have low systemic bioavailability

because of rapid metabolism (189). However, it has been suggested that favorable effects of CUR can be achieved through accumulation of CUR and its metabolites in tissues by long-term exposure. Studies of CUR have focused on colorectal diseases (most notably colorectal cancer) because of the preferential distribution of orally administered CUR in the colon mucosa compared with that in other organs (190). Garcea et al. reported that CUR concentration in human colorectal mucosa after oral consumption of up to 3600 mg may be sufficient to obtain pharmacological effects (191). It has been suggested that epigenetic modifications, which are achievable at lower concentrations, may be involved in the mechanism of chemoprevention by CUR. For example, CUR has been reported to regulate the activity of histone acetyltransferase (HAT), HDAC, and, more recently, DNMT in different model systems (192). Recent studies in our laboratory have demonstrated that CUR decreases the CpG methylation of *Nrf2* and *Neurog 1* in murine tramp C1 prostate cancer cells and human LnCap prostate cancer cells, respectively (87, 89). However, few studies have demonstrated the effect of CUR in modulating the CpG hypermethylation of specific tumor suppressor genes related to colorectal cancer. We believe the development of CUR as an epigenetic agent warrants further studies to explore its diversity and efficacy in preventing colorectal cancer.

Deleted in lung and esophageal cancer 1 (*DLEC1*) was initially discovered in 1999 as a candidate tumor suppressor gene in lung, esophageal, and renal cancers (193). *DLEC1* is located at chromosome 3p22-p21.3, a region recognized as a hot spot likely to contain tumor suppressor genes with frequent genetic abnormalities during carcinogenesis, including colorectal cancer (194). Tumor suppressor genes in this region such as *RASSF1* and *BLU* have been found to be frequently silenced by promoter CpG

methylation (195, 196). Similarly, inactivation of *DLEC1* by promoter CpG hypermethylation has been reported in a wide spectrum of cancers, such as lung (197), hepatocellular (198), ovarian (199), renal (200), nasopharyngeal (201), and breast cancers (202). Additionally, these studies have also provided evidence that overexpression of *DLEC1* significantly suppresses the clonogenicity of tumor cells. Recently, Ying et al. demonstrated for the first time that expression of *DLEC1* was decreased and underwent promoter hypermethylation in various colorectal cancer cell lines and primary tumor samples but not in DKO (HCT116 DNMT1-/- DNMT3B-/-) cells, CCD-841 (normal colon epithelial cells), and paired normal tissues (132). To the best of our knowledge, potential epigenetic interventions targeting *DLEC1* using phytochemicals have not been evaluated. Hence, the present study was undertaken to investigate the involvement of *DLEC1* in the chemopreventive effects of CUR in suppressing anchorage-independent growth of HT29 cells. Furthermore, the potential of CUR to restore *DLEC1* expression in HT29 cells through epigenetic mechanisms was evaluated.

3.2 Materials and Methods

3.2.1 Materials

CUR, azadeoxycytidine (5AZA), trichostatin A (TSA), bacteriological agar, puromycin, ethidium bromide, and Basal Medium Eagle (BME) were purchased from Sigma-Aldrich (St. Louis, MO, USA). All the enzymes used in this study were obtained from New England Biolabs Inc. (Ipswich, MA, USA). The Cell Titer 96 Aqueous One Solution Cell Proliferation Assay Kit, the luciferase reporter vector pGL4.15, the pSV-β-

Galactosidase control vector, the luciferase assay system, and the β-Galactosidase enzyme assay system were purchased from Promega (Madison, WI, USA).

3.2.2 Cell culture, cell viability assay, and lentiviral transduction

The human colorectal adenocarcinoma HT29 and SW48 cell line, human colorectal carcinoma HCT116 cell line, and human embryonic kidney HEK293 cell line were obtained from American Type Culture Collection (ATCC, Manassas, VA, USA). HT29 cells, HCT116 cells, and HEK293 cells were routinely maintained in Dulbecco's modified Eagle medium (DMEM; Gibco, Carlsbad, CA, USA) supplemented with 10% fetal bovine serum (FBS; Gibco). SW48 cells were cultured in RPMI-1640 medium (Gibco) with 10% FBS. All the cells were grown at 37°C in a humidified 5% CO_2 atmosphere.

HT29 cells were seeded in 96-well plates at an initial density of 1,000 cells/well for 24 h. The cells were then treated with CUR (1-25 μM) for 5 days. The medium was changed every other day. On day 5, a MTS assay was performed using the Cell Titer 96 Aqueous One Solution Cell Proliferation Assay Kit as described previously (203).

Lentivirus mediated short hairpin RNAs were used to establish stable mock (scramble control, sh-Mock) and DLEC1 knockdown (sh-DLEC1) HT29 cells. The shRNA clone sets were obtained from Genecopoeia (Rockville, MD, USA), and lentiviral transduction was performed according to the manufacturer's manual. After selection in DMEM medium supplemented with 10% FBS and 2 μg/mL puromycin for 3 weeks, the sh-Mock and sh-DLEC1 cells were further used to evaluate the functional role of DLEC1.

To examine the proliferation rate of sh-Mock and sh-DLEC1 HT29 cells, the cells were seeded in 60-mm tissue culture plates at an initial density of 10,000 cells. The cell number was counted and recorded after 24, 48, and 72 h of incubation using a TC20 automated cell counter (Bio-rad, Hercules, CA, USA).

3.2.3 DNA methylation analysis

HT29 cells were plated in 10-cm plates for 24 h and then treated with 0.1% DMSO (control), 2.5 µM 5AZA and 100 nM TSA, or CUR at 2.5 and 5 µM for 5 days. The medium was changed every other day. For the 5AZA and TSA combined treatment, 100 nM TSA was added 20 h before harvest. On day 5, the cells were harvested for further analyses. Genomic DNA was isolated from the treated cells using the QIAamp DNA Mini Kit (Qiagen, Valencia, CA, USA). Next, 750 ng of genomic DNA was subjected to bisulfite conversion using EZ DNA Methylation Gold Kits (Zymo Research Corp., Orange, CA, USA) following the manufacturer's instructions. To obtain products for sequencing, the converted DNA was amplified by PCR using Platinum PCR Taq DNA polymerase (Invitrogen, Carlsbad, CA, USA) using the forward and reverse primers: 5'- CGA AGA TAT AAA TGT TTA TAA TGA TT-3' and 5'-CAA CTA CAA CCC CAA ATC CTA A-3'. The PCR products were cloned into a pCR4 TOPO vector using the TOPO TA Cloning Kit (Invitrogen), as previously described (26, 87, 89). For each sample, at least 10 clones were randomly selected and sequenced (Genewiz, Piscataway, NJ, USA). The percentage of methylated CpG was calculated as the number of methylated CpG sites over the total number of CpG sites examined.

Methylation-specific PCR (MSP) was performed on bisulfite-converted genomic DNA. The primer sequences for the methylated reactions were 5'-GAT TAT AGC GAT GAC GGG ATT C-3' (forward) and 5'- ACC GGA CTA ATA ACG AAA TTA ACG-3' (reverse), and the primer sequences for the unmethylated reactions were 5'- TGA TTA TAG TGA TGA TGG GAT TTG A-3' (forward) and 5'-CCC AAC TAA TAA CAA AAT TAA CAC C-3' (reverse). The amplification products were separated by agarose gel electrophoresis and visualized by ethidium bromide staining using a Gel Documentation 2000 system (Bio-Rad, Hercules, CA, USA). The bands were semi-quantitated by densitometry using ImageJ (Version 1.48d; NIH, Bethesda, Maryland, USA).

To verify the DNA methylation changes, methylated DNA was captured and quantified using methylated DNA immunoprecipitation coupled with quantitative real-time polymerase chain reaction analysis (MeDIP-qPCR) as described previously (28, 30). Briefly, extracted DNA from treated HT29 cells was sheared in ice-cold water using a Bioruptor sonicator (Diagenode Inc., Sparta, NJ, USA) to approximately 200-1000 base pair. The fragmented DNA was further denatured at 95 °C for 2 min. Methylated DNA was isolated by immunoprecipitation with anti-5'-methylcytosine antibody using Methylamp Methylated DNA capture Kit (Epigentek, Farmingdale, NY, USA) according to the manufacturer's manual. After final purification and elution, the methylation status was quantified by qPCR amplification of MeDIP-enriched DNA using the primer set 5'-AAA CGC GGA GGT CTT AGC-3' (forward) and 5'- GCA GAC GAA GCA GCT GAG -3' (reverse). The enrichment of methylated DNA in each treatment was calculated according to the standard curve of the serial dilution of input DNA. The relative

methylated DNA ratios were then calculated with the basis of the control as 100% of DNA methylation.

3.2.4 RNA isolation and qPCR

Total RNA was extracted from the treated HT29 cells using the RNeasy Mini Kit (Qiagen, Valencia, CA, USA) and reverse-transcribed to cDNA using the SuperScript III First-Strand Synthesis System (Invitrogen, Carlsbad, CA, USA). Relative *DLEC1* mRNA expression was determined by qPCR using cDNA as the template and the Power SYBR Green PCR Master Mix (Applied Biosystems, Carlsbad, CA, USA) in an ABI7900HT system (Applied Biosystems). The forward and reverse primers for *DLEC1* amplification were 5'- CGA ACC CTT CGC CTG AAT AA-3' and 5'- GGG AAA GGT GGC CCA TAA A-3', respectively. Primers for *GAPDH* (internal control) were 5'- GGT GTG AAC CAT GAG AAG TAT GA-3' (forward) and 5'-GAG TCC TTC CAC GAT ACC AAA G-3' (reverse).

3.2.5 Protein lysate preparation and western blotting

Protein lysates were prepared using radioimmunoprecipitation assay (RIPA) buffer (Sigma-Aldrich St. Louis, MO, USA) supplemented with protein inhibitor cocktail (Sigma-Aldrich). The detailed procedure for western blotting was previously described (93). Briefly, 20 μg of total protein as determined using the bicinchoninic acid (BCA) method (Pierce, Rockford, IL, USA) was separated by 4-15% SDS polyacrylamide gel

electrophoresis (Bio-Rad, Hercules, CA, USA) and electro-transferred to polyvinylidene difluoride (PVDF) membranes (Millipore, Bedford, MA, USA). After blocking with 5% BSA (Fisher Scientific, Pittsburgh, PA, USA) in Tris-buffered saline-0.1% Tween 20 (TBST) buffer (Boston Bioproducts, Ashland, MA, USA), the membranes were sequentially incubated with specific primary antibodies and horseradish peroxidase-conjugated secondary antibodies. The blots were visualized using Supersignal West Femto chemiluminescent substrate (Pierce, Rockford, IL, USA) and documented using a Gel Documentation 2000 system (Bio-Rad, Hercules, CA, USA). Densitometry of the bands was analyzed using ImageJ (Version 1.48d; NIH). The primary antibodies were obtained from different sources: anti-β-ACTIN from Santa Cruz Biotechnology (Santa Cruz, CA, USA); anti-DNMT1, 3A, and 3B from IMGENEX (San Diego, CA, USA); anti-HDAC1-7 from Cell Signaling Technology (Boston, MA, USA); and anti-HDAC8 from Proteintech (Chicago, IL, USA). The secondary antibodies were purchased from Santa Cruz Biotechnology.

3.2.6 Plasmids, transfection, and luciferase reporter assay

Human *DLEC1* promoter was amplified from genomic DNA isolated from HT29 cells using the following primers: 5'- GAC ACA AAT GTT TAC AAT GAC C-3' (forward) and 5'- TTT CTC AAC TGC AGC CCC AGA T-3' (reverse). The PCR products were cloned into pCR4 TOPO vector using a TOPO TA Cloning kit (Invitrogen, Carlsbad, CA, USA), digested with KpnI and XhoI enzymes, and inserted into pGL4.15 luc2P/Hygro vector using T4 ligase as previously described (26). All the recombinant

plasmids were verified by sequencing (Genewiz, Piscataway, NJ, USA). To further generate the methylated luciferase reporter, the constructs were treated with methyl-transferase M. SssI. Briefly, 5 µg reporter constructs were incubated with 5 units of M. SssI in NEBuffer 2 (New England Biolabs Inc. Ipswich, MA, USA) supplemented with 160 µM S-adenosylmethionine (SAM, New England Biolabs Inc) at 37°C for 1 h. After the reaction, the methylated luciferase reporter plasmids were purified by gel extraction using the QIAquick gel extraction kit (Qiagen, Valencia, CA, USA). The methylation-dependent HhaI and HpaII restriction endonucleases were used to confirm the efficiency of the methylation reaction.

The transfection efficiency using HT29 cells were not optimal, human colon cancer cell lines HCT116, SW48, and human embryonic kidney HEK293 cells with higher transfection efficiency were used. The cells were seeded in 12-well plates for 24 h, then transfected with 500 ng of the methylated or unmethylated reporter plasmids using Lipofectamine 3000 transfection reagent (Invitrogen, Carlsbad, CA, USA) according to manufacturer's instructions. 500 ng of the pSV-β-Galactosidase control vector was co-transfected as internal control. 24 h after the transfection, the cells were lysed in 1X Reporter Lysis Buffer (Promega, Madison, WI, USA). 10 µL aliquiots of the cell lysate were assayed using the luciferase assay system with a Sirius luminometer (Berthold Technologies, Pforzheim, Germany). 30 µL aliquiots were assayed using the β-Galactosidase enzyme assay system and the absorbance was read at 420 nm by Infinite 200 Pro microplate reader (Tecan, Mannedorf, Switzerland). The transcriptional activities of the methylated or unmethylated constructs were calculated by normalizing the

luciferase activities with the corresponding β-Galactosidase activities, and were reported as the folds of induction compared with the activity of the empty pGL 4.15 vector.

3.2.7 Colony formation assay

The colony-formation assay was performed as described previously with some modifications (93, 204). The HT29, sh-Mock, and sh-DLEC1 cells (8×10^3 / well) were transferred to 1 mL of BME containing 0.33% agar over 3 mL of BME containing 0.5% agar with 10% FBS in 6-well plates. The cells were maintained with 0.1% DMSO, 2.5 µM and 5 µM CUR at 37°C in a humidified 5% CO_2 atmosphere for 14 days.

In another set of experiment, the HT29 cells were first treated with control (0.1% DMSO), or CUR at 2.5 and 5 µM for 5 days similar to that described for the DNA methylation assays. On day 5, the pretreated HT29 cells (8×10^3 / well) were transferred to 1 mL of BME containing 0.33% agar over 3 mL of BME containing 0.5% agar with 10% FBS in 6-well plates. The cells were maintained in soft agar without the presence of CUR at 37°C in a humidified 5% CO_2 atmosphere for additional 14 days.

The colonies were photographed using a computerized microscope system with the Nikon ACT-1 program (Version 2.20) and counted using ImageJ (Version 1.48d; NIH).

3.2.8 Statistical Analysis

The data are presented as the mean ± SEM (standard error of the mean). The statistical analyses were performed using Student's t-test. P values less than 0.05 were considered statistically significant and are indicated with *; P values less than 0.01 are indicated with **.

3.3 Results

3.3.1 CUR suppressed anchorage-independent growth of HT29 cells

To investigate the effect of CUR on the anchorage-independent growth of HT29 cells, the soft agar assay was employed. Firstly, HT29 cells were grown in soft agar containing CUR for 14 days. As illustrated in Figure 7A, colony formation of HT29 cells was significantly reduced by CUR at 2.5 μM and 5 μM by 32.2% and 37.8%, respectively. The cell viability of HT29 cells was not affected by CUR treatment at concentrations of 2.5 μM and 5 μM after 5 days when examined by the MTS assay (Figure 7C). However, a continuous cell counting with trypan blue staining for 14 days revealed that the number of viable cells was significantly reduced by CUR at 5 μM after 12 days (data not shown). To further confirm that the inhibition of colony formation by CUR is not a result from cell death, HT29 cells were pretreated with CUR (2.5 μM and 5 μM) for 5 days before transferred to agar. The pretreated cells were grown in agar for additional 14 days without the presence of CUR. As shown in Figure 7B, although the suppression of colony size by CUR pretreatment is not as pronounced as when CUR is

present in agar medium, HT29 cells pretreated with CUR resulted in a significant reduced

colony number in a similar trend. These results indicated that CUR inhibits the

anchorage-independent growth of HT29 cells in soft agar.
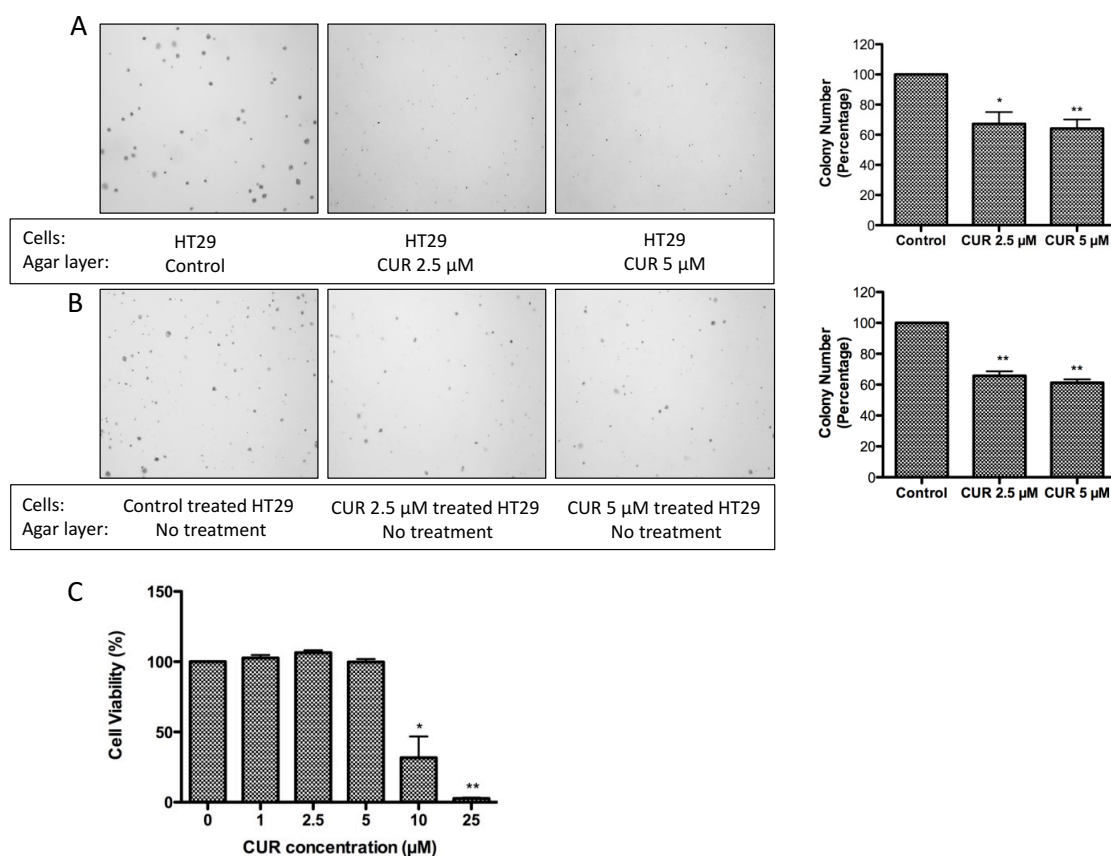
Figure 7: CUR inhibited anchorage-independent growth of HT29 cells.

(A) HT29 cells (8,000 cells/well) were plated in soft agar containing 0.1% DMSO

(Control) and CUR (2.5 μM or 5 μM) in 6-well plates for 14 days. The colonies were

counted under a microscope and analyzed using ImageJ software. The colony number

percentage was calculated by dividing the number of colonies formed in the CUR

treatment groups by the number of colonies formed in the control group. Representative

images of each group under a microscope are shown in the left panel. **(B)** HT29 cells

were firstly treated with 0.1% DMSO (Control) and CUR (2.5 μM or 5 μM) for 5 days. On day 5, pretreated cells (8,000 cells/well) were transferred and grown in agar for additional 14 days without presence of CUR. The colonies were counted under a microscope and analyzed using ImageJ software. The colony number percentage was calculated by dividing the number of colonies formed with pretreated cells by the number of colonies formed in the control group. Representative images of each group under a microscope are shown in the left panel. **(C)** HT29 Cells were plated in 96-well plates at an initial density of 1,000 cells/ well for 24 h. The cells were then incubated in fresh medium with the presence of CUR (1-25 μM) for 5 days. Cell viability was determined by MTS assay.

3.3.2 Knockdown of *DLEC1* reduced the inhibitory effect of CUR against colony formation in HT29 cells

DLEC1 is a candidate tumor suppressor whose overexpression is associated with repression of colony formation in many cancer cell lines (132, 198-201). To investigate whether *DLEC1* plays a critical role in the inhibitory effect of CUR in the anchorage-independent growth of HT29 cells, sh-Mock and sh-DLEC1 cells were established using lentivirus shRNAs vectors. Deficient mRNA expression of *DLEC1* was confirmed in sh-DLEC1 cells by qPCR (Figure 8A). Significantly higher cell proliferation in sh-DLEC1 HT29 cells than in sh-Mock HT29 cells was observed from 24 h to 72 h (Figure 8B). This result was in agreement with previous reports that cells overexpressing DLEC1 grew at a reduced rate (198, 201). Importantly, knockdown of DLEC1 significantly increased the

anchorage-independent growth of HT29-shDLEC1 cells in soft agar by approximately 1.5-fold compared with sh-Mock cells (Figure 8C). Similar to the inhibitory effect in HT29 cells, CUR at the concentrations of 2.5 μM and 5 μM significantly suppressed colony formation of sh-Mock cells by 41% and 45.4%, respectively (Figure 7A and Figure 8C). By contrast, the CUR-mediated inhibition of colony formation was remarkably reduced in sh-DLEC1 cells (Figure 8C and Figure 8D). The inhibition of colony formation by CUR in sh-DLEC1 cells was only approximately 12.8% to 16.4%. These results suggest that DLEC1 played an important role in the CUR-mediated suppression of anchorage-independent growth of HT29 cells.
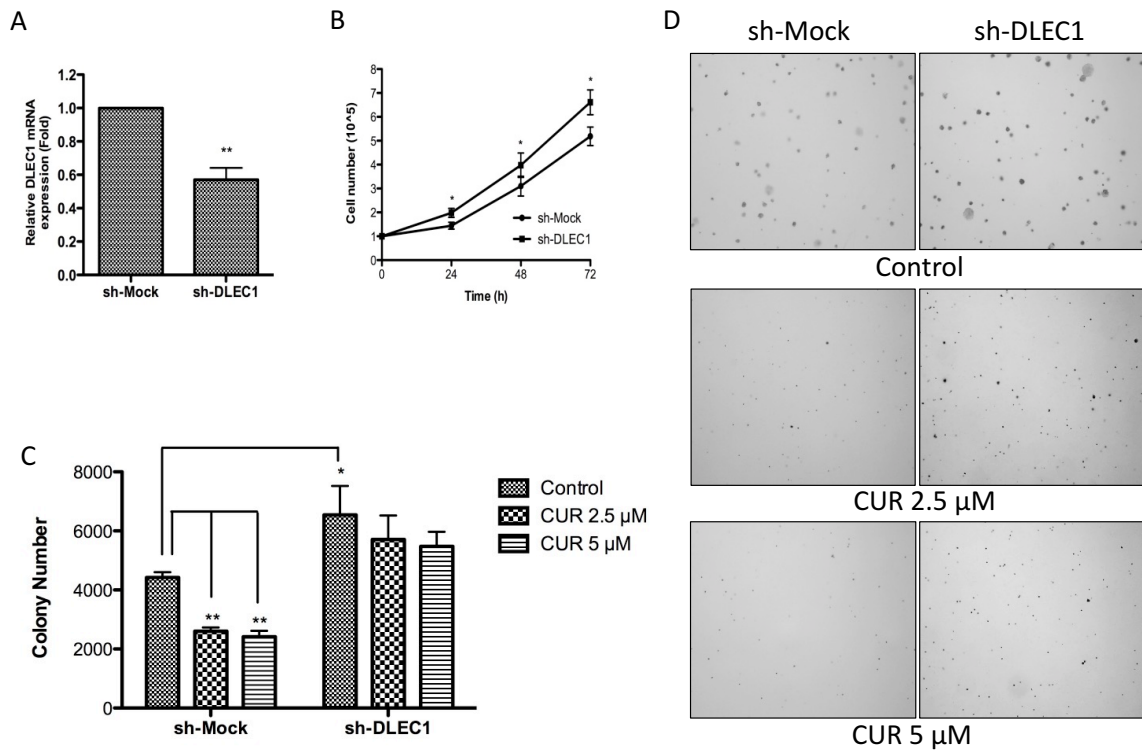
Figure 8: *DLEC1* knockdown increased proliferation and attenuated the inhibitory effects of CUR on the anchorage-independent growth of HT29 cells.

Stable mock (scramble-sequence control, sh-Mock) and DLEC1 knockdown (sh-DLEC1) HT29 cells were established using lenti-virus mediated short hairpin RNAs and were selected with puromycin for 3 weeks. **(A)** Reduced mRNA expression of *DLEC1* in knockdown cells was confirmed by qPCR. **(B)** The growth of HT29 sh-DLEC1 cells was compared with that of sh-Mock cells over a period of 72 h. **(C)** Anchorage-independent growth of sh-Mock and sh-DLEC1 with or without the presence of CUR in soft agar for 14 days. **(D)** Representative images of each group under a microscope.

3.3.3 CUR decreased the methylation of the *DLEC1* promoter in HT29 cells

Considering the role that *DLEC1* played in CUR-mediated inhibition of colony formation in HT29 cells (Figure 8), we further investigated the effect of CUR treatment in regulating *DLEC1* activity. *DLEC1* has been found to be down-regulated in many human colorectal cancer cell lines and colorectal tumors with aberrant hypermethylated promoter regions (132). To test whether CUR treatment could reverse the methylation of the *DLEC1* gene promoter, MSP, bisulfite genomic sequencing, and MeDIP-qPCR were performed. In agreement with previous reports, we found that the methylated MSP gel bands are with higher density than the unmethylated MSP gel bands, indicating that the CpG sites in the promoter of *DLEC1* gene was hypermethylated in HT29 cells (Figure 9A). Sequencing results showed an average of 95.8% methylation in the CpG island (-66 to +516 with translation initiation site designated as +1) in the control sample (data not shown). However, when the cells were treated with 5 μM CUR or a combination of 2.5 μM 5AZA and 100 nM TSA (serving as a positive control as previously described (26,

87, 89, 93)) for 5 days, the density of unmethylated MSP gel bands was significantly increased by approximately 50% (Figure 9A). To further confirm the demethylation effect of CUR observed in MSP, the methylation status of individual CpG site was examined using bisulfite genomic sequencing. The percentage of methylated CpG sites in the CpG island (-66 to +516) was slightly decreased (data not shown). Within this CpG island, the reduction was most significant at CpG sites 10-30 (+15 to +269) after 5 days of treatment with CUR 2.5 µM (p= 0.04) and CUR 5 µM (p=0.005) or a combination of 2.5 µM 5AZA and 100 nM TSA (p=0.004) (Figure 9B). To further quantify the methylation changes by CUR treatment, MeDIP-qPCR analysis was performed. Unlike methods based on bisulfite conversion, MeDIP experiment directly isolates methylated DNA fragments by immunoprecipitation with 5'-methylcytosine-specific antibody. qPCR analysis was then followed to quantitatively measure the enrichment of methylated DNA in the *DLEC1* promoter region. As shown in Figure 9C, 5 µM CUR and the combination of 5AZA/TSA treatment significantly reduced the relative amount of methylated DNA containing *DLEC1* promoter in HT29 cells. Together with the results obtained from MSP and bisulfite genomic sequencing, we showed that CpG methylation of *DLEC1* promoter was decreased by CUR treatment.
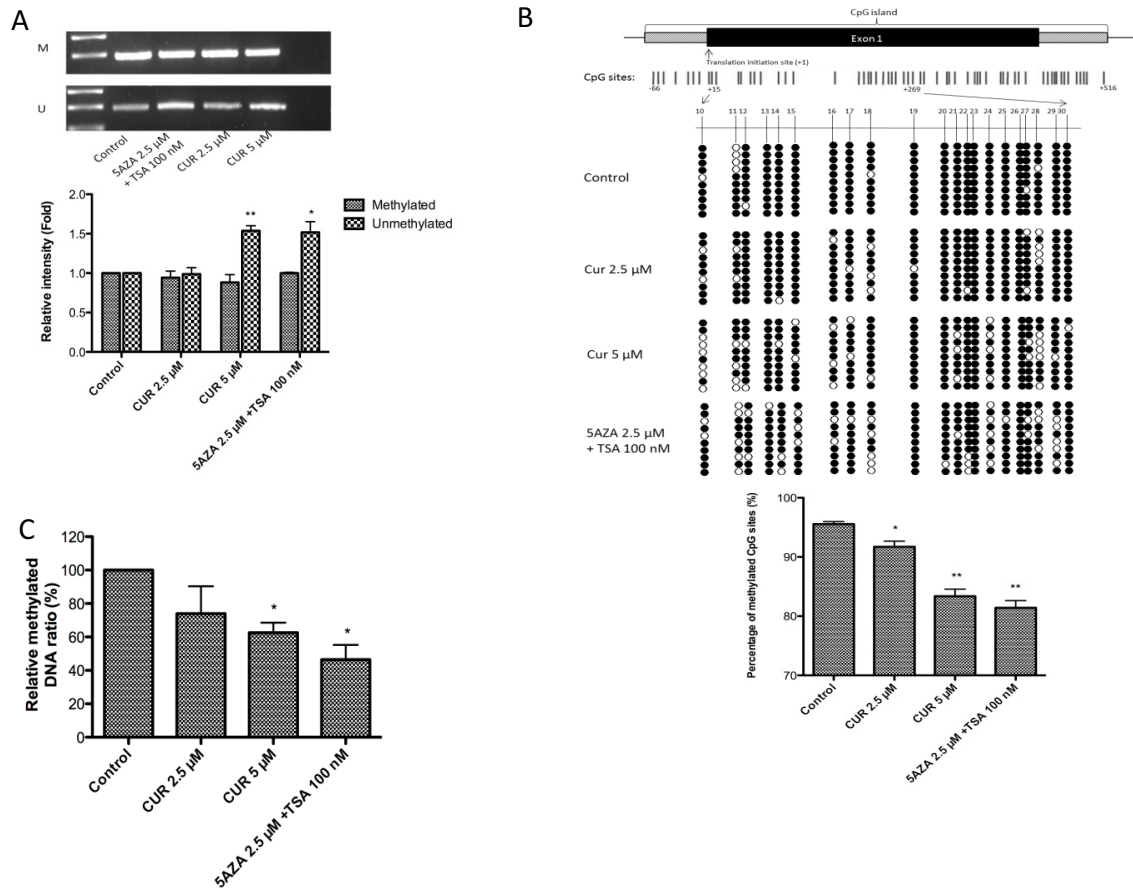
Figure 9: Effects of CUR on CpG methylation in the *DLEC1* promoter region.

HT29 cells (3×10^4 /10-cm dish) were incubated with CUR (2.5 μM and 5 μM) for 5 days. The control group was treated with 0.1% DMSO, and the positive control group was treated with 2.5 μM 5AZA and 100 nM TSA (TSA was added 20 h before harvesting). **(A)** *DLEC1* methylation as measured by methylation-specific PCR (MSP) in HT29 cells after 5 days of treatment. Genomic DNA was extracted, and bisulfite conversion was performed. M: methylated, U: unmethylated. Representative images are presented in the top panel. The relative intensity of the methylated and unmethylated band was measured by ImageJ and presented in the bottom panel. **(B)** The detailed methylation patterns of 10-30 CpGs (+15 to +269) in the promoter regions of the *DLEC1*

gene in HT29 cells were confirmed by bisulfite genomic sequencing. Filled circles indicate methylated CpGs, and empty circles indicate unmethylated CpGs. Ten clones were selected to represent the three independent experiments. The percentage of methylated CpG sites is shown in the bottom panel. The methylation percentage was calculated from three independent experiments as the number of methylated CpG sites over the total number of CpG sites examined. **(C)** The enrichment of the methylated DNA fragments captured by MeDIP was determined by qPCR according to the standard curve from a serial dilution of the inputs. Relative methylatied ratio was calculated by normalizing with control group (defined as 100% methylated DNA).

3.3.4 CUR increased the transcription of *DLEC1* in HT29 cells

It has been reported that down-regulation of *DLEC1* expression is correlated with hypermethylation of the *DLEC1* promoter in various cancer cells and tissues (132, 197-200, 205). In the present study, we constructed a luciferase reporter driven by the *DLEC1* promoter (-66 to +516) to confirm the repression of gene transcription by CpG methylation. *In vitro* CpG methylation of the plasmid by M.sssI CpG methytransferase resulted in a significant decrease in *DLEC1* transcriptional activity by 81.3%, 60.1%, and 51.5% in HCT116, SW48, and HEK293 cell lines, respectively (Figure 10A). Since CUR decreased the methylation of the *DLEC1* promoter in HT29 cells, we hypothesized that the transcriptional activity of the *DLEC1* gene could be enhanced by CUR treatment. qPCR analysis revealed that the mRNA expression of *DLEC1* was significantly induced

in HT29 cells after 5 days of treatment with 5 µM CUR or a combination of 2.5 µM

5AZA and 100 nM TSA (Figure 10B).
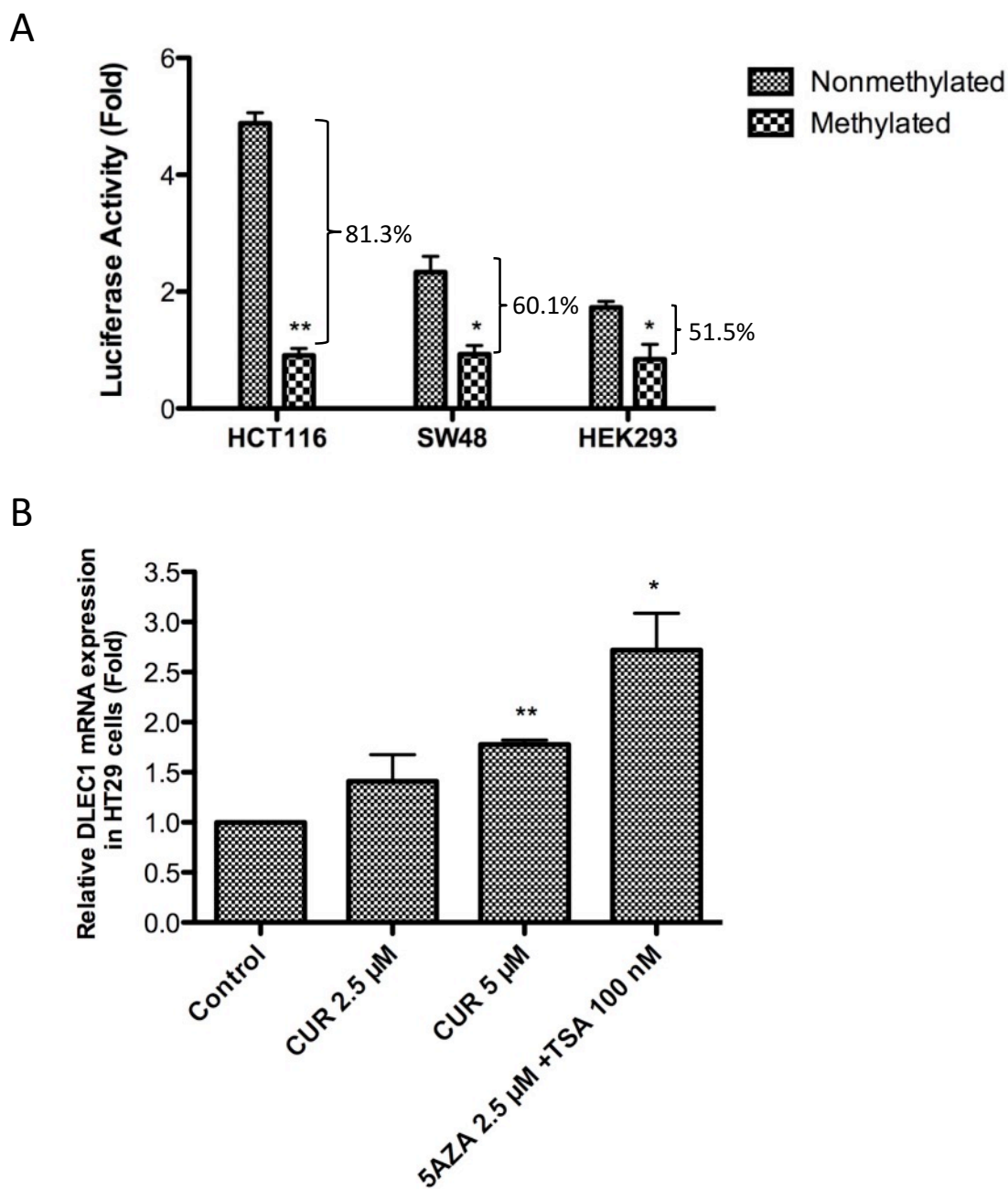
Figure 10: CUR increased the mRNA expression of *DLEC1*.

(A) Methylation of the CpGs inhibited the transcriptional activity of *DLEC1*. The *DLEC1* CpG island (-66 to +516) was amplified from genomic DNA and inserted into pGL4.15 vector. The luciferase reporter construct, either methylated *in vitro* by CpG methyltransferase or not, were co-transfected with β-Galactosidase control vector into several cell lines. And the luciferase activities were measured 24 h post transfection. The luciferase activities were calculated by normalizing the firefly luciferase activities with corresponding β-Galactosidase activities, and are represented as fold change compared with the activity of empty pGL4.15 vector. **(B)** Effect of CUR on the *DLEC1* mRNA expression in HT29 cells. Total mRNA was isolated and analyzed using quantitative real-time PCR.

3.3.5 CUR altered the expression of epigenetic modifying enzymes in HT29 cells

We next examined the effect of CUR on the expression of epigenetic modifying enzymes to explore the epigenetic mechanism by which CUR demethylated the *DLEC1* promoter and increased *DLEC1* transcription. DNA methylation at the 5-position of cytosine through the addition of a methyl group is catalyzed by DNA methyltransferases (DNMTs), including DNMT1, DNMT3A, and DNMT3B (39). As shown in Figure 11, CUR reduced the protein expression of DNMT1, DNMT 3A, and DNMT 3B in a concentration-dependent manner in HT29 cells after 5 days of treatment. In addition, HDAC inhibition activity of CUR was previously reported in a molecular docking study (206). Therefore, western blotting was also performed to evaluate the effect of CUR in modifying the protein expression of HDAC1-8. We found that the protein levels of

HDAC4, HDAC5, HDAC6, and HDAC8 were significantly reduced in a concentration-dependent manner after treatment with CUR for 5 days in HT29 cells, whereas no considerable changes in the protein expression of HDAC1, HDAC2, HDAC3, and HDAC7 were detected (Figure 12). These results suggest that down-regulation of DNMTs and subtypes of HDACs by CUR may result in reduced methylation of *DLEC1* promoter and activation of *DLEC1* transcription in HT29 cells.
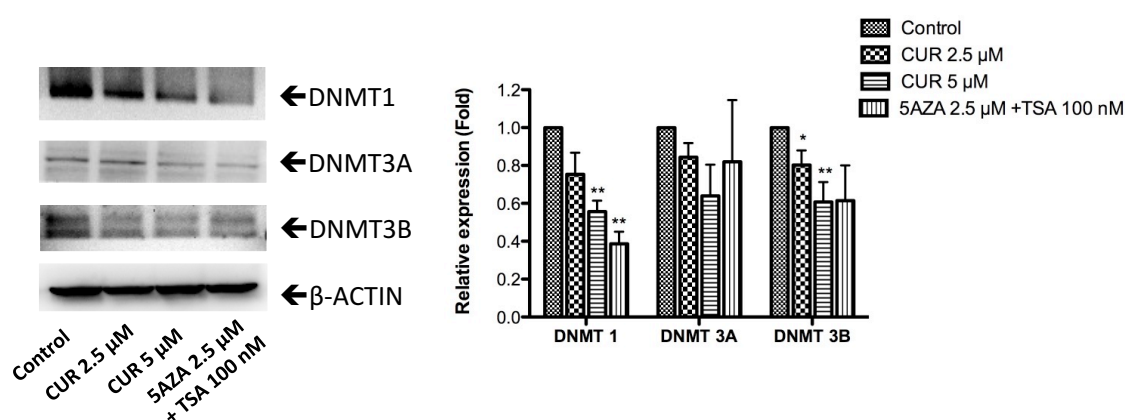
Figure 11: CUR reduced the protein level of DNMTs in HT29 cells.

Proteins were extracted and examined by western blotting. The fold relative expression was calculated by dividing the intensity of each sample by that of the control sample and then normalizing to the intensity of β-actin using ImageJ. Representative bands are shown in the left panel. The bar chart in the right panel presents the mean ± SEM of three independent experiments.
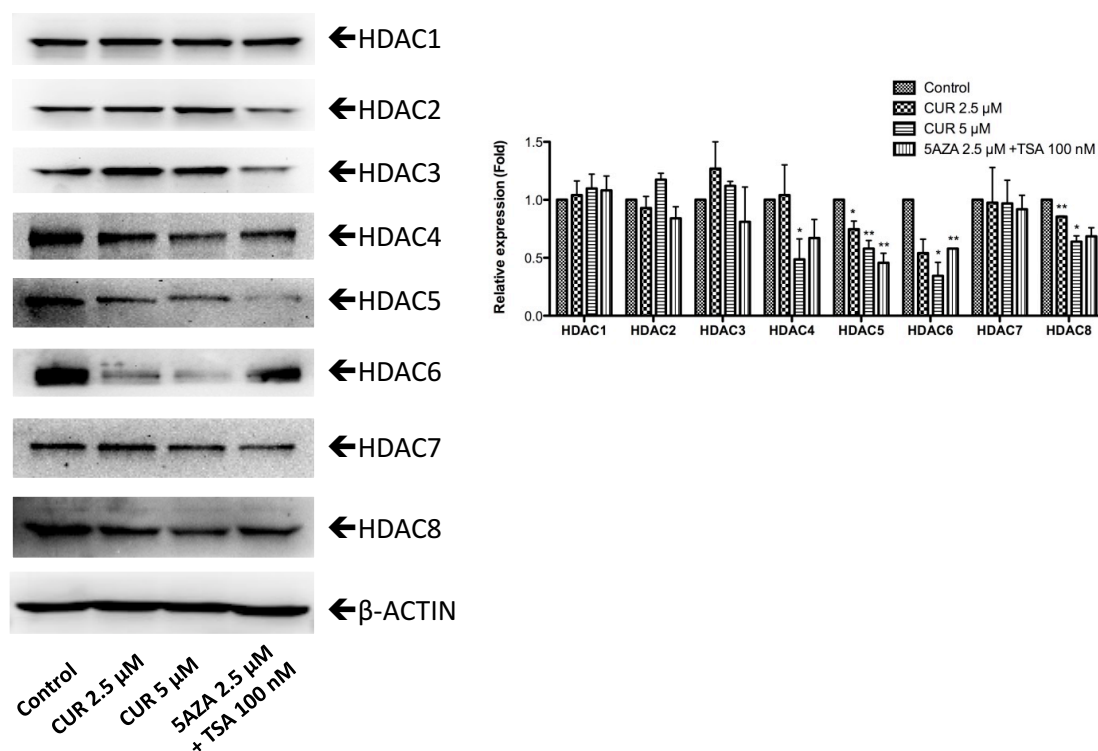
Figure 12: CUR altered the protein level of HDACs in HT29 cells.

Protein expression of HDAC1-8 was measured by western blotting. The fold relative expression was calculated by dividing the intensity of each sample by that of the control sample and then normalizing to the intensity of β-actin using ImageJ. Representative bands are shown in the left panel. The bar chart in the right panel presents the mean ± SEM of three independent experiments.

3.4 Discussion

The tumor-suppressing properties of *DLEC1* have been supported by the observation of tumor-specific reduced transcription and decreased colony formation, in

addition to reduced growth rate, in tumor cells with *DLEC1* exogenous expression (132, 197-200, 205). Moreover, Kwong et al. reported that no tumors formed in nude mice injected with the nasopharyngeal carcinoma cell line HONE1 transfected with *DLEC1* cDNA, whereas tumors with an average size over 200 mm^3 formed in control mice after 55 days (201). However, growth suppression could result from overexpression of any gene; thus, experiments with *DLEC1* knockdown cells are necessary. To further confirm the tumor suppressor role of *DLEC1*, we generated stable DLEC1 knockdown HT29 cells via shRNA expression through lentiviral transduction. We observed a significantly higher proliferation rate (Figure 8B) and enhanced anchorage-independent growth in HT29-shDLEC1 cells compared to HT29-shMock cells (Figure 8C). These observations, together with those of previous reports, demonstrate the tumor suppressor roles of *DLEC1* in colorectal cancer.

Anchorage-independent growth (colony-forming capacity in semisolid medium) is an *in vitro* characteristic of tumorigenic cells and has served as a marker to distinguish transformed cells from normal cells (207). Programmed cell death occurs when non-transformed cells are deprived of attachment for an extended period of time, whereas malignant cells proliferate without attachment to a solid substrate during tumor progression. The anchorage-independent growth of tumor cells has been correlated to their tumorigenic and metastatic potential *in vivo* (208). The potential of suppressing the anchorage-independent growth of cancer cells by numerous phytochemicals, including CUR, has been investigated. Our results (Figure 7A and Figure 7B) are in good agreement with published data supporting that CUR inhibits anchorage-independent growth of colorectal cancer cells (116, 209). Multiple genetic changes such as those

related to the *Myc*, *Notch*, *β-catenin*, and *PI3K/Akt* signaling pathways have been shown to be required for anchorage-independent growth and may be involved in the inhibition of colony formation by chemopreventive agents (210-212). However, the molecular basis for these effects remains complex and poorly understood. Chen et al. reported that CUR inhibited the colony formation of HCT116 cells through down-regulation of the transcription of *Sp-1*, a genetic factor associated with the suppression of anchorage-independent growth in fibrosarcoma cells (209, 213). In our study, inhibition of anchorage-independent growth by CUR was considerably attenuated by the ablation of *DLEC1* expression in HT29 cells (Figure 8C and Figure 8D). Hence, we show for the first time that CUR inhibits the anchorage-independent growth of HT29 cells, at least partially through the modulation of *DLEC1* expression. Since *DLEC1* expression was reported to be associated with cell growth rate and cell cycle (197-200), it is possible that the inhibitory effect of CUR against colony formation of HT29 cells involves cell growth inhibition via *DLEC1*. The involvement of *DLEC1* in the protective role of CUR against colorectal cancer requires further investigation in *in vivo* models.

DLEC1 encodes a 1755-amino-acid protein with no significant homology to any known protein or domains, but contains 27 potential casein kinase II (CK2) phosphorylation sites (193). CK2 regulates the phosphorylation of more than 300 important substrates, and one-third of them are implicated in cell division and the cell cycle. Recently, CK2α (subunit α) was shown to be associated with the malignant transformation of several tissues, including colorectal cancer (214). Based on the finding that ectopic expression of *DLEC1* induced G1 arrest of the hepatocellular carcinoma cell, Qiu et al. proposed that phosphorylation of DLEC1 by CK2 facilitates its nuclear

localization and causes G1 arrest (198). Notably, adhesion of integrin receptors to the extracellular matrix is required for attachment-dependent cells to transit through the G1 phase (211). Thus, the potential involvement of CK2, DLEC1, and G1 cell cycle arrest in the inhibitory effect of CUR on the anchorage-independent growth of HT29 cells should be examined in the future.

CUR is a multi-targeting chemopreventive phytochemical that has been studied extensively in colorectal cancer. Recent studies have recognized the effect of CUR in modifying epigenetic mechanisms. For example, using DNA promoter methylation microarrays and gene expression arrays, Link et al. assessed global methylation and the gene expression profiles in colorectal cancer cells upon CUR treatment (116). Interestingly, the results indicated that CUR modulates gene-specific DNA methylation, whereas the global hypomethylation induced by 5AZA is non-specific. However, data regarding the ability of CUR to regulate the methylation levels of specific genes in colorectal cancer are relatively scarce. Our present study provides evidence that CUR decreases the CpG methylation of the *DLEC1* promoter (Figure 9), which regulates a tumor suppressor gene potentially involved in the anchorage-independent growth of HT29 cells. Consequently, we revealed elevated mRNA expression of *DLEC1* after CUR treatment (Figure 10B), which may be mediated by reduced CpG methylation in the *DLEC1* promoter (Figure 9). Moreover, our results suggest that this demethylation effect may be associated with CUR-mediated inhibition of the protein expression of all subtypes of DNMTs in HT29 cells (Figure 11). Similarly, the importance of DNMT expression in regulating the methylation level and transcriptional activity of *DLEC1* was demonstrated by Ying et al., who showed that the hypermethylated *DLEC1* promoter and down-

regulated *DLEC1* transcription were demethylated and reactivated, respectively, only in HCT116 DKO (deficient in DNMT1 and DNMT3B) cells and not in DNMT1KO or DNMT3BKO cells (132). This finding reflected that the combination of DNMT1 and DNMT3B, but not a specific DNMT, may be crucial for regulating *DLEC1* promoter methylation and transcription. However, the effects of CUR in modulating the expression of DNMTs remain controversial. For example, Liu et al. used a molecular docking approach to suggest that CUR inhibits DNMT1 through covalent binding to the catalytic thiolate of C1226 in DNMT1 (215), whereas little or no alteration of the expression of DNMTs upon CUR treatment was observed in colorectal cancer cells (the specific cell type was not provided) (116) and LnCap cells (89). Here, we clearly showed that CUR reduced the protein expression of DNMT1, DNMT3A, and DNMT3B (the inhibitory effect of DNMT3A was not statistically significant) in a concentration-dependent manner in HT29 cells after 5 days of treatment (Figure 11).

In addition to DNA methylation, deacetylation of histone H3 and H4 at the *DLEC1* promoter may be involved in the epigenetic regulation of *DLEC1* in human ovarian cancer and nasopharyngeal cancer cells (199, 201). Thus, histone modification may also contribute to the regulation of transcriptional activity of *DLEC1*. Molecular docking studies predicted that CUR is a potential HDAC inhibitor (206). Lee et al. reported that total HDAC activity was blocked by CUR treatment in medulloblastoma cells, although HDAC4 was the only HDAC subtype with decreased protein expression (216). Similarly, the effect of CUR in inhibiting HDAC activity in myeloproliferative neoplasm cells was documented as a result of the reduced protein level of HDAC8 (217). In the present study, we found that CUR significantly reduced the protein expression of HDAC4, HDAC5,

HDAC6, and HDAC8 in HT29 cells (Figure 12), possibly resulting in impaired HDAC activity after CUR treatment. Although the exact mechanism of how CUR activates the transcription of *DLEC1* requires further investigation, our results, together with previously reported evidence, suggest that CUR may epigenetically regulate the transcriptional activity of *DLEC1* through alterations of DNMTs and HDACs.

3.5 Conclusion

In conclusion, our present study confirmed the tumor suppressor role of *DLEC1* and suggested the involvement of *DLEC1* in the suppression of anchorage-independent growth of HT29 cells by CUR treatment. Furthermore, we demonstrated that CUR could epigenetically up-regulate *DLEC1* and reducing CpG methylation in HT29 cells, an activity that may be associated with lower protein expression of DNMTs and HDACs. Collectively, we propose a new mechanism underlying the chemopreventive effect of CUR in attenuating the clonogenicity of HT29 cells: the epigenetic regulation of *DLEC1* expression and modification of the protein expression of DNMTs and HDACs. These findings provide valuable information for the future development of CUR and other phytochemicals as epigenetic modulators for preventing colorectal cancer.

4. CHAPTER FOUR

The epigenetic effects of aspirin: the modification of histone H3 lysine 27 acetylation in the prevention of colon carcinogenesis in azoxymethane- and dextran sulfate sodium-treated CF-1 mice [7,8]

4.1 Introduction

Colorectal cancer (CRC) is the third most commonly diagnosed cancer and the third most common cause of cancer death among men and women. It is estimated that 132,700 new cases of CRC will be diagnosed in 2015, and 49,700 patients will die from this disease in 2015 (218). Inflammatory bowel disease (IBD) is one of the top high-risk conditions for CRC, together with hereditary familial adenomatous polyposis syndromes and hereditary nonpolyposis colon cancer syndrome (219). In fact, the risk of developing CRC among patients with IBD (including ulcerative colitis and Crohn's disease) was approximately 2- to 3-fold greater than that in healthy adults (220), indicating a strong association between chronic inflammation and CRC. To investigate the molecular mechanisms that underlie colitis-accelerated colon carcinogenesis (CAC) and to develop effective chemoprevention strategies, azoxymethane (AOM)-initiated and dextran sulfate

---

sodium (DSS)-promoted mouse models were established, and these models are widely used today. AOM is a classic chemical carcinogen used to induce aberrant crypt foci by causing DNA damage in the liver and colon (221), and DSS is an inflammatory stimulus that damages the epithelial lining of the colon and induces colitis (222). When AOM injection (initiation factors) is followed by DSS in drinking water (promotion factors), CAC is induced similar to the multistep carcinogenesis process in humans. This reliable, reproducible, and clinically relevant animal model is a useful tool to simulate the pathogenesis observed in patients with inflammatory CRC and recapitulates many histopathological features of human CRC (223).

The development of CAC is likely multifaceted and involves the accumulation of both genetic and epigenetic alterations (224). Epigenetic modifications, the heritable transcription alterations that do not include changes in DNA sequence, have been implicated in the regulation of gene expression in both normal and cancerous tissue, thereby controlling the transformation from normal epithelium into adenocarcinoma in CRC (5). The covalent modifications of specific residues in the N-terminal tails of the histones, dynamically regulate the transition between heterochromatin (a tightly packed structure with gene repression) and euchromatin (a loosely packed structure with gene activation) (225). Lysine acetylation generally opens the chromatin, increases the accessibility of transcriptional factors to chromatin, and activates gene transcription, whereas deacetylated histone is often associated with gene repression (46). Several lines of evidence have observed differential patterns of histone acetylation in IBD animal models (226, 227), and alterations of histone H3 lysine 27 acetylation (H3K27ac) were observed in patients with sporadic colon cancer (228). However, the alteration of

H3K27ac in the regulation of the inflammatory network during CAC has not yet been investigated.

Histone acetylation is a reversible modification that is dynamically mediated by the epigenetic enzymes histone acetyltransferases (HATs) and histone deacetylases (HDACs), which add and remove acetyl groups, respectively. Of all the epigenetic enzymes, HDACs are perhaps the most extensively characterized epigenetic proteins in chronic inflammatory diseases and CRC. Abnormalities of the expression and activity of HDACs can lead to histone hyperacetylation or histone hypoacetylation, thereby altering the expression of key genes in cancer and inflammation (229). Emerging evidence from *in vitro* cell lines and *in vivo* models of IBD and inflammation-driven tumorigenesis has suggested that the inhibition of HDAC represents a novel therapeutic strategy for CRC (226, 230). Notably, several HDAC inhibitors, including vorinostat, romidepsin, and panobinstat, have been approved by the US Food and Drug Administration (FDA) to treat hematopoietic tumors. Moreover, an increasing number of HDAC inhibitors are currently being evaluated in clinical trials to treat various cancer types. However, some epigenetic agents are toxic. The discovery and development of more specific and safer agents to prevent CRC by targeting HDACs are needed.

Acetylsalicylic acid, also known as aspirin (ASA), is one of the most widely used drugs in the world, particularly for the prevention of cardiovascular diseases. Compelling findings from epidemiological studies, clinical trials, and laboratory data have indicated that ASA can protect against CRC (231). Case-control studies revealed that regular ASA users have a statistically significant lower risk of developing sporadic CRC (OR = 0.62) compared with non-users (232). In addition to preventing sporadic CRC, the effect of

ASA has been evaluated in hereditary CRC. It was found that long-term ASA use (600 mg/day for a mean of 25 months) reduce cancer incidence in carriers of hereditary CRC (233). The use of ASA was also shown to be associated with lower risk of CRC in patients with chronic ulcerative colitis (OR = 0.3) (234). Moreover, preclinical animal models have been used to investigate the mechanisms underlying chemopreventive effect of ASA. Recently, ASA at 200 mg/kg (body weight) for 80 days was found to induce apoptosis in AOM/DSS-induced Balb/c mice by inhibiting IL6-STAT3 pathway, although tumor multiplicity was not significantly changed (235). Thus, we aim to determine if longer exposure (20 wks) of ASA would prevent the carcinogenesis in AOM/DSS-induced CF-1 mice.

The well-characterized mechanism of ASA's action is the modification of the COX enzymes. It has been reported that COX-2-derived prostaglandins played an essential role in tumorigenesis in hereditary and sporadic CRC in which proinflammatory cytokines are not strongly expressed (236). However, studies showed that tumor formation in the AOM/DSS model may not be COX-2 dependent, suggesting that cyclooxygenase-derived prostanoids does not play a major role in inflammatory CRC (236). Notably, although clinical evidence has indicated that regular ASA use reduces the risk of CRC exclusively in individuals with overexpressed COX-2 (237), the effect of low-dose ASA on the activity of COX-2 is marginal (231). Thus, the elucidation of COX-2-independent pathways underlying the effect of ASA in preventing inflammatory CRC is needed. A few recent studies have suggested that epigenetic events are involved in the action of ASA and other non-steroidal anti-inflammatory drugs (NSAIDs) with regard to cancer prevention (238). Hence, the present study investigated the epigenetic effects of

ASA, particularly the modulation of HDACs and H3K27ac, regarding the suppression of inflammatory responses and the prevention of CAC using an AOM/DSS-induced mouse model.

4.2 Materials and Methods

4.2.1 Animals, chemicals, and diets

Male CF-1 mice were purchased from Charles River Laboratory (Wilmington, MA, USA). AOM, hematoxylin, and eosin were obtained from Sigma-Aldrich (St Louis, MO, USA). DSS (MW: 36 000-50 000) was purchased from MP Biomedicals (Solon, OH, USA). ASA was purchased from Sigma-Aldrich and blended with AIN-93M rodent diet at the ratio of 0.02% (w/w) by Research Diet Inc. (New Brunswick, NJ, USA).

4.2.2 Animal experimental procedure

All animal experiments were conducted in accordance with the animal protocol approved by the Institutional Animal Care and Use Committee (IACUC) at Rutgers University. Upon arrival, the mice were housed in sterilized cages in a room held at a controlled temperature (20-22°C), with controlled relative humidity (45-55%) and 12-h light-12-h dark cycles at the Rutgers Animal Care Facility. All of the animals had free access to water and diet throughout the experiment. The experimental protocol is summarized in Figure 13A. Briefly, after one week of acclimatization, mice were

randomly assigned to three groups (n = 12) and started AIN-93M diet with or without ASA. One week later, the CF-1 mice (six weeks old) were injected with AOM (10 mg/kg body weight) or the saline (vehicle) subcutaneously at the lower flank. At seven weeks old, the drinking water for the mice in the AOM/DSS and AOM/DSS+ASA groups was replaced with 1.2% DSS (w/v) in distilled water for seven days, after which the fluid was replaced with drinking water until the end of the experiment. The body weight and consumption of food and water were recorded weekly. The mice were humanely sacrificed via CO_2 asphyxiation 20 weeks after AOM injection. Blood was collected by cardiac puncture. At necropsy, the colons were removed, flushed with saline, and opened longitudinally on filter paper. The number of tumors was counted, and the size of the tumors was measured using a caliper ruler. The tumor volume was estimated using the formula V = 0.5 × (length × width × width) as reported by Carlsson et al. (239). After the removal of the proximal end of the colon and tumors, the remaining tissue was cut into two halves along the main axis. The left portion of the colon was fixed in 10% buffered formalin for 24 h, and the right half was snap frozen in dry ice and stored at -80°C for further analysis.

4.2.3 Clinical scoring of colitis

To monitor the general clinical symptoms of acute colitis, the disease activity index (DAI) was calculated by scoring the percent of weight loss, stool consistency, and bleeding during the administration of DSS as described previously (240). Briefly, each parameter was scored on a scale of 0-4, and the summed score of the three parameters

was recorded as the DAI of each mouse. The percent of weight loss was determined as follows: 0 = weight loss < 1%; 1 = 1% ≤ weight loss < 5%; 2 = 5% ≤ weight loss < 10%; 3 = 10% ≤ weight loss < 20%; and 4 = weight loss ≥ 20%. The stool consistency parameter scores were determined as follows: 0 = well-formed stools; 2 = pasty and loose stools; and 4 = diarrhea (liquid form that adheres to the anus). Bleeding scores were determined as follows: 0 = no bleeding; 2 = blood present in the stool; 4 = gross bleeding.

4.2.4 Histopathological analysis

After fixation in the 10% buffered formalin for 24 h, the left half of the colon was dehydrated, embedded in paraffin, sectioned (4 μm), and mounted on glass slides. The sections were stained with hematoxylin and eosin and evaluated by the histopathologist Dr. Guangxun Li. Colonic neoplasms and dysplasia were classified into three categories: a) dysplasia; b) adenoma; and c) adenocarcinoma according to the criteria previously described (241).

4.2.5 Immunohistochemical analysis

Immunohistochemistry staining was performed as previously described (242) using a primary antibody against H3K27ac (Abcam Cambridge, MA, USA) at a 1:500 dilution. The results of the immunohistochemistry staining were acquired using an Aperio Scanscope scanner (Aperio Technologies, Inc., Vista, CA). The percentage of positive nuclei staining was analyzed using ImageScope software (Aperio Technologies).

4.2.6 RNA isolation and quantitative polymerase chain reaction (qPCR)

Total RNA was extracted from snap-frozen precancerous colonic mucosa using the AllPrep DNA/RNA Mini Kit (Qiagen, Valencia, CA, USA). First-strand cDNA was synthesized from 1 µg of RNA using TaqMan® Reverse Transcription Reagents (Applied Biosystems, Carlsbad, CA, USA). qPCR analysis was performed in an ABI7900HT system (Applied Biosystems) with SYBR Green PCR Master Mix (Applied Biosystems) using cDNA as the template. The primer sequences for tumor necrosis factor alpha (Tnf-α), inducible nitric oxide synthase (iNos), prostaglandin-endoperoxide synthase 2 (Cox-2), and interleukin 6 (iL6) are provided in Table 9.

Table 9: List of primer sequences for qPCR

Gene	Sense primer	Anti-sense primer
Tnf-α	TTG TCT ACT CCC AGG TTC TCT	GAG GTT GAC TTT CTC CTG GTA TG
iNos	GGA ATC TTG AGC GA GTT GT	CCT CTT GTC TTT GAC CCA GTA G
Cox-2	CGG ACT GGA TTC TAT GGT GAA A	CTT GAA GTG GGT CAG GAT GTA G
Gapdh	AAC AGC AAC TCC CAC TCT TC	CCT GTT GCT GTA GCC GTA TT

4.2.7 Chromatin immunoprecipitation assay (ChIP)

The ChIP assay was performed using the MAGnify^{TM} Chromatin Immunoprecipitation System (ThermoFisher Scientific, Waltham, MA, USA) following the manufacturer's instructions. Briefly, chromatin sample was prepared from approximately 50 mg of snap-frozen non-cancerous colonic tissue and sheared to an average length of 200–500 bp via sonication at 4°C using a Bioruptor sonicator (Diagenode Inc., Sparta, NJ, USA). The diluted chromatin solution was immunoprecipitated with 2 µg of anti-H3K27ac antibody (Abcam) or mouse IgG. After washing, cross-link reversal, DNA elution, and DNA purification, the relative amount of immunoprecipitated DNA was quantified via qPCR using the primers listed in Table 10. The enrichment of the precipitated DNA was calibrated using the standard curve from the serial dilution of the inputs, and the data were presented as the fold changes in the signal-to-input ratio normalized to the control.

Table 10: List of primer sequences for ChIP-qPCR

Gene	Sense primer	Anti-sense primer
Tnf-α	CAC ACA CAC CCT CCT GAT TG	TCG GTT TCT TCT CCA TCG C
iNos	CAT GCC ATG TGT GAA TGC TTT A	AGC CTG GTC TAC AGA GTA AGT

Cox-2	GAG CAG CGA GCA CGT CA	TCC AGT GGG GGC CTA AA

4.2.8 Western blotting

Protein sample was isolated from snap-frozen non-cancerous colonic mucosa using radioimmunoprecipitation assay (RIPA) buffer (Cell Signaling Technology, Boston, MA, USA). After homogenization by passing through the syringe with a 21G needle 10 times, resting, and sonication at 4°C, the lysates were cleared via centrifugation at 14,000 g for 10 min at 4°C. The supernatants were collected and quantified using the Pierce™ BCA protein assay kit (ThermoFisher Scientific). Next, 20 μg of total protein was diluted with Laemmli's SDS sample buffer (Boston Bioproducts, Ashland, MA, USA) and denatured at 90°C for 5 min. Then, western blotting was performed as described previously (243). The antibodies were obtained from Cell Signaling Technology (HDAC 1, 2, 3, and 4), Santa Cruz Biotechnology (Santa Cruz, CA, USA, iNOS, β-ACTIN, and all of the secondary antibodies), and Abcam (COX-2 and HDAC5). The protein bands were visualized using the SuperSignal™ West Femto Maximum Sensitivity Substrate (ThermoFisher Scientific) with the Gel Documentation 2000 system (Bio-Rad, Hercules, CA, USA). The relative protein expression was semi-quantitated via densitometry using ImageJ (Version 1.48d; NIH) and presented as fold changes by calculating the density of each sample compared with the control sample and then normalized to the intensity of β-ACTIN.

4.2.9 Enzyme-linked immunosorbent assay (ELISA)

The Tnf-α and iL6 level was determined using the protein lysate as prepared in western blotting and plasma using the Mouse Tnf-α and iL6 ELISA kit (ThermoFisher Scientific), respectively, according to the manufacturer's protocol. The level of Tnf-α and iL-6 (pg/mg) was calculated by dividing the concentration of the total protein (mg/mL) by the concentration of Tnf-α and iL-6 (pg/mL).

4.2.10 HDAC activity assay

The HDAC activity in non-cancerous colonic tissue was determined using an Epigenase HDAC Activity/Inhibition Direct Assay Kit (Epigentek, Farmingdale, NY, USA) following the manufacturer's instruction. The nuclear extract was prepared from snap-frozen colonic mucosa using NE-PER^{TM} Nuclear and Cytoplasmic Protein Extraction Reagents (ThermoFisher Scientific) and quantitated. The relative HDAC activity was calculated as the ratio of the HDAC activity of the AOM/DSS- or AOM/DSS+ASA group compared with that of the control group.

4.2.11 Statistical analysis

The data are presented as mean ± SEM. One-way ANOVA with Tukey's multiple comparison tests were used to test comparisons among multiple groups, and two-tailed

Student's t-tests were employed for simple comparisons between two groups. A P-value of less than 0.05 was regarded as significant.

4.3 Results

4.3.1 ASA at the dose of 0.02% attenuates AOM/DSS-induced acute colitis and colon tumorigenesis in CF-1 mice

DSS treatment after AOM injection was used to induce acute colitis. The clinical severity of colitis was estimated by assessing the DAI from day 0 to day 7 during the DSS treatment. The DAI has been widely used as an estimator of colitis severity and is associated with the presence of erosions and inflammation (244). As Figure 13B shows, the DAI score in the AOM/DSS group was increased gradually, but AOM/DSS+ASA slightly attenuated the increase in DAI starting at day 3, and the inhibition was significant at day 7. This result suggests that ASA protects against DSS-induced acute colitis. The effect of ASA in AOM/DSS-induced colon tumorigenesis was examined 20 weeks after AOM injection. As shown in Figure 13D, 7 of the 12 animals in the AOM/DSS group showed tumor growth in the colon, and the tumor multiplicity was 6.5 ± 2.7 tumors per mouse. This finding is comparable with that of previous publication with a similar experimental design in CF-1 mice (241). The dietary supplementation of 0.02% ASA for 21 weeks resulted in only 2 of the 12 mice showing tumor growth and a significantly lower tumor multiplicity (0.2 ± 0.1 tumors per mouse; Figure 13D). However, the tumor volume was only slightly reduced by AOM/DSS+ASA (13.7 ± 1.6 mm^3 in the AOM/DSS group and 9.3 ± 8.2 mm^3 in AOM/DSS+ASA group; $P > 0.05$; Figure 13E), possibly

because of the large variability in the tumors in the AOM/DSS+ASA group due to the limited number of tumors. Weekly monitoring throughout the animal experiments showed no noticeable body weight loss in mice fed with diet supplemented with 0.02% ASA compared with the mice fed the control diet (Figure 13C).
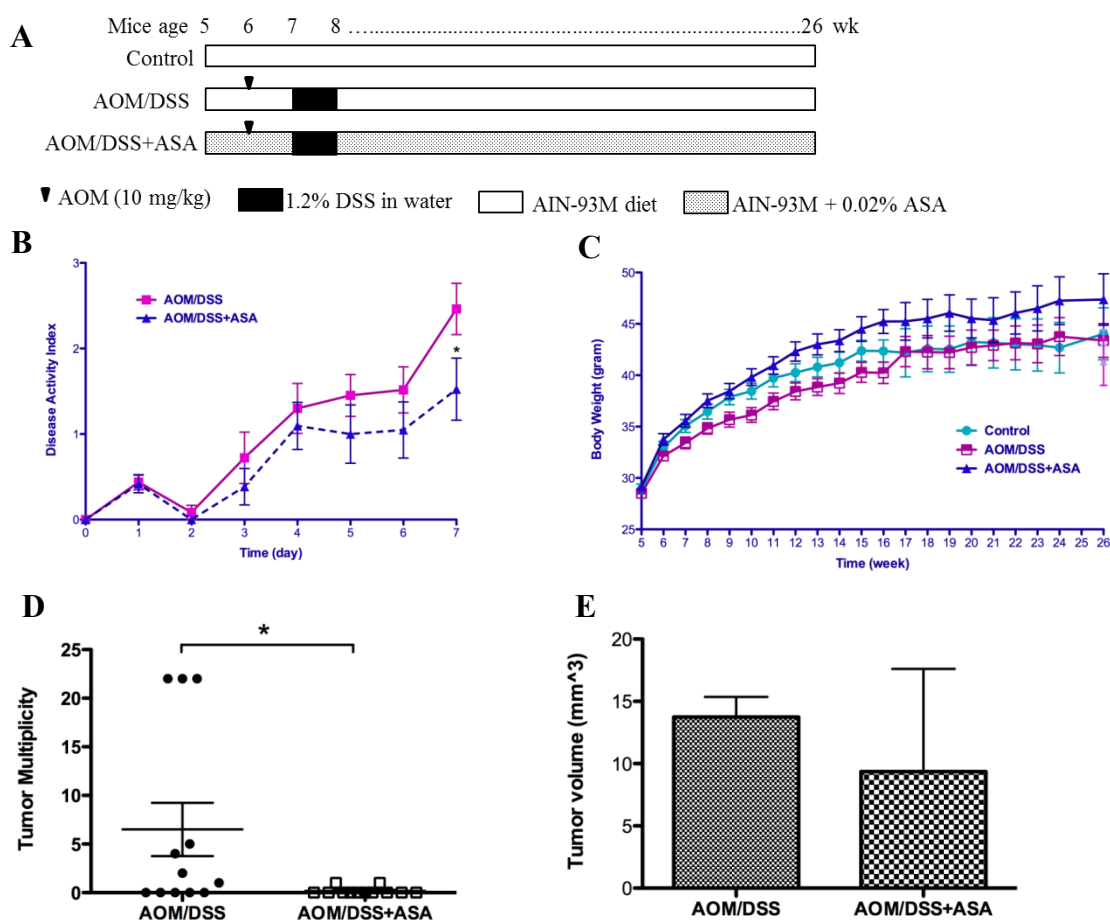
Figure 13: The dietary administration of ASA inhibits CAC in AOM/DSS-induced CF-1 mice.

(A) The experimental protocol for a chemoprevention study with ASA using the AOM/DSS model. **(B)** AOM/DSS+ASA suppressed the elevated DAI starting at day 3 of

DSS administration, and the suppression was significant at day 7. **(C)** The administration of ASA did not cause significant weight loss. **(D)** AOM/DSS+ASA decreased tumor incidence and tumor multiplicity. **(E)** The effect of ASA on tumor volume. * $P < 0.05$ versus AOM/DSS

A histopathologist subsequently examined and characterized the histological alterations using hematoxylin and eosin staining. As shown in Figure 14, AOM/DSS treatment induces severe crypt dysplasia, adenomas, and adenocarcinomas in the colon. The adenomas observed were associated with inflammation, an increased nucleus-to-cytoplasm ratio, nuclear crowding, mitosis, and nuclear hyperchromasia (Figure 14C displays a representative image). Inflammation, leukocyte infiltration into the lumen, nuclear hyperchromasia, nuclear mitosis, and the loss of nuclear polarity with respect to the basement membrane were observed in the adenocarcinomas of AOM/DSS-treated mice (Figure 14D). Administering ASA attenuated inflammation severity and cancer lesions. As Figure 14E-F show, mice in the AOM/DSS+ASA group exhibited normal colon morphology or dysplasia with inflammation.
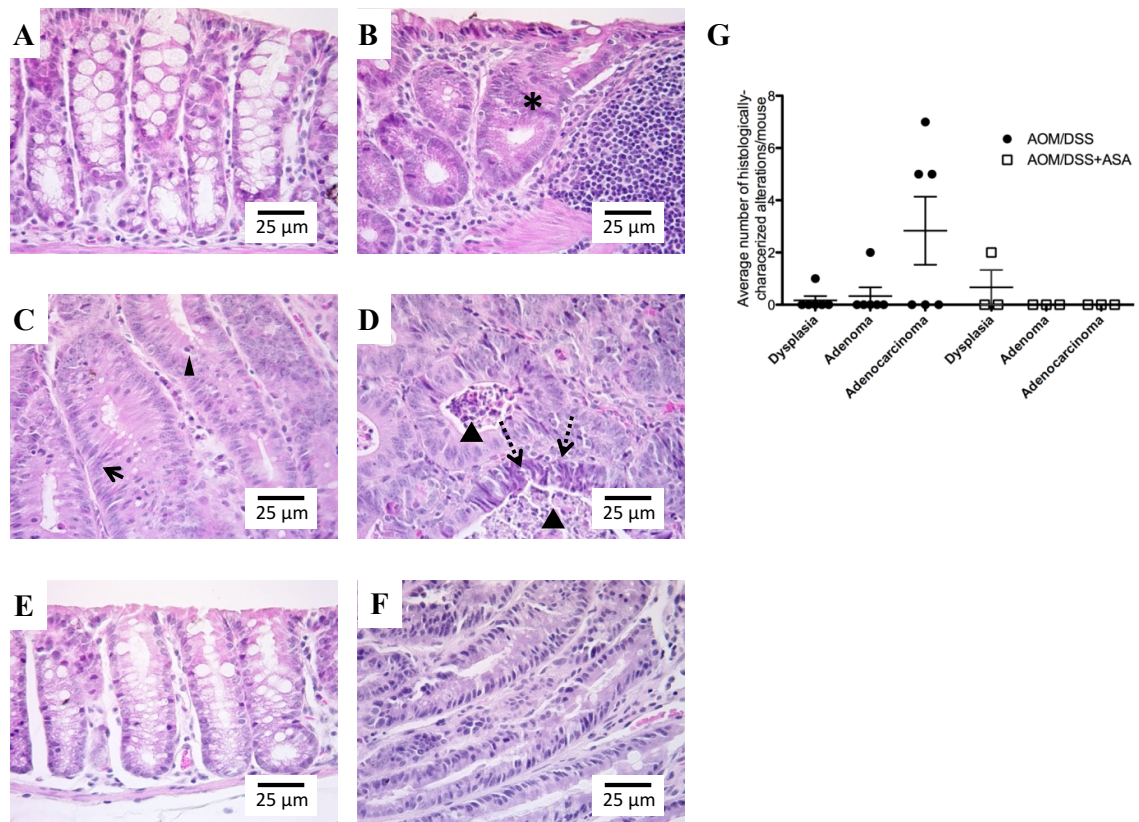
Figure 14: Histologic characterization of colonic tumors and lesions in AOM/DSS-treated CF-1 mice.

Normal mucosa was observed in the mice in the control groups **(A)**. AOM/DSS resulted in crypt dysplasia (black star) with the loss of goblet cells in the crypts **(B)**; adenomas with inflammation, increased nucleus to cytoplasm ratios, nuclear crowding (solid arrow), and mitosis (arrow head) **(C)**; adenocarcinoma with inflammation; leukocytes infiltrated into the diluted lumen (triangle) composed of a pattern of cribriform glands, nucleus hyperchromasia (dotted arrow), and mitosis **(D)**. The colon from AOM/DSS+ASA-treated mice showed attenuated inflammation severity and cancer lesions, normal mucosa **(E)** or dysplasia with inflammation **(F)**. The average number of histologically

characterized alterations, including dysplasia, adenoma, and adenocarcinoma, per mouse are presented **(G)**.

Together, these results demonstrate that dietary feeding of ASA at 0.02% effectively suppresses acute colitis and tumor growth in AOM/DSS-induced CF-1 mice without affecting body weight.

4.3.2 ASA at the dose of 0.02% suppresses AOM/DSS-induced HDAC activity

Emerging evidence has suggested that HDACs are important modulators of the inflammatory response and colon cancer progression (229), and HDAC inhibitors might be a promising therapeutic option in IBD and colon cancer (245, 246). As shown in Figure 15A and B, the protein expression levels of HDAC 1, 2, 3, 4, and 5 are significantly elevated in precancerous colonic tissue from AOM/DSS-treated mice. Accordingly, the HDAC activity was significantly higher in the colonic mucosa of AOM/DSS-treated mice (Figure 15C). AOM/DSS+ASA significantly suppressed the protein expression of HDACs (subtypes 2-5) and HDAC activity compared with the AOM/DSS group (Figure 15A-C). These findings implicated that the activation of the HDACs may be involved in the CAC induced by AOM/DSS and ASA treatment at the dose of 0.02% effectively inhibits HDACs.
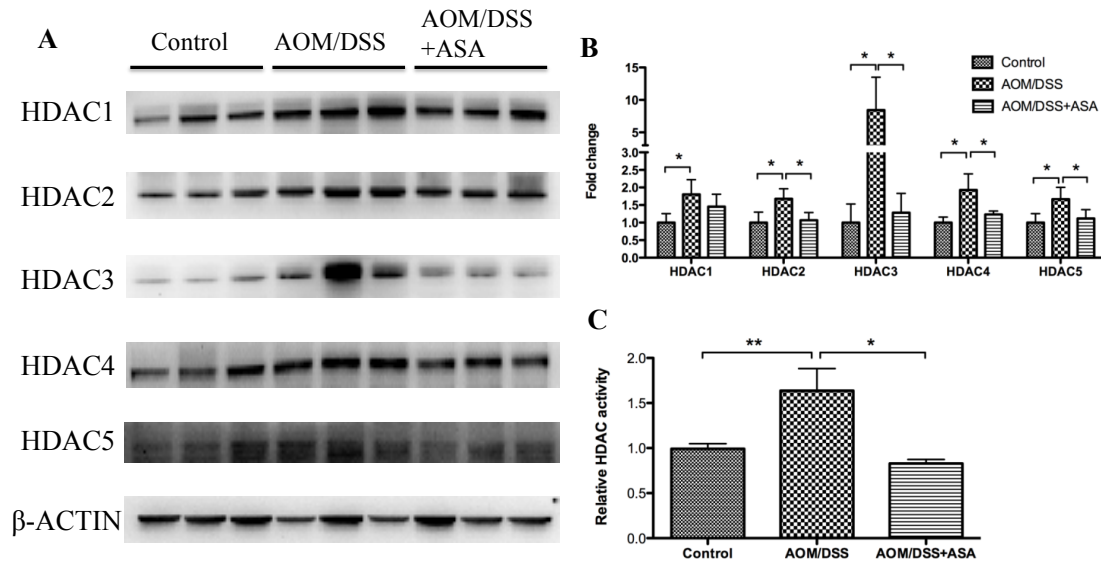
Figure 15: The effect of ASA on the protein expression of HDAC 1-5 and HDAC activity.

Total proteins were extracted and examined via western blotting. AOM/DSS treatment significantly increased the protein expression of HDAC 1-5, whereas AOM/DSS+ASA effectively inhibited the protein expression of HDAC 2-5. Representative bands are shown **(A)**, and the bar graph presents the fold change of the blot density determined by ImageJ **(B)**. Nuclear proteins were extracted and assayed for HDAC activity. AOM/DSS+ASA strongly suppressed significantly elevated HDAC activity in AOM/DSS-treated mice **(C)**. * P < 0.05; ** P < 0.01

4.3.3 AOM/DSS and ASA alter the level of H3K27ac

The activity and expression of HDAC regulate histone acetylation. Immunohistochemical staining was performed to investigate the level of H3K27ac in formalin-fixed paraffin embedded tissues. Although the tissues from all three groups revealed pronounced positive nuclear staining for H3K27ac, the percentage of H3K27ac positive cells analyzed using ImageScope software was dramatically lower in the AOM/DSS-treated mice (Figure 16A-D). AOM/DSS+ASA significantly increased H3K27ac staining compared with AOM/DSS, and the percentage of H3K27ac-positive cells was similar to that of the mice in the control group (Figure 16A-D). These results suggest that the exposure of AOM/DSS diminishes the overall H3K27ac level in the colon, whereas AOM/DSS+ASA restores H3K27ac expression.

Aberrant modifications of H3K27ac at specific genetic regions have been reported in DSS-induced colitis (247). We performed a ChIP-qPCR analysis to investigate the level of H3K27ac in the promoter regions of selective pro-inflammatory genes in non-cancerous colonic tissue. In contrast to reducing the H3K27ac level globally, AOM/DSS treatment increased the enrichment of H3K27ac at the promoters of iNos, Tnf-α, and iL6 by 2.99 ± 0.32, 1.20 ± 0.11, and 1.91 ± 0.18-fold, respectively, compared with the control (Figure 16E-G). AOM/DSS+ASA led to 33.4%, 26.7%, and 39.8% decrease in the H3K27ac level at the promoter regions of iNos, Tnf-α, and iL6, respectively, compared with AOM/DSS (Figure 16E-G). However, the level of H3K27ac at the Cox-2 promoter was not significantly affected by AOM/DSS with or without ASA (Figure 16H).
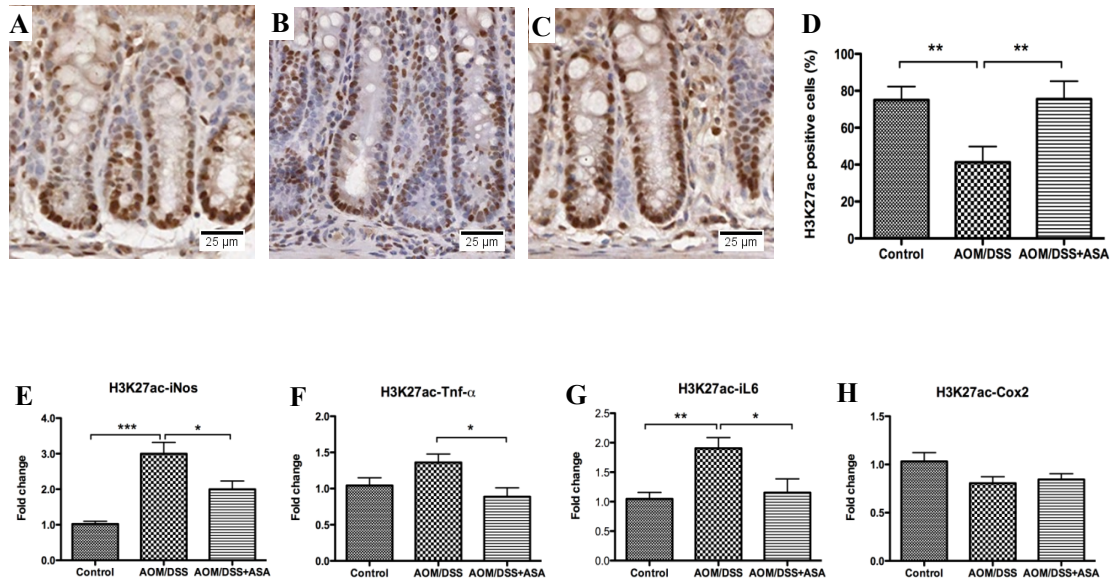
Figure 16: AOM/DSS+ASA counters the AOM/DSS-induced alteration of H3K27ac expression.

The expression of H3K27ac was examined by immunohistochemical staining. Representative images of the control **(A)**, AOM/DSS **(B)**, and AOM/DSS+ASA **(C)** are presented. The percentage of H3K27ac-positive cells was analyzed using ImageScope software, indicating that AOM/DSS significantly suppress nuclear staining, whereas AOM/DSS+ASA restores reduced H3K27ac staining **(D)**. The enrichment of the H3K27ac mark in the promoter regions of selective pro-inflammatory genes was determined using a ChIP-qPCR assay. AOM/DSS+ASA significantly suppressed the increased relative abundance of H3K27ac following AOM/DSS in the promoter regions of iNos **(E)**, Tnf-α **(F)**, and iL6 **(G)**. No significant changes in the H3K27ac level in the Cox-2 promoter were observed **(H)**. * $P < 0.05$; ** $P < 0.01$; *** $P < 0.005$

Our results suggest that AOM/DSS exposure introduces differential patterns of alterations at the global H3K27ac level as well as H3K27ac enrichment at specific loci, whereas AOM/DSS+ASA resulted in the opposite modification of the H3K27ac level compared with AOM/DSS and exhibited similar H3K27ac levels to the control group.

4.3.4 AOM suppresses the AOM/DSS-induced expression of pro-inflammatory genes

The H3K27ac mark is associated with an open chromatin configuration and transcriptional activation (46). Because AOM/DSS treatment in CF-1 mice led to local hyperacetylation at H3K27 in the promoters of iNos, Tnf-α, and iL6 and because AOM/DSS+ASA suppressed this hyperacetylation, we examined whether this modification at the H3K27ac mark influenced the transcription activity of iNos, Tnf-α, and iL6. A qPCR analysis revealed that the mRNA expressions of iNos, Tnf-α, and iL6 were dramatically increased in non-cancerous colonic tissue exposed to AOM/DSS by 55.10 ± 19.06, 3.92 ± 0.22, and 5.59 ± 1.25-fold, respectively, compared with the control (Figure 17A-C). The mRNA expressions of iNos, Tnf-α, and iL6 from AOM/DSS+ASA group were only 1.96 ± 0.61, 1.53 ± 0.29, and 1.77 ± 0.86-fold, respectively, compared with the control, leading to a 96.4%, 61.0%, and 68.3% decreases in the mRNA expressions of iNos, Tnf-α, and iL6, respectively, compared with the AOM/DSS-treated mice (Figure 17A-C). We also examined the protein expressions of iNOS, TNF-α, and iL6 via western blotting and ELISA, respectively. Figure 17E showed that the blotting of iNOS was only detectable in the protein extracted from the AOM/DSS group,

demonstrating that AOM/DSS+ASA reduced the dramatically elevated level of iNOS protein expression. AOM/DSS+ASA significantly decreased the induction of the TNF-α protein level in the AOM/DSS group by 59.9% (Figure 17F). Since the iL6 protein level is below the detection limit in protein lysate (data now shown), we examined the iL6 level in plasma samples instead. As shown in Figure 17G, the dramatically elevated iL6 concentration in AOM/DSS group was significantly decreased in AOM/DSS+ASA group by 80.8%. In accordance with the unchanged H3K27ac abundance in the Cox-2 promoter, neither AOM/DSS nor AOM/DSS+ASA significantly influenced the mRNA and protein levels of Cox-2 (Figure 17D and E). These data demonstrate that AOM/DSS+ASA significantly attenuated the AOM/DSS-induced mRNA and protein expressions of iNos, Tnf-α, and iL6.
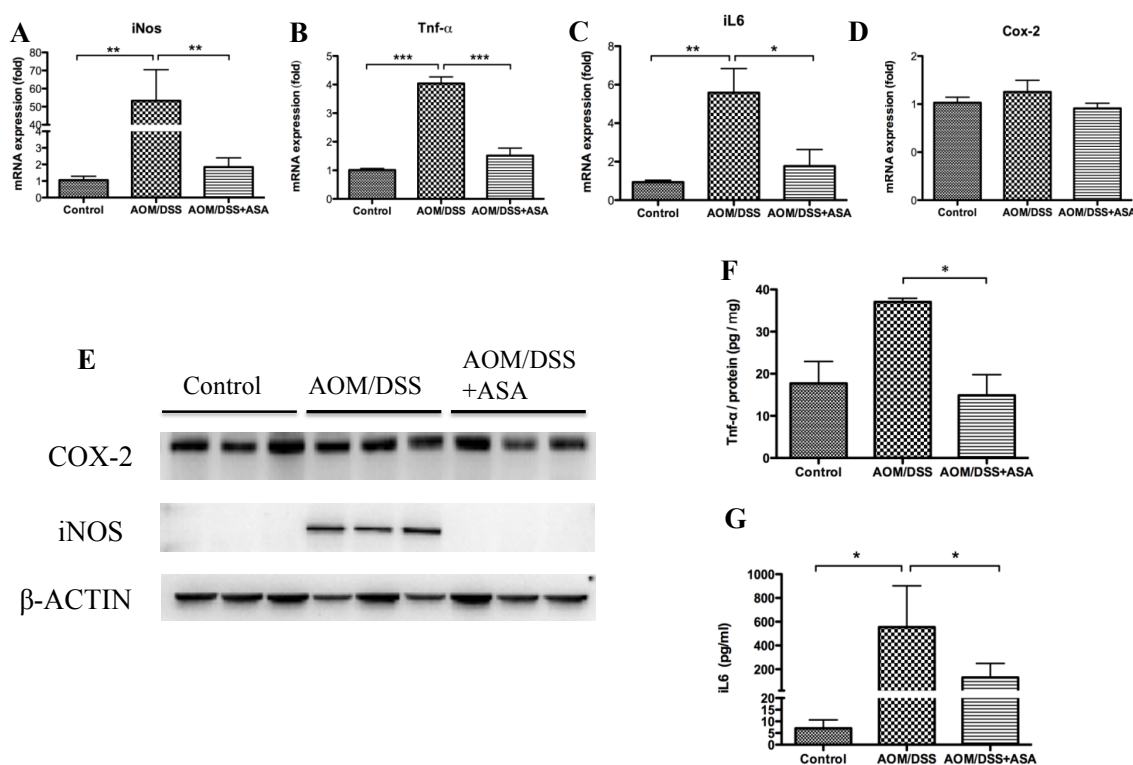
Figure 17: The effect of ASA on the expressions of iNos, Tnf-α, iL6, and Cox-2. The mRNA expression of pro-inflammatory genes was examined using qPCR.

AOM/DSS+ASA strikingly suppressed the AOM/DSS-induced mRNA expressions of iNos **(A)**, Tnf-α **(B)**, and iL6 **(C)**. However, the mRNA expression of Cox-2 was not changed in any treatment group **(D)**. The average CT value for the house keeping gene Gapdh is: 17.67 in control, 17.36 in AOM/DSS, and 17.37 in AOM/DSS+ASA. The average CT value for iNos gene is: 27.52 in control, 22.10 in AOM/DSS, and 26.82 in AOM/DSS+ASA. The average CT value in Tnf-α gene is: 25.14 in control, 22.88 in AOM/DSS, and 24.58 in AOM/DSS+ASA. The average CT value in iL6 is: 29.98 in control, 29.15 in AOM/DSS, and 29.51 in AOM/DSS+ASA. The average CT value in Cox-2 gene is: 26.16 in control, 26.07 in AOM/DSS, and 25.63 in AOM/DSS+ASA. The protein expressions of COX-2 and iNOS were determined using western blotting, and the representative blots are presented. AOM/DSS+ASA strongly inhibited the protein expression of iNOS, but the COX-2 protein was not inhibited **(E)**. The protein expression of TNF-α and iL6 was quantified using ELISA, and the results demonstrated that AOM/DSS+ASA effectively inhibits the protein concentration of TNF-α **(F)** and iL6 **(G)**, respectively. Normal appearing colonic mucosa was used in the assay, except that iL6 concentration was determined in plasma sample. * $P < 0.05$; ** $P < 0.01$; *** $P < 0.005$

4.4 Discussion

Old, even abandoned drugs might hold promise for cancer therapy by targeting epigenetic mechanisms. For example, azacitidine (Vidaza; an epigenetic drug used to

treat myelodysplastic syndromes) was originally developed as a cytotoxic agent that was rejected by the FDA more than 25 years ago. The elucidation of epigenetic modifications in cancer and the discovery that azacitidine is a hypomethylating agent have prompted its re-evaluation and led to its approval in 2004 (248). The investigation of ASA in the context of epigenetic modifications might reveal novel insights into its mechanisms and provide useful information regarding the dosage regimen when used as an epigenetic modulator in cancer chemoprevention. In the present study, ASA was administered in mouse diets at a dose of 0.02% for 21 weeks (equivalent to a dose of approximately 110 mg/day in humans using conversion based on body surface area as suggested by FDA). At this dosing regimen, ASA remarkably reduced tumor multiplicity and strongly suppressed HDAC activity and the enrichment of H3K27ac in the promoter regions of iNos, Tnf-α, and iL6 in CF-1 mice (Figure 13D, Figure 15A-C, and Figure 16E-G). A recently published study investigated the effect of ASA in AOM+DSS-induced Balb/c mice. However, ASA at a similar dose for a shorter duration (less than 12 weeks) failed to significantly inhibit the tumor number (235), possibly due to different variability to DSS in these two mouse strains and different cycles of DSS used in these two studies. Although clinical trials and observational studies have suggested that the long-term use of ASA at both low (81-160 mg/day) and high doses (300-325 mg/day) can reduce cancer risk (249), the optimal dose and duration of ASA needed to prevent CAC have not yet been established. Interestingly, one randomized trial suggested that the reduction in the risk of recurrent adenomas was found only with lower dose of ASA (81-160 mg/day), whereas several observational studies indicated that higher dose of ASA (300-325 mg/day) may be required for the prevention of CRC (249). Our present study provides

useful information suggesting that the chronic use of ASA at a low dose (~110 mg/day) might be a reasonable starting point for investigating ASA's role in modulating histone acetylation to prevent CAC in humans.

In the current study, we did not observe any induction of COX-2 in AOM/DSS-treated mice, and AOM/DSS+ASA did not suppress the expression of COX-2 (Figure 17D and E). The relatively unchanged COX-2 expression observed in our study might be explained by the fact that the precancerous mucosa (rather than tumor samples) was examined and up-regulated COX-2 was predominantly located in the tumor tissue of the colonic mucosa but not the adjacent normal tissue (250). Notably, the normal appearing colonic mucosa was used in all the molecular assays in the current study to elucidate the epigenetic effect of ASA. The use of non-cancerous tissue was partly due to the limit quantity of tumor samples in this study, especially accounting for the extremely low tumor multiplicity in AOM/DSS+ASA group (Figure 13D). Cancer epigenomic studies have indicated that DNA methylation abnormalities in malignant tumors are already accumulated in the precancerous stages in the kidney, liver, lung, urinary tract, pancreas, and gastric mucosa obtained from patients with carcinomas (251, 252). These data suggested that abnormal epigenetic pattern may have already established in precancerous tissues and further determines the tumor development and patient outcome. Thus, the modification of HDACs and H3K27ac we observed in precancerous tissue in the current study may reveal the early epigenetic events during colon carcinogenesis in AOM/DSS-induced CF-1 mice.

Recently, evidence has suggested that epigenetic modifications are involved in the chemopreventive actions of ASA. The chronic use of ASA is associated with the reduced

prevalence of E-cadherin (CDH1) promoter methylation in human gastric mucosa, suggesting that ASA protects against promoter DNA methylation (253). In the context of histone acetylation, both the induction and inhibition of HDACs by ASA have been reported. Kamble et al. showed that ASA induces Sirtuin 1 (SIRT1, a class III HDAC) in liver cells (254). A total of 33 cellular proteins (including histones) were identified as targets of ASA-mediated acetylation in colon cancer HCT-116 cells, implying that histone acetylation plays a role in the action of ASA in colon cancer (255). Another study that investigated the mechanisms of ASA in atherosclerosis found that a low concentration of ASA inhibited HDAC activities and increased the expression of acetylated H3, thereby promoting the transcription of netrin-1 in TNF-α-treated cells (256). The present study provides the first evidence suggesting that the inhibition of the protein expression of HDACs and the activity of HDAC are involved in the prevention of CAC in AOM/DSS-induced CF-1 mice by ASA at the dose of 0.02% (Figure 15A-C). Additional investigations are needed to determine whether the inhibition of HDACs by ASA is in dose-dependent manner and to delineate the mechanisms that underlie the actin of ASA in modifying HDAC activity and histone acetylation.

Up-regulated HDACs might be associated with abnormal histone acetylation, which can lead to the massive deregulation of gene transcription during the course of cancer. Reduced histone acetylation marks, including H3ac, H4ac, H4K16ac, H3K18ac, and H3K9/14ac, are implicated in CRC (257). In addition, aberrant histone acetylation, particularly H4K8ac and H4K12ac, was observed in the inflamed mucosa of a murine colitis model (227). However, the alteration of H3K27ac in CAC has not yet been determined. Recently, Karczmarski et al. showed that the level of H3K27ac is increased

in patients with sporadic colon cancer (228). Contrary to this finding, our results showed that the expression of H3K27ac in the colons of CF-1 mice was significantly reduced in the AOM/DSS group (Figure 16B and D). Importantly, AOM/DSS+ASA significantly restored the reduction of H3K27ac, possibly through the inhibition of HDAC (Figure 15 and Figure 16C-D). Nevertheless, the involvement of other epigenetic enzymes (e.g., HATs) in the control of the H3K27ac mark by ASA should be investigated in the future. We postulated that the reduction of the H3K27ac mark predisposes the epigenetic trait in the epithelium in favor of tumor growth in CAC, and the preventive effect of ASA might be associated with the restoration of H3K27ac expression.

Experimental results showed that the abundance of histone acetylation marks (e.g., H4K12ac and H4K16ac) are altered in the promoter regions of pro-inflammatory genes, including Cox2, iNos, Tnf-α, and iL6 under inflammation conditions, thereby influencing the expression of these genes (258-261). It would be important to examine whether AOM/DSS or AOM/DSS+ASA influences the expression of H3K27ac in the promoters of these genes. Interestingly, although AOM/DSS diminished global H3K27ac expression, the relative abundance of H3K27ac was increased in the promoters of iNos, Tnf-α, and iL6. AOM/DSS+ASA significantly countered the effect of AOM/DSS on the H3K27ac mark, both globally and locally (Figure 16). The H3K27ac mark is frequently associated with active transcriptional enhancers and chromatin-accessible transcription factor binding regions; moreover, it predicts active transcription (262). Notably, AOM/DSS+ASA dramatically suppressed the abnormally high levels of the transcription and protein expression of iNos, Tnf-α, and iL6 in the non-cancerous colonic tissue from AOM/DSS-induced mice, possibly as a result of the modifications in the abundance of

the H3K27ac mark in the promoter regions. Given the critical roles that iNos, Tnf-α, and iL6 play in the CAC (263, 264), the suppressive effect of ASA in AOM/DSS-induced colon cancer might be partially attributed to the inhibitions of iNos, Tnf-α, and iL6 via histone modification. Future research should determine whether other histone marks such as H3K27me1, 2, and 3, as well as H3K9ac are associated with CAC, plus whether the epigenetic effect of ASA involves the modifications of these histone marks. In addition, ChIP coupled with next-generation sequencing (ChIP-seq) might identify the potential genetic locus regulated by histone modification upon ASA use. Furthermore, it would be important to investigate whether the transcriptional factor network shift upon the chromatin conformational changes are involved in the epigenetic regulation of pro-inflammatory genes by ASA treatment. Moreover, ASA was administered prior to the injection AOM in the current study. Thus, whether ASA interfere with the metabolism of AOM and thereby inhibit tumor initiation should be investigated by future experiments.

4.5 Conclusion

In conclusion, we used an AOM/DSS-induced CAC model to demonstrate the preventive effect of the chronic use of low-dose ASA, suggesting that the *in vivo* mechanism for ASA may be COX-2-independent and appear to involve epigenetic modifications. Specifically, ASA at the dose of 0.02% inhibited the protein expression and activity of HDACs, as well as restoring the global H3K27ac level. In addition, ASA dramatically reduced the expressions of iNos, Tnf-α, and iL6, activities that might be associated with the suppression of the local enrichment of the H3K27ac mark in promoter

regions. These findings provide novel insights for the future development of old drug ASA as a potential epigenetic modulator in the prevention of inflammatory CRC.

5. CHAPTER FIVE

Mechanisms of colitis-accelerated colon carcinogenesis and its prevention with the combination of aspirin and curcumin: transcriptomic analysis using RNA-seq [9],[10]

5.1 Introduction

Colorectal cancer (CRC) is the third most common malignancy and the fourth leading cause of cancer-related deaths worldwide, which is estimated to account for more than 49,190 deaths in 2016 in the United States (265). Chronic inflammation is one of the hallmarks of cancer (266) and has been linked to the pathogenesis of tumors in multiple

---

[9] Part of this chapter has been published in Biochemical Pharmacology. 2017
[10] **Key Words**: Colitis-associated colorectal cancer; aspirin; curcumin; RNA-seq

human cancers, including CRC (267). Colitis-accelerated colon cancer (CAC) is a subtype of CRC with a high mortality that is closely associated with inflammatory bowel disease (IBD) (268). As one of the top high-risk conditions for CRC, epidemiological studies show that patients with long-standing IBD have a significantly higher risk of developing CRC (269). The azoxymethane (AOM)-initiated and dextran sulfate sodium (DSS)-promoted mouse model has been widely used to simulate the pathogenesis observed in patients with CAC (223). Specifically, the multistep carcinogenesis process is induced by an AOM injection [an initiation factor that induces aberrant crypt foci (ACF) by causing DNA damage] and DSS in the drinking water (a promotion factor that induces colitis by imposing inflammatory damage in the epithelial lining of the colon) in rodents.

Although the efficacy of CRC treatment has improved in recent years, the side effects of these treatment strategies, such as surgery, radiation therapy, chemotherapy, and targeted therapy, cannot be neglected. CRC is highly associated with environmental and lifestyle factors and usually undergoes a relatively long precancerous stage that provides individuals with opportunities to interfere before adenomas progress into malignancies. Hence, chemoprevention, the intake of agents with a relatively low toxicity to prevent the progression of cancer at a premalignant stage, has gained increasing attention in the management of CRC as a cost-effective alternative to CRC treatment (270). Among proposed chemopreventive interventions, aspirin (ASA, acetylsalicylic acid) is perhaps the agent with the most extensive evidence that long-term and regular use lowers the risk of different types of CRC (249), including sporadic CRC (232), hereditary CRC (233), and CAC (234). In addition, recent studies from our laboratory demonstrated

that dietary administration of ASA (0.02% w/w, equivalent to a dose of approximately 110 mg/day in humans) for 20 weeks effectively prevented carcinogenesis in AOM/DSS-induced CF-1 mice (271). Curcumin (CUR), the main component of turmeric (also called curry powder), is another widely studied chemopreventive candidate for CRC with a promising effect in suppressing inflammation and colon cancer cell growth (243, 272) with no reported adverse effects. In a phase IIa clinical trial, CUR at a dose of 4 g/day for 30 days significantly reduced ACF formation (273). Although CUR has been shown to effectively inhibit tumor growth in AOM-induced rats (274, 275), its effect in suppressing AOM/DSS-induced CAC has not yet been determined.

The potential side effects of gastrointestinal bleeding from chronic use of high-dose ASA have limited its use in the general population for the prevention of CRC. With regards to CUR, although up to 12 g/day was well-tolerated in humans (276), chronic administration of CUR at a very high dose may lead to poor patient compliance. Co-administration of two or more chemopreventive agents with different molecular mechanisms at a lower dosage may act as a promising strategy to maximize efficacies and minimize toxicities. For example, a synergistic effect has been observed in the combination of green tea polyphenols and atorvastatin in the inhibition of lung tumorigenesis (277), atorvastatin and celecoxib in the suppression of prostate tumors (278), and metformin and ASA in the inhibition of pancreatic cancer (279). In addition, data from two different randomized clinical trials suggested a synergistic interaction between calcium supplementation and the use of ASA in the reduction of the risk of advanced colorectal adenomas; however, the combination of calcium and ASA failed to exert a synergistic action in the suppression of ACF formation in AOM-induced rodent

models (280). Regarding the combinational action of ASA and CUR, Thakkar et al. reported a synergistic effect of ASA, CUR, and sulforaphane in the reduction of pancreatic cancer cell viability (281). Furthermore, Perkins et al. found that ASA and CUR exerted an optimal adenoma-retarding effect at different stages in Apc$^{min/+}$ mice, although synergism was not achieved when CUR and ASA were administered sequentially (282). In the present study, we aimed to investigate the combinatorial effect of concomitant administration of ASA and CUR at half the dose of their single treatment in the prevention of AOM/DSS-induced CAC.

Previous studies have indicated that both ASA and CUR are multi-target chemopreventive agents that impact various signaling pathways and molecules involved in inflammation, tumor initiation, and tumor progression (217, 249). However, an overview of the genes and signaling pathways associated with the chemopreventive actions of ASA and CUR in AOM/DSS-induced CAC remains relatively understudied. In particular, the molecular targets influenced by the combination of these two agents have not yet been investigated. RNA sequencing (RNA-seq) is a recently developed deep-sequencing approach in transcriptome profiling that offers a relatively unbiased and more precise measurement of the levels of transcripts and their isoforms (283). Because RNA-seq technology provides several key advantages over hybridization-based microarrays for transcriptome profiling, it is rapidly becoming an attractive tool to identify the differentially expressed genes in multiple experimental conditions. To depict a comprehensive picture of the molecular mechanisms underlying the chemopreventive effect of ASA and CUR, especially their combination at a lower dose, the present study utilized RNA-seq to analyze the differential gene expression and pathways in tumors

induced by AOM/DSS with or without treatment with ASA and CUR, alone or in combination, in a rodent CAC model.

5.2 Materials and methods

5.2.1 Animals and diets

Animal experiments were conducted under an animal protocol (01-016) approved by the Institutional Animal Care and Use Committee (IACUC) of Rutgers University. C57BL/6 mice were obtained from Jackson Laboratory (Bar Harbor, ME, USA) at the age of 4 weeks old. Upon arrival, the animals were maintained at a controlled temperature (20-22°C), controlled relative humidity (45-55%), and 12-h light and 12-h dark cycles at the Rutgers Animal Care Facility. After 1 week of acclimatization, mice at the age of 5 weeks were randomly assigned to 5 experimental groups (n = 14-15) and fed with AIN-93M rodent diet (Research Diet Inc. New Brunswick, NJ, USA) or special diet (Research Diet Inc.) supplemented with ASA, CUR, or their combination ad libitum. ASA was purchased from Sigma-Aldrich (St Louis, MO, USA) and blended into AIN-93M rodent diet at a final concentration of 0.02% as previously described (271). Curcumin C3 Complex® was a kind gift from Sabinsa Corporation (East Windsor, NJ, USA) and mixed into the AIN-93M rodent diet at a final concentration of 2%. The diet containing the combination of ASA and CUR was prepared by simultaneously mixing ASA and CUR into AIN-93M diet at a final concentration of 0.01% and 1%, respectively.

5.2.2 Experimental procedure

The AOM/DSS model was carried out as previously described (271, 284) and is summarized in Figure 18. Briefly, 6-week-old mice were injected with AOM (Sigma-Aldrich) subcutaneously in the lower flank at a dose of 10 mg/kg body weight. The mice in the control group instead received an injection of saline (Thermo Fisher Scientific, Waltham, MA, USA). One week later, the drinking water for the mice, other than the control group, was replaced with DSS (MP Biomedicals, Solon, OH, USA) at a concentration of 1.2% (w/v) for 7 days. The disease activity index (DAI) was calculated daily during the administration of DSS to monitor the symptoms of acute colitis using the scoring system published previously (271). The body weight and the consumption of food and fluid were recorded weekly during the entire experiment. Twenty-two weeks after the AOM injection, all mice were sacrificed by CO_2 asphyxiation. Colons were removed, cleaned, and opened longitudinally followed by careful examination of the tumors. The left portion of the colon was saved for histological analysis. After removing the proximal end and palpable tumors, the remaining right portion of the colon was snap frozen and stored at -80°C for molecular assays.
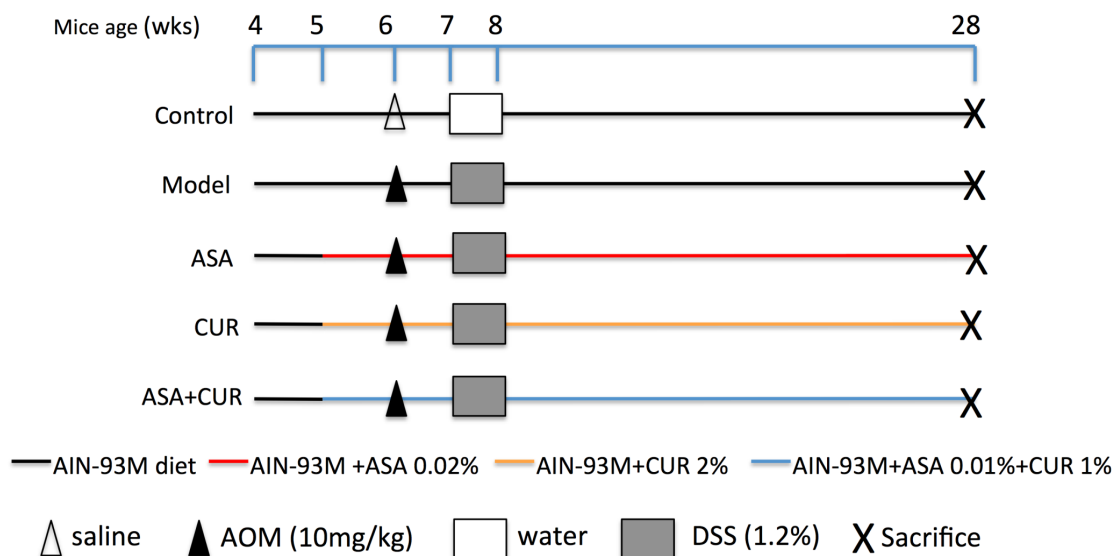
Figure 18: The experimental protocol for a chemoprevention study with ASA and CUR, alone or in combination, in AOM/DSS-induced C57/BL6 mice.

Mice at 5 weeks of age were fed the AIN-93M diet or this diet supplemented with 0.02% ASA, 2% CUR, or 0.01% ASA+1% CUR until the end of the experiment. Mice in groups other than the control group received a subcutaneous injection of AOM at 10 mg/kg at the age of 6 weeks, followed by the administration of water containing DSS at 1.2% (w/v) for 7 consecutive days. Twenty-two weeks after AOM initiation, the mice were sacrificed for further analysis.

5.2.3 Histopathological analysis

The histopathological analysis was performed as described previously (271). The left portion of the colon was fixed in 10% buffered formalin (Thermo Fisher Scientific) for 24 h, serially dehydrated, embedded in paraffin (Thermo Fisher Scientific), and stored

at 4°C. The tissue blocks were then serially sectioned at 4 μm and mounted on glass slides. Histopathological abnormalities in the colon were examined by hematoxylin and eosin staining and evaluated by the histopathologist, Dr. Guangxun Li.

5.2.4 RNA extraction, library preparation, and next-generation sequencing

Total RNA was isolated from snap-frozen colonic tissue from the control group and tumor samples from the experimental groups (model, ASA, CUR, and ASA+CUR) using the AllPrep DNA/RNA Mini Kit (Qiagen, Valencia, CA, USA). The quality and quantity of the extracted RNA samples were determined with an Agilent 2100 Bioanalyzer and NanoDrop, respectively. A total of 10 RNA samples [2 samples per group x 5 groups (control, model, ASA, CUR, and ASA+CUR)] were sent to RUCDR for library preparation and sequencing. Briefly, the library was constructed using the Illumina TruSeq RNA preparation kit (Illumina, San Diego, CA, USA) according to the manufacturer's manual. Samples were sequenced on the Illumina NextSeq 500 instrument with 50-75 bp paired-end reads, to a minimum depth of 30 million reads per sample.

5.2.5 Computational analyses of RNA-seq data

The reads were aligned to the mouse genome (mm10) with TopHat v2.0.9 (285). Reference gene annotations from UCSC were supplied to TopHat (-G genes.gtf); otherwise, default parameters were used. The Cufflinks v2.2.1 (286) program cuffdiff

was used to calculate expression levels, using the UCSC gene annotations and default parameters.

5.2.6 Ingenuity Pathway Analysis (IPA)

Isoforms that exhibited a log2 fold change greater than 1 and a false detection rate (FDR) less than 0.05 were subjected to Ingenuity Pathway Analysis (IPA 4.0, Ingenuity Systems, www.Ingenuity.com). The input isoforms were mapped to IPA's knowledge bases, and the relevant biological functions, networks, and pathways related to the treatment of ASA, CUR, and their combination were identified.

5.2.7 Quantitative polymerase chain reaction (qPCR)

qPCR was used to validate selected differentially expressed genes observed in RNA-seq. After synthesis of first-strand cDNA from 500 ng of RNA using TaqMan® Reverse Transcription reagents (Applied Biosystems, Carlsbad, CA, USA), qPCR was performed using a QuantStudio^{TM} 5 Real-Time PCR System (Applied Biosystems) with SYBR Green PCR Master Mix (Applied Biosystems). The results were normalized to the expression of Glyceraldehyde 3-phosphate dehydrogenase (Gapdh) using the $2^{-\Delta\Delta CT}$ method. All of the primers were designed and ordered from Integrated DNA Technologies (IDT, Coralville, Iowa, USA).

5.2.8 Statistical analysis

The data are presented as the mean ± SD. Comparisons among multiple groups were analyzed using one-way analysis of variance (ANOVA) with Tukey's multiple comparison test. The DAI data were analyzed with the repeated measure ANOVA method. A P-value less than 0.05 was considered statistically significant.

5.3 Results

5.3.1 Effects of ASA, CUR, and their combination in the prevention of colon tumorigenesis

The clinical symptoms of colitis were evaluated by recording the DAI during DSS treatment. It is widely accepted that the DAI is associated with colitis severity as well as erosions and inflammation (244). As shown in Figure 19A, the DAI score increased gradually in the model group, indicating elevated clinical colitis symptoms in the mice that received AOM/DSS treatment. Dietary administration of ASA (0.02%) slightly attenuated the increase of the DAI starting at day 5, whereas treatment of CUR (2%) and the combination (ASA 0.01% + CUR 1%) started to exhibit effective suppression of the DAI at day 4. Notably, the inhibitory effect of the combination treatment, although at only half the dose of the single compound, was statistically significant by repeated measure ANOVA.

We did not observe any noticeable body weight loss in mice fed the diet supplemented with ASA, CUR, or the combination compared with mice fed the control

diet (data not shown). Twenty-two weeks after the AOM injection, the tumors in the colon were carefully examined and recorded. As shown in Figure 19B and C, 8 of the 15 mice in the model group developed tumors in the colon with a tumor multiplicity of 1.80 ± 0.60 tumors per animal, which is comparable to a previous publication with a similar experimental protocol in C57BL/6 mice (284). Although mice fed the diet supplemented with ASA at the level of 0.02% developed slightly fewer tumors (1.33 ± 0.6 tumors per mouse), the tumor incidence was not decreased. Compared to the model group, dietary administration of CUR at 2% resulted in a lower tumor incidence as well as significantly decreased tumor multiplicity (0.40 ± 0.19 tumors per animal). The combination treatment with only half of the dose compared to the single treatment exhibited the lowest tumor incidence among the four experimental groups and resulted in significantly lower tumor multiplicity (0.41 ± 0.24 tumors in each mouse).
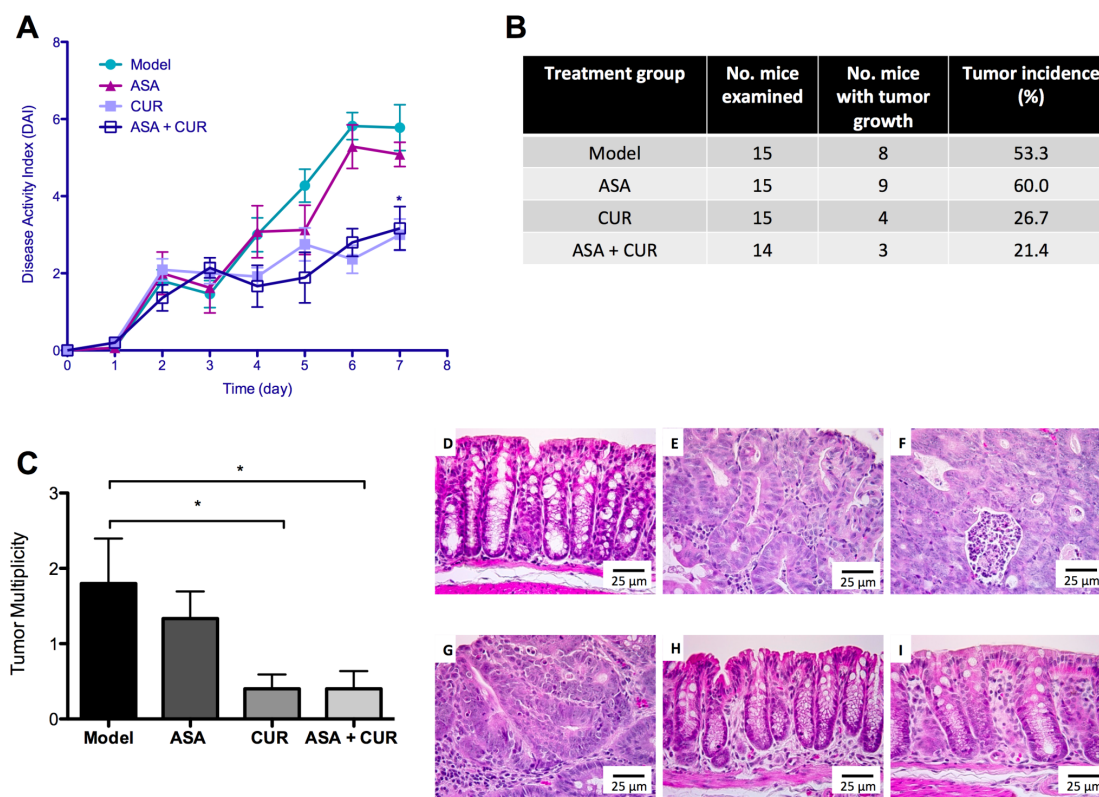
Figure 19: The effect of dietary administration of ASA, CUR, and their combination in AOM/DSS-induced CAC.

(A) The suppression of the DAI by 0.02% ASA, 2% CUR, and 0.01% ASA+1% CUR. **(B)** The effect of ASA, CUR, and their low-dose combination on tumor incidence in AOM/DSS-induced CAC. The tumor incidence (%) of each group was calculated from the number of mice with tumor growth over the number of mice examined. **(C)** The effect of ASA and CUR, alone or in combination, in decreasing tumor multiplicity in AOM/DSS-induced CAC. Tumor multiplicity was calculated from the total number of tumors in each group divided by the number of mice in each group. **(D-I)** Histological observation of the control group **(D)**, the model group with AOM/DSS administration **(E,**

F), mice treated with 0.02% ASA **(G)**, mice treated with 2% CUR **(H)**, and mice treated with 0.01% ASA+1% CUR **(I)**. * P < 0.05 versus the model group.

Hematoxylin and eosin staining showed that AOM/DSS-treated mice had severe colonic damage including crypt dysplasia, adenomas, and adenocarcinoma. Inflammation, an increased nucleus to cytoplasm ratio, nuclear crowding, mitosis, and nuclear hyperchromasia were observed in the adenomas (Figure 19E). Adenocarcinomas were associated with severe inflammation, infiltration of leukocytes into the lumen, the composition of cribriform glands, the loss of nuclear polarity to the basement membrane, nuclear hyperchromasia, and mitosis (Figure 19F). Although ASA (0.02%) treatment attenuated inflammation, hyperplasia and adenomas were observed (Figure 19G). CUR (2%) treatment and the combination treatment (ASA 0.01% + CUR 1%) suppressed inflammation severity and cancer lesions, and treated animals exhibited normal colon morphology (Figure 19H-I).

Taken together, these results demonstrate that the dietary administration of CUR at 2% showed a superior inhibitory effect in colitis and colon tumorigenesis over ASA at 0.02%. The combination of ASA and CUR at only half of the dose effectively and significantly suppressed acute colitis and tumor growth in AOM/DSS-induced mice without affecting body weight. One of the limitations of our present study is that we did not include a group of animals administered with 1% CUR alone, thus it is possible that 1% CUR is more effective than 2% CUR. Several studies have indicated a dose-dependent effect of CUR in suppressing AOM-induced tumors. For example, 2% CUR exhibited superior effect in inhibiting AOM-induced ACFs than 0.2% CUR (287) and 2% CUR showed better inhibition of AOM-induced adenomas and adenocarcinomas than 0.5%

CUR (288). In addition, Pereira et al. reported that AOM-induced animals developed less adenoma upon treatment with 1.6% CUR than 0.8% CUR (274). Therefore, we postulate that 1% CUR may not be as effective as 2% CUR and ASA increased the efficacy of CUR such that combination treatment with only half of the dose was effective as 2% CUR alone. Thus, combining these two compounds at a lower dosage may provide a promising effect in colon cancer prevention.

5.3.2 Top differentially expressed genes and canonical pathways affected in the model group compared to the control group

To understand the mechanisms underlying the carcinogenicesis process from normal colonic tissue to tumor tissue, we compared the gene expression profiles of tumors induced by AOM/DSS in the model group to those of age-matched colonic tissue in the control group. We found that a total of 1,291 differentially expressed genes showed a log2 fold change greater than 1 and an FDR less than 0.05. The top 10 down-regulated and up-regulated genes under this comparison are presented in Table 11. The dramatic fold change of these genes (as low as 0.021-fold or as high as 389.9-fold) could be due to the different nature and cell populations of the tumor mass compared to those of normal colon tissue or to alterations triggered by AOM/DSS treatment. To understand the possible biological functions associated with these differentially expressed genes observed in the model group versus the control group, canonical pathway analysis in IPA was used. Based on the ratio of the number of differentially expressed genes in our dataset to the total number of reference genes in the corresponding pathways in the IPA

knowledge bases, IPA utilized Fisher's exact test to determine the significant canonical pathways associated with differentially expressed genes observed from RNA-seq. Using a cutoff P-value less than 0.05, a total of 378 canonical pathways were identified as being significantly correlated with the alterations of gene expression in AOM/DSS-induced tumors compared to normal colonic tissue. Table 12 displays the 10 most significant pathways, their –log (P-value), the ratio of affected genes over total genes in that particular pathway, and the details of significant expressed genes in our dataset contained in that specific pathway. These results suggested that AOM/DSS-induced tumors displayed substantially differentially expressed genes with dramatic mRNA expression changes compared to age-matched normal colon tissue.

Table 11: Top 10 down-regulated and up-regulated genes in tumors from mice in Model group compared to Control group.

Fold change larger than 1 indicates higher expression in tumors in Model group. Fold change smaller than 1 indicates lower expression in tumors in Model group.

Gene ID	Gene name	Fold Change	FDR
Down-regulated			
RETNLB	resistin like beta	0.021	2.12E-03
CA3	carbonic anhydrase III	0.028	3.89E-03
NOS1	nitric oxide synthase 1 (neuronal)	0.031	1.45E-02
SYCN	syncollin	0.031	2.12E-03
ZCCHC12	zinc finger, CCHC domain containing 12	0.032	3.28E-02
CHRNA3	cholinergic receptor, nicotinic, alpha 3	0.036	1.34E-02
SST	somatostatin	0.037	2.12E-03

NAALAD	N-acetylated alpha-linked acidic	0.041	2.12E-03
Pln	phospholamban	0.042	9.63E-03
STMN3	stathmin-like 3	0.044	5.44E-03
Up-regulated			
MMP7	matrix metallopeptidase 7	389.911	2.12E-03
LYZ	lysozyme	328.329	2.12E-03
CXCL6	chemokine (C-X-C motif) ligand 6	181.900	3.63E-02
WIF1	WNT inhibitory factor 1	167.266	2.12E-03
PNLIPRP1	pancreatic lipase-related protein 1	154.236	2.12E-03
SLC30A2	solute carrier family 30 (zinc transporter),	124.673	6.89E-03
CLCA4	chloride channel accessory 4	114.246	2.12E-03
ALOX15	arachidonate 15-lipoxygenase	92.411	6.89E-03
MMP10	matrix metallopeptidase 10	91.456	2.12E-03
ALB	albumin	87.913	2.12E-03

Table 12: The 10 most significant canonical pathways regulated by AOM/DSS-induced tumors compared to normal colonic tissue in Control group. Genes in bold are down-regulated in tumors.

Canonical Pathways	-log (p value)	Ratio	Target genes
Hepatic Fibrosis / Hepatic Stellate Cell Activation	19.8	50/187 (0.267)	CCR5,COL9A3,MMP13,**COL8A1**,IL1R2,TGFB1,LAMA1,SERPINE1,PDGFRB,TNFRSF11B,IL4R,COL4A1,**MYH14**,MMP2,IGFBP5,PDGFB,MYL7,**MYL9**,**ACTA2**,IL10RA,COL6A5,TNF,CCR7,COL7A1,IGFBP4,ICAM1,FN1,IL1RL1,**EGF**,CCL5,COL4A2,**MYH11**,PDGFC,COL15A1,PGF,COL1A2,**NGFR**,PDGFRA,LBP,TNFRSF1B,COL18A1,VCAM1,COL5A2,COL12A1,**FGF1**,COL1A1,COL5A3,IL1B,EDNRA,MMP9
Atherosclerosis Signaling	13.9	34/125 (0.272)	APOE,ICAM1,**APOB**,MMP3,**PLA2G10**,CMA1,MMP13,ALOX12,PLA2G7,PDGFC,**PRDX6**,COL1A2,LYZ,Pla2g2a,TGFB1,COL18A1,PLA2G

			12A,ALOX15,VCAM1,CXCR4,**PLA2G3**,F3,PDGFB,TPSAB1/TPSB2,SELPLG,COL1A1,ITGB2,COL5A3,ALB,SELP,IL1B,TNF,MMP9,CLU
Granulocyte Adhesion and Diapedesis	13.1	40/179 (0.223)	MMP7,ICAM1,MMP3,**CLDN15**,IL1RL1,MMP14,MMP13,CCL22,CCL5,Cxcl9,IL1R2,CLDN4,**SDC2**,**CCL28**,**NGFR**,CXCL14,MMP11,TNFRSF1B,MMP12,**Ccl6**,**MMP17**,TNFRSF11B,VCAM1,CXCR4,PF4,MMP10,THY1,MMP2,CXCL6,SELPLG,ITGB2,CXCL16,ITGAM,SELP,CDH5,**CLDN8**,IL1B,TNF,MMP9,**HSPB1**
LPS/IL-1 Mediated Inhibition of RXR Function	12.9	45/224 (0.201)	**GAL3ST2**,APOE,**CYP3A7**,**CHST4**,**GSTM5**,IL1RL1,ABCC2,**CYP2C9**,ABCG1,**HMGCS2**,SOD3,ABCA1,CHST2,IL1R2,**GSTT2/GSTT2B**,**MAOB**,**ALDH1A1**,ACSBG1,ALDH1A3,**Gstm3**,**NGFR**,**PPARGC1B**,CHST11,FABP5,LBP,TNFRSF1B,**ALDH6A1**,TNFRSF11B,GSTA3,**GSTM1**,**ALDH1B1**,**ABCB1**,**MGST1**,**SULT1C2**,**CHST12**,**Sult1d1**,**SULT2B1**,HS3ST3B1,**FABP2**,**ALDH1A2**,IL1B,**ABCC3**,TNF,**SULT1B1**,**MAOA**
Agranulocyte Adhesion and Diapedesis	11.5	39/190 (0.205)	MMP7,ICAM1,FN1,MMP3,**CLDN15**,MMP14,MMP13,CCL22,**MYH11**,CCL5,Cxcl9,CLDN4,**CCL28**,CXCL14,MMP11,**ACTG2**,MMP12,**Ccl6**,**MMP17**,ACTA1,VCAM1,CXCR4,PF4,**MYH14**,MMP10,MMP2,CXCL6,SELPLG,MYL7,**MYL9**,ITGB2,CXCL16,SELP,CDH5,**CLDN8**,**ACTA2**,IL1B,TNF,MMP9
Xenobiotic Metabolism Signaling	7.73	41/274 (0.15)	**GAL3ST2**,**CYP3A7**,**CHST4**,**GSTM5**,**CAMK1D**,ABCC2,**CYP2C9**,SOD3,CHST2,HMOX1,**GSTT2/GSTT2B**,**MAOB**,**CES1**,**ALDH1A1**,ALDH1A3,**Gstm3**,**Ugt1a7c**,CHST11,**PRKCE**,NOS2,PRKD1,**ALDH6A1**,GSTA3,**GSTM1**,**ALDH1B1**,**ABCB1**,**MGST1**,**SULT1C2**,**UGT2B10**,**CHST12**,**Sult1d1**,**SULT2B1**,**Ces1e**,HS3ST3B1,**PRKCD**,**ALDH1A2**,IL1B,**ABCC3**,TNF,**SULT1B1**,**MAOA**
Leukocyte Extravasation Signaling	7.69	34/204 (0.167)	RAC2,MMP7,ICAM1,MMP3,**CLDN15**,MMP14,MMP13,CLDN4,CYBA,CYBB,**PRKCE**,MMP11,**ACTG2**,MMP12,PRKD1,**MMP17**,ACTA1,VCAM1,CXCR4,THY1,MMP10,PLCG1,MMP2,NCF4,SELPLG,ITGB2,NCF1,ITGAM,**EDIL3**,CDH5,**CLDN8**,**ACTA2**,**PRKCD**,MMP9
Role of Macrophages, Fibroblasts and Endothelial Cells in Rheumatoid Arthritis	7.43	43/302 (0.142)	FZD10,SOCS3,TCF4,FN1,ICAM1,MMP3,IL1RL1,LTB,MMP13,WNT6,CCL5,PDGFC,FCGR1A,CCND1,PGF,**PLCD1**,IL1R2,WIF1,**PLCE1**,TGFB1,DKK3,**NGFR**,TLR7,DKK2,**PRKCE**,TNFRSF1B,NOS2,FCGR3A/FCGR3B,PRKD1,TNFRSF11B,ADAMTS4,VCAM1,PLCG1,**CREB3L4**,PDGFB,TLR2,**PRKCD**,Tlr13,IL1B,LEF1,TN

			F,Tcf7,WNT5A
Complement System	7	13/38 (0.342)	C1R,C4A/C4B,ITGB2,SERPING1,ITGAM,C3, C1QA,C1QC,CFH,C1QB,C3AR1,C2,ITGAX
Axonal Guidance Signaling	6.9	54/440 (0.123)	RAC2,**ADAMTS8**,BMP4,MMP13,WNT6,ADAMTS2,ADAM8,**PLCE1**,**CFL2**,PTCH2,PRKD1, ADAMTS4,**TUBB3**,PAPPA,MMP2,RAC3,PDGFB,MYL7,**MYL9**,ADAMTS6,ADAM12,**PRKCD**,EPHA2,FZD10,ADAMTS7,MMP7,**BMP3**,**EGF**,PDGFC,ROBO1,SEMA4C,PGF,TUBB2B,**PLCD1**,**SDC2**,**NGFR**,**PRKCE**,PLXNB1,MMP11,TUBB4A,**SEMA4A**,SEMA3F,BMP1,**GNG4**,PLXNC1,CXCR4,MMP10,PLCG1,PLXND1,**SEMA4G**,BMP7,MMP9,SEMA7A,WNT5A

5.3.3 Overview of differentially expressed genes regulated by the treatment of ASA, CUR, and their combination compared to the model group

To determine how ASA, CUR, and their combination exerted a preventive effect in AOM/DSS-induced CAC, we compared the global gene expression profiles of AOM/DSS-induced tumors to those treated by ASA, CUR, or their combination. A cut-off value of a log2 fold change greater than 1 and an FDR less than 0.05 were used to extract the differentially expressed genes. We identified 99 differentially expressed genes in the comparison of tumors from ASA 0.02% treated mice versus tumors from the model group (64 genes were up-regulated by ASA treatment, while 35 genes were down-regulated by ASA treatment). We observed 189 genes with differential expression in comparison with tumors from CUR 2% treated mice versus tumors from the model group (108 genes were up-regulated by CUR treatment, while 81 genes were down-regulated by CUR treatment). The combination of ASA and CUR at only half the dose of the single compound was found to modulate more genes than ASA or CUR alone when compared to the model group. A total of 344 genes that showed significantly differential expression levels were identified (155 genes were up-regulated while 189 genes were down-

regulated by combination treatment compared to the model group). This result indicated that dietary administration of CUR at 2% alone modulated a larger number of genes than ASA at 0.02%, whereas the combined treatment was able to regulate an even broader gene set. Of the genes increased by ASA, 56% (36/64) were also up-regulated by the combination of ASA and CUR (Figure 20A), whereas 74% (26/35) of the down-regulated genes in tumors from ASA-treated mice were also decreased in the tumors from combination-treated animals (Figure 20B). However, the differentially expressed genes regulated by CUR treatment showed less commonality with those regulated by the combination treatment. As shown in Figure 20A and B, only 22% (24/108) and 48% (36/81) of the up-regulated and down-regulated genes, respectively, also appeared in the subset of the differentially expressed genes regulated by the combination treatment.
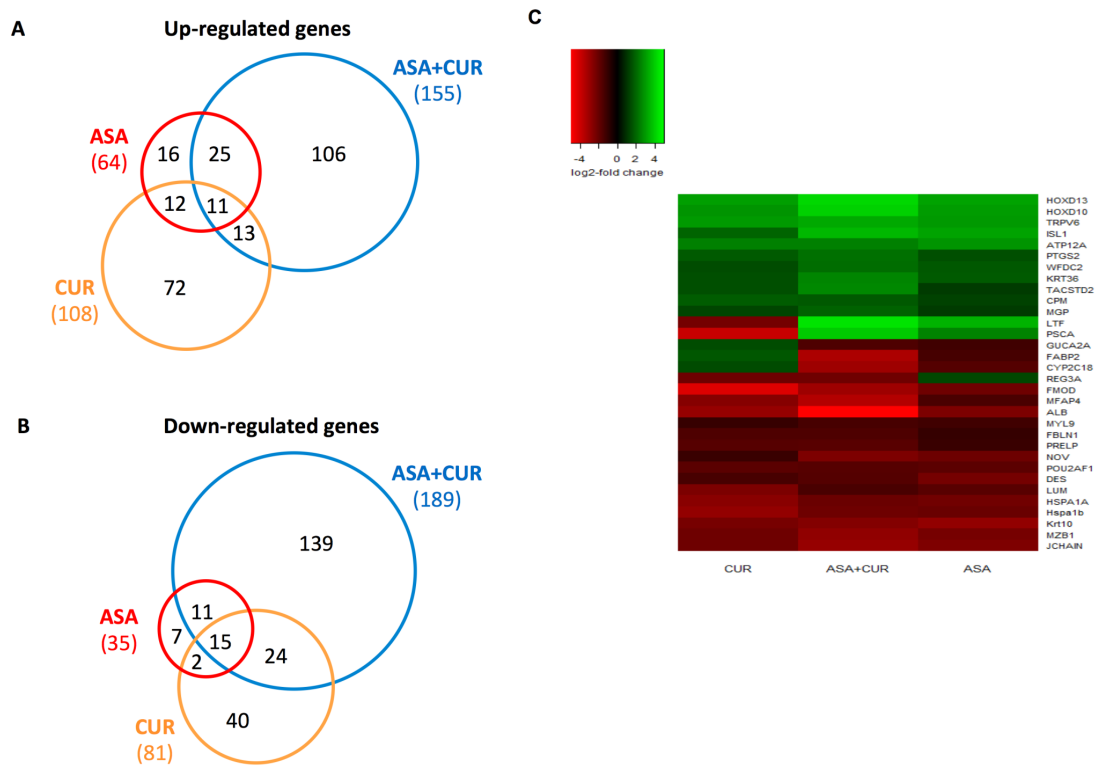
Figure 20: Overview of the genes regulated by ASA and CUR, alone or in combination, compared to the model group.

(A, B) Venn diagrams comparing the number of up-regulated genes **(A)** and down-regulated genes **(B)** in tumors from mice treated with 0.02% ASA, 2% CUR, or 0.01% ASA+1% CUR compared to tumors from mice treated with AOM/DSS alone. Genes with log2 fold changes greater than 1 and an FDR less than 0.05 were counted. **(C)** Heat map of 32 genes with differential expression that appeared in all three treatment groups (ASA, CUR, and ASA+CUR) compared to the model group.

In addition, we identified a total of 32 genes that appeared in all three treatment groups (ASA, CUR, and their combination) compared to the model group. Of the differentially expressed genes in these three groups, 81% (26/32) showed the same direction of regulation (either up-regulated or down-regulated). As shown in the heat map (Figure 20C), the color of the combination group was overall slightly brighter than that of the ASA and CUR groups, suggesting that combined treatment with ASA and CUR may regulate the expression of these shared genes at a higher fold change than treatment with the single compound. We randomly selected 6 genes from this set of shared genes and validated their expression in tumor samples from the model, ASA, CUR, and ASA+CUR groups using qPCR analysis. As shown in Figure 21, the fold change determined by qPCR (bar with black color) was consistent with that observed in RNA-seq (bar with white color) for all 6 selected genes, confirming the quantitative properties of the RNA-seq analysis used in this study. Furthermore, it was found that ASA at 0.02% and CUR at 2% could down-regulate the expression of Alb and Mfap4, and the combination treatment (ASA 0.01%+CUR 1%) resulted in the lowest expression of Alb and Mfap4 among the

four groups. The mRNA expression of Krt36, Tacstd2, Hoxd10, and Hoxd13 was up-regulated by treatment with ASA, CUR, or their combination compared with their levels in tumors in the model group, whereas the combination treatment was able to induce this mRNA expression to a slightly higher level than was induced by the single treatment.
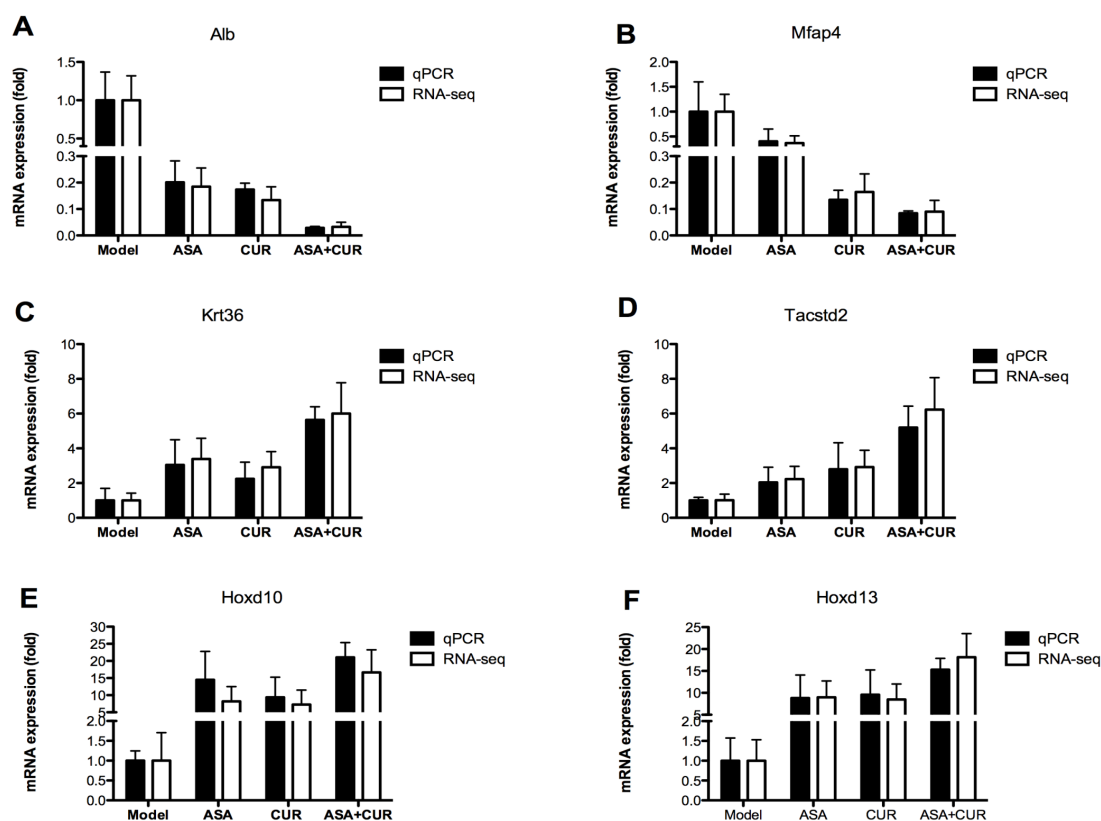
Figure 21: Validation of the mRNA expression of selected genes regulated by ASA, CUR, or their combination compared to the model group.

mRNA isolated from tumors in mice from the model, 0.02% ASA, 2% CUR, and 0.01% ASA+1% CUR groups was subjected to qPCR analysis. Black bar: the qPCR results are presented as the fold change compared with the model group using Gapdh as the

endogenous control. White bar: fold change from the RNA-seq analysis. The data are presented as the mean ± SD (n = 2).

Altogether, these data showed that combination treatment with ASA and CUR at half of the dose of the single compound had an impact on more gene targets than ASA alone or CUR alone. In addition, for the gene sets regulated by all three treatments (ASA, CUR, and their combination), the combination treatment resulted in a slightly higher fold change than the single compound.

5.3.4 Top differentially expressed genes and canonical pathways modulated by ASA, CUR, and their combination

Upon further examination of the significant differentially expressed gene profiles of tumors treated by ASA, CUR, or their combination compared to those in the model group, we listed the top 10 down-regulated or up-regulated genes (ranked by fold change) for these three treatments, as shown in Table 13 and Table 14. A fold change lower than 1 indicated that the expression of the gene was decreased by this particular treatment compared to the expression in the model group, whereas a fold change higher than 1 suggested an elevated mRNA expression in tumors receiving that treatment compared to the expression with AOM/DSS alone. Interestingly, Alb was among the top 10 down-regulated genes in all the three comparisons (Table 13), and its relative expression was only 0.185, 0.134, and 0.032 in tumors treated by ASA, CUR, and ASA+CUR, respectively (expression of Alb in AOM/DSS alone was set as 1). As shown in Figure 21A, the expression of Alb was validated in tumor samples by qPCR analysis, confirming

that its expression was decreased by these treatments and that the combination was able to decrease its expression to a higher magnitude. Similarly, Hoxd13 was among the top 10 up-regulated genes in all three comparisons (Table 14), and its expression was 9.044-, 8.497-, and 18.126-fold higher in tumors treated by ASA, CUR, and the combination, respectively, compared to the expression in the model group, and this trend was also confirmed by qPCR analysis (Figure 21F).

Table 13: Top 10 down-regulated genes in tumors from mice treated by ASA, CUR, and their combination compared to Model group.

The expression of these genes in Model group was set to 1.

Gene ID	Gene name	Fold Change	FDR
ASA			
IGFBP2	insulin-like growth factor binding protein 2	0.078	4.94E-02
Krt10	keratin 10	0.141	2.12E-03
JCHAIN	joining chain of multimeric IgA and IgM	0.184	2.12E-03
ALB	albumin	0.185	2.12E-03
MZB1	marginal zone B and B1 cell-specific protein	0.206	2.12E-03
DES	desmin	0.207	2.12E-03
HSPA1A	heat shock 70kDa protein 1A	0.217	3.89E-03
FMOD	fibromodulin	0.225	3.37E-02
NOV	nephroblastoma overexpressed	0.230	2.12E-03
HSPA1B	heat shock protein 1B	0.242	2.12E-03
CUR			
Defa3	defensin, alpha, 3	0.048	6.89E-
FMOD	fibromodulin	0.051	2.12E-
PSCA	prostate stem cell antigen	0.069	4.86E-

Gene ID	Gene name		
GPC3	glypican 3	0.071	2.12E-
AFM	afamin	0.095	3.18E-
ANGPT4	angiopoietin 4	0.095	1.68E-
ALB	albumin	0.134	2.12E-
Hspa1b	heat shock protein 1B	0.139	2.12E-
HSPA1A	heat shock 70kDa protein 1A	0.159	2.12E-
MFAP4	microfibrillar-associated protein 4	0.164	2.12E-
ASA+CUR			
B3GNT6	UDP-GlcNAc:betaGal beta-1,3-N- acetylglucosaminyltransferase 6	0.032	8.28E- 03
ALB	albumin	0.032	2.12E-
GPC3	glypican 3	0.046	2.12E-
TMIGD1	transmembrane and immunoglobulin domain containing 1	0.046	5.44E- 03
Apol7e	apolipoprotein L 7e	0.050	2.12E-
KRT1	keratin 1, type II	0.070	4.39E-
B4GALNT	beta-1,4-N-acetyl-galactosaminyl transferase	0.072	2.12E-
ACTA1	actin, alpha 1, skeletal muscle	0.073	2.12E-
MFAP4	microfibrillar-associated protein 4	0.077	2.12E-
FABP2	fatty acid binding protein 2, intestinal	0.090	2.12E-

Table 14: Top 10 up-regulated genes in tumors from mice treated by ASA, CUR, and their combination compared to Model group.

The expression of these genes in Model group was set to 1.

Gene ID	Gene name	Fold Change	FDR
ASA			

LTF	lactotransferrin	11.096	2.12E-03
LIX1	limb and CNS expressed 1	10.541	1.68E-02
KRT5	keratin 5, type II	9.044	2.12E-03
HOXD13	homeobox D13	9.044	2.12E-03
ISL1	ISL LIM homeobox 1	8.982	2.12E-03
HOXD10	homeobox D10	8.938	1.45E-02
TRPV6	transient receptor potential cation channel,	8.179	2.11E-02
KRT84	keratin 84, type II	7.890	2.12E-03
ATP12A	ATPase, H+/K+ transporting, nongastric,	7.600	2.12E-03
GBP2	Guanylate binding protein 2	7.321	2.12E-03
CUR			
HOXD12	homeobox D12	12.951	4.62E-02
HOXD13	homeobox D13	8.497	2.12E-03
TRPV6	transient receptor potential cation channel,	7.989	2.11E-02
IDO1	indoleamine 2,3-dioxygenase 1	7.989	2.12E-03
SLFN12L	schlafen family member 12-like	7.765	2.12E-03
HOXD10	homeobox D10	7.738	1.68E-02
GABRA4	gamma-aminobutyric acid (GABA) A	7.280	1.45E-02
BTNL2	butyrophilin-like 2	7.190	3.28E-02
Tgtp1	T cell specific GTPase 1	6.723	2.12E-03
Cxcl9	chemokine (C-X-C motif) ligand 9	6.498	2.12E-03
ASA+CUR			
HOXD12	homeobox D12	48.068	6.89E-03
KLK15	kallikrein-related peptidase 15	45.192	2.21E-02
LTF	lactotransferrin	21.511	2.12E-03
CNTN3	contactin 3 (plasmacytoma associated)	21.511	1.79E-02
KRT5	keratin 5, type II	20.649	2.12E-03
SHH	sonic hedgehog	20.224	8.28E-03

HOXD13	homeobox D13	19.685	2.12E-03
HOXD10	homeobox D10	18.126	5.44E-03
Xlr3c	X-linked lymphocyte-regulated 3C	16.656	1.22E-02
PSCA	prostate stem cell antigen	16.427	2.12E-03

Among the top 10 down-regulated genes in the ASA+CUR treated group, the expression of genes such as B3gnt6, Alb, Gpc3, Tmigd1, and Apol7e was more than 20-fold lower than that in tumors from the AOM/DSS group without any treatment. Similarly, the combined treatment with ASA and CUR increased the mRNA expression of Hoxd12, Klk15, Ltf, Cntn3, Krt5, and Shh by more than 20-fold compared to treatment with AOM/DSS alone. Because the combination treatment with ASA and CUR at half the dose of the single treatment effectively prevented colitis and colon carcinogenesis in our study, modulated broader targets, and induced/suppressed genes at higher fold change, we continued to investigate the possible biological function and pathways that were influenced by the combination regimen. Similar to the canonical pathway analysis we performed using the contrast of the control versus AOM/DSS-induced tumors, we were also interested in finding the significant pathways associated with the alterations of gene expression in ASA+CUR-treated tumors versus those treated with AOM/DSS alone. We identified a total of 235 canonical pathways significantly associated with the differentially expressed genes in the combination compared to the model group, with a P-value less than 0.05. The top 10 most significant pathways are displayed in Table 15. Interestingly, 6 of the top 10 pathways modulated by combination treatment compared to AOM/DSS alone, including hepatic fibrosis/hepatic stellate cell activation; agranulocyte adhesion and diapedesis; granulocyte adhesion and diapedesis;

atherosclerosis signaling; LPS/IL-1 mediated inhibition of RXR function; and the role of macrophages, fibroblasts and endothelial cells in rheumatoid arthritis, were also recognized as the top 10 pathways associated with differentially expressed genes in AOM/DSS-induced tumors compared to normal colonic tissue. This finding may suggest that these pathways not only play an important role in the carcinogenesis process induced by AOM/DSS but also contain the molecular targets potentially modulated by the combination treatment. Notably, some of the molecules in these pathways showed the opposite direction of change when contrasting the combination versus the model and the model versus the control group. For example, Mmp9 was significantly up-regulated in AOM/DSS-induced tumors compared to its expression in normal tissue, whereas its expression was down-regulated in tumors from the combination treatment compared to that in AOM/DSS-induced tumors.

Table 15: The 10 most significant canonical pathways regulated by ASA 0.01%+CUR 1% compared to tumors in Model group.

Genes in bold are down-regulated in the combination treatment.

Canonical Pathways	-log (p value)	Ratio	Target genes
Hepatic Fibrosis / Hepatic Stellate Cell Activation	6.75	15/187 (0.08)	IL1RL1,BAMBI,MMP13,**MYH11**,**CCL5**,**MYL7**,**MYL9**,CXCL3,NGFR,HGF,SERPI,NE1,COL9A2,**MMP9**,COL7A1,TNFRSF11B
Agranulocyte Adhesion and Diapedesis	5.9	14/190 (0.07)	**CLDN15**,Ppbp,ITGA6,MMP13,**MYH11**,**CCL5**,**MYL7**,MYL9,CXCL3,

			Cxcl3,**Ccl6**,**ACTA1**,**MMP9**,MMP19
Granulocyte Adhesion and Diapedesis	5.45	13/179 (0.07)	**CLDN15**,IL1RL1,Ppbp,ITGA6,MMP13,**CCL5**,CXCL3,NGFR,Cxcl3,**Ccl6**,**MMP9**,MMP19,TNFRSF11B
LXR/RXR Activation	4.59	10/128 (0.08)	**ALB**,**APOB**,IL1RL1,NGFR,**SAA1**,**LPL**,PTGS2,**NOS2**,**MMP9**,TNFRSF11B
Atherosclerosis Signaling	3.92	9/125 (0.07)	**ALOX15**,**ALB**,**APOB**,**LPL**,MMP13,ALOX12,F3,**TPSAB1/TPSB2**,**MMP9**
Glucocorticoid Receptor Signaling	3.43	13/281 (0.05)	**Hspa1b**,**HSPA1A/HSPA1B**,**TAT**,**PCK1**,**CCL5**,KRT36,**CD3G**,CXCL3,ANXA1,PTGS2,NRIP1,**NOS2**,SERPINE1
Role of IL-17A in Arthritis	2.81	5/56 (0.09)	CXCL3,MMP13,**CCL5**,PTGS2,**NOS2**
LPS/IL-1 Mediated Inhibition of RXR Function	2.65	10/224 (0.04)	**ALDH1B1**,**HS3ST3B1**,**FABP2**,ALDH1A3,IL1RL1,NGFR,**FABP4**,**CYP2C9**,**HMGCS2**,TNFRSF11B
Role of Macrophages, Fibroblasts and Endothelial Cells in Rheumatoid Arthritis	2.64	12/302 (0.04)	WNT10A,IL1RL1,NGFR,DKK2,**LTB**,MMP13,**FZD9**,**SFRP1**,**CCL5**,**NOS2**,**FZD2**,TNFRSF11B
Role of Osteoblasts, Osteoclasts and Chondrocytes in Rheumatoid Arthritis	2.63	10/225 (0.04)	WNT10A,IL1RL1,NGFR,DKK2,MMP13,**FZD9**,**SFRP1**,**FZD2**,IL11,TNFRSF11B

5.3.5 The subset of genes modified by AOM/DSS-induced tumors was also influenced by ASA+CUR

In light of the finding that some molecules in the shared pathways changed in the opposite direction, we further compared the significant differentially expressed genes in the following two data sets: the model versus the control and the combination versus the model groups. A total of 54 genes were found to be regulated by AOM/DSS and the combination treatment in the opposite direction (Figure 22). Specifically, 13 genes that were significantly down-regulated by AOM/DSS alone (the expression in the control colon tissue was set to 1) were further up-regulated by the combination treatment when we set the expression in the AOM/DSS group to 1. Forty-one significantly up-regulated genes in tumors induced with AOM/DSS alone were decreased by the combined treatment of ASA+CUR. Thus, these 54 genes might represent a set of molecular targets that underlies the preventive action of the combination of ASA+CUR in the AOM/DSS-induced model.
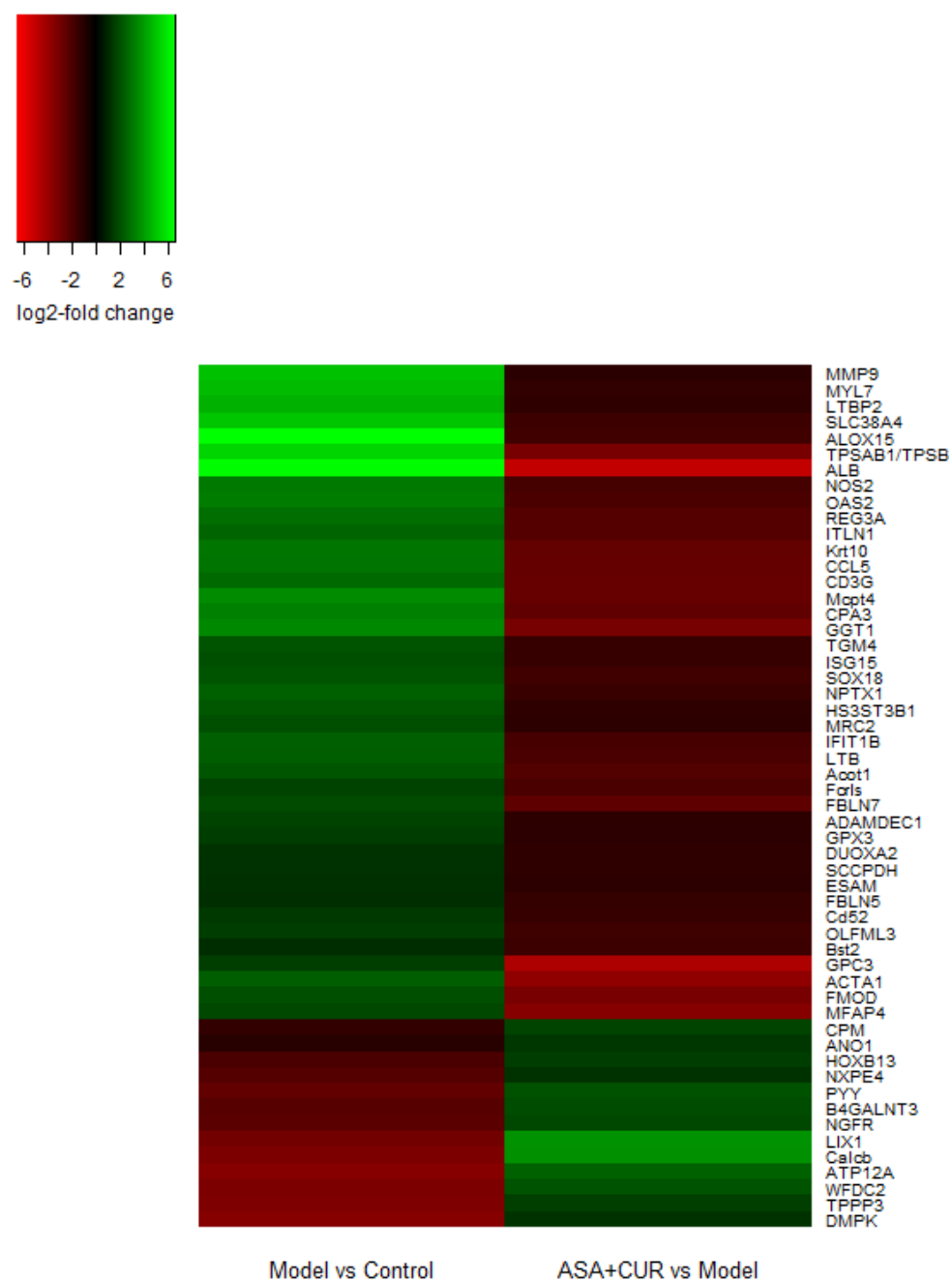
Figure 22: The list of 54 genes that showed regulation in the opposite direction when comparing the model versus the control and the combination versus the model groups.

There were 13 genes that were down-regulated in the model group compared to the control group, and their expression was up-regulated by the combination of ASA and CUR. There were 41 genes that were up-regulated in the model group compared to control group, and their expression was down-regulated by the combination of ASA and CUR.
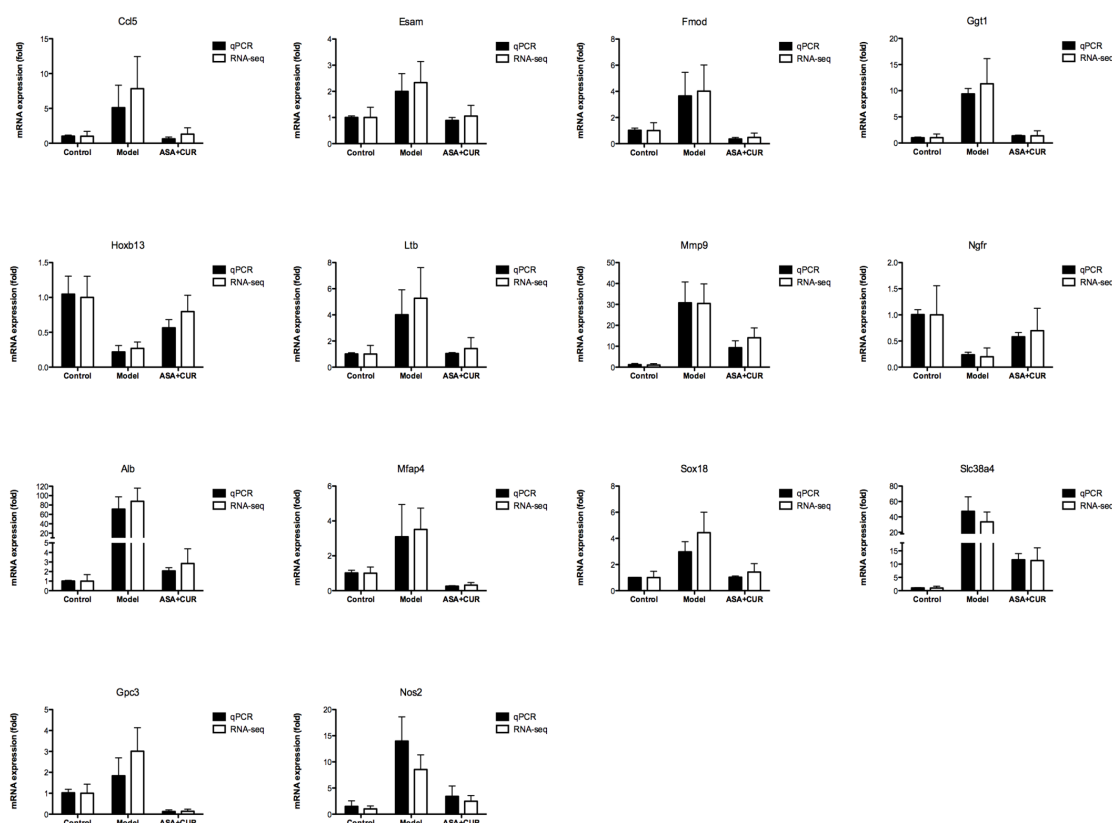
Figure 23: Validation of the mRNA expression of selected genes that showed regulation in the opposite direction when comparing AOM/DSS alone and the combination of ASA and CUR.

mRNA isolated from the colonic tissues of mice from the control group and tumors from mice receiving 0.01%ASA+1% CUR was subjected to qPCR analysis. Black bar: the

qPCR results are presented as the fold change compared with the control group using Gapdh as the endogenous control. White bar: fold change from the RNA-seq analysis. The data are presented as the mean ± SD (n = 2).

Given the potential functional role of the set of genes presented in Figure 22, we randomly selected 14 genes and validated their expression using qPCR analysis. As shown in Figure 23, the trend of fold change determined by qPCR (black bar) was overall in accordance with the fold change observed by RNA-seq (white bar). Among these 14 genes, the relative mRNA expression of Hoxb13 and Ngfr was suppressed in AOM/DSS-induced tumors, whereas ASA+CUR treatment could alleviate this suppression. Furthermore, the mRNA expression of Ccl5, Esam, Fmod, Ggt1, Ltb, Mmp9, Alb, Mfap4, Sox18, Slc38a4, Gpc3, and Nos2 were all increased in AOM/DSS-induced tumors, although combined treatment with ASA+CUR could ameliorate this induction.

5.4 Discussion

In the present study, we investigated the preventive effect of dietary administration of ASA and CUR in AOM/DSS-induced CAC in C57/BL6 mice. Although oral feeding of CUR at a dose of 2% has been shown to prevent tumor formation in AOM-induced mice and Apc$^{min/+}$ mice previously (272, 288), our study provides the first evidence that dietary administration of CUR (2%) effectively suppresses tumor multiplicity and tumor incidence in inflammation-related CRC induced by AOM/DSS (Figure 19B and C). However, to our surprise, ASA treatment in the current study in C57BL/6 mice was not as effective as in our recent study in AOM/DSS-induced CF-1 mice (271). In addition,

another recent study found that ASA at a similar dose failed to significantly inhibit the tumor number in AOM/DSS-induced Balb/c mice (235). The discrepancy in the effect of ASA in these two previous studies and our current study could possibly be explained by the presence of strain differences in the susceptibility to AOM/DSS-induced colonic tumorigenesis (289), suggesting that the chemopreventive effect of ASA in AOM/DSS-induced CAC might be strain specific. Further studies comparing the preventive effect of ASA against CRC in different strains of animals and different ethnicities of patients should be considered.

The highlight of the current study is that we investigated the effect of concomitant administration of ASA and CUR in an AOM/DSS-induced CAC model for the first time. Our results indicate that combined treatment with ASA and CUR is effective at reducing tumor incidence and tumor multiplicity (Figure 19B and C). Although mice in the combination group received a low dose of ASA (0.01%) and CUR (1%), the tumor incidence and multiplicity were similar to those for CUR alone at a higher dose (2%) and much lower than those for ASA alone at 0.02%. Notably, the equivalent human dose of the combinational treatment in the present study is approximately 55 mg/day ASA + 5.5 g/day CUR, which is more feasible and will possibly lead to less adverse effects from chronic use of ASA in humans compared to single treatment with ASA at 110 mg/day or CUR at 11 g/day. With the help of RNA-seq, we established, for the first time, a global transcriptome profile associated with ASA, CUR, and their combination in AOM/DSS-induced tumors. When comparing the gene expression profiles of tumors from these three treatment groups (ASA, CUR, and both) to those from AOM/DSS induction alone without any intervention, we found that the combination treatment, even at a lower dose,

had an impact on a larger gene set (344 differentially expressed genes) than for ASA alone (99 differentially expressed genes) or CUR alone (189 differentially expressed genes) (Figure 20A and B). In addition, when we looked at a smaller set of significant differentially expressed genes modulated by all three treatment groups (ASA, CUR, and their combination), the combined treatment with ASA+CUR resulted in a slightly higher fold change than ASA alone or CUR alone (Figure 20C and Figure 21). These results suggest that co-administration of ASA and CUR at a lower dose may provide a promising preventive regimen against CAC, possibility by targeting more molecular targets and magnifying the fold change of certain genes. Interestingly, other than the impact at the molecular level, as we showed in the current study by combination of ASA and CUR, a previous study reported that the stability of CUR could be improved in the presence of ASA, whereas the stability of ASA was not affected by the presence of CUR (290). In addition, the cellular uptake of CUR and the cytotoxicity of CUR in HCT116 cells could be enhanced when incubated with ASA (290). Moreover, it was postulated that the acidic properties and antioxidant potential of ASA could provide favorable conditions for stabilizing CUR and prevent the degradation of CUR (291). Therefore, further studies should be carried out to determine if co-administration of ASA and CUR could enhance the absorption and half-life of CUR in humans.

In addition to investigating the effect of the chemopreventive agents ASA, CUR, and their combination in the AOM/DSS-induced CAC model, the present study also aimed to identify the global profile of gene expression changes related to AOM/DSS-induced tumors. The top-ranked genes with decreased or increased expression that are listed in Table 11 may provide novel insight to facilitate the discovery of critical genes

driving the carcinogenesis process in AOM/DSS-induced CAC as well as potential therapeutic targets and biomarkers for the prevention of CAC. For example, the expression levels of two matrix metalloproteinases [MMP7 (fold change = 389.9) and MMP10 (fold change = 91.5)] were dramatically up-regulated in AOM/DSS-induced tumors compared to the levels in normal colonic tissue (Table 11). MMPs comprise a large family of zinc-dependent endopeptidases that are involved in the physiological and pathological remodeling of the extracellular matrix in proliferation, angiogenesis, tumor invasion, and metastasis (292). However, their function in inflammation-associated colorectal cancer remains largely unknown. Our observation of increased expression of MMP7 in tumors from AOM/DSS-treated mice was in accordance with various previous studies showing that MMP7 is overexpressed in advanced stages of CRC (293) and is a potential prognostic marker (294, 295). On the contrary, the function of MMP10 in CRC is more ambiguous. Although the overexpression of MMP10 in the serum of CRC patients is considered to be a prognostic marker (295) and the expression of MMP10 is up-regulated in DSS-induced colitis in mice (296), MMP10 knockout mice develop more severe colitis after DSS exposure, suggesting that MMP10 may play a beneficial role in favor of colitis resolution (296). Our results show for the first time that MMP10 is dramatically elevated in AOM/DSS-induced tumors; however, the mechanisms underlying the role of MMP10 in tumorigenesis and metastasis require further investigation. In addition, chemokine (C-X-C motif) ligand 6 (CXCL6) is another target that showed significantly higher expression in tumors than in normal tissue (fold change = 181.9, Table 11). CXCL6 belongs to the family of ELR$^+$ CXC chemokines that play important roles in the activation and recruitment of neutrophils at sites of inflammation

(297), and CXCL6 has been shown to be overexpressed in the inflamed tissue of IBD patients (298). Nevertheless, Rubie et al. found that although other members of the ELR$^+$ CXC chemokine family (CXCL1 and CXCL5) were up-regulated in colorectal adenoma and carcinoma tissue specimens, the expression of CXCL6 was not significantly altered (299). Thus, it is possible that CXCL6 only plays a pivotal role in CRC associated with IBD instead of hereditary CRC, but this hypothesis requires further investigation. Furthermore, a member of the carbonic anhydrases, CA III, was shown for the first time to be down-regulated in AOM/DSS-induced tumors (fold change = 0.028, Table 11). CA isozymes have been considered to be important players in maintaining the pH homeostasis in tumors and thereby modulate the behavior of cancer cells. Among these isozymes, CA I, II, IV, VII, and XIII were implicated as potential tumor suppressors in CRC with down-regulated expression in CRC specimens compared to normal tissue (300-302). Specifically, it was found that promoter hypermethylation may contribute to the silence of CA IV in CRC, where its tumor suppressor action involves the inhibition of the Wnt signaling pathway (301). The expression of CA III may be associated with the invasiveness and metastasis of liver cancer (303); however, its role in CRC has not yet been investigated. Based on our current observation that the expression of CA III was down-regulated in AOM/DSS-induced tumors, the tumor suppressive potential of CA III and the mechanism leading to the inactivation of CA III in CAC should be explored in human specimens.

Our canonical pathway analysis highlighted "Hepatic Fibrosis/Hepatic Stellate Cell Activation" as the most significantly regulated pathway influenced by AOM/DSS-induced tumors (Table 12). Interestingly, this pathway was also recognized as the most

significant pathway containing the differentially expressed genes regulated by ASA+CUR compared to the model group (Table 15). Hepatic stellate cells (HSCs) are considered to be critical players in colon cancer-induced liver metastasis. It was found that colonic tumor-derived factors lead to the activation of HSCs in the liver, and in turn, activated HSCs promote hepatic fibrosis and produce cytokines, chemokines, and matrix-degrading MMPs to enhance metastatic growth in the liver (304). Our results show that up-regulation of cytokines (such as CCL5, IL1B, and TNF), growth factors (such as PGF and TGFB1), and MMPs (such as MMP2, MMP9, and MMP13) in colonic tumors may be involved in the activation of HSCs in the liver in AOM/DSS-induced CAC. In addition, concomitant administration of ASA and CUR significantly down-regulated the expression of CCL5 and MMP9, which showed elevated expression in AOM/DSS-induced colonic tumors in the hepatic fibrosis/HSC activation pathway. However, our current study did not examine the effects of ASA, CUR, or their combination on the inhibition of colon cancer-induced liver metastasis, which may be worth investigating in the future. Other canonical pathways worth noting are the "Agranulocyte Adhesion and Diapedesis" and "Granulocyte Adhesion and Diapedesis" pathways. These two pathways are associated with the migration of leukocytes and immune cells from the vascular system to sites of inflammation. Our results suggested that these two pathways were the top significant pathways involved in AOM/DSS-induced colonic tumorigenesis and contain the molecular targets that underlie the preventive action of the combined treatment of ASA and CUR (Table 12 and Table 15). Further research is warranted to understand the pivotal role of agranulocytes, granulocytes, and their mediators in the constitution of the tumor microenvironment during the progression of CAC and how the

combination of ASA and CUR suppresses CAC by modulating the infiltration of these inflammatory cells.

Additionally, we identified a subset of 54 differentially expressed genes as the potential molecular targets underlying the protective action of the concomitant administration of ASA and CUR in AOM/DSS-induced CAC. Among these genes, the overexpression of 41 genes was found in AOM/DSS-induced tumors, while their expression was down-regulated by ASA+CUR (Figure 22). Some of these genes, such as REG3A (305), MMP9 (306), NOS2 (271), CCL5 (307), LTB (308), DUOXA2 (309), and BST2 (310), were also found to be overexpressed in AOM/DSS-induced CAC, CRC specimens, or CRC cell lines in previous reports, and inhibition of these targets has been implicated as a promising therapeutic strategy in CRC. On the contrary, 13 genes were identified with a decreased expression in tumors from the model group, and their expression was restored by the combination of ASA and CUR (Figure 22). Some of these genes, such as HOXB13 (311) and NGFR (312), have been suggested to be tumor suppressors with diminished expression in CRC in previous studies. The modulation of the genes listed in Figure 22, except for MMP9 and NOS2 (271), following treatment with ASA, CUR, or the combination of ASA and CUR has not been investigated previously. However, we also noticed that the alterations of several genes in our list were not in accordance with previous reports. For example, ANO1, a gene with decreased expression in AOM/DSS-induced tumors in our study, was reported to be overexpressed in CRC cell lines (313). In addition, GPX3 expression was increased in tumors from the model group, whereas Barrett et al. showed that GPX3 was down-regulated in AOM/DSS-treated mice (314). Although further detailed mechanistic studies are needed,

our current study provides a novel list of genes that may be responsible for the preventive effect of concomitant administration of ASA and CUR in AOM/DSS-induced CAC.

Unlike the 54 genes regulated by AOM/DSS versus the ASA/CUR combination treatment displayed opposite direction, we observed 104 genes showed same direction of regulation by AOM/DSS and the combination treatment (data not shown). Interestingly, several tumor suppressor genes were in this set of genes and their expression was down-regulated by AOM/DSS and concomitant administration of ASA and CUR could further decrease their expression in tumors. For instance, the relative expression of CDX2 (a widely known tumor suppressor gene (315), with decreased expression in ~30% human CRC (316)) was 0.48 in AOM/DSS-induced tumors and 0.05 in tumors from combination group (the expression of CDX2 in control group was set as 1). The inhibition of these tumor suppressor genes by the combination treatment may be one of the reasons for the tumor growth in the presence of these chemopreventive agents ASA/CUR. In addition, the expression of several membrane transporters in tumors was altered by the combination of ASA and CUR, which could change the influx or efflux of the chemopreventive agents in tumor cells. The altered expression of transporters could also influence the uptake of essential nutrients for tumor growth and survival, therefore making the tumors resistant to ASA and CUR and leading to the tumor growth in the presence of chemopreventive agents.

5.5 Conclusions

In summary, our study is the first to show that concomitant administration of ASA 0.01% + CUR 1% effectively attenuates tumor growth in the AOM/DSS-induced CAC model. Our results provide a quantitative gene expression profile of AOM/DSS-induced tumors as well as tumors from mice treated with ASA, CUR, and their combination at half of the dose. Furthermore, a small set of genes was postulated as potential molecular targets involved in the action of ASA+CUR in the prevention of AOM/DSS-induced CAC. These findings provide novel insights that further the understanding of the carcinogenesis of inflammatory CRC as well as the mechanisms underlying the preventive effect of ASA and CUR in CAC.

6. Summary

Emerging evidence has suggested that epigenetic modifications frequently occur in the development of colorectal cancer. Accumulation of both genetic and epigenetic alterations transform normal epithelium into adenocarcinomas (182). There have been major advances in our understanding of cancer epigenetics over the last decade and some of these identified epigenetic alterations have been developed to clinical biomarkers in the diagnostic, prognostic, preventive, and therapeutic application of colon cancer (182). In Chapter 2 of this dissertation, we obtained the global DNA methylation profile in the well-established Apc $^{min/+}$ intestinal tumorigenesis mouse model using MeDIP-seq approach and identified extensive aberrant DNA methylation in polyps. It was found that these differentially methylated genes were mainly attributed to functions and networks in cancer, the cell cycle, and gastrointestinal diseases and were situated in several important canonical pathways. In Chapter 3 of this dissertation, we focused on DLEC1 gene, confirmed its role as tumor suppressor, determined its DNA methylation status, and found its involvement in the suppression of anchorage-independent growth. In Chapter 4 of this dissertation, we investigated the histone modification in AOM/DSS-induced inflammation associated colorectal cancer. Our results suggested that colitis-accelerated colorectal cancer induced by AOM/DSS is accompanied with activation of the HDACs, reduced level of global H3K27ac, and increased accumulation of H3K27ac mark at the promoters of several pro-inflammatory genes. Furthermore, we provided a quantitative gene expression profiles in AOM/DSS-induced colonic tumors in Chapter 5 of this dissertation. Taken together, the differentially methylated genes we identified, the

methylation status of DLEC1, the changes in HDACs and H3K27ac level, as well as the differentially expressed genes we observed in this dissertation provided fundamental information to understand the involvement of epigenetic and genetic modifications in colorectal cancer. Further studies are needed to validate these findings in clinical samples.

Colorectal cancer is a disease highly associated with environmental and lifestyle factors and usually undergoes a long precancerous stage. Hence, chemoprevention has gained increasing interest as an attractive option in the management of colorectal cancer. We focused on two promising chemopreventive agents, curcumin and aspirin in this dissertation research and elucidated their potential molecular mechanisms in the epigenetic perspective. Results from Chapter 3 proposed a novel epigenetic mechanism underlying the chemopreventive effect of curcumin in attenuating clonogenicity of HT29 cells: the reduction of CpG methylation of DLEC1 promoter and the modification of the protein expression of DNMTs and HDACs. In Chapter 4 of this dissertation, we demonstrated the preventive effect of the chronic use of low-dose aspirin and its role in histone modification in inflammatory colorectal cancer animal model. We found that aspirin inhibited HDAC activity, restored overall H3K27ac, and reduced H3K27ac enrichment in Tnf-α, iNos, and iL6 promoters, likely leading to the suppression of pro-inflammatory genes. In Chapter 5 of this dissertation, we showed that low dose combination of curcumin and aspirin effectively inhibited tumor growth in AOM/DSS-induced colorectal cancer animal model and a small set of genes was postulated as potential molecular targets involved in the action of curcumin and aspirin. Collectively, this dissertation have provided convincing results in support of chemopreventive potential of aspirin and curcumin and its plausible mechanisms in colon cancer cell lines

and animal models. The ultimate proof of the efficacy of aspirin and curcumin, especially

their combination, in colon cancer prevention requires well-designed clinical trials.

Appendix 1

Epigenetic regulation of keap1-nrf2 signaling [11],[12]

A1.1 Introduction

Mammalian cells are constantly exposed to oxidative stresses that are regarded as some of the most important and ubiquitous causes of neoplastic, metabolic, cardiovascular, neurodegenerative, and many other chronic diseases. To deal with the deleterious effects of oxidative stresses, cells have evolved elaborate and powerful cellular defense machinery against reactive oxygen species (ROS). Central to this cellular defensive machinery is the transcription factor nuclear factor erythroid 2-related factor 2 (Nrf2) and its negative regulator kelch-like ECH-associated protein 1 (Keap1). Under basal conditions, Keap1 acts as an adaptor between Nrf2 and the ubiquitination ligase Cullin-3 (Cul3) and promotes the proteasomal degradation of Nrf2. Upon modification of specific thiols, Keap1 allows Nrf2 to translocate into nucleus and activate the expression of a wide array of antioxidative metabolizing/detoxifying and many other genes by binding to the antioxidant response element (ARE) in their regulatory regions (317). In addition to the Keap1-Nrf2 interaction, the transcriptional activity of Nrf2 is regulated by a complex signaling network (318).

---

[11] Part of this chapter has been published in Free Radical Biology and Medicine 2015 Nov; 88(Pt B): 337-49

[12] **Key Words**: DNA methylation; Epigenetic; Histone modification; Keap1; MicroRNAs; Nrf2

The Keap1-Nrf2 signaling axis is the pivotal coordinator of cytoprotective responses towards oxidative/electrophilic stimuli and protects cells against chemical insults. Therefore, activation of Keap1-Nrf2 signaling has been widely accepted as an important strategy to prevent oxidative damage-related chronic diseases, including cancer (319). However, upregulated Nrf2 activity in cancerous cells leads to resistance to radio- and chemotherapies (320). Furthermore, activation of Nrf2 confers neoplastic cells with growth and survival advantages during their transformation and progression (321). Indeed, although Nrf2-knockout mice were more susceptible to chemical-induced carcinogenesis than control mice, high expression of Nrf2 in tumors predicts a poor prognosis, and inhibition of Nrf2 sensitizes cancer cells to chemotherapeutic drugs (322). Such apparently paradoxical roles of Nrf2 in different stages of cancer initiation and progression are essentially arose from the "double-edged sword" nature of ROS in cancer, and have been extensively investigated and reviewed (321). However, the roles of Nrf2 in other ROS-related diseases such as neurodegenerative diseases, diabetes, and cardiovascular disease are simply protective. Thus, the mechanisms regulating Keap1-Nrf2 signaling are expected to produce different even opposite outcomes, and the preventive or therapeutic applications of Keap1-Nrf2 signaling modulators have to be carefully evaluated according to the context.

Importantly, very different expression levels and activities of Keap1 and Nrf2 have been observed at different stages of different pathological processes. Functional somatic mutations or single nucleotide polymorphisms (SNPs) of Keap1 or Nrf2 occur in many types of cancer and have been utilized to explain the variations in expression and activity of Keap1 and Nrf2 (320). However, although the expression of Keap1 and Nrf2

exhibits significant inter-individual variations in these cancers, somatic mutations exist in only a small portion of cancer tissues (323, 324). For example, Solis et al. detected nuclear Nrf2 expression in 26% and low or absent Keap1 expression in 56% of non-small cell lung cancers (NSCLCs), and found that this expression correlated with clinicopathologic characteristics; nevertheless, mutations in the NFE2L2 and KEAP1 genes were very uncommon in the examined samples (324). Therefore, alternative mechanisms must exist to regulate Keap1 and Nrf2 expression. Recently, a body of evidence is emerging that shows that the Keap1-Nrf2 signaling can be regulated by epigenetic mechanisms in cancers as well as in other diseases, and the present chapter will focus on the epigenetic regulation of Keap1-Nrf2 signaling as schematically depicted in Figure 24.

Figure 24: Schematic model depicting epigenetic modifications of Nrf2 and Keap1.

Left and right panel shows epigenetic modifications that lead to down- and up-regulation of Keap1-Nrf2 signaling, respectively.

A1.2 Epigenetic modifications

The term epigenetics refers to the study of heritable alterations in gene expression that are not due to changes in the primary DNA sequence. DNA-based mechanisms (DNA methylation and histone modification) and RNA-based mechanisms (non-coding RNA) are known to mediate these heritable gene expression alterations (4). The addition of a methyl group to cytosine bases and covalent modifications of histones at a given promoter can modulate DNA accessibility and chromatin structure, ultimately regulating gene transcription (4). By targeting mRNA degradation, translation inhibition, and chromatin architecture, non-coding RNAs interfere with various levels of gene expression (325). Furthermore, interactions between DNA methylation, histone modification, and non-coding RNAs in controlling the epigenome landscape have been recognized; however, the regulatory network remains elusive.

A1.2.1 Epigenetic modifications and human diseases

Epigenetic mechanisms, together with genetic factors, are fundamental for maintaining cellular differentiation and mammalian development (326). However, the disruption of either epigenetic modifications or genetic functions is associated with

abnormalities in various signaling pathways and can lead to the pathogenesis of many human disorders. Unlike genetic changes, aberrant epigenetic marks tend to be acquired in a gradual process (327). Long-lasting effects of environmental factors and the aging process introduce alterations in the landscape of the epigenome (328, 329). Thus, studies of epigenetic disruptions are primarily focused on chronic diseases, especially cancer. Studies of epigenetic abnormalities associated with carcinogenesis suggest that epigenetic alterations may interact with genetic dysregulation at all stages to initiate and promote cancer (6, 7). Global DNA hypomethylation, regional hypermethylation at specific promoters, global reduction of monoacetylated H4K16, and overall microRNA (miRNA) down-regulation are characteristics of cancer cells (143, 330). In addition, the important role of epigenetic modifications in diabetes (331), autoimmune diseases (332), cardiovascular diseases (333), and neurodegenerative diseases (334) has been recognized.

A1.2.2 Epigenetic therapy

Unlike genetic mutations, epigenetic disruptions in diseases are potentially reversible. For example, genes that have been transcriptionally silenced by epigenetic modifications can be reactivated through epigenetic mechanisms because these genes remain intact, whereas genetic mutations are permanent. Given that epigenetic abnormalities play an important role in human diseases, including cancer, increasing efforts have been focused on the development of agents that target epigenetic mechanisms. Successful examples of the use of epigenetic therapies in the treatment of cancer include hypomethylating drugs and histone deacetylase inhibitors that have been

approved by the US Food and Drug Administration (FDA) (335). In addition, the second generation of novel potential epigenetic therapies, such as histone methyltrasferase inhibitors and epigenetic reader protein inhibitors, have been discovered and are currently under investigation (336). Furthermore, numerous studies have suggested that the consumption of dietary phytochemicals may alter epigenetic modifications and reverse abnormal gene transcription, thereby preventing certain diseases, including cancer (124).

A1.2.3 Epigenetic modifications and oxidative stress

Oxidative stresses are involved in almost all chronic diseases including ageing. Interestingly, epigenetic mechanisms have been reported to be profoundly involved in oxidative stress responses. ROS, such as hydroxyl radicals, can cause serious DNA lesions and lead to mutagenesis; such lesions can also result in global DNA hypomethylation (337, 338). For instance, the DNA oxidization product 8-OHdG strongly inhibits the methylation of adjacent cytosines and impairs the binding of methyl-CpG-binding domain proteins (MBDs) (338). Moreover, demethylation of methyl-CpG by Ten-eleven translocation (TET) enzymes, a family of Fe(II)/α-ketoglutarate-dependent dioxygenases, is a highly oxidative stress labile process. It involves serial oxidation of 5-methylcytosine to 5-hydroxymethylcytosine, which inhibits DNA methyltransferase 1 (DNMT1) recognition, then to 5-formylcytosine and 5-carboxylcytosine, and finally be excised from DNA by glycosylases (337). Furthermore, histone modifications can also be modulated by oxidative stresses (339). In addition, many Nrf2-activating chemopreventive compounds have been identified as epigenetic modulators, and the

expression of several Nrf2-target genes has been found to be regulated epigenetically (340-343). Therefore, it is expectable that complex interactions exist between Keap1-Nrf2 signaling and epigenetic modifications.

A1.3 Regulation of the Keap1-Nrf2 signaling pathway by DNA methylation

DNA methylation is widely observed in organisms ranging from prokaryotic bacteria to vertebrates; however, in vertebrates, heritable methylation only occurs at the 5 position of the cytosine pyrimidine ring in CpG dinucleotides. CpG methylation serves as an epigenetic mechanism to memorize the transcriptional state (120). In mammalian cells, DNA methylation patterns are established during embryogenesis and development or under certain physiological and pathological conditions by de novo DNMT3a and DNMT3b, then maintained by DNMT1 during DNA replication. On the other hand, DNA demethylation can occur through active demethylation by TET enzymes or through passive demethylation caused by the absence of DNMT1 activity during DNA replication (344). Approximately 60% of human genes contain clusters of CpG sites called CpG islands in their GC-rich promoter regions, and their expression can be epigenetically regulated by DNA methylation (345). The methyl moiety lies in the major groove of the DNA helix and can potentially interact with many DNA-binding proteins. CpG methylation in the binding sequences can inhibit the binding of transcription factors and the initiation of transcription, or it can attract MBDs, such as MBD1, MBD2, and MeCP2, which can recruit co-repressor complexes to silence gene transcription (345). In addition, DNA methylation also collaborates with histone modifications to regulate chromatin

accessibility and gene transcription. MBDs often associate with histone deacetylases (HDACs) and histone lysine methyltransferases (HKMTs) to regulate histone modifications (120).

The hypermethylation of several genes regulated by Keap1-Nrf2 signaling has been investigated for decades. For example, the hypermethylation of CpG islands in the promoter region and expression silencing of pi class glutathione S-transferase (GSTPi) have been observed in prostate cancers (342). NAD(P)H:quinone oxidoreductase 1 (NQO1), UDP-glucuronosyltransferases 1A1 (UGT1A1), glutathione peroxidase (GPX), and manganese superoxide dismutase (MnSOD) have also been reported to be regulated by promoter methylation (341, 346-348). Regulation of Keap1 and Nrf2 expression by DNA methylation has been investigated in recent years and is discussed below and summarized in Table 16.

Table 16: DNA methylation regulates Keap1-Nrf2 signaling pathway.

Target	Diseases	Methylation	Experimental Model	Impact on Keap1-Nrf2	Outcomes	Ref
Nrf2	Prostate cancer	↑	TRAMP mice and TRAMP-C1 cells	↓ Nrf2, NQO1, GST mu	Prostate carcinogenesis	(26, 349, 350)
		↑	Human prostate cancer tissues	↓ Nrf2	Advanced stages	(351)
		↓	TRAMP-C1 or LNCap cells treated by 5-Aza/TSA	↑ Nrf2, NQO1, HO-1 ↓ DNMTs, HDACs	Not Applicable	(26, 351)
		↓	TRAMP-C1 cells or TRAMP mice treated by γ-TmT, curcumin, sulforaphane, 3,3'-diindolylmethane, or Z-Ligustilide	↑ Nrf2, NQO1, HO-1 ↓ DNMT, HDAC	Inhibition of carcinogenesis	(27-30, 87)
	Skin cancer	↓	Mouse skin epidermal JB6 P+ cells treated by sulforaphane, apigenin, or Tanshinone IIA	↑ Nrf2, NQO1, HO-1 ↓ DNMT, HDAC	Inhibition of TPA-induced transformation	(68, 93, 107)
Keap1	Lung cancer	↑	Human lung cancer tissues and cell lines	↓ Keap1	Not Applicable	(352, 353)
			Human non-small cell lung cancer	Not Applicable	Worse prognosis	(354)
	Gliomas	↑	Human malignant gliomas	↓ Keap1	Better prognosis	(355)
	Breast cancer	↑	Primary breast cancers and pre-invasive lesions	↓ Keap1	Higher mortality in triple-negative; reduced relapse	(356)
	Colorectal cancer	↑	Colorectal cancer cell lines and surgical specimens	↓ Keap1 ↑ Nrf2, NQO1, AKR1C1	Not Applicable	(357)
	Prostate cancer	↑	Prostate cancer cell lines	↓ Keap1; ↑ Nrf2, HO-1, NQO1, Gclc	Increased tumor growth, enhanced chemo- and radio-resistance	(358)
	Thyroid	↑	Papillary thyroid carcinoma	↓ Keap1	Not Applicable	(359)

cancers			↑ Nrf2-regulated genes		
Age-related cataracts	↓	Cataractous lenses with increasing age or in diabetes patients; human lens epithelial cells treated by homocysteine, valproic acid, methylglyoxal or selenite	↑ Keap1, TET1 ↓ Nrf2, CAT, GST, DNMT	Elevated ROS, age-related cataracts	(360-366)
Diabetic cardiomyopathy	↓	Myocardial biopsies of non-diabetic and type-2 diabetic cardiomyopathy patients	↓ Keap1 ↑ Nrf2-regulated genes	Failure of Nrf2 mediated antioxidant system	(367)

A1.3.1 Regulation of Nrf2 expression by DNA methylation

The protein expression of Nrf2 and the Nrf2-targeted gene heme oxygenase 1 (HO-1) was abolished in skin tumors in a skin cancer mouse model (368). Similar results were obtained in a transgenic adenocarcinoma of mouse prostate (TRAMP) model, in which the expression of Nrf2 and its downstream target genes, such as UGT1A1, glutathione S-transferase Mu 1 (GSTM1), and NQO1, were gradually down-regulated in prostate tumors during tumorigenesis (349). Frolich et al. also reported that the expression of Nrf2 and GST mu family genes was significantly decreased in TRAMP prostate tumors (350). More importantly, the expression of Nrf2 and several downstream genes such as GST and NQO1 has been found to be decreased in human prostate cancers compared with normal epithelia or localized adenoma (26, 350). Yu et al. identified CpG islands in the promoter regions of human, rat, and mouse NFE2L2 genes and demonstrated that the suppression of Nrf2 expression in TRAMP prostate tumors and TRAMP C1 cells was mediated by the hypermethylation of specific CpG sites in the Nrf2 promoter (26, 350). Further study by Khor et al. using human prostate cancer samples identified three specific CpG sites in the Nrf2 promoter that were hypermethylated during prostate cancer progression (351). Moreover, treatment of TRAMP cells with the DNMT inhibitor 5-aza-2'-deoxycytidine (5-aza) and the HDAC inhibitor trichostatin A (TSA) could restore Nrf2 expression, which was accompanied by the dissociation of MBD2, MeCP2, and methylated histones (26).

Interestingly, inhibition of methylation or demethylation of the Nrf2 promoter has been found to be involved in the action of many chemopreventive chemicals. Dietary feeding of a γ-tocopherol–rich mixture of tocopherols (γ-TmT) dose-dependently

suppressed prostate tumorigenesis and hypermethylation of the Nrf2 promoter in TRAMP mice and was associated with higher Nrf2 and NQO1 protein levels. γ-TmT treatment inhibited the protein expression of DNMT1, DNMT3a, and DNMT3b in the prostate of TRAMP mice, suggesting that γ-TmT inhibited both de novo and sustained methylation (27). It has been well documented that many dietary cancer chemopreventive compounds, including curcumin (243), isothiocyanates (369), tea polyphenols (370), and genistein (77), are epigenetic modifiers (340). Some of these compounds, such as curcumin, sulforaphane, 3,3'-diindolylmethane, and Z‑Ligustilide (from the traditional Chinese medicine Radix *Angelicae Sinensis),* were also found to demethylate the Nrf2 promoter and re-activate Nrf2 signaling in the prostate of TRAMP mice or TRAMP C1 cells, possibly through the inhibition of DNMT and HDAC expression (28-30, 87). The CpG sites in the promoter region of Nrf2 are heavily methylated in mouse skin epidermal JB6 P+ cells and could be demethylated by sulforaphane, apigenin, or Tanshinone IIA. Such demethylation was associated with suppression of TPA-induced transformation, reactivation of Nrf2 signaling, and expression of Nrf2 target genes, along with the inhibition of protein expression of DNMTs and HDACs (68, 93, 107). These findings suggest that Nrf2 expression during carcinogenesis can be epigenetically regulated through DNA methylation at specific CpG sites in its promoter and that such mechanisms could be targeted for cancer prevention. However, given the paradoxical roles of Nrf2 in the process of carcinogenesis, the exact impact of Nrf2 modulators on cancer would be context-sensitive.

A1.3.2 Regulation of Keap1 expression by DNA methylation

Loss of Keap1 function has been observed in many cancer tissues and is regarded as the main cause of Nrf2 over-activation. In addition to somatic mutations, the epigenetic regulation of Keap1 has been investigated in human tissues and cells of different diseases. Wang et al. first showed that Keap1 is highly expressed in BEAS-2B human normal bronchial epithelial cells but is down-regulated in a series of lung cancer cell lines and human lung cancer tissues. This down-regulation was accompanied by the hypermethylation of CpG sites in the Keap1 promoter region and could be restored by 5-aza treatment (352). Further studies by the same group suggested that hypermethylation of the Keap1 promoter abrogated the binding of stimulating protein-1 (SP-1), and 5-aza treatment restored SP-1 binding to the Keap1 promoter (353). In another study, using 47 pairs of NSCLC tissues and normal specimens, promoter methylation was detected in 47% of NSCLCs but in none of the normal tissues, whereas somatic mutations were detected in 15% of NSCLCs; patients harboring both alterations had the worst prognosis (354).

Similar results have been obtained in other cancers, including malignant gliomas and breast, colorectal, prostate, thyroid, and head and neck cancer cells. Frequent promoter hypermethylation and correlated down-regulation of Keap1 expression were observed in malignant gliomas and contributed to resistance to therapies and disease progression (355). Aberrant Keap1 promoter methylation was detected in more than half of primary breast cancers and pre-invasive lesions but not in normal breast tissues, whereas no Keap1 mutations were detected in examined breast cancer cases. Methylation was more frequent in ER-positive, HER2-negative than in triple-negative breast cancers, and Keap1 promoter hypermethylation predicted higher mortality risk in triple-negative patients

(356). Keap1 promoter methylation was also observed in 53% of colorectal cancer tissues, in 25% of adjacent normal mucosa, and in 8 out of 10 colorectal cancer cell lines analyzed (357, 371). Loss of Keap1 function in prostate cancer cells causes chemoresistance and radioresistance and promotes tumor growth. In addition to point mutations of Keap1 in various prostate cancer cell lines, down-regulation of Keap1 expression by promoter hypermethylation was identified in DU-145 prostate cancer cells (358). Hypermethylation is the major inactivating mechanism of Keap1 in thyroid cancers (70.6%) and head and neck cancers (29.3%) and is associated with a worse prognosis (359). Here again we saw the uncertainty of the outcomes produced by epigenetic regulation of Keap1-Nrf2 signaling in cancers: while silencing of Nrf2 by DNA methylation is implicated in carcinogenesis, activation of Nrf2 signaling by hypermethylation of Keap1 promoter is also associated with tumor progression and resistance to therapies.

On the other hand, Keap1 promoter hypermethylation in oxidative stress-related diseases other than cancers plays mainly protective roles. Increased oxidative stress during chronic aging is a major pathological factor of age-related cataracts (ARCs), especially in diabetes patients; therefore, impaired Keap1-Nrf2 signaling is proposed to be involved in the pathogenesis of ARCs (360). Although no SNPs in Nrf2 or Keap1 were found to be associated with Alzheimer's disease or age-related cataracts (372), demethylation of the Keap1 promoter accompanied by increased Keap1 and decreased Nrf2 expression was identified in cataractous lenses with increasing age or in diabetes patients, which may lead to failure of the cytoprotective system and increased oxidative stress (361, 362). Exposure to homocysteine resulted in endoplasmic reticulum (ER)

stress and the suppression of Keap1-Nrf2 signaling by ER-associated degradation (ERAD) and demethylation of the Keap1 promoter, elevated ROS generation and lens oxidation (360). Treatment of human lens epithelial cells (HLEC) with acetyllcarnitine prevented the effects of homocysteine and significantly increased the levels of Nrf2 and downstream antioxidant genes (363). Sodium selenite has been employed to induce cataracts in animal models and can suppress Keap1-Nrf2 signaling in HLECs by ERAD and Keap1 promoter demethylation, possibly by both reducing DNMT1/3a protein levels and inducing Tet1 expression (364). Methylglyoxal and valproic acid promote lenticular protein oxidation and cataract formation by almost the same mechanisms as selenite (365, 366). In addition, demethylation of the Keap1 promoter and increased Keap1 expression have been observed in diabetic cardiomyopathy, thus suppressing Nrf2 activity and disturbing the redox balance (367).

According to the observations described above, it would be of therapeutic interest to determine whether demethylation of the Keap1 promoter in neoplastic tissues could suppress tumor progression and resistance to therapies or whether the activation of Nrf2 signaling in lens epithelial cells could prevent cataract formation or the onset of other oxidative stress-initiated diseases.

A1.4 Histone modifications and the Keap1-Nrf2 signaling pathway

Eukaryotic DNA is wrapped by octomers of four core histone proteins into repeating nucleosomes, which are further folded into chromatin fibers (42). This highly organized and dynamic protein-DNA complex has two structurally and functionally

distinguishable configurations, namely, heterochromatin and euchromatin. Heterochromatin represents a highly condensed structure with repressed gene transcription as a result of low accessibility of transcription factors and RNA polymerase II to their recognition sequences, whereas euchromatin is loosely packed and more easily transcribed (373). It is suggested that posttranslational modifications of specific residues on the N-terminal tails of histones play a pivotal role in the modulation of the chromatin structure; ultimately, they regulate the transcriptional activity of a wide variety of genes. Here, we review and discuss the mutual effects of histone modifications and the Keap1-Nrf2 signaling pathway. Histone modifications shown to regulate the Keap1-Nrf2 signaling are summarized in Table 17.

Table 17: Histone modifications regulate Keap1-Nrf2 signaling pathway.

Target	Diseases	Modifications	Enzymes	Experimental Model	Impact on Keap1-Nrf2 and outcomes	Ref
Nrf2	Neuroinflammation and neurodegenerative diseases	Deacetylation of histones H3 and H4	HDACs	Astrocyte-rich cultures exposed to conditioned medium	High level of HDAC activity leads to: ↓Nrf2 and γGCL-M; ↓Nrf2-mediated antioxidant defense	(374)
	Chronic obstructive pulmonary disease	Histone acetylation	HDAC2	Human airway epithelial BEAS2B cells, monocyte-derived macrophages from COPD patients	Treatment of HDAC inhibitor leads to: ↓Nrf2 stability; ↓Nrf2-regulated HO-1 expression; ↑sensitivity to oxidative stress	(375)
	Human non-small cell lung cancer	H3K27me3	EZH2	A549 cells, human non-small cell lung cancer patients, nu/nu mice	Low expression of EZH2 leads to: ↑Nrf2, NQO1, and HO-1	(376)
Keap1	Cerebral ischemic injury	Histone acetylation	HDACs	Permanent middle cerebral artery occlusion model in mice, cortical neuronal cells, and RAW 264.7 cells	Treatment of HDAC inhibitor leads to: ↓Keap1; ↑Nrf2 nuclear translocation; ↑Nrf2-ARE binding; ↑HO-1, NQO1, and GCLC; ↑neuronal cell viability; and ↓cerebral ischemic injury	(377)
	Diebetic retinopathy	H3K4me1	SetD7	Bovine retinal endothelial cells, retina from rats and human donors	Hyperglycemia leads to: ↑SetD7; ↑binding of Sp1 at Keap1; ↑Keap1; and ↓Nrf2, Gclc, and HO-1.	(378)
HO-1 E1 enhancer	Pathological processes of inflammation and cancer	Histone hypoacetylation	HDAC3	HepG2, HEK293, and L929 cells	↓ ARE-dependent gene expression	(379)
Sod2	Diebetic retinopathy	H3K4 methylation	LSD1	Bovine retinal endothelial cells, retina from rats and human donors	Hyperglycemia leads to: ↑binding of LSD1 and Sp1 at Sod2; ↓Sod2 expression.	(380)
Gclc-ARE4	Diebetic retinopathy	H3K4 methylation	LSD1, KDM5A	Bovine retinal endothelial cells, retina from rats and human donors	Hyperglycemia leads to: ↓binding of Nrf2 at Gclc-ARE4 and Gclc transcripts	(381)

A1.4.1 Histone acetylation and the Keap1-Nrf2 signaling pathway

There is compelling evidence that the acetylation of histones neutralizes the positive charge, destabilizes the nucleosome structure, and promotes the accessibility of transcriptional factors to a genetic locus, thereby activating gene transcription, whereas histone deacetylation leads to gene silencing (382). Histone acetyltransferases (HATs) and HDACs, which add and remove the acetyl groups, respectively, constitute a group of enzymes that dynamically regulate histone acetylation/deacetylation and gene transcriptional activity. Liu et al. reported that class 1 HDACs (1, 2, and 3) inhibit ARE-dependent gene expression. Furthermore, this study demonstrated that the Nf-kB subunit p65 suppresses the Nrf2-ARE pathway via selective deprivation of CREB-binding protein (CBP, a member of HAT) from Nrf2 and promotion of the recruitment of HDAC3 to ARE. Specifically, p65 enhances the interaction of HDAC3 with MafK (a known dimerization partner with Nrf2), facilitates the recruitment of endogenous HDAC3 to the ARE element, helps to maintain the histone hypoacetylation state in the local chromosome and hence represses ARE-dependent gene expression (379). This mechanism provides direct evidence regarding the involvement of HDAC3 in the negative regulation of the Nrf2 pathway by NF-κB in response to inflammatory-related stimuli. Similarly, the impact of HDACs on the inhibition of Nrf2-mediated antioxidant defense in neuroinflammation has been investigated. Exposure to conditioned medium from lipopolysaccharide (LPS)-treated microglia (MCM_{10}) induced HDAC activity in astrocyte-rich cultures, which correlated with decreased acetylation in histones (H3 and H4) and reduced expression of Nrf2 and its target gene γ-glutamyl cysteine ligase modulatory subunit (γGCL-M). Notably, treatment with HDAC inhibitors, such as

valproic acid and TSA, markedly elevated acetylation in H3 and H4, restored the Nrf2-mediated anti-oxidant responses, and thus resulted in an increased resistance to oxidative stress (H_2O_2) in astrocyte-rich cultures exposed to MCM_{10} (374). In addition to protecting against neuroinflammation, the HDAC inhibitor also exhibited a promising effect in the protection of neuronal cell viability from oxygen-glucose deprivation and the attenuation of cerebral ischemic injury in the ischemic stroke mouse model via Nrf2 activation. Experimental evidence clearly showed that HDAC inhibitors activated the Nrf2 signaling pathway and up-regulated the Nrf2 downstream targets HO-1, NQO1, and glutamate-cysteine ligase catalytic subunit (GCLC) by suppressing Keap1 and promoting dissociation of Keap1 from Nrf2, Nrf2 nuclear translocation, and Nrf2-ARE binding. Importantly, the protective effect of HDAC inhibitors in cerebral ischemia was abolished in Nrf2-deficient mice (377). Therefore, activation of Nrf2 through HDAC inhibition may provide a promising therapeutic strategy for preventing neural damage in ischemic stroke.

However, inhibition of HDAC does not always lead to Nrf2 activation. Mercado et al. reported that Nrf2 activity is impaired as a result of decreased Nrf2 stability in the presence of TSA (an HDAC inhibitor) in BEAS2B (human airway epithelial) cells or in HDAC2-knockdown cells. TSA treatment also significantly ameliorated the elevation of HO-1 expression in mice exposed to cigarette smoke. In addition, a significant correlation between the expression of HDAC2 and Nrf2 was found in monocyte-derived macrophages obtained from chronic obstructive pulmonary disease (COPD) patients (375). Thus, a vicious circle in the pathogenesis of COPD is proposed: reduced HDAC2 activity observed in COPD as a result of oxidative stress could suppress Nrf2 stability

and activity, thereby increasing oxidative stress due to limited antioxidant responses, which then further impairs HDAC2 activity (375). In fact, several studies have suggested that Nrf2 plays an important role in lung inflammation by modulating HDAC activity. For example, Nrf2-deficient mice were found to have diminished HDAC2 levels in the lungs and increased susceptibility to chronic cigarette smoke- and LPS-induced lung inflammation, which were not reversed by steroid therapy (383). HDAC6, a critical regulator of autophagy-mediated airway inflammatory responses, was elevated in the lungs of Nrf2-deficient mice in response to cigarette smoke exposure (384). Taken together, these findings show that the activity of the Keap1-Nrf2 signaling pathway is epigenetically regulated by HDACs; conversely, Nrf2-mediated oxidative stress responses may have an epigenetic impact on other signaling pathways through the modulation of HDAC activity. The involvement of the Nrf2-HDAC axis in the pathogenesis of human disorders, especially in inflammatory diseases, requires further investigation.

The detailed mechanisms underlying the regulation of the Keap1-Nrf2 pathway by HDAC/HAT are not yet fully understood. It appears that HDAC and HAT and their inhibitors not only regulate Nrf2 activity and ARE-dependent gene expression via the adjustment of histone acetylation in the promoter regions (374, 379) but also selectively modulate the acetylation of Nrf2 independently of histones (385, 386). Lysine residues within the Nrf2 Neh1 DNA-binding domain can be acetylated directly by HAT (p300/CBP) in response to sodium arsenite-induced stress, and this acetylation is followed by the elevated expression of ARE-dependent genes (386). hMOF, the HAT required for histone H4K16 acetylation, can acetylate Nrf2 at Lys^{588}. In human NSCLC

tissues, hMOF-mediated acetylation of Nrf2 increased its nuclear retention and the transcription of its downstream genes, subsequently modulating tumor growth and drug resistance (387). In addition, the acetylation of Lys^{588} and Lys^{591} in the Neh3 domain by a selective inhibitor of sirtuin 1 (SIRT1, a class III HDAC) favors the nuclear localization of Nrf2, resulting in enhanced binding of Nrf2 to ARE and thereby increasing Nrf2-mediated gene expression. By contrast, a SIRT1 activator induces deacetylation, suppressing Nrf2 signaling accordingly (385).

The regulation of phase II detoxification enzymes by histone acetylation/deacetylation has also been investigated. It was previously reported that the acetylation of histones H3 and H4 on the chromatin of the promoter regions of the glutathione S-transferase placental form (GSTP) and GSTP enhancer 1 (GPE1) occurred in the H4IIE hepatoma cell line, where GSTP expression is activated, but not in the normal liver (388). Monocytic leukemia zinc-finger protein (MOZ), a member of HAT, stimulates GSTP promoter activity in the presence of Nrf2. Although the precise mechanism by which histone acetylation regulates the gene transcription of GSTP remains unclear, the elevation of both MOZ and Nrf2 levels may be required (389). UGT1A is another example of phase II enzymes regulated by histone acetylation. Gender-specific repression of UGT1A is controlled via chromatin remodeling through the recruitment of estrogen receptor alpha (ERα), HDAC1, and HDAC 2 to the xenobiotic response element (XRE) sites (390).

A1.4.1 Histone methylation and the Keap1-Nrf2 signaling pathway

Histone methylation is also a critical player in the regulation of chromatin compaction and gene expression. The methylation of histones occurs on all basic residues, including arginines, lysines, and histidines. Different lysine sites can be mono (me1), di (me2) or tri (me3) methylated (391). Depending on which residue is methylated and the degree of methylation, histone methylation can lead to either gene activation or suppression. For example, enhancer of zeste homolog 2 (EZH2) specifically catalyzes the trimethylation of histone H3 lysine 27 (H3K27me3) and leads to transcription repression (392), whereas histone-lysine N-methyltransferase (SetD7) monomethylates histone H3 lysine 4 (H3K4me1) and favors the binding of the transcription factor (393). Abnormal expression of histone methyltransferases (HMT) and histone demethyltransferases (HDMs) may write an aberrant epigenetic mark on the histone tail, influencing gene expression and resulting in disease. The proteasome inhibitor MG132 increases the degradation of EZH2 through a compensatory Nrf1- and Nrf2-dependent increase in the proteasome subunit level (394). Li and coworkers showed that decreased EZH2 expression significantly correlated with the elevated expression of Nrf2, NQO1, and HO1 in lung cancer tissues and cell lines, which was mainly attributed to a decrease in H3K27me3 in the Nrf2 promoter but not the NQO1 or HO1 promoter. Interestingly, the inhibitory effect of EZH2 on lung cancer growth in vitro and in vivo was abolished by Nrf2 deficiency (376). Collectively, these data suggest that EZH2 suppresses lung cancer growth by inhibiting Nrf2 expression via H3K27 trimethylation in the promoter region. However, the up-regulated EZH2 level in a number of cancers, including prostate cancer, breast cancer, lymphomas, gastric cancer, hepatocellular carcinoma, and bladder cancer

(see review (392)), suggests that EZH2 can be tumorigenic. The correlation of overexpression of EZH2 and the Keap1-Nrf2 signaling pathway in cancer tissues needs to be investigated. Furthermore, given the promising effect of EZH2 inhibitors in the treatment of cancer (395, 396), it will be interesting to explore the effect of EZH2 inhibitors on the Nrf2 pathway in cancer cells.

The modification of the Keap1-Nrf2 signaling pathway by methylation of histone 3 lysine 4 in diabetic retinopathy has been identified (378, 380, 381). The diabetic environment induces oxidant production in the retina and its capillary cells and decreases the antioxidant response (397). Mitochondrial superoxide dismutase (Sod2), an Nrf2 downstream target, becomes subnormal in diabetes due to lysine-specific demethylase-1 (LSD1)-mediated reduction of H3K4me1 and -me2 levels at the retinal Sod2 promoter. Sod2 inhibition may result in increased mitochondrial superoxide and the development of diabetic retinopathy (380). In addition to Sod2, suppression of GCLC, an enzyme that is important for the biosynthesis of GSH, has been implicated in the progression of diabetic retinopathy. Specifically, reduced H3K4me1 and H3K4me3 and increased H3K4me2 at Gclc-ARE4 in the retina in diabetes results in impaired binding of Nrf2 at Gclc-ARE4. One possible reason for such an increase in H3K4me2 could be that activated JARID family protein (KDM5A), an H3K4me3 demethylase, demethylates H3K4me3, resulting in elevated H3K4me2 (381). As an upper regulator, the association of Keap1 and Nrf2 could be regulated through epigenetic mechanisms, further impairing the antioxidant responses in diabetes. Indeed, hyperglycemia increases the binding of Sp1 at the Keap1 promoter through enrichment of H3K4me1 due to the activation of SetD7. In line with this finding, SetD7 knockdown leads to a lower H3K4me1 level at the Keap1 promoter

and reduced Sp1 binding, accompanied by the restoration of Nrf2 in high-glucose conditions. Following Nrf2 restoration, the binding of Nrf2 at the Gclc promoter and the expression of GCLC and HO-1 were enhanced, which is beneficial to rebalance the oxidative stress in a diabetic environment (378). In addition, as epigenetic modifications can persist in a system, the above-mentioned alterations of the histone methylation level may continue to suppress the expression of antioxidant genes, resulting in high oxidative stress, even after the termination of the hyperglycemic challenge, known as metabolic memory phenomenon. The reestablishment of normal glucose conditions failed to reverse the abnormal methylation marks of H3K4 at the Sod2, Gclc-ARE4, and Keap1 promoters; therefore, the activity of Nrf2 and its downstream genes continues to be compromised (378, 380, 381). According to these studies, the knockdown of the key enzymes that catalyze histone methylation appears to be effective in restoring the antioxidant defense system; thus, specific inhibitors of these enzymes may potentially protect diabetic retinopathy by regulating the Keap1-Nrf2 signaling pathway.

A1.4.1 Histone readers and the Keap1-Nrf2 signaling pathway

Histone readers are the proteins that recognize the histone modifications that are deposited or removed by histone writers or erasers (44). These readers play an essential role in the translation of a "histone code" for gene transcription. The bromodomain and extraterminal (BET) proteins are perhaps the most thoroughly characterized acetyl-lysine readers (398). After binding to acetylated lysine residues, BET proteins may interact with transcription factors and chromatin remodeling complexes, recruiting them to gene

promoters and thus activating or inactivating gene transcription (399). It was recently found that BET proteins are involved in the regulation of antioxidant gene expression (400, 401). BET proteins act as negative regulators of Nrf2 signaling; inhibition of BET proteins by genetic knockdown or the specific inhibitor JQ1 activates Nrf2-dependent transcription, increases the expression of the antioxidant genes HO-1, NQO1, and GCLC, and further ameliorates the ROS production induced by H_2O_2. BET proteins may interact directly with Nrf2 and are constitutively present at Nrf2-binding sites on the promoters of HO-1 and NQO1 (400). In addition, Hussong et al. showed that BRD4, a member of the BET protein family, is a key mediator of Keap1 transcription under stress. However, under normal conditions, BRD4 appears to modulate anti-oxidative responses by directly targeting Sp-1 binding sites in the inducible heme oxygenase 1 (HMOX1) promoter (401). However, the roles of histone readers in the interpretation of the histone code, chromatin remodeling, and recruitment of the repressive complex or co-activators to the Nrf2-regulated gene promoter remain unclear and need to be investigated in depth in the future.

A1.5 Interaction of miRNAs and the Keap1-Nrf2 signaling pathway

miRNAs are endogenous short non-coding RNAs that usually contain 20-22 nucleotides. By complementary pairing with mRNA sequences, miRNAs inhibit the translation of mRNAs in ribosomes and/or facilitate the degradation of mRNA molecules. Thus, miRNAs represent another category of epigenetic mechanism, which regulates gene expression at the post-transcriptional level, mostly in a "fine-tuning" manner. During recent decades, increasing efforts have been made to profile miRNA expression

patterns and characterize miRNA functions to identify novel diagnostic markers and therapeutic targets. Among these studies, a number of miRNAs have been reported to affect the Keap1-Nrf2 signaling pathway at several nodes (summarized in Table 18).

Table 18: miRNAs regulate Keap1-Nrf2 signaling pathway

Target	miRNA	Experimental model	Impact on Keap1-Nrf2	Outcomes	Ref
Nrf2	miR-144	K562 cell line, primary erythroid progenitor cells	↓Nrf2 levels, ↓glutathione regeneration ↓antioxidant capacity	Associated with anemia severity in sickle cell disease	(402)
	miR-27a,-142-5p,-144, -153	SH-SY5Y cells	↓Gclc, Gsr levels	Not applicable	(403)
	miR-28	MCF-7 cell line	↓Nrf2 mRNA	Increased anchorage-independent growth	(404)
	miR-93	E2-induced breast carcinognesis in ACI rats	↓Nrf2 and Nrf2 regulated genes	Decreased apoptosis, increased DNA damage	(405)
Keap1	miR-200a	MDA-MB-231 cell line	Keap1 mRNA degradation, ↑Nrf2 nuclear accumulation, ↑NQO1	Inhibits anchorage-independent growth	(406)
Cul3	miR-101	hypoxic condition	↑Nrf2 nuclear accumulation, ↑HO-1	Improves neovascularization and blood flow in ischemia	(407)
Bach1	let-7	Huh7 cell line	↑HO-1	Increased resistance against oxidant injury against tBuOOH	(408)
	miR-155	primary HUVECs	↑HO-1	Cytoprotective during inflammation	(409)

A1.5.1 miRNAs regulate Nrf2 activity by directly targeting the mRNA of Nrf2

As miRNAs function as post-transcriptional repressors of gene expression, miRNAs that directly target Nrf2 usually negatively regulate the Keap1-Nrf2 pathway. Notably, inefficient activation of Nrf2 results in alteration of Nrf2-dependent redox homeostasis, thus potentially triggering disease outcomes. Erythrocytes from patients with homozygous sickle cell disease (HbSS) have a reduced tolerance for oxidative stress. In a subset of HbSS patients with more severe anemia, higher erythrocytic miR-144 expression has been observed (402). In the same study, Sangokoya et al. found that the 3' UTR of Nrf2 is directly targeted by miR-144 in K562 cells and primary erythroid progenitor cells. Therefore, increased miR-144 may contribute to the attenuated Nrf2 levels in HbSS erythrocytes, which could account for the decrease in glutathione regeneration and impaired oxidative stress tolerance. By employing bioinformatic analysis of the human Nrf2 3' UTR sequences for miRNA binding sites, Narasimhan et al. reported an in-silico prediction of 4 different miRNAs targeting human Nrf2, including hsa-miR27a, hsa-miR153, hsa-miR142-5p, as well as the already reported hsa-miR144 (403). The direct interaction between the four identified miRNAs and Nrf2 was further validated using luciferase constructs carrying either the 3' UTR of human Nrf2 or mutated miRNA binding sites within the Nrf2 3' UTR. Moreover, ectopic expression of the corresponding miRNA mimics affected cellular Nrf2 mRNA levels as well as the nucleo-cytoplasmic concentration of the Nrf2 protein in a Keap1-independent manner, which consequently lessens GCLC and glutathione reductase (GSR) expression.

In the context of cancer, a variety of miRNAs have been implicated in cell differentiation, cell proliferation/apoptosis, and tumor suppression (58, 410). Specifically

in the Keap1-Nrf2 pathway, miR-28 expression has been reported to be reversibly correlated with Nrf2 mRNA levels in human mammary epithelial cells and the breast cancer MCF-7 cell line (404). Yang et al. also demonstrated that miR-28 regulates the Nrf2 pathway by targeting the 3' UTR region, thereby facilitating the degradation of Nrf2 mRNA. In addition, Nrf2 shRNA or ectopic expression of miR-28 inhibited the anchorage-independent cell growth of MCF-7 cells, suggesting that miR-28 might influence breast cancer motility and growth by regulating the Nrf2 pathway. Similarly, in 17β-estradiol (E2)-induced rat breast carcinogenesis, an E2-mediated increase in miR-93 levels was associated with decreased expression of Nrf2 (405). Furthermore, in human breast cell lines, miR-93 has been shown to have oncogenic potential, including the ability to increase colony formation, mammosphere formation, cell migration, and DNA damage and to decrease apoptosis.

A1.5.2 miRNAs regulate Nrf2 activity by interacting with cellular Nrf2 regulators

On the other hand, those miRNAs that interact with cellular Nrf2 regulators are expected to influence Nrf2/ARE signaling as well. Keap1 has been most extensively studied as a cellular suppressor of Nrf2. In human breast cancer MDA-MB-231 cells, Eades et al. reported that miR-200a could interact with the Keap1 3'UTR, facilitating its mRNA degradation (406). Therefore, the decreased miR-200a levels in breast cancer may provide a novel mechanistic explanation for the deregulation of the Nrf2 pathway. By inducing the re-expression of miR-200a, the reduction in Keap1 levels subsequently enhances Nrf2 nuclear accumulation and NQO1 gene transcription. Furthermore, this

study demonstrates that Nrf2 activation consequently inhibits the anchorage-independent growth of breast cancer cells in vitro and carcinogen-induced mammary hyperplasia in vivo. Cul3 is an important component of the Keap-1 protein complex that promotes Keap1-dependent Nrf2 ubiquitination and proteasomal degradation (407). Kim et al. demonstrated that Cul3 is a target of miR-101. Under hypoxic conditions, miR-101 is up-regulated in a HIF-1a-dependent manner, thereby stabilizing Nrf2 protein and inducing HO-1. Local overexpression of miR-101 improves neovascularization and blood flow in a mouse model of hindlimb ischemia. A mechanistic study indicated that a positive feedback loop between the Nrf2/HO-1 and VEGF/eNOS axes is implicated in miR-101-mediated post-ischemic vascular remodeling and angiogenesis. Bach1 is a MAF-related transcription factor that plays critical role in specific of HO-1 gene regulation. In cells naïve to oxidative stress, Bach1 conceals the ARE sequences; thus, it antagonizes Nrf2 binding and represses HO-1 gene transcriptional activation (411). In an earlier report, MacLeod et al. demonstrated the specificity attributes to that only HO-1 contains the necessary multiple *cis*-elements required for efficient Bach1 binding among human ARE-driven gene battery (412). Hou et al. reported that let-7 miRNAs (let-7b, 7c) enhanced HO-1 gene transcription by down-regulating Bach1 protein levels (408). Ectopic expression of the let-7 miRNA in Huh-7 cells resulted in increased resistance against oxidant injury induced by tert-butyl-hydroperoxide (tBuOOH), whereas the enhanced anti-oxidative capacity was counteracted by Bach1 over-expression. It is worth mentioning that the pro-inflammatory miR-155 also targets Bach1 degradation and induces subsequent elevation of HO-1 expression in endothelial cells (409). It has been proposed that the cytoprotective response to inflammation results from the miR-155-

mediated regulation of HO-1 rather than direct induction via the NF-κB pathway. This study provides a novel mechanistic insight by introducing miRNA in the cross-talk between the inflammatory and oxidative stress pathways. However, in lipopolysaccharide-stimulated murine RAW264.7 macrophages, either sulforaphane or allyl-isothiocyanate treatment leads to decrease in miR-155 levels, accompanied by HO-1 induction (413). Given that each miRNA could have multiple target genes while being controlled by a variety of upstream signals, the precise mechanisms by which miR-155 affects the Nrf2-mediated cellular protective system remain to be fully elucidated.

A1.5.3 Transcriptional regulation of miRNAs by Nrf2

The biogenesis of miRNAs is similar to that of other RNA molecules and starts with the transcription of the genes that encode immature primary miRNA (pri-miRNA) by RNA polymerase II. It is possible that the transcription of pri-miRNAs could be regulated by transcription factors (TFs) such as Nrf2. Indeed, recent studies provide evidence that a number of miRNAs can be regulated by Nrf2, reviewed by (414). In addition, a systematic analysis of the interactors and regulators of Nrf2 conducted by Papp et al. predicted 85 miRNA-Nrf2 mRNA interactions (415). Interestingly, 35 TFs regulated by Nrf2 could increase the levels of 63 out of the 85 miRNAs mentioned above. This model indicates that miRNAs are involved in the fine-tuning feedback loops in Nrf2 signaling.

A1.6 Cross-talk of epigenetic mechanisms in the modulation of the Keap1-Nrf2 signaling pathway

Circumstantial evidence suggests that different epigenetic layers may be engaged in complex crosstalk to establish and maintain different chromatin states. Thus, the above-mentioned epigenetic modifications may not function alone, but they may be linked to each other and work in combination to regulate gene transcription (176). Studies in our laboratory suggested that hypermethylated CpG islands in TRAMP C1 cells were associated with MBD2 and histone modifications, indicating interplay between DNA methylation and histone modification in the regulation of Nrf2 transcription activity. Chromatin immunoprecipitation assays showed that MBD2 and tri-methylated histone 3-lys9 (H3K9me3) are enriched in methylated CpGs in the Nrf2 promoter, whereas acetylated histone 3 (H3Ac) is associated with unmethylated CpGs (26). Additionally, recent research has reported that nutritional phytochemicals, including sulforaphane, apigenin, 3,3'-diindolylmethane, and tanshinone IIA, epigenetically re-activate the expression of Nrf2 through the inhibition of both DNMT and HDAC (29, 30, 68, 93, 107). Although these studies suggest an intimate communication and confounding actions between DNA methylation and histone acetylation/methylation in the silencing/activation of the Nrf2 gene, the fundamental question regarding which epigenetic event initiates and steers the crosstalk and Nrf2 silencing remains to be answered. Two different sequential models have been proposed to describe the interplay of DNA methylation and histone modification in gene silencing (reviewed in (416)). In one scenario, partial DNA methylation trigged by environmental and intrinsic signals attracts the binding of MePC2 and HDAC to the CpG sites, leads to deacetylated histone and inactive chromatin

configuration, and further recruits DNMT1 to amplify the silencing signals. In another scenario, imbalanced HAT and HDAC activities induce chromatin hypoacetylation, a chromatin state that will be recognized by de novo DNMTs and result in a local hypermethylation state. Future studies are necessary to understand the mechanisms underlying the combination of the epigenetic events in the regulation of Keap1-Nrf2 signaling pathways.

These epigenetic modifications not only work in combination to interact with Keap1-Nrf2 signaling pathways, but are also known to cross-regulate each other in a manner that diversifies their functions and ultimately influences cellular activity. For example, the miR-200 family was previously shown to be aberrantly silenced by epigenetic mechanisms in breast cancer (417), and impaired miR-200a activity led to the overexpression of SIRT1 (class III HDAC) (418). It is noteworthy that the epigenetic silencing of miR-200a by histone acetylation might contribute to the overexpression of Keap1 and loss of the Nrf2-dependent antioxidant pathway in breast cancer cells. Furthermore, Eades and coworkers found that treatment with the HDAC inhibitor suberoylanilide hydroxamic acid re-expressed miR-200a, which corresponded to decreased Keap1 expression, increased Nrf2 translocation, and elevated Nrf2-dependent NQO1 expression (406). More recently, another study reported similar results: the HDAC inhibitor MS-275 efficiently reduces the deacetylation in the miR-200a promoter region and reactivates miR-200a. As a consequence, mature miR-200a destabilizes Keap1 mRNA, leads to enhanced translocation and binding of Nrf2 to the polyamine-responsive element of the spermidine/spermine N^1-acetyltransferase (SSAT) promoter, and ultimately results in reduced polyamine synthesis and growth inhibition (419). These

studies suggested that cross-regulation of epigenetic modifications modulates Keap1-Nrf2 signaling. Therefore, more in-depth understanding will be necessary to exploit this complex regulatory network to combat dysregulation of the Keap1-Nrf2 pathway in chronic diseases.

A1.7 Conclusions and perspectives

Keap1-Nrf2 signaling plays important roles in a variety of physiological, pathological, pharmacological, and toxicological processes and is subjected to multiple layers of regulation at transcriptional, translational, and post-translational levels. In recent years, the epigenetic regulation of Keap1 and Nrf2 expression in various oxidative stress-related diseases has begun to be unveiled. As depicted schematically in Figure 24, Keap1 and Nrf2 expression could be regulated by methylation/demethylation of CpGs in the promoter regions, acetylation/deacetylation and methylation/demethylation of histones, or targeting of mRNAs by miRNAs. In addition, Nrf2 has also been implicated in the transcriptional regulation of certain non-coding RNAs. However, although oxidative stresses are profoundly engaged in epigenetic modifications and chromatin organization, it is not clear whether Keap1-Nrf2 signaling directly or indirectly regulates epigenetic processes other than miRNA transcription.

To date, most epigenetic regulation of Keap1-Nrf2 signaling has been identified in the context of cancer. Because oxidative stresses and Keap1-Nrf2 signaling are widely involved in almost all major chronic diseases, the participation of epigenetic mechanisms in the regulation of Keap1-Nrf2 signaling in these diseases will be interesting to elucidate.

Indeed, investigations have revealed the important roles of the demethylation of the Keap1 promoter in ARCs and cardiomyopathy and the reactivation of Nrf2 by HDAC inhibitors in neuroinflammation and cerebral ischemic injury, and further investigations in other oxidative stress-related diseases are guaranteed. Moreover, given the complexity of the crosstalk between genetic/epigenetic modifications and the Keap1-Nrf2 signaling networks, the exact mechanisms of epigenetic regulation of Keap1-Nrf2 signaling and their physiological significance remain open for further investigation.

References

1. Hanahan D, Weinberg RA. The hallmarks of cancer. Cell. 2000;100(1):57-70. PubMed PMID: 10647931.
2. Sharma S, Kelly TK, Jones PA. Epigenetics in cancer. Carcinogenesis. 2010;31(1):27-36. doi: 10.1093/carcin/bgp220. PubMed PMID: 19752007; PMCID: 2802667.
3. Waddington CH. The epigenotype. 1942. International journal of epidemiology. 2012;41(1):10-3. doi: 10.1093/ije/dyr184. PubMed PMID: 22186258.
4. Wolffe AP, Matzke MA. Epigenetics: regulation through repression. Science. 1999;286(5439):481-6. PubMed PMID: 10521337.
5. Feinberg AP, Tycko B. The history of cancer epigenetics. Nature reviews Cancer. 2004;4(2):143-53. doi: 10.1038/nrc1279. PubMed PMID: 14732866.
6. Sandoval J, Esteller M. Cancer epigenomics: beyond genomics. Current opinion in genetics & development. 2012;22(1):50-5. doi: 10.1016/j.gde.2012.02.008. PubMed PMID: 22402447.
7. You JS, Jones PA. Cancer genetics and epigenetics: two sides of the same coin? Cancer cell. 2012;22(1):9-20. doi: 10.1016/j.ccr.2012.06.008. PubMed PMID: 22789535; PMCID: 3396881.
8. Dhanak D, Jackson P. Development and classes of epigenetic drugs for cancer. Biochemical and biophysical research communications. 2014. doi: 10.1016/j.bbrc.2014.07.006. PubMed PMID: 25016182.
9. Kantarjian HM, Giles FJ, Greenberg PL, Paquette RL, Wang ES, Gabrilove JL, Garcia-Manero G, Hu K, Franklin JL, Berger DP. Phase 2 study of romiplostim in patients with low- or intermediate-risk myelodysplastic syndrome receiving azacitidine therapy. Blood. 2010;116(17):3163-70. doi: 10.1182/blood-2010-03-274753. PubMed PMID: 20631375; PMCID: 3324162.
10. Dolinoy DC, Weidman JR, Jirtle RL. Epigenetic gene regulation: linking early developmental environment to adult disease. Reproductive toxicology. 2007;23(3):297-307. doi: 10.1016/j.reprotox.2006.08.012. PubMed PMID: 17046196.
11. Lee KW, Bode AM, Dong Z. Molecular targets of phytochemicals for cancer prevention. Nature reviews Cancer. 2011;11(3):211-8. doi: 10.1038/nrc3017. PubMed PMID: 21326325.
12. Surh YJ. Cancer chemoprevention with dietary phytochemicals. Nature reviews Cancer. 2003;3(10):768-80. doi: 10.1038/nrc1189. PubMed PMID: 14570043.
13. Bird A. DNA methylation patterns and epigenetic memory. Genes Dev. 2002;16(1):6-21. doi: 10.1101/gad.947102. PubMed PMID: 11782440.
14. Wang Y, Leung FC. An evaluation of new criteria for CpG islands in the human genome as gene markers. Bioinformatics. 2004;20(7):1170-7. doi: 10.1093/bioinformatics/bth059. PubMed PMID: 14764558.
15. Suzuki MM, Bird A. DNA methylation landscapes: provocative insights from epigenomics. Nature reviews Genetics. 2008;9(6):465-76. doi: 10.1038/nrg2341. PubMed PMID: 18463664.
16. Baylin SB, Herman JG. DNA hypermethylation in tumorigenesis: epigenetics joins genetics. Trends in genetics : TIG. 2000;16(4):168-74. PubMed PMID: 10729832.

17. Prendergast GC, Ziff EB. Methylation-sensitive sequence-specific DNA binding by the c-Myc basic region. Science. 1991;251(4990):186-9. PubMed PMID: 1987636.

18. Nan X, Ng HH, Johnson CA, Laherty CD, Turner BM, Eisenman RN, Bird A. Transcriptional repression by the methyl-CpG-binding protein MeCP2 involves a histone deacetylase complex. Nature. 1998;393(6683):386-9. doi: 10.1038/30764. PubMed PMID: 9620804.

19. Jones PA, Baylin SB. The fundamental role of epigenetic events in cancer. Nature reviews Genetics. 2002;3(6):415-28. doi: 10.1038/nrg816. PubMed PMID: 12042769.

20. Esteller M, Toyota M, Sanchez-Cespedes M, Capella G, Peinado MA, Watkins DN, Issa JP, Sidransky D, Baylin SB, Herman JG. Inactivation of the DNA repair gene O6-methylguanine-DNA methyltransferase by promoter hypermethylation is associated with G to A mutations in K-ras in colorectal tumorigenesis. Cancer research. 2000;60(9):2368-71. PubMed PMID: 10811111.

21. Simpkins SB, Bocker T, Swisher EM, Mutch DG, Gersell DJ, Kovatich AJ, Palazzo JP, Fishel R, Goodfellow PJ. MLH1 promoter methylation and gene silencing is the primary cause of microsatellite instability in sporadic endometrial cancers. Human molecular genetics. 1999;8(4):661-6. PubMed PMID: 10072435.

22. Hall GL, Shaw RJ, Field EA, Rogers SN, Sutton DN, Woolgar JA, Lowe D, Liloglou T, Field JK, Risk JM. p16 Promoter methylation is a potential predictor of malignant transformation in oral epithelial dysplasia. Cancer epidemiology, biomarkers & prevention : a publication of the American Association for Cancer Research, cosponsored by the American Society of Preventive Oncology. 2008;17(8):2174-9. doi: 10.1158/1055-9965.EPI-07-2867. PubMed PMID: 18708411.

23. Wemmert S, Bettscheider M, Alt S, Ketter R, Kammers K, Feiden W, Steudel WI, Rahnenfuhrer J, Urbschat S. p15 promoter methylation - a novel prognostic marker in glioblastoma patients. International journal of oncology. 2009;34(6):1743-8. PubMed PMID: 19424593.

24. Carvalho JR, Filipe L, Costa VL, Ribeiro FR, Martins AT, Teixeira MR, Jeronimo C, Henrique R. Detailed analysis of expression and promoter methylation status of apoptosis-related genes in prostate cancer. Apoptosis : an international journal on programmed cell death. 2010;15(8):956-65. doi: 10.1007/s10495-010-0508-6. PubMed PMID: 20464497.

25. Narayan G, Arias-Pulido H, Koul S, Vargas H, Zhang FF, Villella J, Schneider A, Terry MB, Mansukhani M, Murty VV. Frequent promoter methylation of CDH1, DAPK, RARB, and HIC1 genes in carcinoma of cervix uteri: its relationship to clinical outcome. Molecular cancer. 2003;2:24. PubMed PMID: 12773202; PMCID: 156646.

26. Yu S, Khor TO, Cheung KL, Li W, Wu TY, Huang Y, Foster BA, Kan YW, Kong AN. Nrf2 expression is regulated by epigenetic mechanisms in prostate cancer of TRAMP mice. PLoS One. 2010;5(1):e8579. doi: 10.1371/journal.pone.0008579. PubMed PMID: 20062804; PMCID: 2799519.

27. Huang Y, Khor TO, Shu L, Saw CL, Wu TY, Suh N, Yang CS, Kong AN. A gamma-tocopherol-rich mixture of tocopherols maintains Nrf2 expression in prostate tumors of TRAMP mice via epigenetic inhibition of CpG methylation. The Journal

of nutrition. 2012;142(5):818-23. doi: 10.3945/jn.111.153114. PubMed PMID: 22457388; PMCID: 3327740.

28. Su ZY, Khor TO, Shu L, Lee JH, Saw CL, Wu TY, Huang Y, Suh N, Yang CS, Conney AH, Wu Q, Kong AN. Epigenetic reactivation of Nrf2 in murine prostate cancer TRAMP C1 cells by natural phytochemicals Z-ligustilide and Radix angelica sinensis via promoter CpG demethylation. Chemical research in toxicology. 2013;26(3):477-85. doi: 10.1021/tx300524p. PubMed PMID: 23441843.

29. Wu TY, Khor TO, Su ZY, Saw CL, Shu L, Cheung KL, Huang Y, Yu S, Kong AN. Epigenetic modifications of Nrf2 by 3,3'-diindolylmethane in vitro in TRAMP C1 cell line and in vivo TRAMP prostate tumors. The AAPS journal. 2013;15(3):864-74. doi: 10.1208/s12248-013-9493-3. PubMed PMID: 23658110; PMCID: 3691436.

30. Zhang C, Su ZY, Khor TO, Shu L, Kong AN. Sulforaphane enhances Nrf2 expression in prostate cancer TRAMP C1 cells through epigenetic regulation. Biochemical pharmacology. 2013;85(9):1398-404. doi: 10.1016/j.bcp.2013.02.010. PubMed PMID: 23416117; PMCID: 4123317.

31. Feinberg AP, Vogelstein B. Hypomethylation distinguishes genes of some human cancers from their normal counterparts. Nature. 1983;301(5895):89-92. PubMed PMID: 6185846.

32. Feinberg AP, Gehrke CW, Kuo KC, Ehrlich M. Reduced genomic 5-methylcytosine content in human colonic neoplasia. Cancer research. 1988;48(5):1159-61. PubMed PMID: 3342396.

33. Rodriguez J, Frigola J, Vendrell E, Risques RA, Fraga MF, Morales C, Moreno V, Esteller M, Capella G, Ribas M, Peinado MA. Chromosomal instability correlates with genome-wide DNA demethylation in human primary colorectal cancers. Cancer research. 2006;66(17):8462-9468. doi: 10.1158/0008-5472.CAN-06-0293. PubMed PMID: 16951157.

34. Baylin SB, Makos M, Wu JJ, Yen RW, de Bustros A, Vertino P, Nelkin BD. Abnormal patterns of DNA methylation in human neoplasia: potential consequences for tumor progression. Cancer cells. 1991;3(10):383-90. PubMed PMID: 1777359.

35. Kim GD, Ni J, Kelesoglu N, Roberts RJ, Pradhan S. Co-operation and communication between the human maintenance and de novo DNA (cytosine-5) methyltransferases. The EMBO journal. 2002;21(15):4183-95. PubMed PMID: 12145218; PMCID: 126147.

36. Suetake I, Shinozaki F, Miyagawa J, Takeshima H, Tajima S. DNMT3L stimulates the DNA methylation activity of Dnmt3a and Dnmt3b through a direct interaction. The Journal of biological chemistry. 2004;279(26):27816-23. doi: 10.1074/jbc.M400181200. PubMed PMID: 15105426.

37. Aapola U, Kawasaki K, Scott HS, Ollila J, Vihinen M, Heino M, Shintani A, Kawasaki K, Minoshima S, Krohn K, Antonarakis SE, Shimizu N, Kudoh J, Peterson P. Isolation and initial characterization of a novel zinc finger gene, DNMT3L, on 21q22.3, related to the cytosine-5-methyltransferase 3 gene family. Genomics. 2000;65(3):293-8. doi: 10.1006/geno.2000.6168. PubMed PMID: 10857753.

38. Robertson KD, Uzvolgyi E, Liang G, Talmadge C, Sumegi J, Gonzales FA, Jones PA. The human DNA methyltransferases (DNMTs) 1, 3a and 3b: coordinate mRNA

expression in normal tissues and overexpression in tumors. Nucleic acids research. 1999;27(11):2291-8. PubMed PMID: 10325416; PMCID: 148793.

39. Subramaniam D, Thombre R, Dhar A, Anant S. DNA methyltransferases: a novel target for prevention and therapy. Frontiers in oncology. 2014;4:80. doi: 10.3389/fonc.2014.00080. PubMed PMID: 24822169; PMCID: 4013461.

40. Tahiliani M, Koh KP, Shen Y, Pastor WA, Bandukwala H, Brudno Y, Agarwal S, Iyer LM, Liu DR, Aravind L, Rao A. Conversion of 5-methylcytosine to 5-hydroxymethylcytosine in mammalian DNA by MLL partner TET1. Science. 2009;324(5929):930-5. doi: 10.1126/science.1170116. PubMed PMID: 19372391; PMCID: 2715015.

41. Kohli RM, Zhang Y. TET enzymes, TDG and the dynamics of DNA demethylation. Nature. 2013;502(7472):472-9. doi: 10.1038/nature12750. PubMed PMID: 24153300; PMCID: 4046508.

42. Kornberg RD, Lorch Y. Twenty-five years of the nucleosome, fundamental particle of the eukaryote chromosome. Cell. 1999;98(3):285-94. PubMed PMID: 10458604.

43. Strahl BD, Allis CD. The language of covalent histone modifications. Nature. 2000;403(6765):41-5. doi: 10.1038/47412. PubMed PMID: 10638745.

44. Jenuwein T, Allis CD. Translating the histone code. Science. 2001;293(5532):1074-80. doi: 10.1126/science.1063127. PubMed PMID: 11498575.

45. Fullgrabe J, Kavanagh E, Joseph B. Histone onco-modifications. Oncogene. 2011;30(31):3391-403. doi: 10.1038/onc.2011.121. PubMed PMID: 21516126.

46. Struhl K. Histone acetylation and transcriptional regulatory mechanisms. Genes & development. 1998;12(5):599-606. PubMed PMID: 9499396.

47. Thakur VS, Deb G, Babcook MA, Gupta S. Plant phytochemicals as epigenetic modulators: role in cancer chemoprevention. The AAPS journal. 2014;16(1):151-63. doi: 10.1208/s12248-013-9548-5. PubMed PMID: 24307610; PMCID: 3889536.

48. Fraga MF, Ballestar E, Villar-Garea A, Boix-Chornet M, Espada J, Schotta G, Bonaldi T, Haydon C, Ropero S, Petrie K, Iyer NG, Perez-Rosado A, Calvo E, Lopez JA, Cano A, Calasanz MJ, Colomer D, Piris MA, Ahn N, Imhof A, Caldas C, Jenuwein T, Esteller M. Loss of acetylation at Lys16 and trimethylation at Lys20 of histone H4 is a common hallmark of human cancer. Nature genetics. 2005;37(4):391-400. doi: 10.1038/ng1531. PubMed PMID: 15765097.

49. Hardy TM, Tollefsbol TO. Epigenetic diet: impact on the epigenome and cancer. Epigenomics. 2011;3(4):503-18. doi: 10.2217/epi.11.71. PubMed PMID: 22022340; PMCID: 3197720.

50. Vakoc CR, Sachdeva MM, Wang H, Blobel GA. Profile of histone lysine methylation across transcribed mammalian chromatin. Molecular and cellular biology. 2006;26(24):9185-95. doi: 10.1128/MCB.01529-06. PubMed PMID: 17030614; PMCID: 1698537.

51. Jackson JP, Lindroth AM, Cao X, Jacobsen SE. Control of CpNpG DNA methylation by the KRYPTONITE histone H3 methyltransferase. Nature. 2002;416(6880):556-60. doi: 10.1038/nature731. PubMed PMID: 11898023.

52. Dawson MA, Kouzarides T. Cancer epigenetics: from mechanism to therapy. Cell. 2012;150(1):12-27. doi: 10.1016/j.cell.2012.06.013. PubMed PMID: 22770212.

53. Kim W, Bird GH, Neff T, Guo G, Kerenyi MA, Walensky LD, Orkin SH. Targeted disruption of the EZH2-EED complex inhibits EZH2-dependent cancer. Nature

chemical biology. 2013;9(10):643-50. doi: 10.1038/nchembio.1331. PubMed PMID: 23974116; PMCID: 3778130.

54. Jansson MD, Lund AH. MicroRNA and cancer. Molecular oncology. 2012;6(6):590-610. doi: 10.1016/j.molonc.2012.09.006. PubMed PMID: 23102669.

55. Calin GA, Dumitru CD, Shimizu M, Bichi R, Zupo S, Noch E, Aldler H, Rattan S, Keating M, Rai K, Rassenti L, Kipps T, Negrini M, Bullrich F, Croce CM. Frequent deletions and down-regulation of micro- RNA genes miR15 and miR16 at 13q14 in chronic lymphocytic leukemia. Proceedings of the National Academy of Sciences of the United States of America. 2002;99(24):15524-9. doi: 10.1073/pnas.242606799. PubMed PMID: 12434020; PMCID: 137750.

56. Faraoni I, Antonetti FR, Cardone J, Bonmassar E. miR-155 gene: a typical multifunctional microRNA. Biochimica et biophysica acta. 2009;1792(6):497-505. doi: 10.1016/j.bbadis.2009.02.013. PubMed PMID: 19268705.

57. Volinia S, Calin GA, Liu CG, Ambs S, Cimmino A, Petrocca F, Visone R, Iorio M, Roldo C, Ferracin M, Prueitt RL, Yanaihara N, Lanza G, Scarpa A, Vecchione A, Negrini M, Harris CC, Croce CM. A microRNA expression signature of human solid tumors defines cancer gene targets. Proceedings of the National Academy of Sciences of the United States of America. 2006;103(7):2257-61. doi: 10.1073/pnas.0510565103. PubMed PMID: 16461460; PMCID: 1413718.

58. Takamizawa J, Konishi H, Yanagisawa K, Tomida S, Osada H, Endoh H, Harano T, Yatabe Y, Nagino M, Nimura Y, Mitsudomi T, Takahashi T. Reduced expression of the let-7 microRNAs in human lung cancers in association with shortened postoperative survival. Cancer research. 2004;64(11):3753-6. doi: 10.1158/0008-5472.CAN-04-0637. PubMed PMID: 15172979.

59. Fabbri M, Garzon R, Cimmino A, Liu Z, Zanesi N, Callegari E, Liu S, Alder H, Costinean S, Fernandez-Cymering C, Volinia S, Guler G, Morrison CD, Chan KK, Marcucci G, Calin GA, Huebner K, Croce CM. MicroRNA-29 family reverts aberrant methylation in lung cancer by targeting DNA methyltransferases 3A and 3B. Proc Natl Acad Sci U S A. 2007;104(40):15805-10. doi: 10.1073/pnas.0707628104. PubMed PMID: 17890317; PMCID: 2000384.

60. Bouchie A. First microRNA mimic enters clinic. Nature biotechnology. 2013;31(7):577. doi: 10.1038/nbt0713-577. PubMed PMID: 23839128.

61. Shukla S, Gupta S. Dietary agents in the chemoprevention of prostate cancer. Nutrition and cancer. 2005;53(1):18-32. doi: 10.1207/s15327914nc5301_3. PubMed PMID: 16351503.

62. Tan S, Wang C, Lu C, Zhao B, Cui Y, Shi X, Ma X. Quercetin is able to demethylate the p16INK4a gene promoter. Chemotherapy. 2009;55(1):6-10. doi: 10.1159/000166383. PubMed PMID: 18974642.

63. Xiao X, Shi D, Liu L, Wang J, Xie X, Kang T, Deng W. Quercetin suppresses cyclooxygenase-2 expression and angiogenesis through inactivation of P300 signaling. PloS one. 2011;6(8):e22934. doi: 10.1371/journal.pone.0022934. PubMed PMID: 21857970; PMCID: 3152552.

64. Lee WJ, Chen YR, Tseng TH. Quercetin induces FasL-related apoptosis, in part, through promotion of histone H3 acetylation in human leukemia HL-60 cells. Oncology reports. 2011;25(2):583-91. doi: 10.3892/or.2010.1097. PubMed PMID: 21165570.

65. Vargas JE, Filippi-Chiela EC, Suhre T, Kipper FC, Bonatto D, Lenz G. Inhibition of HDAC increases the senescence induced by natural polyphenols in glioma cells. Biochemistry and cell biology = Biochimie et biologie cellulaire. 2014;92(4):297-304. doi: 10.1139/bcb-2014-0022. PubMed PMID: 25070040.

66. Lam TK, Shao S, Zhao Y, Marincola F, Pesatori A, Bertazzi PA, Caporaso NE, Wang E, Landi MT. Influence of quercetin-rich food intake on microRNA expression in lung cancer tissues. Cancer epidemiology, biomarkers & prevention : a publication of the American Association for Cancer Research, cosponsored by the American Society of Preventive Oncology. 2012;21(12):2176-84. doi: 10.1158/1055-9965.EPI-12-0745. PubMed PMID: 23035181; PMCID: 3538163.

67. MacKenzie TN, Mujumdar N, Banerjee S, Sangwan V, Sarver A, Vickers S, Subramanian S, Saluja AK. Triptolide induces the expression of miR-142-3p: a negative regulator of heat shock protein 70 and pancreatic cancer cell proliferation. Molecular cancer therapeutics. 2013;12(7):1266-75. doi: 10.1158/1535-7163.MCT-12-1231. PubMed PMID: 23635652; PMCID: 3707985.

68. Paredes-Gonzalez X, Fuentes F, Su ZY, Kong AN. Apigenin reactivates Nrf2 anti-oxidative stress signaling in mouse skin epidermal JB6 P + cells through epigenetics modifications. The AAPS journal. 2014;16(4):727-35. doi: 10.1208/s12248-014-9613-8. PubMed PMID: 24830944; PMCID: 4070251.

69. Pandey M, Kaur P, Shukla S, Abbas A, Fu P, Gupta S. Plant flavone apigenin inhibits HDAC and remodels chromatin to induce growth arrest and apoptosis in human prostate cancer cells: in vitro and in vivo study. Molecular carcinogenesis. 2012;51(12):952-62. doi: 10.1002/mc.20866. PubMed PMID: 22006862; PMCID: 4019962.

70. Chakrabarti M, Banik NL, Ray SK. miR-138 overexpression is more powerful than hTERT knockdown to potentiate apigenin for apoptosis in neuroblastoma in vitro and in vivo. Experimental cell research. 2013;319(10):1575-85. doi: 10.1016/j.yexcr.2013.02.025. PubMed PMID: 23562653; PMCID: 3661724.

71. Gao Z, Xu Z, Hung MS, Lin YC, Wang T, Gong M, Zhi X, Jablon DM, You L. Promoter demethylation of WIF-1 by epigallocatechin-3-gallate in lung cancer cells. Anticancer research. 2009;29(6):2025-30. PubMed PMID: 19528461.

72. Mirza S, Sharma G, Parshad R, Gupta SD, Pandya P, Ralhan R. Expression of DNA methyltransferases in breast cancer patients and to analyze the effect of natural compounds on DNA methyltransferases and associated proteins. Journal of breast cancer. 2013;16(1):23-31. doi: 10.4048/jbc.2013.16.1.23. PubMed PMID: 23593078; PMCID: 3625766.

73. Deb G, Thakur VS, Limaye AM, Gupta S. Epigenetic induction of tissue inhibitor of matrix metalloproteinase-3 by green tea polyphenols in breast cancer cells. Molecular carcinogenesis. 2014. doi: 10.1002/mc.22121. PubMed PMID: 24481780.

74. Wang H, Bian S, Yang CS. Green tea polyphenol EGCG suppresses lung cancer cell growth through upregulating miR-210 expression caused by stabilizing HIF-1alpha. Carcinogenesis. 2011;32(12):1881-9. doi: 10.1093/carcin/bgr218. PubMed PMID: 21965273; PMCID: 3220612.

75. Gordon MW, Yan F, Zhong X, Mazumder PB, Xu-Monette ZY, Zou D, Young KH, Ramos KS, Li Y. Regulation of p53-targeting microRNAs by polycyclic aromatic hydrocarbons: Implications in the etiology of multiple myeloma. Molecular

carcinogenesis. 2014. doi: 10.1002/mc.22175. PubMed PMID: 24798859; PMCID: 4223015.

76. Nandakumar V, Vaid M, Katiyar SK. (-)-Epigallocatechin-3-gallate reactivates silenced tumor suppressor genes, Cip1/p21 and p16INK4a, by reducing DNA methylation and increasing histones acetylation in human skin cancer cells. Carcinogenesis. 2011;32(4):537-44. doi: 10.1093/carcin/bgq285. PubMed PMID: 21209038; PMCID: 3066414.

77. Xie Q, Bai Q, Zou LY, Zhang QY, Zhou Y, Chang H, Yi L, Zhu JD, Mi MT. Genistein inhibits DNA methylation and increases expression of tumor suppressor genes in human breast cancer cells. Genes, chromosomes & cancer. 2014;53(5):422-31. doi: 10.1002/gcc.22154. PubMed PMID: 24532317.

78. Hirata H, Hinoda Y, Shahryari V, Deng G, Tanaka Y, Tabatabai ZL, Dahiya R. Genistein downregulates onco-miR-1260b and upregulates sFRP1 and Smad4 via demethylation and histone modification in prostate cancer cells. British journal of cancer. 2014;110(6):1645-54. doi: 10.1038/bjc.2014.48. PubMed PMID: 24504368; PMCID: 3960620.

79. Xia J, Cheng L, Mei C, Ma J, Shi Y, Zeng F, Wang Z, Wang Z. Genistein inhibits cell growth and invasion through regulation of miR-27a in pancreatic cancer cells. Current pharmaceutical design. 2014;20(33):5348-53. PubMed PMID: 24479798.

80. Zhu W, Qin W, Zhang K, Rottinghaus GE, Chen YC, Kliethermes B, Sauter ER. Trans-resveratrol alters mammary promoter hypermethylation in women at increased risk for breast cancer. Nutrition and cancer. 2012;64(3):393-400. doi: 10.1080/01635581.2012.654926. PubMed PMID: 22332908; PMCID: 3392022.

81. Qin W, Zhang K, Clarke K, Weiland T, Sauter ER. Methylation and miRNA effects of resveratrol on mammary tumors vs. normal tissue. Nutrition and cancer. 2014;66(2):270-7. doi: 10.1080/01635581.2014.868910. PubMed PMID: 24447120.

82. Venturelli S, Berger A, Bocker A, Busch C, Weiland T, Noor S, Leischner C, Schleicher S, Mayer M, Weiss TS, Bischoff SC, Lauer UM, Bitzer M. Resveratrol as a pan-HDAC inhibitor alters the acetylation status of histone [corrected] proteins in human-derived hepatoblastoma cells. PloS one. 2013;8(8):e73097. doi: 10.1371/journal.pone.0073097. PubMed PMID: 24023672; PMCID: 3758278.

83. Liu P, Liang H, Xia Q, Li P, Kong H, Lei P, Wang S, Tu Z. Resveratrol induces apoptosis of pancreatic cancers cells by inhibiting miR-21 regulation of BCL-2 expression. Clinical & translational oncology : official publication of the Federation of Spanish Oncology Societies and of the National Cancer Institute of Mexico. 2013;15(9):741-6. doi: 10.1007/s12094-012-0999-4. PubMed PMID: 23359184.

84. Sheth S, Jajoo S, Kaur T, Mukherjea D, Sheehan K, Rybak LP, Ramkumar V. Resveratrol reduces prostate cancer growth and metastasis by inhibiting the Akt/MicroRNA-21 pathway. PloS one. 2012;7(12):e51655. doi: 10.1371/journal.pone.0051655. PubMed PMID: 23272133; PMCID: 3521661.

85. Chen CQ, Yu K, Yan QX, Xing CY, Chen Y, Yan Z, Shi YF, Zhao KW, Gao SM. Pure curcumin increases the expression of SOCS1 and SOCS3 in myeloproliferative neoplasms through suppressing class I histone deacetylases. Carcinogenesis. 2013;34(7):1442-9. doi: 10.1093/carcin/bgt070. PubMed PMID: 23430957.

86. Collins HM, Abdelghany MK, Messmer M, Yue B, Deeves SE, Kindle KB, Mantelingu K, Aslam A, Winkler GS, Kundu TK, Heery DM. Differential effects of

garcinol and curcumin on histone and p53 modifications in tumour cells. BMC Cancer. 2013;13:37. doi: 10.1186/1471-2407-13-37. PubMed PMID: 23356739; PMCID: 3583671.

87. Khor TO, Huang Y, Wu TY, Shu L, Lee J, Kong AN. Pharmacodynamics of curcumin as DNA hypomethylation agent in restoring the expression of Nrf2 via promoter CpGs demethylation. Biochem Pharmacol. 2011;82(9):1073-8. doi: 10.1016/j.bcp.2011.07.065. PubMed PMID: 21787756.

88. Kronski E, Fiori ME, Barbieri O, Astigiano S, Mirisola V, Killian PH, Bruno A, Pagani A, Rovera F, Pfeffer U, Sommerhoff CP, Noonan DM, Nerlich AG, Fontana L, Bachmeier BE. miR181b is induced by the chemopreventive polyphenol curcumin and inhibits breast cancer metastasis via down-regulation of the inflammatory cytokines CXCL1 and -2. Molecular oncology. 2014;8(3):581-95. doi: 10.1016/j.molonc.2014.01.005. PubMed PMID: 24484937.

89. Shu L, Khor TO, Lee JH, Boyanapalli SS, Huang Y, Wu TY, Saw CL, Cheung KL, Kong AN. Epigenetic CpG demethylation of the promoter and reactivation of the expression of Neurog1 by curcumin in prostate LNCaP cells. AAPS J. 2011;13(4):606-14. doi: 10.1208/s12248-011-9300-y. PubMed PMID: 21938566; PMCID: 3231852.

90. Zhao SF, Zhang X, Zhang XJ, Shi XQ, Yu ZJ, Kan QC. Induction of microRNA-9 mediates cytotoxicity of curcumin against SKOV3 ovarian cancer cells. Asian Pacific journal of cancer prevention : APJCP. 2014;15(8):3363-8. PubMed PMID: 24870723.

91. Hsu A, Wong CP, Yu Z, Williams DE, Dashwood RH, Ho E. Promoter de-methylation of cyclin D2 by sulforaphane in prostate cancer cells. Clinical epigenetics. 2011;3:3. doi: 10.1186/1868-7083-3-3. PubMed PMID: 22303414; PMCID: 3257546.

92. Shan Y, Zhang L, Bao Y, Li B, He C, Gao M, Feng X, Xu W, Zhang X, Wang S. Epithelial-mesenchymal transition, a novel target of sulforaphane via COX-2/MMP2, 9/Snail, ZEB1 and miR-200c/ZEB1 pathways in human bladder cancer cells. The Journal of nutritional biochemistry. 2013;24(6):1062-9. doi: 10.1016/j.jnutbio.2012.08.004. PubMed PMID: 23159064.

93. Su ZY, Zhang C, Lee JH, Shu L, Wu TY, Khor TO, Conney AH, Lu YP, Kong AN. Requirement and epigenetics reprogramming of Nrf2 in suppression of tumor promoter TPA-induced mouse skin cell transformation by sulforaphane. Cancer prevention research. 2014;7(3):319-29. doi: 10.1158/1940-6207.CAPR-13-0313-T. PubMed PMID: 24441674.

94. Li Q, Yao Y, Eades G, Liu Z, Zhang Y, Zhou Q. Downregulation of miR-140 promotes cancer stem cell formation in basal-like early stage breast cancer. Oncogene. 2014;33(20):2589-600. doi: 10.1038/onc.2013.226. PubMed PMID: 23752191; PMCID: 3883868.

95. Yu C, Gong AY, Chen D, Solelo Leon D, Young CY, Chen XM. Phenethyl isothiocyanate inhibits androgen receptor-regulated transcriptional activity in prostate cancer cells through suppressing PCAF. Molecular nutrition & food research. 2013;57(10):1825-33. doi: 10.1002/mnfr.201200810. PubMed PMID: 23661605.

96. Liu Y, Chakravarty S, Dey M. Phenethylisothiocyanate alters site- and promoter-specific histone tail modifications in cancer cells. PloS one. 2013;8(5):e64535. doi: 10.1371/journal.pone.0064535. PubMed PMID: 23724058; PMCID: 3665791.

97. Wang LG, Beklemisheva A, Liu XM, Ferrari AC, Feng J, Chiao JW. Dual action on promoter demethylation and chromatin by an isothiocyanate restored GSTP1 silenced in prostate cancer. Molecular carcinogenesis. 2007;46(1):24-31. doi: 10.1002/mc.20258. PubMed PMID: 16921492.

98. Tang H, Kong Y, Guo J, Tang Y, Xie X, Yang L, Su Q, Xie X. Diallyl disulfide suppresses proliferation and induces apoptosis in human gastric cancer through Wnt-1 signaling pathway by up-regulation of miR-200b and miR-22. Cancer letters. 2013;340(1):72-81. doi: 10.1016/j.canlet.2013.06.027. PubMed PMID: 23851184.

99. Altonsy MO, Habib TN, Andrews SC. Diallyl disulfide-induced apoptosis in a breast-cancer cell line (MCF-7) may be caused by inhibition of histone deacetylation. Nutrition and cancer. 2012;64(8):1251-60. doi: 10.1080/01635581.2012.721156. PubMed PMID: 23163853.

100. Kong D, Heath E, Chen W, Cher ML, Powell I, Heilbrun L, Li Y, Ali S, Sethi S, Hassan O, Hwang C, Gupta N, Chitale D, Sakr WA, Menon M, Sarkar FH. Loss of let-7 up-regulates EZH2 in prostate cancer consistent with the acquisition of cancer stem cell signatures that are attenuated by BR-DIM. PloS one. 2012;7(3):e33729. doi: 10.1371/journal.pone.0033729. PubMed PMID: 22442719; PMCID: 3307758.

101. Jin Y. 3,3'-Diindolylmethane inhibits breast cancer cell growth via miR-21-mediated Cdc25A degradation. Molecular and cellular biochemistry. 2011;358(1-2):345-54. doi: 10.1007/s11010-011-0985-0. PubMed PMID: 21761201.

102. Li Y, Li X, Guo B. Chemopreventive agent 3,3'-diindolylmethane selectively induces proteasomal degradation of class I histone deacetylases. Cancer research. 2010;70(2):646-54. doi: 10.1158/0008-5472.CAN-09-1924. PubMed PMID: 20068155; PMCID: 2808120.

103. Wong CP, Hsu A, Buchanan A, Palomera-Sanchez Z, Beaver LM, Houseman EA, Williams DE, Dashwood RH, Ho E. Effects of sulforaphane and 3,3'-diindolylmethane on genome-wide promoter methylation in normal prostate epithelial cells and prostate cancer cells. PloS one. 2014;9(1):e86787. doi: 10.1371/journal.pone.0086787. PubMed PMID: 24466240; PMCID: 3899342.

104. Kang KA, Kim HS, Kim DH, Hyun JW. The role of a ginseng saponin metabolite as a DNA methyltransferase inhibitor in colorectal cancer cells. International journal of oncology. 2013;43(1):228-36. doi: 10.3892/ijo.2013.1931. PubMed PMID: 23652987.

105. An IS, An S, Kwon KJ, Kim YJ, Bae S. Ginsenoside Rh2 mediates changes in the microRNA expression profile of human non-small cell lung cancer A549 cells. Oncology reports. 2013;29(2):523-8. doi: 10.3892/or.2012.2136. PubMed PMID: 23152132.

106. Wu N, Wu GC, Hu R, Li M, Feng H. Ginsenoside Rh2 inhibits glioma cell proliferation by targeting microRNA-128. Acta pharmacologica Sinica. 2011;32(3):345-53. doi: 10.1038/aps.2010.220. PubMed PMID: 21372826.

107. Wang L, Zhang C, Guo Y, Su ZY, Yang Y, Shu L, Kong AN. Blocking of JB6 cell transformation by tanshinone IIA: epigenetic reactivation of Nrf2 antioxidative

stress pathway. The AAPS journal. 2014;16(6):1214-25. doi: 10.1208/s12248-014-9666-8. PubMed PMID: 25274607.

108. Tu J, Xing Y, Guo Y, Tang F, Guo L, Xi T. TanshinoneIIA ameliorates inflammatory microenvironment of colon cancer cells via repression of microRNA-155. International immunopharmacology. 2012;14(4):353-61. doi: 10.1016/j.intimp.2012.08.015. PubMed PMID: 22982040.

109. Gong Y, Li Y, Abdolmaleky HM, Li L, Zhou JR. Tanshinones inhibit the growth of breast cancer cells through epigenetic modification of Aurora A expression and function. PloS one. 2012;7(4):e33656. doi: 10.1371/journal.pone.0033656. PubMed PMID: 22485147; PMCID: 3317444.

110. Woo J, Kim HY, Byun BJ, Chae CH, Lee JY, Ryu SY, Park WK, Cho H, Choi G. Biological evaluation of tanshindiols as EZH2 histone methyltransferase inhibitors. Bioorganic & medicinal chemistry letters. 2014;24(11):2486-92. doi: 10.1016/j.bmcl.2014.04.010. PubMed PMID: 24767850.

111. Takahashi M, Sung B, Shen Y, Hur K, Link A, Boland CR, Aggarwal BB, Goel A. Boswellic acid exerts antitumor effects in colorectal cancer cells by modulating expression of the let-7 and miR-200 microRNA family. Carcinogenesis. 2012;33(12):2441-9. doi: 10.1093/carcin/bgs286. PubMed PMID: 22983985; PMCID: 3510738.

112. Shen Y, Takahashi M, Byun HM, Link A, Sharma N, Balaguer F, Leung HC, Boland CR, Goel A. Boswellic acid induces epigenetic alterations by modulating DNA methylation in colorectal cancer cells. Cancer biology & therapy. 2012;13(7):542-52. doi: 10.4161/cbt.19604. PubMed PMID: 22415137; PMCID: 3364790.

113. Wang J, Li Y, Wang X, Jiang C. Ursolic acid inhibits proliferation and induces apoptosis in human glioblastoma cell lines U251 by suppressing TGF-beta1/miR-21/PDCD4 pathway. Basic & clinical pharmacology & toxicology. 2012;111(2):106-12. doi: 10.1111/j.1742-7843.2012.00870.x. PubMed PMID: 22353043.

114. Lee WJ, Shim JY, Zhu BT. Mechanisms for the inhibition of DNA methyltransferases by tea catechins and bioflavonoids. Molecular pharmacology. 2005;68(4):1018-30. doi: 10.1124/mol.104.008367. PubMed PMID: 16037419.

115. Du L, Xie Z, Wu LC, Chiu M, Lin J, Chan KK, Liu S, Liu Z. Reactivation of RASSF1A in breast cancer cells by curcumin. Nutr Cancer. 2012;64(8):1228-35. doi: 10.1080/01635581.2012.717682. PubMed PMID: 23145775.

116. Link A, Balaguer F, Shen Y, Lozano JJ, Leung HC, Boland CR, Goel A. Curcumin modulates DNA methylation in colorectal cancer cells. PLoS One. 2013;8(2):e57709. doi: 10.1371/journal.pone.0057709. PubMed PMID: 23460897; PMCID: 3584082.

117. Nagaraju GP, Zhu S, Wen J, Farris AB, Adsay VN, Diaz R, Snyder JP, Mamoru S, El-Rayes BF. Novel synthetic curcumin analogues EF31 and UBS109 are potent DNA hypomethylating agents in pancreatic cancer. Cancer letters. 2013;341(2):195-203. doi: 10.1016/j.canlet.2013.08.002. PubMed PMID: 23933177.

118. Gonzalez-Vallinas M, Molina S, Vicente G, Zarza V, Martin-Hernandez R, Garcia-Risco MR, Fornari T, Reglero G, Ramirez de Molina A. Expression of microRNA-15b and the glycosyltransferase GCNT3 correlates with antitumor efficacy of

Rosemary diterpenes in colon and pancreatic cancer. PloS one. 2014;9(6):e98556. doi: 10.1371/journal.pone.0098556. PubMed PMID: 24892299; PMCID: 4043684.

119. Berdasco M, Esteller M. Aberrant epigenetic landscape in cancer: how cellular identity goes awry. Developmental cell. 2010;19(5):698-711. doi: 10.1016/j.devcel.2010.10.005. PubMed PMID: 21074720.

120. Jones PA, Takai D. The role of DNA methylation in mammalian epigenetics. Science. 2001;293(5532):1068-70. doi: 10.1126/science.1063852. PubMed PMID: 11498573.

121. Jones PA, Baylin SB. The epigenomics of cancer. Cell. 2007;128(4):683-92. doi: 10.1016/j.cell.2007.01.029. PubMed PMID: 17320506; PMCID: 3894624.

122. Herman JG, Baylin SB. Gene silencing in cancer in association with promoter hypermethylation. The New England journal of medicine. 2003;349(21):2042-54. doi: 10.1056/NEJMra023075. PubMed PMID: 14627790.

123. Vogelstein B, Fearon ER, Hamilton SR, Kern SE, Preisinger AC, Leppert M, Nakamura Y, White R, Smits AM, Bos JL. Genetic alterations during colorectal-tumor development. The New England journal of medicine. 1988;319(9):525-32. doi: 10.1056/NEJM198809013190901. PubMed PMID: 2841597.

124. Guo Y, Su Z-Y, Kong A-NT. Current Perspectives on Epigenetic Modifications by Dietary Chemopreventive and Herbal Phytochemicals. Current Pharmacology Reports. 2015:1-13.

125. Harrison S, Benziger H. The molecular biology of colorectal carcinoma and its implications: a review. The surgeon : journal of the Royal Colleges of Surgeons of Edinburgh and Ireland. 2011;9(4):200-10. doi: 10.1016/j.surge.2011.01.011. PubMed PMID: 21672660.

126. Kinzler KW, Vogelstein B. Lessons from hereditary colorectal cancer. Cell. 1996;87(2):159-70. PubMed PMID: 8861899.

127. Morin PJ, Sparks AB, Korinek V, Barker N, Clevers H, Vogelstein B, Kinzler KW. Activation of beta-catenin-Tcf signaling in colon cancer by mutations in beta-catenin or APC. Science. 1997;275(5307):1787-90. PubMed PMID: 9065402.

128. Tetsu O, McCormick F. Beta-catenin regulates expression of cyclin D1 in colon carcinoma cells. Nature. 1999;398(6726):422-6. doi: 10.1038/18884. PubMed PMID: 10201372.

129. Pancione M, Remo A, Colantuoni V. Genetic and epigenetic events generate multiple pathways in colorectal cancer progression. Pathology research international. 2012;2012:509348. doi: 10.1155/2012/509348. PubMed PMID: 22888469; PMCID: 3409552.

130. Shima K, Nosho K, Baba Y, Cantor M, Meyerhardt JA, Giovannucci EL, Fuchs CS, Ogino S. Prognostic significance of CDKN2A (p16) promoter methylation and loss of expression in 902 colorectal cancers: Cohort study and literature review. International journal of cancer Journal international du cancer. 2011;128(5):1080-94. doi: 10.1002/ijc.25432. PubMed PMID: 20473920; PMCID: 2958235.

131. Belshaw NJ, Pal N, Tapp HS, Dainty JR, Lewis MP, Williams MR, Lund EK, Johnson IT. Patterns of DNA methylation in individual colonic crypts reveal aging and cancer-related field defects in the morphologically normal mucosa. Carcinogenesis. 2010;31(6):1158-63. doi: 10.1093/carcin/bgq077. PubMed PMID: 20395289.

132. Ying J, Poon FF, Yu J, Geng H, Wong AH, Qiu GH, Goh HK, Rha SY, Tian L, Chan AT, Sung JJ, Tao Q. DLEC1 is a functional 3p22.3 tumour suppressor silenced by promoter CpG methylation in colon and gastric cancers. British journal of cancer. 2009;100(4):663-9. doi: 10.1038/sj.bjc.6604888. PubMed PMID: 19156137; PMCID: 2653732.

133. Guo Y, Shu L, Zhang C, Su ZY, Kong AN. Curcumin inhibits anchorage-independent growth of HT29 human colon cancer cells by targeting epigenetic restoration of the tumor suppressor gene DLEC1. Biochemical pharmacology. 2015. doi: 10.1016/j.bcp.2015.01.009. PubMed PMID: 25640947.

134. Hibi K, Mizukami H, Shirahata A, Goto T, Sakata M, Saito M, Ishibashi K, Kigawa G, Nemoto H, Sanada Y. Aberrant methylation of the UNC5C gene is frequently detected in advanced colorectal cancer. Anticancer research. 2009;29(1):271-3. PubMed PMID: 19331160.

135. Li X, Lu P, Li B, Zhang W, Luo K. Effects of iodine-125 seeds on the methylation of SFRP and P16 in colorectal cancer. Experimental and therapeutic medicine. 2013;6(5):1225-8. doi: 10.3892/etm.2013.1298. PubMed PMID: 24223648; PMCID: 3820808.

136. Halberg RB, Katzung DS, Hoff PD, Moser AR, Cole CE, Lubet RA, Donehower LA, Jacoby RF, Dove WF. Tumorigenesis in the multiple intestinal neoplasia mouse: Redundancy of negative regulators and specificity of modifiers. P Natl Acad Sci USA. 2000;97(7):3461-6. doi: DOI 10.1073/pnas.050585597. PubMed PMID: WOS:000086195200091.

137. Fearon ER, Vogelstein B. A genetic model for colorectal tumorigenesis. Cell. 1990;61(5):759-67. PubMed PMID: 2188735.

138. Khor TO, Cheung WK, Prawan A, Reddy BS, Kong AN. Chemoprevention of familial adenomatous polyposis in Apc(Min/+) mice by phenethyl isothiocyanate (PEITC). Molecular carcinogenesis. 2008;47(5):321-5. doi: 10.1002/mc.20390. PubMed PMID: 17932952.

139. Yang AY, Lee JH, Shu L, Zhang C, Su ZY, Lu Y, Huang MT, Ramirez C, Pung D, Huang Y, Verzi M, Hart RP, Kong AN. Genome-wide analysis of DNA methylation in UVB- and DMBA/TPA-induced mouse skin cancer models. Life sciences. 2014. doi: 10.1016/j.lfs.2014.07.031. PubMed PMID: 25093921.

140. Trapnell C, Roberts A, Goff L, Pertea G, Kim D, Kelley DR, Pimentel H, Salzberg SL, Rinn JL, Pachter L. Differential gene and transcript expression analysis of RNA-seq experiments with TopHat and Cufflinks. Nature protocols. 2012;7(3):562-78. doi: 10.1038/nprot.2012.016. PubMed PMID: 22383036; PMCID: 3334321.

141. Zhu LJ, Gazin C, Lawson ND, Pages H, Lin SM, Lapointe DS, Green MR. ChIPpeakAnno: a Bioconductor package to annotate ChIP-seq and ChIP-chip data. BMC bioinformatics. 2010;11:237. doi: 10.1186/1471-2105-11-237. PubMed PMID: 20459804; PMCID: 3098059.

142. Polyak K, Weinberg RA. Transitions between epithelial and mesenchymal states: acquisition of malignant and stem cell traits. Nature reviews Cancer. 2009;9(4):265-73. doi: 10.1038/nrc2620. PubMed PMID: 19262571.

143. Esteller M. Cancer epigenomics: DNA methylomes and histone-modification maps. Nature reviews Genetics. 2007;8(4):286-98. doi: 10.1038/nrg2005. PubMed PMID: 17339880.

144. Down TA, Rakyan VK, Turner DJ, Flicek P, Li H, Kulesha E, Graf S, Johnson N, Herrero J, Tomazou EM, Thorne NP, Backdahl L, Herberth M, Howe KL, Jackson DK, Miretti MM, Marioni JC, Birney E, Hubbard TJ, Durbin R, Tavare S, Beck S. A Bayesian deconvolution strategy for immunoprecipitation-based DNA methylome analysis. Nature biotechnology. 2008;26(7):779-85. doi: 10.1038/nbt1414. PubMed PMID: 18612301; PMCID: 2644410.

145. Alisch RS, Wang T, Chopra P, Visootsak J, Conneely KN, Warren ST. Genome-wide analysis validates aberrant methylation in fragile X syndrome is specific to the FMR1 locus. BMC medical genetics. 2013;14:18. doi: 10.1186/1471-2350-14-18. PubMed PMID: 23356558; PMCID: 3599197.

146. Fang WJ, Zheng Y, Wu LM, Ke QH, Shen H, Yuan Y, Zheng SS. Genome-wide analysis of aberrant DNA methylation for identification of potential biomarkers in colorectal cancer patients. Asian Pacific journal of cancer prevention : APJCP. 2012;13(5):1917-21. PubMed PMID: 22901147.

147. Ruike Y, Imanaka Y, Sato F, Shimizu K, Tsujimoto G. Genome-wide analysis of aberrant methylation in human breast cancer cells using methyl-DNA immunoprecipitation combined with high-throughput sequencing. BMC genomics. 2010;11:137. doi: 10.1186/1471-2164-11-137. PubMed PMID: 20181289; PMCID: 2838848.

148. Grimm C, Chavez L, Vilardell M, Farrall AL, Tierling S, Bohm JW, Grote P, Lienhard M, Dietrich J, Timmermann B, Walter J, Schweiger MR, Lehrach H, Herwig R, Herrmann BG, Morkel M. DNA-methylome analysis of mouse intestinal adenoma identifies a tumour-specific signature that is partly conserved in human colon cancer. PLoS genetics. 2013;9(2):e1003250. doi: 10.1371/journal.pgen.1003250. PubMed PMID: 23408899; PMCID: 3567140.

149. Tan LJ, Zhu H, He H, Wu KH, Li J, Chen XD, Zhang JG, Shen H, Tian Q, Krousel-Wood M, Papasian CJ, Bouchard C, Perusse L, Deng HW. Replication of 6 obesity genes in a meta-analysis of genome-wide association studies from diverse ancestries. PloS one. 2014;9(5):e96149. doi: 10.1371/journal.pone.0096149. PubMed PMID: 24879436; PMCID: 4039436.

150. Huhn S, Ingelfinger D, Bermejo JL, Bevier M, Pardini B, Naccarati A, Steinke V, Rahner N, Holinski-Feder E, Morak M, Schackert HK, Gorgens H, Pox CP, Goecke T, Kloor M, Loeffler M, Buttner R, Vodickova L, Novotny J, Demir K, Cruciat CM, Renneberg R, Huber W, Niehrs C, Boutros M, Propping P, Vodieka P, Hemminki K, Forsti A. Polymorphisms in CTNNBL1 in relation to colorectal cancer with evolutionary implications. International journal of molecular epidemiology and genetics. 2011;2(1):36-50. PubMed PMID: 21537400; PMCID: 3077237.

151. Ogino S, Kawasaki T, Kirkner GJ, Ogawa A, Dorfman I, Loda M, Fuchs CS. Down-regulation of p21 (CDKN1A/CIP1) is inversely associated with microsatellite instability and CpG island methylator phenotype (CIMP) in colorectal cancer. The Journal of pathology. 2006;210(2):147-54. doi: 10.1002/path.2030. PubMed PMID: 16850502.

152. Baylin SB. DNA methylation and gene silencing in cancer. Nat Clin Pract Oncol. 2005;2 Suppl 1:S4-11. doi: 10.1038/ncponc0354. PubMed PMID: 16341240.

153. De Carvalho DD, Sharma S, You JS, Su SF, Taberlay PC, Kelly TK, Yang X, Liang G, Jones PA. DNA methylation screening identifies driver epigenetic events of

cancer cell survival. Cancer cell. 2012;21(5):655-67. doi: 10.1016/j.ccr.2012.03.045. PubMed PMID: 22624715; PMCID: 3395886.

154. Bardhan K, Liu K. Epigenetics and colorectal cancer pathogenesis. Cancers (Basel). 2013;5(2):676-713. doi: 10.3390/cancers5020676. PubMed PMID: 24216997; PMCID: 3730326.

155. Kalluri R, Weinberg RA. The basics of epithelial-mesenchymal transition. The Journal of clinical investigation. 2009;119(6):1420-8. doi: 10.1172/JCI39104. PubMed PMID: 19487818; PMCID: 2689101.

156. Kang Y, Massague J. Epithelial-mesenchymal transitions: twist in development and metastasis. Cell. 2004;118(3):277-9. doi: 10.1016/j.cell.2004.07.011. PubMed PMID: 15294153.

157. Thiery JP. Epithelial-mesenchymal transitions in tumour progression. Nature reviews Cancer. 2002;2(6):442-54. doi: 10.1038/nrc822. PubMed PMID: 12189386.

158. Chen X, Halberg RB, Burch RP, Dove WF. Intestinal adenomagenesis involves core molecular signatures of the epithelial-mesenchymal transition. Journal of molecular histology. 2008;39(3):283-94. doi: 10.1007/s10735-008-9164-3. PubMed PMID: 18327651; PMCID: 2544376.

159. Lee K, Nelson CM. New insights into the regulation of epithelial-mesenchymal transition and tissue fibrosis. International review of cell and molecular biology. 2012;294:171-221. doi: 10.1016/B978-0-12-394305-7.00004-5. PubMed PMID: 22364874.

160. Kiesslich T, Pichler M, Neureiter D. Epigenetic control of epithelial-mesenchymal-transition in human cancer. Molecular and clinical oncology. 2013;1(1):3-11. doi: 10.3892/mco.2012.28. PubMed PMID: 24649114; PMCID: 3956244.

161. Cieslik M, Hoang SA, Baranova N, Chodaparambil S, Kumar M, Allison DF, Xu X, Wamsley JJ, Gray L, Jones DR, Mayo MW, Bekiranov S. Epigenetic coordination of signaling pathways during the epithelial-mesenchymal transition. Epigenetics & chromatin. 2013;6(1):28. doi: 10.1186/1756-8935-6-28. PubMed PMID: 24004852; PMCID: 3847279.

162. Sodir NM, Chen X, Park R, Nickel AE, Conti PS, Moats R, Bading JR, Shibata D, Laird PW. Smad3 deficiency promotes tumorigenesis in the distal colon of ApcMin/+ mice. Cancer research. 2006;66(17):8430-8. doi: 10.1158/0008-5472.CAN-06-1437. PubMed PMID: 16951153.

163. Lo HW, Hsu SC, Xia W, Cao X, Shih JY, Wei Y, Abbruzzese JL, Hortobagyi GN, Hung MC. Epidermal growth factor receptor cooperates with signal transducer and activator of transcription 3 to induce epithelial-mesenchymal transition in cancer cells via up-regulation of TWIST gene expression. Cancer research. 2007;67(19):9066-76. doi: 10.1158/0008-5472.CAN-07-0575. PubMed PMID: 17909010; PMCID: 2570961.

164. Scartozzi M, Bearzi I, Mandolesi A, Giampieri R, Faloppi L, Galizia E, Loupakis F, Zaniboni A, Zorzi F, Biscotti T, Labianca R, Falcone A, Cascinu S. Epidermal growth factor receptor (EGFR) gene promoter methylation and cetuximab treatment in colorectal cancer patients. British journal of cancer. 2011;104(11):1786-90. doi: 10.1038/bjc.2011.161. PubMed PMID: 21559018; PMCID: 3111171.

165. Fang X, Cai Y, Liu J, Wang Z, Wu Q, Zhang Z, Yang CJ, Yuan L, Ouyang G. Twist2 contributes to breast cancer progression by promoting an epithelial-

mesenchymal transition and cancer stem-like cell self-renewal. Oncogene. 2011;30(47):4707-20. doi: 10.1038/onc.2011.181. PubMed PMID: 21602879.

166. Yu H, Jin GZ, Liu K, Dong H, Yu H, Duan JC, Li Z, Dong W, Cong WM, Yang JH. Twist2 is a valuable prognostic biomarker for colorectal cancer. World journal of gastroenterology : WJG. 2013;19(15):2404-11. doi: 10.3748/wjg.v19.i15.2404. PubMed PMID: 23613636; PMCID: 3631994.

167. Raval A, Lucas DM, Matkovic JJ, Bennett KL, Liyanarachchi S, Young DC, Rassenti L, Kipps TJ, Grever MR, Byrd JC, Plass C. TWIST2 demonstrates differential methylation in immunoglobulin variable heavy chain mutated and unmutated chronic lymphocytic leukemia. Journal of clinical oncology : official journal of the American Society of Clinical Oncology. 2005;23(17):3877-85. doi: 10.1200/JCO.2005.02.196. PubMed PMID: 15809452.

168. Thathia SH, Ferguson S, Gautrey HE, van Otterdijk SD, Hili M, Rand V, Moorman AV, Meyer S, Brown R, Strathdee G. Epigenetic inactivation of TWIST2 in acute lymphoblastic leukemia modulates proliferation, cell survival and chemosensitivity. Haematologica. 2012;97(3):371-8. doi: 10.3324/haematol.2011.049593. PubMed PMID: 22058208; PMCID: 3291591.

169. Dhir M, Montgomery EA, Glockner SC, Schuebel KE, Hooker CM, Herman JG, Baylin SB, Gearhart SL, Ahuja N. Epigenetic regulation of WNT signaling pathway genes in inflammatory bowel disease (IBD) associated neoplasia. Journal of gastrointestinal surgery : official journal of the Society for Surgery of the Alimentary Tract. 2008;12(10):1745-53. doi: 10.1007/s11605-008-0633-5. PubMed PMID: 18716850; PMCID: 3976145.

170. Wang LS, Kuo CT, Huang TH, Yearsley M, Oshima K, Stoner GD, Yu J, Lechner JF, Huang YW. Black raspberries protectively regulate methylation of Wnt pathway genes in precancerous colon tissue. Cancer prevention research. 2013;6(12):1317-27. doi: 10.1158/1940-6207.CAPR-13-0077. PubMed PMID: 24129635; PMCID: 3902171.

171. Wang LS, Kuo CT, Stoner K, Yearsley M, Oshima K, Yu J, Huang TH, Rosenberg D, Peiffer D, Stoner G, Huang YW. Dietary black raspberries modulate DNA methylation in dextran sodium sulfate (DSS)-induced ulcerative colitis. Carcinogenesis. 2013;34(12):2842-50. doi: 10.1093/carcin/bgt310. PubMed PMID: 24067901; PMCID: 3845896.

172. Barker N, Ridgway RA, van Es JH, van de Wetering M, Begthel H, van den Born M, Danenberg E, Clarke AR, Sansom OJ, Clevers H. Crypt stem cells as the cells-of-origin of intestinal cancer. Nature. 2009;457(7229):608-11. doi: 10.1038/nature07602. PubMed PMID: 19092804.

173. Clevers H. Wnt/beta-catenin signaling in development and disease. Cell. 2006;127(3):469-80. doi: 10.1016/j.cell.2006.10.018. PubMed PMID: 17081971.

174. Miao CG, Yang YY, He X, Xu T, Huang C, Huang Y, Zhang L, Lv XW, Jin Y, Li J. New advances of microRNAs in the pathogenesis of rheumatoid arthritis, with a focus on the crosstalk between DNA methylation and the microRNA machinery. Cellular signalling. 2013;25(5):1118-25. doi: 10.1016/j.cellsig.2013.01.024. PubMed PMID: 23385088.

175. Cedar H, Bergman Y. Linking DNA methylation and histone modification: patterns and paradigms. Nature reviews Genetics. 2009;10(5):295-304. doi: 10.1038/nrg2540. PubMed PMID: 19308066.

176. Kondo Y. Epigenetic cross-talk between DNA methylation and histone modifications in human cancers. Yonsei medical journal. 2009;50(4):455-63. doi: 10.3349/ymj.2009.50.4.455. PubMed PMID: 19718392; PMCID: 2730606.

177. Tahara T, Yamamoto E, Madireddi P, Suzuki H, Maruyama R, Chung W, Garriga J, Jelinek J, Yamano HO, Sugai T, Kondo Y, Toyota M, Issa JP, Estecio MR. Colorectal carcinomas with CpG island methylator phenotype 1 frequently contain mutations in chromatin regulators. Gastroenterology. 2014;146(2):530-38 e5. doi: 10.1053/j.gastro.2013.10.060. PubMed PMID: 24211491; PMCID: 3918446.

178. Zhang GJ, Xiao HX, Tian HP, Liu ZL, Xia SS, Zhou T. Upregulation of microRNA-155 promotes the migration and invasion of colorectal cancer cells through the regulation of claudin-1 expression. International journal of molecular medicine. 2013;31(6):1375-80. doi: 10.3892/ijmm.2013.1348. PubMed PMID: 23588589.

179. Sims RJ, 3rd, Millhouse S, Chen CF, Lewis BA, Erdjument-Bromage H, Tempst P, Manley JL, Reinberg D. Recognition of trimethylated histone H3 lysine 4 facilitates the recruitment of transcription postinitiation factors and pre-mRNA splicing. Mol Cell. 2007;28(4):665-76. doi: 10.1016/j.molcel.2007.11.010. PubMed PMID: 18042460; PMCID: 2276655.

180. Grady WM, Carethers JM. Genomic and epigenetic instability in colorectal cancer pathogenesis. Gastroenterology. 2008;135(4):1079-99. doi: 10.1053/j.gastro.2008.07.076. PubMed PMID: 18773902; PMCID: 2866182.

181. Wood LD, Parsons DW, Jones S, Lin J, Sjoblom T, Leary RJ, Shen D, Boca SM, Barber T, Ptak J, Silliman N, Szabo S, Dezso Z, Ustyanksky V, Nikolskaya T, Nikolsky Y, Karchin R, Wilson PA, Kaminker JS, Zhang Z, Croshaw R, Willis J, Dawson D, Shipitsin M, Willson JK, Sukumar S, Polyak K, Park BH, Pethiyagoda CL, Pant PV, Ballinger DG, Sparks AB, Hartigan J, Smith DR, Suh E, Papadopoulos N, Buckhaults P, Markowitz SD, Parmigiani G, Kinzler KW, Velculescu VE, Vogelstein B. The genomic landscapes of human breast and colorectal cancers. Science. 2007;318(5853):1108-13. doi: 10.1126/science.1145720. PubMed PMID: 17932254.

182. Lao VV, Grady WM. Epigenetics and colorectal cancer. Nat Rev Gastroenterol Hepatol. 2011;8(12):686-700. doi: 10.1038/nrgastro.2011.173. PubMed PMID: 22009203; PMCID: 3391545.

183. Glockner SC, Dhir M, Yi JM, McGarvey KE, Van Neste L, Louwagie J, Chan TA, Kleeberger W, de Bruine AP, Smits KM, Khalid-de Bakker CA, Jonkers DM, Stockbrugger RW, Meijer GA, Oort FA, Iacobuzio-Donahue C, Bierau K, Herman JG, Baylin SB, Van Engeland M, Schuebel KE, Ahuja N. Methylation of TFPI2 in stool DNA: a potential novel biomarker for the detection of colorectal cancer. Cancer research. 2009;69(11):4691-9. doi: 10.1158/0008-5472.CAN-08-0142. PubMed PMID: 19435926; PMCID: 3062162.

184. Yi JM, Dhir M, Guzzetta AA, Iacobuzio-Donahue CA, Heo K, Yang KM, Suzuki H, Toyota M, Kim HM, Ahuja N. DNA methylation biomarker candidates for early detection of colon cancer. Tumour biology : the journal of the International Society

for Oncodevelopmental Biology and Medicine. 2012;33(2):363-72. doi: 10.1007/s13277-011-0302-2. PubMed PMID: 22238052; PMCID: 3593674.

185. van Engeland M, Derks S, Smits KM, Meijer GA, Herman JG. Colorectal cancer epigenetics: complex simplicity. Journal of clinical oncology : official journal of the American Society of Clinical Oncology. 2011;29(10):1382-91. doi: 10.1200/JCO.2010.28.2319. PubMed PMID: 21220596.

186. Miyamoto K, Ushijima T. Diagnostic and therapeutic applications of epigenetics. Japanese journal of clinical oncology. 2005;35(6):293-301. doi: 10.1093/jjco/hyi088. PubMed PMID: 15930038.

187. Wargovich MJ. Experimental evidence for cancer preventive elements in foods. Cancer letters. 1997;114(1-2):11-7. PubMed PMID: 9103245.

188. Shehzad A, Wahid F, Lee YS. Curcumin in cancer chemoprevention: molecular targets, pharmacokinetics, bioavailability, and clinical trials. Archiv der Pharmazie. 2010;343(9):489-99. doi: 10.1002/ardp.200900319. PubMed PMID: 20726007.

189. Hsu CH, Cheng AL. Clinical studies with curcumin. Advances in experimental medicine and biology. 2007;595:471-80. doi: 10.1007/978-0-387-46401-5_21. PubMed PMID: 17569225.

190. Garcea G, Jones DJ, Singh R, Dennison AR, Farmer PB, Sharma RA, Steward WP, Gescher AJ, Berry DP. Detection of curcumin and its metabolites in hepatic tissue and portal blood of patients following oral administration. British journal of cancer. 2004;90(5):1011-5. doi: 10.1038/sj.bjc.6601623. PubMed PMID: 14997198; PMCID: 2409622.

191. Garcea G, Berry DP, Jones DJ, Singh R, Dennison AR, Farmer PB, Sharma RA, Steward WP, Gescher AJ. Consumption of the putative chemopreventive agent curcumin by cancer patients: assessment of curcumin levels in the colorectum and their pharmacodynamic consequences. Cancer epidemiology, biomarkers & prevention : a publication of the American Association for Cancer Research, cosponsored by the American Society of Preventive Oncology. 2005;14(1):120-5. PubMed PMID: 15668484.

192. Reuter S, Gupta SC, Park B, Goel A, Aggarwal BB. Epigenetic changes induced by curcumin and other natural compounds. Genes & nutrition. 2011;6(2):93-108. doi: 10.1007/s12263-011-0222-1. PubMed PMID: 21516481; PMCID: 3092901.

193. Daigo Y, Nishiwaki T, Kawasoe T, Tamari M, Tsuchiya E, Nakamura Y. Molecular cloning of a candidate tumor suppressor gene, DLC1, from chromosome 3p21.3. Cancer research. 1999;59(8):1966-72. PubMed PMID: 10213508.

194. Imreh S, Klein G, Zabarovsky ER. Search for unknown tumor-antagonizing genes. Genes, chromosomes & cancer. 2003;38(4):307-21. doi: 10.1002/gcc.10271. PubMed PMID: 14566849.

195. Agathanggelou A, Dallol A, Zochbauer-Muller S, Morrissey C, Honorio S, Hesson L, Martinsson T, Fong KM, Kuo MJ, Yuen PW, Maher ER, Minna JD, Latif F. Epigenetic inactivation of the candidate 3p21.3 suppressor gene BLU in human cancers. Oncogene. 2003;22(10):1580-8. doi: 10.1038/sj.onc.1206243. PubMed PMID: 12629521.

196. Hesson L, Bieche I, Krex D, Criniere E, Hoang-Xuan K, Maher ER, Latif F. Frequent epigenetic inactivation of RASSF1A and BLU genes located within the

critical 3p21.3 region in gliomas. Oncogene. 2004;23(13):2408-19. doi: 10.1038/sj.onc.1207407. PubMed PMID: 14743209.

197. Seng TJ, Currey N, Cooper WA, Lee CS, Chan C, Horvath L, Sutherland RL, Kennedy C, McCaughan B, Kohonen-Corish MR. DLEC1 and MLH1 promoter methylation are associated with poor prognosis in non-small cell lung carcinoma. British journal of cancer. 2008;99(2):375-82. doi: 10.1038/sj.bjc.6604452. PubMed PMID: 18594535; PMCID: 2480971.

198. Qiu GH, Salto-Tellez M, Ross JA, Yeo W, Cui Y, Wheelhouse N, Chen GG, Harrison D, Lai P, Tao Q, Hooi SC. The tumor suppressor gene DLEC1 is frequently silenced by DNA methylation in hepatocellular carcinoma and induces G1 arrest in cell cycle. Journal of hepatology. 2008;48(3):433-41. doi: 10.1016/j.jhep.2007.11.015. PubMed PMID: 18191269.

199. Kwong J, Lee JY, Wong KK, Zhou X, Wong DT, Lo KW, Welch WR, Berkowitz RS, Mok SC. Candidate tumor-suppressor gene DLEC1 is frequently downregulated by promoter hypermethylation and histone hypoacetylation in human epithelial ovarian cancer. Neoplasia. 2006;8(4):268-78. doi: 10.1593/neo.05502. PubMed PMID: 16756719; PMCID: 1600675.

200. Zhang Q, Ying J, Li J, Fan Y, Poon FF, Ng KM, Tao Q, Jin J. Aberrant promoter methylation of DLEC1, a critical 3p22 tumor suppressor for renal cell carcinoma, is associated with more advanced tumor stage. The Journal of urology. 2010;184(2):731-7. doi: 10.1016/j.juro.2010.03.108. PubMed PMID: 20639048.

201. Kwong J, Chow LS, Wong AY, Hung WK, Chung GT, To KF, Chan FL, Daigo Y, Nakamura Y, Huang DP, Lo KW. Epigenetic inactivation of the deleted in lung and esophageal cancer 1 gene in nasopharyngeal carcinoma. Genes, chromosomes & cancer. 2007;46(2):171-80. doi: 10.1002/gcc.20398. PubMed PMID: 17099870.

202. Park SY, Kwon HJ, Lee HE, Ryu HS, Kim SW, Kim JH, Kim IA, Jung N, Cho NY, Kang GH. Promoter CpG island hypermethylation during breast cancer progression. Virchows Archiv : an international journal of pathology. 2011;458(1):73-84. doi: 10.1007/s00428-010-1013-6. PubMed PMID: 21120523.

203. Saw CL, Guo Y, Yang AY, Paredes-Gonzalez X, Ramirez C, Pung D, Kong AN. The berry constituents quercetin, kaempferol, and pterostilbene synergistically attenuate reactive oxygen species: Involvement of the Nrf2-ARE signaling pathway. Food and chemical toxicology : an international journal published for the British Industrial Biological Research Association. 2014;72:303-11. doi: 10.1016/j.fct.2014.07.038. PubMed PMID: 25111660.

204. Wang L, Zhang C, Guo Y, Su ZY, Yang Y, Shu L, Kong AN. Blocking of JB6 Cell Transformation by Tanshinone IIA: Epigenetic Reactivation of Nrf2 Antioxidative Stress Pathway. The AAPS journal. 2014. doi: 10.1208/s12248-014-9666-8. PubMed PMID: 25274607.

205. Wang Z, Li L, Su X, Gao Z, Srivastava G, Murray PG, Ambinder R, Tao Q. Epigenetic silencing of the 3p22 tumor suppressor DLEC1 by promoter CpG methylation in non-Hodgkin and Hodgkin lymphomas. Journal of translational medicine. 2012;10:209. doi: 10.1186/1479-5876-10-209. PubMed PMID: 23050586; PMCID: 3540012.

206. Bora-Tatar G, Dayangac-Erden D, Demir AS, Dalkara S, Yelekci K, Erdem-Yurter H. Molecular modifications on carboxylic acid derivatives as potent histone

deacetylase inhibitors: Activity and docking studies. Bioorganic & medicinal chemistry. 2009;17(14):5219-28. doi: 10.1016/j.bmc.2009.05.042. PubMed PMID: 19520580.

207. Cifone MA, Fidler IJ. Correlation of patterns of anchorage-independent growth with in vivo behavior of cells from a murine fibrosarcoma. Proceedings of the National Academy of Sciences of the United States of America. 1980;77(2):1039-43. PubMed PMID: 6928659; PMCID: 348419.

208. Mori S, Chang JT, Andrechek ER, Matsumura N, Baba T, Yao G, Kim JW, Gatza M, Murphy S, Nevins JR. Anchorage-independent cell growth signature identifies tumors with metastatic potential. Oncogene. 2009;28(31):2796-805. doi: 10.1038/onc.2009.139. PubMed PMID: 19483725; PMCID: 3008357.

209. Chen CC, Sureshbabul M, Chen HW, Lin YS, Lee JY, Hong QS, Yang YC, Yu SL. Curcumin Suppresses Metastasis via Sp-1, FAK Inhibition, and E-Cadherin Upregulation in Colorectal Cancer. Evidence-based complementary and alternative medicine : eCAM. 2013;2013:541695. doi: 10.1155/2013/541695. PubMed PMID: 23970932; PMCID: 3736531.

210. Sjolund J, Johansson M, Manna S, Norin C, Pietras A, Beckman S, Nilsson E, Ljungberg B, Axelson H. Suppression of renal cell carcinoma growth by inhibition of Notch signaling in vitro and in vivo. The Journal of clinical investigation. 2008;118(1):217-28. doi: 10.1172/JCI32086. PubMed PMID: 18079963; PMCID: 2129233.

211. Orford K, Orford CC, Byers SW. Exogenous expression of beta-catenin regulates contact inhibition, anchorage-independent growth, anoikis, and radiation-induced cell cycle arrest. The Journal of cell biology. 1999;146(4):855-68. PubMed PMID: 10459019; PMCID: 2156133.

212. Dang CV, O'Donnell KA, Zeller KI, Nguyen T, Osthus RC, Li F. The c-Myc target gene network. Seminars in cancer biology. 2006;16(4):253-64. doi: 10.1016/j.semcancer.2006.07.014. PubMed PMID: 16904903.

213. Lou Z, O'Reilly S, Liang H, Maher VM, Sleight SD, McCormick JJ. Down-regulation of overexpressed sp1 protein in human fibrosarcoma cell lines inhibits tumor formation. Cancer research. 2005;65(3):1007-17. PubMed PMID: 15705902.

214. Zou J, Luo H, Zeng Q, Dong Z, Wu D, Liu L. Protein kinase CK2alpha is overexpressed in colorectal cancer and modulates cell proliferation and invasion via regulating EMT-related genes. Journal of translational medicine. 2011;9:97. doi: 10.1186/1479-5876-9-97. PubMed PMID: 21702981; PMCID: 3132712.

215. Liu Z, Xie Z, Jones W, Pavlovicz RE, Liu S, Yu J, Li PK, Lin J, Fuchs JR, Marcucci G, Li C, Chan KK. Curcumin is a potent DNA hypomethylation agent. Bioorganic & medicinal chemistry letters. 2009;19(3):706-9. doi: 10.1016/j.bmcl.2008.12.041. PubMed PMID: 19112019.

216. Lee SJ, Krauthauser C, Maduskuie V, Fawcett PT, Olson JM, Rajasekaran SA. Curcumin-induced HDAC inhibition and attenuation of medulloblastoma growth in vitro and in vivo. BMC Cancer. 2011;11:144. doi: 10.1186/1471-2407-11-144. PubMed PMID: 21501498; PMCID: 3090367.

217. Park W, Amin AR, Chen ZG, Shin DM. New perspectives of curcumin in cancer prevention. Cancer Prev Res (Phila). 2013;6(5):387-400. doi: 10.1158/1940-6207.CAPR-12-0410. PubMed PMID: 23466484; PMCID: 3693758.

218. Howlader N NA, Krapcho M. SEER Cancer Statistics Review Bethesda, MD: National Cancer Institute; 1975-2012.

219. Triantafillidis JK, Nasioulas G, Kosmidis PA. Colorectal cancer and inflammatory bowel disease: epidemiology, risk factors, mechanisms of carcinogenesis and prevention strategies. Anticancer Res. 2009;29(7):2727-37. PubMed PMID: 19596953.

220. von Roon AC, Reese G, Teare J, Constantinides V, Darzi AW, Tekkis PP. The risk of cancer in patients with Crohn's disease. Dis Colon Rectum. 2007;50(6):839-55. doi: 10.1007/s10350-006-0848-z. PubMed PMID: 17308939.

221. Delker DA, McKnight SJ, 3rd, Rosenberg DW. The role of alcohol dehydrogenase in the metabolism of the colon carcinogen methylazoxymethanol. Toxicol Sci. 1998;45(1):66-71. doi: 10.1006/toxs.1998.2499. PubMed PMID: 9848112.

222. Perse M, Cerar A. Dextran sodium sulphate colitis mouse model: traps and tricks. J Biomed Biotechnol. 2012;2012:718617. doi: 10.1155/2012/718617. PubMed PMID: 22665990; PMCID: PMC3361365.

223. De Robertis M, Massi E, Poeta ML, Carotti S, Morini S, Cecchetelli L, Signori E, Fazio VM. The AOM/DSS murine model for the study of colon carcinogenesis: From pathways to diagnosis and therapy studies. J Carcinog. 2011;10:9. doi: 10.4103/1477-3163.78279. PubMed PMID: 21483655; PMCID: 3072657.

224. Hartnett L, Egan LJ. Inflammation, DNA methylation and colitis-associated cancer. Carcinogenesis. 2012;33(4):723-31. doi: 10.1093/carcin/bgs006. PubMed PMID: 22235026.

225. Guo Y, Su ZY, Kong AT. Current Perspectives on Epigenetic Modifications by Dietary Chemopreventive and Herbal Phytochemicals. Curr Pharmacol Rep. 2015;1(4):245-57. doi: 10.1007/s40495-015-0023-0. PubMed PMID: 26328267; PMCID: 4552355.

226. Glauben R, Batra A, Fedke I, Zeitz M, Lehr HA, Leoni F, Mascagni P, Fantuzzi G, Dinarello CA, Siegmund B. Histone hyperacetylation is associated with amelioration of experimental colitis in mice. J Immunol. 2006;176(8):5015-22. PubMed PMID: 16585598.

227. Tsaprouni LG, Ito K, Powell JJ, Adcock IM, Punchard N. Differential patterns of histone acetylation in inflammatory bowel diseases. J Inflamm (Lond). 2011;8(1):1. doi: 10.1186/1476-9255-8-1. PubMed PMID: 21272292; PMCID: 3040698.

228. Karczmarski J, Rubel T, Paziewska A, Mikula M, Bujko M, Kober P, Dadlez M, Ostrowski J. Histone H3 lysine 27 acetylation is altered in colon cancer. Clin Proteomics. 2014;11(1):24. doi: 10.1186/1559-0275-11-24. PubMed PMID: 24994966; PMCID: 4071346.

229. Villagra A, Sotomayor EM, Seto E. Histone deacetylases and the immunological network: implications in cancer and inflammation. Oncogene. 2010;29(2):157-73. doi: 10.1038/onc.2009.334. PubMed PMID: 19855430.

230. Glauben R, Batra A, Stroh T, Erben U, Fedke I, Lehr HA, Leoni F, Mascagni P, Dinarello CA, Zeitz M, Siegmund B. Histone deacetylases: novel targets for prevention of colitis-associated cancer in mice. Gut. 2008;57(5):613-22. doi: 10.1136/gut.2007.134650. PubMed PMID: 18194985.

231. Sostres C, Gargallo CJ, Lanas A. Aspirin, cyclooxygenase inhibition and colorectal cancer. World J Gastrointest Pharmacol Ther. 2014;5(1):40-9. doi: 10.4292/wjgpt.v5.i1.40. PubMed PMID: 24605250; PMCID: 3944468.

232. Algra AM, Rothwell PM. Effects of regular aspirin on long-term cancer incidence and metastasis: a systematic comparison of evidence from observational studies versus randomised trials. Lancet Oncol. 2012;13(5):518-27. doi: 10.1016/S1470-2045(12)70112-2. PubMed PMID: 22440112.

233. Burn J, Gerdes AM, Macrae F, Mecklin JP, Moeslein G, Olschwang S, Eccles D, Evans DG, Maher ER, Bertario L, Bisgaard ML, Dunlop MG, Ho JW, Hodgson SV, Lindblom A, Lubinski J, Morrison PJ, Murday V, Ramesar R, Side L, Scott RJ, Thomas HJ, Vasen HF, Barker G, Crawford G, Elliott F, Movahedi M, Pylvanainen K, Wijnen JT, Fodde R, Lynch HT, Mathers JC, Bishop DT, Investigators C. Long-term effect of aspirin on cancer risk in carriers of hereditary colorectal cancer: an analysis from the CAPP2 randomised controlled trial. Lancet. 2011;378(9809):2081-7. doi: 10.1016/S0140-6736(11)61049-0. PubMed PMID: 22036019; PMCID: 3243929.

234. Velayos FS, Loftus EV, Jr., Jess T, Harmsen WS, Bida J, Zinsmeister AR, Tremaine WJ, Sandborn WJ. Predictive and protective factors associated with colorectal cancer in ulcerative colitis: A case-control study. Gastroenterology. 2006;130(7):1941-9. doi: 10.1053/j.gastro.2006.03.028. PubMed PMID: 16762617.

235. Tian Y, Ye Y, Gao W, Chen H, Song T, Wang D, Mao X, Ren C. Aspirin promotes apoptosis in a murine model of colorectal cancer by mechanisms involving downregulation of IL-6-STAT3 signaling pathway. Int J Colorectal Dis. 2011;26(1):13-22. doi: 10.1007/s00384-010-1060-0. PubMed PMID: 20886344.

236. Ishikawa TO, Herschman HR. Tumor formation in a mouse model of colitis-associated colon cancer does not require COX-1 or COX-2 expression. Carcinogenesis. 2010;31(4):729-36. doi: 10.1093/carcin/bgq002. PubMed PMID: 20061361; PMCID: 2847091.

237. Chan AT, Ogino S, Fuchs CS. Aspirin and the risk of colorectal cancer in relation to the expression of COX-2. N Engl J Med. 2007;356(21):2131-42. doi: 10.1056/NEJMoa067208. PubMed PMID: 17522398.

238. Yiannakopoulou E. Targeting epigenetic mechanisms and microRNAs by aspirin and other non steroidal anti-inflammatory agents--implications for cancer treatment and chemoprevention. Cell Oncol (Dordr). 2014;37(3):167-78. doi: 10.1007/s13402-014-0175-7. PubMed PMID: 24996792.

239. Carlsson G, Gullberg B, Hafstrom L. Estimation of liver tumor volume using different formulas - an experimental study in rats. J Cancer Res Clin Oncol. 1983;105(1):20-3. PubMed PMID: 6833336.

240. Qualls JE, Kaplan AM, van Rooijen N, Cohen DA. Suppression of experimental colitis by intestinal mononuclear phagocytes. J Leukoc Biol. 2006;80(4):802-15. doi: 10.1189/jlb.1205734. PubMed PMID: 16888083.

241. Ju J, Hao X, Lee MJ, Lambert JD, Lu G, Xiao H, Newmark HL, Yang CS. A gamma-tocopherol-rich mixture of tocopherols inhibits colon inflammation and carcinogenesis in azoxymethane and dextran sulfate sodium-treated mice. Cancer Prev Res (Phila). 2009;2(2):143-52. doi: 10.1158/1940-6207.CAPR-08-0099. PubMed PMID: 19155443; PMCID: PMC2821738.

242. Lee JH, Lee KR, Su ZY, Boyanapalli SS, Barman DN, Huang MT, Chen L, Magesh S, Hu L, Kong AN. In vitro and in vivo anti-inflammatory effects of a novel 4,6-bis ((E)-4-hydroxy-3-methoxystyryl)-1-phenethylpyrimidine-2(1H)-thione. Chem Res Toxicol. 2014;27(1):34-41. doi: 10.1021/tx400315u. PubMed PMID: 24304388.

243. Guo Y, Shu L, Zhang C, Su ZY, Kong AN. Curcumin inhibits anchorage-independent growth of HT29 human colon cancer cells by targeting epigenetic restoration of the tumor suppressor gene DLEC1. Biochemical pharmacology. 2015;94(2):69-78. doi: 10.1016/j.bcp.2015.01.009. PubMed PMID: 25640947.

244. Murthy SN, Cooper HS, Shim H, Shah RS, Ibrahim SA, Sedergran DJ. Treatment of dextran sulfate sodium-induced murine colitis by intracolonic cyclosporin. Dig Dis Sci. 1993;38(9):1722-34. PubMed PMID: 8359087.

245. Tampakis A, Tampaki EC, Nebiker CA, Kouraklis G. Histone deacetylase inhibitors and colorectal cancer: what is new? Anticancer Agents Med Chem. 2014;14(9):1220-7. PubMed PMID: 25246306.

246. Glauben R, Siegmund B. Inhibition of histone deacetylases in inflammatory bowel diseases. Mol Med. 2011;17(5-6):426-33. doi: 10.2119/molmed.2011.00069. PubMed PMID: 21365125; PMCID: 3105130.

247. Chahar S, Gandhi V, Yu S, Desai K, Cowper-Sal-lari R, Kim Y, Perekatt AO, Kumar N, Thackray JK, Musolf A, Kumar N, Hoffman A, Londono D, Vazquez BN, Serrano L, Shin H, Lupien M, Gao N, Verzi MP. Chromatin profiling reveals regulatory network shifts and a protective role for hepatocyte nuclear factor 4alpha during colitis. Mol Cell Biol. 2014;34(17):3291-304. doi: 10.1128/MCB.00349-14. PubMed PMID: 24980432; PMCID: PMC4135557.

248. Issa JP, Kantarjian HM, Kirkpatrick P. Azacitidine. Nat Rev Drug Discov. 2005;4(4):275-6. doi: 10.1038/nrd1698. PubMed PMID: 15861567.

249. Garcia-Albeniz X, Chan AT. Aspirin for the prevention of colorectal cancer. Best Pract Res Clin Gastroenterol. 2011;25(4-5):461-72. doi: 10.1016/j.bpg.2011.10.015. PubMed PMID: 22122763; PMCID: 3354696.

250. Roelofs HM, Te Morsche RH, van Heumen BW, Nagengast FM, Peters WH. Over-expression of COX-2 mRNA in colorectal cancer. BMC Gastroenterol. 2014;14:1. doi: 10.1186/1471-230X-14-1. PubMed PMID: 24383454; PMCID: 3880419.

251. Yamanoi K, Arai E, Tian Y, Takahashi Y, Miyata S, Sasaki H, Chiwaki F, Ichikawa H, Sakamoto H, Kushima R, Katai H, Yoshida T, Sakamoto M, Kanai Y. Epigenetic clustering of gastric carcinomas based on DNA methylation profiles at the precancerous stage: its correlation with tumor aggressiveness and patient outcome. Carcinogenesis. 2015;36(5):509-20. doi: 10.1093/carcin/bgv013. PubMed PMID: 25740824; PMCID: 4417340.

252. Arai E, Kanai Y. DNA methylation profiles in precancerous tissue and cancers: carcinogenetic risk estimation and prognostication based on DNA methylation status. Epigenomics. 2010;2(3):467-81. doi: 10.2217/epi.10.16. PubMed PMID: 22121905.

253. Tahara T, Shibata T, Nakamura M, Yamashita H, Yoshioka D, Okubo M, Maruyama N, Kamano T, Kamiya Y, Fujita H, Nagasaka M, Iwata M, Takahama K, Watanabe M, Hirata I, Arisawa T. Chronic aspirin use suppresses CDH1 methylation in human gastric mucosa. Dig Dis Sci. 2010;55(1):54-9. doi: 10.1007/s10620-008-0701-4. PubMed PMID: 19184424.

254. Kamble P, Selvarajan K, Aluganti Narasimhulu C, Nandave M, Parthasarathy S. Aspirin may promote mitochondrial biogenesis via the production of hydrogen peroxide and the induction of Sirtuin1/PGC-1alpha genes. Eur J Pharmacol. 2013;699(1-3):55-61. doi: 10.1016/j.ejphar.2012.11.051. PubMed PMID: 23228932; PMCID: 3619195.

255. Marimuthu S, Chivukula RS, Alfonso LF, Moridani M, Hagen FK, Bhat GJ. Aspirin acetylates multiple cellular proteins in HCT-116 colon cancer cells: Identification of novel targets. Int J Oncol. 2011;39(5):1273-83. doi: 10.3892/ijo.2011.1113. PubMed PMID: 21743961.

256. Passacquale G, Phinikaridou A, Warboys C, Cooper M, Lavin B, Alfieri A, Andia ME, Botnar RM, Ferro A. Aspirin-induced histone acetylation in endothelial cells enhances synthesis of the secreted isoform of netrin-1 thus inhibiting monocyte vascular infiltration. Br J Pharmacol. 2015;172(14):3548-64. doi: 10.1111/bph.13144. PubMed PMID: 25824964; PMCID: 4507159.

257. Gargalionis AN, Piperi C, Adamopoulos C, Papavassiliou AG. Histone modifications as a pathogenic mechanism of colorectal tumorigenesis. Int J Biochem Cell Biol. 2012;44(8):1276-89. doi: 10.1016/j.biocel.2012.05.002. PubMed PMID: 22583735.

258. Narayan V, Ravindra KC, Liao C, Kaushal N, Carlson BA, Prabhu KS. Epigenetic regulation of inflammatory gene expression in macrophages by selenium. J Nutr Biochem. 2015;26(2):138-45. doi: 10.1016/j.jnutbio.2014.09.009. PubMed PMID: 25458528; PMCID: 4302047.

259. Yu Z, Zhang W, Kone BC. Histone deacetylases augment cytokine induction of the iNOS gene. J Am Soc Nephrol. 2002;13(8):2009-17. PubMed PMID: 12138131.

260. Sullivan KE, Reddy AB, Dietzmann K, Suriano AR, Kocieda VP, Stewart M, Bhatia M. Epigenetic regulation of tumor necrosis factor alpha. Molecular and cellular biology. 2007;27(14):5147-60. doi: 10.1128/MCB.02429-06. PubMed PMID: 17515611; PMCID: 1951949.

261. Zimmermann M, Aguilera FB, Castellucci M, Rossato M, Costa S, Lunardi C, Ostuni R, Girolomoni G, Natoli G, Bazzoni F, Tamassia N, Cassatella MA. Chromatin remodelling and autocrine TNFalpha are required for optimal interleukin-6 expression in activated human neutrophils. Nat Commun. 2015;6:6061. doi: 10.1038/ncomms7061. PubMed PMID: 25616107.

262. Rada-Iglesias A, Bajpai R, Swigut T, Brugmann SA, Flynn RA, Wysocka J. A unique chromatin signature uncovers early developmental enhancers in humans. Nature. 2011;470(7333):279-83. doi: 10.1038/nature09692. PubMed PMID: 21160473; PMCID: 4445674.

263. Erdman SE, Rao VP, Poutahidis T, Rogers AB, Taylor CL, Jackson EA, Ge Z, Lee CW, Schauer DB, Wogan GN, Tannenbaum SR, Fox JG. Nitric oxide and TNF-alpha trigger colonic inflammation and carcinogenesis in Helicobacter hepaticus-infected, Rag2-deficient mice. Proc Natl Acad Sci U S A. 2009;106(4):1027-32. doi: 10.1073/pnas.0812347106. PubMed PMID: 19164562; PMCID: 2633549.

264. Grivennikov S, Karin E, Terzic J, Mucida D, Yu GY, Vallabhapurapu S, Scheller J, Rose-John S, Cheroutre H, Eckmann L, Karin M. IL-6 and Stat3 are required for survival of intestinal epithelial cells and development of colitis-associated cancer.

Cancer Cell. 2009;15(2):103-13. doi: 10.1016/j.ccr.2009.01.001. PubMed PMID: 19185845; PMCID: 2667107.

265. Howlader N NA, Krapcho M. . SEER Cancer Statistics Review. In: Institute NC, editor. 2012.

266. Hanahan D, Weinberg RA. Hallmarks of cancer: the next generation. Cell. 2011;144(5):646-74. doi: 10.1016/j.cell.2011.02.013. PubMed PMID: 21376230.

267. Lasry A, Zinger A, Ben-Neriah Y. Inflammatory networks underlying colorectal cancer. Nat Immunol. 2016;17(3):230-40. doi: 10.1038/ni.3384. PubMed PMID: 26882261.

268. Feagins LA, Souza RF, Spechler SJ. Carcinogenesis in IBD: potential targets for the prevention of colorectal cancer. Nat Rev Gastroenterol Hepatol. 2009;6(5):297-305. doi: 10.1038/nrgastro.2009.44. PubMed PMID: 19404270.

269. Soderlund S, Brandt L, Lapidus A, Karlen P, Brostrom O, Lofberg R, Ekbom A, Askling J. Decreasing time-trends of colorectal cancer in a large cohort of patients with inflammatory bowel disease. Gastroenterology. 2009;136(5):1561-7; quiz 818-9. PubMed PMID: 19422077.

270. Sporn MB, Suh N. Chemoprevention: an essential approach to controlling cancer. Nat Rev Cancer. 2002;2(7):537-43. doi: 10.1038/nrc844. PubMed PMID: 12094240.

271. Guo Y, Liu Y, Zhang C, Su ZY, Li W, Huang MT, Kong AN. The epigenetic effects of aspirin: the modification of histone H3 lysine 27 acetylation in the prevention of colon carcinogenesis in azoxymethane- and dextran sulfate sodium-treated CF-1 mice. Carcinogenesis. 2016;37(6):616-24. doi: 10.1093/carcin/bgw042. PubMed PMID: 27207670.

272. Murphy EA, Davis JM, McClellan JL, Gordon BT, Carmichael MD. Curcumin's effect on intestinal inflammation and tumorigenesis in the ApcMin/+ mouse. J Interferon Cytokine Res. 2011;31(2):219-26. doi: 10.1089/jir.2010.0051. PubMed PMID: 20950131; PMCID: 3064532.

273. Carroll RE, Benya RV, Turgeon DK, Vareed S, Neuman M, Rodriguez L, Kakarala M, Carpenter PM, McLaren C, Meyskens FL, Jr., Brenner DE. Phase IIa clinical trial of curcumin for the prevention of colorectal neoplasia. Cancer Prev Res (Phila). 2011;4(3):354-64. doi: 10.1158/1940-6207.CAPR-10-0098. PubMed PMID: 21372035; PMCID: 4136551.

274. Pereira MA, Grubbs CJ, Barnes LH, Li H, Olson GR, Eto I, Juliana M, Whitaker LM, Kelloff GJ, Steele VE, Lubet RA. Effects of the phytochemicals, curcumin and quercetin, upon azoxymethane-induced colon cancer and 7,12-dimethylbenz[a]anthracene-induced mammary cancer in rats. Carcinogenesis. 1996;17(6):1305-11. PubMed PMID: 8681447.

275. Rao CV, Simi B, Reddy BS. Inhibition by dietary curcumin of azoxymethane-induced ornithine decarboxylase, tyrosine protein kinase, arachidonic acid metabolism and aberrant crypt foci formation in the rat colon. Carcinogenesis. 1993;14(11):2219-25. PubMed PMID: 8242846.

276. Vareed SK, Kakarala M, Ruffin MT, Crowell JA, Normolle DP, Djuric Z, Brenner DE. Pharmacokinetics of curcumin conjugate metabolites in healthy human subjects. Cancer Epidemiol Biomarkers Prev. 2008;17(6):1411-7. doi: 10.1158/1055-9965.EPI-07-2693. PubMed PMID: 18559556; PMCID: 4138955.

277. Lu G, Xiao H, You H, Lin Y, Jin H, Snagaski B, Yang CS. Synergistic inhibition of lung tumorigenesis by a combination of green tea polyphenols and atorvastatin. Clin Cancer Res. 2008;14(15):4981-8. doi: 10.1158/1078-0432.CCR-07-1860. PubMed PMID: 18676773.

278. Zheng X, Cui XX, Gao Z, Zhao Y, Lin Y, Shih WJ, Huang MT, Liu Y, Rabson A, Reddy B, Yang CS, Conney AH. Atorvastatin and celecoxib in combination inhibits the progression of androgen-dependent LNCaP xenograft prostate tumors to androgen independence. Cancer Prev Res (Phila). 2010;3(1):114-24. doi: 10.1158/1940-6207.CAPR-09-0059. PubMed PMID: 20051379; PMCID: 2803700.

279. Yue W, Zheng X, Lin Y, Yang CS, Xu Q, Carpizo D, Huang H, DiPaola RS, Tan XL. Metformin combined with aspirin significantly inhibit pancreatic cancer cell growth in vitro and in vivo by suppressing anti-apoptotic proteins Mcl-1 and Bcl-2. Oncotarget. 2015;6(25):21208-24. doi: 10.18632/oncotarget.4126. PubMed PMID: 26056043; PMCID: 4673260.

280. Liu Y, Ju J, Xiao H, Simi B, Hao X, Reddy BS, Huang MT, Newmark H, Yang CS. Effects of combination of calcium and aspirin on azoxymethane-induced aberrant crypt foci formation in the colons of mice and rats. Nutr Cancer. 2008;60(5):660-5. doi: 10.1080/01635580802290215. PubMed PMID: 18791930.

281. Thakkar A, Sutaria D, Grandhi BK, Wang J, Prabhu S. The molecular mechanism of action of aspirin, curcumin and sulforaphane combinations in the chemoprevention of pancreatic cancer. Oncol Rep. 2013;29(4):1671-7. doi: 10.3892/or.2013.2276. PubMed PMID: 23404329; PMCID: 3621734.

282. Perkins S, Clarke AR, Steward W, Gescher A. Age-related difference in susceptibility of Apc(Min/+) mice towards the chemopreventive efficacy of dietary aspirin and curcumin. Br J Cancer. 2003;88(9):1480-3. doi: 10.1038/sj.bjc.6600900. PubMed PMID: 12778080; PMCID: 2741037.

283. Wang Z, Gerstein M, Snyder M. RNA-Seq: a revolutionary tool for transcriptomics. Nat Rev Genet. 2009;10(1):57-63. doi: 10.1038/nrg2484. PubMed PMID: 19015660; PMCID: 2949280.

284. Cheung KL, Khor TO, Huang MT, Kong AN. Differential in vivo mechanism of chemoprevention of tumor formation in azoxymethane/dextran sodium sulfate mice by PEITC and DBM. Carcinogenesis. 2010;31(5):880-5. doi: 10.1093/carcin/bgp285. PubMed PMID: 19959557; PMCID: 2864406.

285. Kim D, Pertea G, Trapnell C, Pimentel H, Kelley R, Salzberg SL. TopHat2: accurate alignment of transcriptomes in the presence of insertions, deletions and gene fusions. Genome Biol. 2013;14(4):R36. doi: 10.1186/gb-2013-14-4-r36. PubMed PMID: 23618408; PMCID: 4053844.

286. Trapnell C, Williams BA, Pertea G, Mortazavi A, Kwan G, van Baren MJ, Salzberg SL, Wold BJ, Pachter L. Transcript assembly and quantification by RNA-Seq reveals unannotated transcripts and isoform switching during cell differentiation. Nat Biotechnol. 2010;28(5):511-5. doi: 10.1038/nbt.1621. PubMed PMID: 20436464; PMCID: 3146043.

287. Kubota M, Shimizu M, Sakai H, Yasuda Y, Terakura D, Baba A, Ohno T, Tsurumi H, Tanaka T, Moriwaki H. Preventive effects of curcumin on the development of azoxymethane-induced colonic preneoplastic lesions in male C57BL/KsJ-db/db

obese mice. Nutr Cancer. 2012;64(1):72-9. doi: 10.1080/01635581.2012.630554. PubMed PMID: 22172229.

288. Huang MT, Lou YR, Ma W, Newmark HL, Reuhl KR, Conney AH. Inhibitory effects of dietary curcumin on forestomach, duodenal, and colon carcinogenesis in mice. Cancer Res. 1994;54(22):5841-7. PubMed PMID: 7954412.

289. Suzuki R, Kohno H, Sugie S, Nakagama H, Tanaka T. Strain differences in the susceptibility to azoxymethane and dextran sodium sulfate-induced colon carcinogenesis in mice. Carcinogenesis. 2006;27(1):162-9. doi: 10.1093/carcin/bgi205. PubMed PMID: 16081511.

290. Choi HA, Kim MR, Park KA, Hong J. Interaction of over-the-counter drugs with curcumin: influence on stability and bioactivities in intestinal cells. J Agric Food Chem. 2012;60(42):10578-84. doi: 10.1021/jf303534e. PubMed PMID: 23025432.

291. Dinis TC, Maderia VM, Almeida LM. Action of phenolic derivatives (acetaminophen, salicylate, and 5-aminosalicylate) as inhibitors of membrane lipid peroxidation and as peroxyl radical scavengers. Arch Biochem Biophys. 1994;315(1):161-9. PubMed PMID: 7979394.

292. Gialeli C, Theocharis AD, Karamanos NK. Roles of matrix metalloproteinases in cancer progression and their pharmacological targeting. FEBS J. 2011;278(1):16-27. doi: 10.1111/j.1742-4658.2010.07919.x. PubMed PMID: 21087457.

293. Polistena A, Cucina A, Dinicola S, Stene C, Cavallaro G, Ciardi A, Orlando G, Arena R, D'Ermo G, Cavallaro A, Johnson LB, De Toma G. MMP7 expression in colorectal tumours of different stages. In Vivo. 2014;28(1):105-10. PubMed PMID: 24425843.

294. Koskensalo S, Louhimo J, Nordling S, Hagstrom J, Haglund C. MMP-7 as a prognostic marker in colorectal cancer. Tumour Biol. 2011;32(2):259-64. doi: 10.1007/s13277-010-0080-2. PubMed PMID: 21207220.

295. Klupp F, Neumann L, Kahlert C, Diers J, Halama N, Franz C, Schmidt T, Koch M, Weitz J, Schneider M, Ulrich A. Serum MMP7, MMP10 and MMP12 level as negative prognostic markers in colon cancer patients. BMC Cancer. 2016;16:494. doi: 10.1186/s12885-016-2515-7. PubMed PMID: 27431388; PMCID: 4950722.

296. Koller FL, Dozier EA, Nam KT, Swee M, Birkland TP, Parks WC, Fingleton B. Lack of MMP10 exacerbates experimental colitis and promotes development of inflammation-associated colonic dysplasia. Lab Invest. 2012;92(12):1749-59. doi: 10.1038/labinvest.2012.141. PubMed PMID: 23044923; PMCID: 3510327.

297. Wang D, Dubois RN, Richmond A. The role of chemokines in intestinal inflammation and cancer. Curr Opin Pharmacol. 2009;9(6):688-96. doi: 10.1016/j.coph.2009.08.003. PubMed PMID: 19734090; PMCID: 2787713.

298. Gijsbers K, Van Assche G, Joossens S, Struyf S, Proost P, Rutgeerts P, Geboes K, Van Damme J. CXCR1-binding chemokines in inflammatory bowel diseases: down-regulated IL-8/CXCL8 production by leukocytes in Crohn's disease and selective GCP-2/CXCL6 expression in inflamed intestinal tissue. Eur J Immunol. 2004;34(7):1992-2000. doi: 10.1002/eji.200324807. PubMed PMID: 15214047.

299. Rubie C, Frick VO, Wagner M, Schuld J, Graber S, Brittner B, Bohle RM, Schilling MK. ELR+ CXC chemokine expression in benign and malignant colorectal conditions. BMC Cancer. 2008;8:178. doi: 10.1186/1471-2407-8-178. PubMed PMID: 18578857; PMCID: 2459188.

300. Kummola L, Hamalainen JM, Kivela J, Kivela AJ, Saarnio J, Karttunen T, Parkkila S. Expression of a novel carbonic anhydrase, CA XIII, in normal and neoplastic colorectal mucosa. BMC Cancer. 2005;5:41. doi: 10.1186/1471-2407-5-41. PubMed PMID: 15836783; PMCID: 1097719.

301. Zhang J, Tsoi H, Li X, Wang H, Gao J, Wang K, Go MY, Ng SC, Chan FK, Sung JJ, Yu J. Carbonic anhydrase IV inhibits colon cancer development by inhibiting the Wnt signalling pathway through targeting the WTAP-WT1-TBL1 axis. Gut. 2016;65(9):1482-93. doi: 10.1136/gutjnl-2014-308614. PubMed PMID: 26071132.

302. Yang GZ, Hu L, Cai J, Chen HY, Zhang Y, Feng D, Qi CY, Zhai YX, Gong H, Fu H, Cai QP, Gao CF. Prognostic value of carbonic anhydrase VII expression in colorectal carcinoma. BMC Cancer. 2015;15:209. doi: 10.1186/s12885-015-1216-y. PubMed PMID: 25885898; PMCID: 4406128.

303. Dai HY, Hong CC, Liang SC, Yan MD, Lai GM, Cheng AL, Chuang SE. Carbonic anhydrase III promotes transformation and invasion capability in hepatoma cells through FAK signaling pathway. Mol Carcinog. 2008;47(12):956-63. doi: 10.1002/mc.20448. PubMed PMID: 18444244.

304. Kang N, Gores GJ, Shah VH. Hepatic stellate cells: partners in crime for liver metastases? Hepatology. 2011;54(2):707-13. doi: 10.1002/hep.24384. PubMed PMID: 21520207; PMCID: 3145026.

305. Ye Y, Xiao L, Wang SJ, Yue W, Yin QS, Sun MY, Xia W, Shao ZY, Zhang H. Up-regulation of REG3A in colorectal cancer cells confers proliferation and correlates with colorectal cancer risk. Oncotarget. 2016;7(4):3921-33. doi: 10.18632/oncotarget.6473. PubMed PMID: 26646797; PMCID: 4826180.

306. Garg P, Sarma D, Jeppsson S, Patel NR, Gewirtz AT, Merlin D, Sitaraman SV. Matrix metalloproteinase-9 functions as a tumor suppressor in colitis-associated cancer. Cancer Res. 2010;70(2):792-801. doi: 10.1158/0008-5472.CAN-09-3166. PubMed PMID: 20068187; PMCID: 2821688.

307. Chang LY, Lin YC, Mahalingam J, Huang CT, Chen TW, Kang CW, Peng HM, Chu YY, Chiang JM, Dutta A, Day YJ, Chen TC, Yeh CT, Lin CY. Tumor-derived chemokine CCL5 enhances TGF-beta-mediated killing of CD8(+) T cells in colon cancer by T-regulatory cells. Cancer Res. 2012;72(5):1092-102. doi: 10.1158/0008-5472.CAN-11-2493. PubMed PMID: 22282655.

308. Ihara A, Wada K, Yoneda M, Fujisawa N, Takahashi H, Nakajima A. Blockade of leukotriene B4 signaling pathway induces apoptosis and suppresses cell proliferation in colon cancer. J Pharmacol Sci. 2007;103(1):24-32. PubMed PMID: 17220595.

309. MacFie TS, Poulsom R, Parker A, Warnes G, Boitsova T, Nijhuis A, Suraweera N, Poehlmann A, Szary J, Feakins R, Jeffery R, Harper RW, Jubb AM, Lindsay JO, Silver A. DUOX2 and DUOXA2 form the predominant enzyme system capable of producing the reactive oxygen species H2O2 in active ulcerative colitis and are modulated by 5-aminosalicylic acid. Inflamm Bowel Dis. 2014;20(3):514-24. doi: 10.1097/01.MIB.0000442012.45038.0e. PubMed PMID: 24492313.

310. Mukai S, Oue N, Oshima T, Mukai R, Tatsumoto Y, Sakamoto N, Sentani K, Tanabe K, Egi H, Hinoi T, Ohdan H, Yasui W. Overexpression of Transmembrane Protein BST2 is Associated with Poor Survival of Patients with Esophageal, Gastric, or Colorectal Cancer. Ann Surg Oncol. 2016. doi: 10.1245/s10434-016-5100-z. PubMed PMID: 26832883.

311. Jung C, Kim RS, Zhang H, Lee SJ, Sheng H, Loehrer PJ, Gardner TA, Jeng MH, Kao C. HOXB13 is downregulated in colorectal cancer to confer TCF4-mediated transactivation. Br J Cancer. 2005;92(12):2233-9. doi: 10.1038/sj.bjc.6602631. PubMed PMID: 15928669; PMCID: 2361828.

312. Yang Z, Chen H, Huo L, Yang Z, Bai Y, Fan X, Ni B, Fang L, Hu J, Peng J, Wang L, Wang J. Epigenetic inactivation and tumor-suppressor behavior of NGFR in human colorectal cancer. Mol Cancer Res. 2015;13(1):107-19. doi: 10.1158/1541-7786.MCR-13-0247. PubMed PMID: 25244921.

313. Sui Y, Sun M, Wu F, Yang L, Di W, Zhang G, Zhong L, Ma Z, Zheng J, Fang X, Ma T. Inhibition of TMEM16A expression suppresses growth and invasion in human colorectal cancer cells. PLoS One. 2014;9(12):e115443. doi: 10.1371/journal.pone.0115443. PubMed PMID: 25541940; PMCID: 4277312.

314. Barrett CW, Ning W, Chen X, Smith JJ, Washington MK, Hill KE, Coburn LA, Peek RM, Chaturvedi R, Wilson KT, Burk RF, Williams CS. Tumor suppressor function of the plasma glutathione peroxidase gpx3 in colitis-associated carcinoma. Cancer Res. 2013;73(3):1245-55. doi: 10.1158/0008-5472.CAN-12-3150. PubMed PMID: 23221387; PMCID: 3563732.

315. Hryniuk A, Grainger S, Savory JG, Lohnes D. Cdx1 and Cdx2 function as tumor suppressors. J Biol Chem. 2014;289(48):33343-54. doi: 10.1074/jbc.M114.583823. PubMed PMID: 25320087; PMCID: 4246091.

316. Baba Y, Nosho K, Shima K, Freed E, Irahara N, Philips J, Meyerhardt JA, Hornick JL, Shivdasani RA, Fuchs CS, Ogino S. Relationship of CDX2 loss with molecular features and prognosis in colorectal cancer. Clin Cancer Res. 2009;15(14):4665-73. doi: 10.1158/1078-0432.CCR-09-0401. PubMed PMID: 19584150; PMCID: 2777758.

317. Itoh K, Wakabayashi N, Katoh Y, Ishii T, Igarashi K, Engel JD, Yamamoto M. Keap1 represses nuclear activation of antioxidant responsive elements by Nrf2 through binding to the amino-terminal Neh2 domain. Genes Dev. 1999;13(1):76-86. PubMed PMID: 9887101; PMCID: 316370.

318. Wakabayashi N, Slocum SL, Skoko JJ, Shin S, Kensler TW. When NRF2 talks, who's listening? Antioxidants & redox signaling. 2010;13(11):1649-63. doi: 10.1089/ars.2010.3216. PubMed PMID: 20367496; PMCID: 2966480.

319. Jeong WS, Jun M, Kong AN. Nrf2: a potential molecular target for cancer chemoprevention by natural compounds. Antioxidants & redox signaling. 2006;8(1-2):99-106. doi: 10.1089/ars.2006.8.99. PubMed PMID: 16487042.

320. Hayes JD, McMahon M. NRF2 and KEAP1 mutations: permanent activation of an adaptive response in cancer. Trends in biochemical sciences. 2009;34(4):176-88. doi: 10.1016/j.tibs.2008.12.008. PubMed PMID: 19321346.

321. Sporn MB, Liby KT. NRF2 and cancer: the good, the bad and the importance of context. Nature reviews Cancer. 2012;12(8):564-71. doi: 10.1038/nrc3278. PubMed PMID: 22810811; PMCID: 3836441.

322. Wang XJ, Sun Z, Villeneuve NF, Zhang S, Zhao F, Li Y, Chen W, Yi X, Zheng W, Wondrak GT, Wong PK, Zhang DD. Nrf2 enhances resistance of cancer cells to chemotherapeutic drugs, the dark side of Nrf2. Carcinogenesis. 2008;29(6):1235-43. doi: 10.1093/carcin/bgn095. PubMed PMID: 18413364; PMCID: 3312612.

323. Singh A, Misra V, Thimmulappa RK, Lee H, Ames S, Hoque MO, Herman JG, Baylin SB, Sidransky D, Gabrielson E, Brock MV, Biswal S. Dysfunctional KEAP1-NRF2 interaction in non-small-cell lung cancer. PLoS medicine. 2006;3(10):e420. doi: 10.1371/journal.pmed.0030420. PubMed PMID: 17020408; PMCID: 1584412.

324. Solis LM, Behrens C, Dong W, Suraokar M, Ozburn NC, Moran CA, Corvalan AH, Biswal S, Swisher SG, Bekele BN, Minna JD, Stewart DJ, Wistuba, II. Nrf2 and Keap1 abnormalities in non-small cell lung carcinoma and association with clinicopathologic features. Clinical cancer research : an official journal of the American Association for Cancer Research. 2010;16(14):3743-53. doi: 10.1158/1078-0432.CCR-09-3352. PubMed PMID: 20534738; PMCID: 2920733.

325. Mattick JS, Makunin IV. Non-coding RNA. Human molecular genetics. 2006;15 Spec No 1:R17-29. doi: 10.1093/hmg/ddl046. PubMed PMID: 16651366.

326. Li E. Chromatin modification and epigenetic reprogramming in mammalian development. Nature reviews Genetics. 2002;3(9):662-73. doi: 10.1038/nrg887. PubMed PMID: 12209141.

327. Egger G, Liang G, Aparicio A, Jones PA. Epigenetics in human disease and prospects for epigenetic therapy. Nature. 2004;429(6990):457-63. doi: 10.1038/nature02625. PubMed PMID: 15164071.

328. Teschendorff AE, West J, Beck S. Age-associated epigenetic drift: implications, and a case of epigenetic thrift? Human molecular genetics. 2013;22(R1):R7-R15. doi: 10.1093/hmg/ddt375. PubMed PMID: 23918660; PMCID: 3782071.

329. Feil R, Fraga MF. Epigenetics and the environment: emerging patterns and implications. Nature reviews Genetics. 2011;13(2):97-109. doi: 10.1038/nrg3142. PubMed PMID: 22215131.

330. Portela A, Esteller M. Epigenetic modifications and human disease. Nature biotechnology. 2010;28(10):1057-68. doi: 10.1038/nbt.1685. PubMed PMID: 20944598.

331. Ling C, Groop L. Epigenetics: a molecular link between environmental factors and type 2 diabetes. Diabetes. 2009;58(12):2718-25. doi: 10.2337/db09-1003. PubMed PMID: 19940235; PMCID: 2780862.

332. Martino D, Kesper DA, Amarasekera M, Harb H, Renz H, Prescott S. Epigenetics in immune development and in allergic and autoimmune diseases. Journal of reproductive immunology. 2014;104-105:43-8. doi: 10.1016/j.jri.2014.05.003. PubMed PMID: 25034262.

333. Handy DE, Castro R, Loscalzo J. Epigenetic modifications: basic mechanisms and role in cardiovascular disease. Circulation. 2011;123(19):2145-56. doi: 10.1161/CIRCULATIONAHA.110.956839. PubMed PMID: 21576679; PMCID: 3107542.

334. Marques SC, Oliveira CR, Pereira CM, Outeiro TF. Epigenetics in neurodegeneration: a new layer of complexity. Progress in neuro-psychopharmacology & biological psychiatry. 2011;35(2):348-55. doi: 10.1016/j.pnpbp.2010.08.008. PubMed PMID: 20736041.

335. Gronbaek K, Hother C, Jones PA. Epigenetic changes in cancer. APMIS : acta pathologica, microbiologica, et immunologica Scandinavica. 2007;115(10):1039-59. doi: 10.1111/j.1600-0463.2007.apm_636.xml.x. PubMed PMID: 18042143.

336. Dhanak D, Jackson P. Development and classes of epigenetic drugs for cancer. Biochemical and biophysical research communications. 2014;455(1-2):58-69. doi: 10.1016/j.bbrc.2014.07.006. PubMed PMID: 25016182.

337. Shen L, Song CX, He C, Zhang Y. Mechanism and function of oxidative reversal of DNA and RNA methylation. Annual review of biochemistry. 2014;83:585-614. doi: 10.1146/annurev-biochem-060713-035513. PubMed PMID: 24905787.

338. Franco R, Schoneveld O, Georgakilas AG, Panayiotidis MI. Oxidative stress, DNA methylation and carcinogenesis. Cancer letters. 2008;266(1):6-11. doi: 10.1016/j.canlet.2008.02.026. PubMed PMID: 18372104.

339. Niu Y, DesMarais TL, Tong Z, Yao Y, Costa M. Oxidative stress alters global histone modification and DNA methylation. Free radical biology & medicine. 2015;82:22-8. doi: 10.1016/j.freeradbiomed.2015.01.028. PubMed PMID: 25656994.

340. Su ZY, Shu L, Khor TO, Lee JH, Fuentes F, Kong AN. A perspective on dietary phytochemicals and cancer chemoprevention: oxidative stress, nrf2, and epigenomics. Topics in current chemistry. 2013;329:133-62. doi: 10.1007/128_2012_340. PubMed PMID: 22836898; PMCID: 3924422.

341. Tada M, Yokosuka O, Fukai K, Chiba T, Imazeki F, Tokuhisa T, Saisho H. Hypermethylation of NAD(P)H: quinone oxidoreductase 1 (NQO1) gene in human hepatocellular carcinoma. Journal of hepatology. 2005;42(4):511-9. doi: 10.1016/j.jhep.2004.11.024. PubMed PMID: 15763338.

342. Meiers I, Shanks JH, Bostwick DG. Glutathione S-transferase pi (GSTP1) hypermethylation in prostate cancer: review 2007. Pathology. 2007;39(3):299-304. doi: 10.1080/00313020701329906. PubMed PMID: 17558856.

343. Belanger AS, Tojcic J, Harvey M, Guillemette C. Regulation of UGT1A1 and HNF1 transcription factor gene expression by DNA methylation in colon cancer cells. BMC molecular biology. 2010;11:9. doi: 10.1186/1471-2199-11-9. PubMed PMID: 20096102; PMCID: 2835698.

344. Schubeler D. Function and information content of DNA methylation. Nature. 2015;517(7534):321-6. doi: 10.1038/nature14192. PubMed PMID: 25592537.

345. Li E, Zhang Y. DNA methylation in mammals. Cold Spring Harbor perspectives in biology. 2014;6(5):a019133. doi: 10.1101/cshperspect.a019133. PubMed PMID: 24789823.

346. Gagnon JF, Bernard O, Villeneuve L, Tetu B, Guillemette C. Irinotecan inactivation is modulated by epigenetic silencing of UGT1A1 in colon cancer. Clinical cancer research : an official journal of the American Association for Cancer Research. 2006;12(6):1850-8. doi: 10.1158/1078-0432.CCR-05-2130. PubMed PMID: 16551870.

347. Hurt EM, Thomas SB, Peng B, Farrar WL. Molecular consequences of SOD2 expression in epigenetically silenced pancreatic carcinoma cell lines. British journal of cancer. 2007;97(8):1116-23. doi: 10.1038/sj.bjc.6604000. PubMed PMID: 17895890; PMCID: 2360443.

348. Mohamed MM, Sabet S, Peng DF, Nouh MA, El-Shinawi M, El-Rifai W. Promoter hypermethylation and suppression of glutathione peroxidase 3 are associated with inflammatory breast carcinogenesis. Oxidative medicine and cellular longevity.

2014;2014:787195. doi: 10.1155/2014/787195. PubMed PMID: 24790704; PMCID: 3980917.

349. Barve A, Khor TO, Nair S, Reuhl K, Suh N, Reddy B, Newmark H, Kong AN. Gamma-tocopherol-enriched mixed tocopherol diet inhibits prostate carcinogenesis in TRAMP mice. International journal of cancer Journal international du cancer. 2009;124(7):1693-9. doi: 10.1002/ijc.24106. PubMed PMID: 19115203.

350. Frohlich DA, McCabe MT, Arnold RS, Day ML. The role of Nrf2 in increased reactive oxygen species and DNA damage in prostate tumorigenesis. Oncogene. 2008;27(31):4353-62. doi: 10.1038/onc.2008.79. PubMed PMID: 18372916.

351. Khor TO, Fuentes F, Shu L, Paredes-Gonzalez X, Yang AY, Liu Y, Smiraglia DJ, Yegnasubramanian S, Nelson WG, Kong AN. Epigenetic DNA Methylation of Antioxidative Stress Regulator NRF2 in Human Prostate Cancer. Cancer prevention research. 2014;7(12):1186-97. doi: 10.1158/1940-6207.CAPR-14-0127. PubMed PMID: 25266896; PMCID: 4256109.

352. Wang R, An J, Ji F, Jiao H, Sun H, Zhou D. Hypermethylation of the Keap1 gene in human lung cancer cell lines and lung cancer tissues. Biochemical and biophysical research communications. 2008;373(1):151-4. doi: 10.1016/j.bbrc.2008.06.004. PubMed PMID: 18555005.

353. Guo D, Wu B, Yan J, Li X, Sun H, Zhou D. A possible gene silencing mechanism: hypermethylation of the Keap1 promoter abrogates binding of the transcription factor Sp1 in lung cancer cells. Biochemical and biophysical research communications. 2012;428(1):80-5. doi: 10.1016/j.bbrc.2012.10.010. PubMed PMID: 23047008.

354. Muscarella LA, Parrella P, D'Alessandro V, la Torre A, Barbano R, Fontana A, Tancredi A, Guarnieri V, Balsamo T, Coco M, Copetti M, Pellegrini F, De Bonis P, Bisceglia M, Scaramuzzi G, Maiello E, Valori VM, Merla G, Vendemiale G, Fazio VM. Frequent epigenetics inactivation of KEAP1 gene in non-small cell lung cancer. Epigenetics : official journal of the DNA Methylation Society. 2011;6(6):710-9. PubMed PMID: 21610322.

355. Muscarella LA, Barbano R, D'Angelo V, Copetti M, Coco M, Balsamo T, la Torre A, Notarangelo A, Troiano M, Parisi S, Icolaro N, Catapano D, Valori VM, Pellegrini F, Merla G, Carella M, Fazio VM, Parrella P. Regulation of KEAP1 expression by promoter methylation in malignant gliomas and association with patient's outcome. Epigenetics : official journal of the DNA Methylation Society. 2011;6(3):317-25. PubMed PMID: 21173573; PMCID: 3092680.

356. Barbano R, Muscarella LA, Pasculli B, Valori VM, Fontana A, Coco M, la Torre A, Balsamo T, Poeta ML, Marangi GF, Maiello E, Castelvetere M, Pellegrini F, Murgo R, Fazio VM, Parrella P. Aberrant Keap1 methylation in breast cancer and association with clinicopathological features. Epigenetics : official journal of the DNA Methylation Society. 2013;8(1):105-12. doi: 10.4161/epi.23319. PubMed PMID: 23249627; PMCID: 3549873.

357. Hanada N, Takahata T, Zhou Q, Ye X, Sun R, Itoh J, Ishiguro A, Kijima H, Mimura J, Itoh K, Fukuda S, Saijo Y. Methylation of the KEAP1 gene promoter region in human colorectal cancer. BMC cancer. 2012;12:66. doi: 10.1186/1471-2407-12-66. PubMed PMID: 22325485; PMCID: 3296656.

358. Zhang P, Singh A, Yegnasubramanian S, Esopi D, Kombairaju P, Bodas M, Wu H, Bova SG, Biswal S. Loss of Kelch-like ECH-associated protein 1 function in prostate cancer cells causes chemoresistance and radioresistance and promotes tumor growth. Molecular cancer therapeutics. 2010;9(2):336-46. doi: 10.1158/1535-7163.MCT-09-0589. PubMed PMID: 20124447; PMCID: 2821808.

359. Martinez VD, Vucic EA, Pikor LA, Thu KL, Hubaux R, Lam WL. Frequent concerted genetic mechanisms disrupt multiple components of the NRF2 inhibitor KEAP1/CUL3/RBX1 E3-ubiquitin ligase complex in thyroid cancer. Molecular cancer. 2013;12(1):124. doi: 10.1186/1476-4598-12-124. PubMed PMID: 24138990; PMCID: 4016213.

360. Elanchezhian R, Palsamy P, Madson CJ, Lynch DW, Shinohara T. Age-related cataracts: homocysteine coupled endoplasmic reticulum stress and suppression of Nrf2-dependent antioxidant protection. Chemico-biological interactions. 2012;200(1):1-10. doi: 10.1016/j.cbi.2012.08.017. PubMed PMID: 22964297; PMCID: 3586200.

361. Palsamy P, Ayaki M, Elanchezhian R, Shinohara T. Promoter demethylation of Keap1 gene in human diabetic cataractous lenses. Biochemical and biophysical research communications. 2012;423(3):542-8. doi: 10.1016/j.bbrc.2012.05.164. PubMed PMID: 22683333.

362. Gao Y, Yan Y, Huang T. Human agerelated cataracts: Epigenetic suppression of the nuclear factor erythroid 2related factor 2mediated antioxidant system. Molecular medicine reports. 2015;11(2):1442-7. doi: 10.3892/mmr.2014.2849. PubMed PMID: 25370996.

363. Yang SP, Yang XZ, Cao GP. Acetyllcarnitine prevents homocysteineinduced suppression of Nrf2/Keap1 mediated antioxidation in human lens epithelial cells. Molecular medicine reports. 2015;12(1):1145-50. doi: 10.3892/mmr.2015.3490. PubMed PMID: 25776802.

364. Palsamy P, Bidasee KR, Shinohara T. Selenite cataracts: activation of endoplasmic reticulum stress and loss of Nrf2/Keap1-dependent stress protection. Biochimica et biophysica acta. 2014;1842(9):1794-805. doi: 10.1016/j.bbadis.2014.06.028. PubMed PMID: 24997453; PMCID: 4293018.

365. Palsamy P, Bidasee KR, Ayaki M, Augusteyn RC, Chan JY, Shinohara T. Methylglyoxal induces endoplasmic reticulum stress and DNA demethylation in the Keap1 promoter of human lens epithelial cells and age-related cataracts. Free radical biology & medicine. 2014;72:134-48. doi: 10.1016/j.freeradbiomed.2014.04.010. PubMed PMID: 24746615.

366. Palsamy P, Bidasee KR, Shinohara T. Valproic acid suppresses Nrf2/Keap1 dependent antioxidant protection through induction of endoplasmic reticulum stress and Keap1 promoter DNA demethylation in human lens epithelial cells. Experimental eye research. 2014;121:26-34. doi: 10.1016/j.exer.2014.01.021. PubMed PMID: 24525405; PMCID: 4293019.

367. Liu ZZ, Zhao XZ, Zhang XS, Zhang M. Promoter DNA demethylation of Keap1 gene in diabetic cardiomyopathy. International journal of clinical and experimental pathology. 2014;7(12):8756-62. PubMed PMID: 25674242; PMCID: 4313971.

368. Xu C, Huang MT, Shen G, Yuan X, Lin W, Khor TO, Conney AH, Kong AN. Inhibition of 7,12-dimethylbenz(a)anthracene-induced skin tumorigenesis in

C57BL/6 mice by sulforaphane is mediated by nuclear factor E2-related factor 2. Cancer research. 2006;66(16):8293-6. doi: 10.1158/0008-5472.CAN-06-0300. PubMed PMID: 16912211.

369. Gerhauser C. Epigenetic impact of dietary isothiocyanates in cancer chemoprevention. Current opinion in clinical nutrition and metabolic care. 2013;16(4):405-10. doi: 10.1097/MCO.0b013e328362014e. PubMed PMID: 23657153.

370. Fang MZ, Wang Y, Ai N, Hou Z, Sun Y, Lu H, Welsh W, Yang CS. Tea polyphenol (-)-epigallocatechin-3-gallate inhibits DNA methyltransferase and reactivates methylation-silenced genes in cancer cell lines. Cancer research. 2003;63(22):7563-70. PubMed PMID: 14633667.

371. Jazirehi AR, Wenn PB, Arle D. Is there a decrease in Keap1 RNA expression in colorectal cancer cells, and is this decrease in expression due to hypermethylation? Epigenomics. 2012;4(3):253-4. PubMed PMID: 22872918.

372. von Otter M, Landgren S, Nilsson S, Zetterberg M, Celojevic D, Bergstrom P, Minthon L, Bogdanovic N, Andreasen N, Gustafson DR, Skoog I, Wallin A, Tasa G, Blennow K, Nilsson M, Hammarsten O, Zetterberg H. Nrf2-encoding NFE2L2 haplotypes influence disease progression but not risk in Alzheimer's disease and age-related cataract. Mechanisms of ageing and development. 2010;131(2):105-10. doi: 10.1016/j.mad.2009.12.007. PubMed PMID: 20064547.

373. Huisinga KL, Brower-Toland B, Elgin SC. The contradictory definitions of heterochromatin: transcription and silencing. Chromosoma. 2006;115(2):110-22. doi: 10.1007/s00412-006-0052-x. PubMed PMID: 16506022.

374. Correa F, Mallard C, Nilsson M, Sandberg M. Activated microglia decrease histone acetylation and Nrf2-inducible anti-oxidant defence in astrocytes: restoring effects of inhibitors of HDACs, p38 MAPK and GSK3beta. Neurobiology of disease. 2011;44(1):142-51. doi: 10.1016/j.nbd.2011.06.016. PubMed PMID: 21757005; PMCID: 3341174.

375. Mercado N, Thimmulappa R, Thomas CM, Fenwick PS, Chana KK, Donnelly LE, Biswal S, Ito K, Barnes PJ. Decreased histone deacetylase 2 impairs Nrf2 activation by oxidative stress. Biochemical and biophysical research communications. 2011;406(2):292-8. doi: 10.1016/j.bbrc.2011.02.035. PubMed PMID: 21320471; PMCID: 3061319.

376. Li Z, Xu L, Tang N, Xu Y, Ye X, Shen S, Niu X, Lu S, Chen Z. The polycomb group protein EZH2 inhibits lung cancer cell growth by repressing the transcription factor Nrf2. FEBS letters. 2014;588(17):3000-7. doi: 10.1016/j.febslet.2014.05.057. PubMed PMID: 24928441.

377. Wang B, Zhu X, Kim Y, Li J, Huang S, Saleem S, Li RC, Xu Y, Dore S, Cao W. Histone deacetylase inhibition activates transcription factor Nrf2 and protects against cerebral ischemic damage. Free radical biology & medicine. 2012;52(5):928-36. doi: 10.1016/j.freeradbiomed.2011.12.006. PubMed PMID: 22226832.

378. Mishra M, Zhong Q, Kowluru RA. Epigenetic modifications of Keap1 regulate its interaction with the protective factor Nrf2 in the development of diabetic retinopathy. Investigative ophthalmology & visual science. 2014;55(11):7256-65. doi: 10.1167/iovs.14-15193. PubMed PMID: 25301875; PMCID: 4231994.

379. Liu GH, Qu J, Shen X. NF-kappaB/p65 antagonizes Nrf2-ARE pathway by depriving CBP from Nrf2 and facilitating recruitment of HDAC3 to MafK. Biochimica et biophysica acta. 2008;1783(5):713-27. doi: 10.1016/j.bbamcr.2008.01.002. PubMed PMID: 18241676.

380. Zhong Q, Kowluru RA. Epigenetic modification of Sod2 in the development of diabetic retinopathy and in the metabolic memory: role of histone methylation. Investigative ophthalmology & visual science. 2013;54(1):244-50. doi: 10.1167/iovs.12-10854. PubMed PMID: 23221071; PMCID: 3590072.

381. Mishra M, Zhong Q, Kowluru RA. Epigenetic modifications of Nrf2-mediated glutamate-cysteine ligase: implications for the development of diabetic retinopathy and the metabolic memory phenomenon associated with its continued progression. Free radical biology & medicine. 2014;75:129-39. doi: 10.1016/j.freeradbiomed.2014.07.001. PubMed PMID: 25016074.

382. Ura K, Kurumizaka H, Dimitrov S, Almouzni G, Wolffe AP. Histone acetylation: influence on transcription, nucleosome mobility and positioning, and linker histone-dependent transcriptional repression. The EMBO journal. 1997;16(8):2096-107. doi: 10.1093/emboj/16.8.2096. PubMed PMID: 9155035; PMCID: 1169812.

383. Adenuga D, Caito S, Yao H, Sundar IK, Hwang JW, Chung S, Rahman I. Nrf2 deficiency influences susceptibility to steroid resistance via HDAC2 reduction. Biochemical and biophysical research communications. 2010;403(3-4):452-6. doi: 10.1016/j.bbrc.2010.11.054. PubMed PMID: 21094147; PMCID: 3031165.

384. Lam HC, Cloonan SM, Bhashyam AR, Haspel JA, Singh A, Sathirapongsasuti JF, Cervo M, Yao H, Chung AL, Mizumura K, An CH, Shan B, Franks JM, Haley KJ, Owen CA, Tesfaigzi Y, Washko GR, Quackenbush J, Silverman EK, Rahman I, Kim HP, Mahmood A, Biswal SS, Ryter SW, Choi AM. Histone deacetylase 6-mediated selective autophagy regulates COPD-associated cilia dysfunction. The Journal of clinical investigation. 2013;123(12):5212-30. doi: 10.1172/JCI69636. PubMed PMID: 24200693; PMCID: 3859407.

385. Kawai Y, Garduno L, Theodore M, Yang J, Arinze IJ. Acetylation-deacetylation of the transcription factor Nrf2 (nuclear factor erythroid 2-related factor 2) regulates its transcriptional activity and nucleocytoplasmic localization. The Journal of biological chemistry. 2011;286(9):7629-40. doi: 10.1074/jbc.M110.208173. PubMed PMID: 21196497; PMCID: 3045017.

386. Sun Z, Chin YE, Zhang DD. Acetylation of Nrf2 by p300/CBP augments promoter-specific DNA binding of Nrf2 during the antioxidant response. Molecular and cellular biology. 2009;29(10):2658-72. doi: 10.1128/MCB.01639-08. PubMed PMID: 19273602; PMCID: 2682049.

387. Chen Z, Ye X, Tang N, Shen S, Li Z, Niu X, Lu S, Xu L. The histone acetylranseferase hMOF acetylates Nrf2 and regulates anti-drug responses in human non-small cell lung cancer. British journal of pharmacology. 2014;171(13):3196-211. doi: 10.1111/bph.12661. PubMed PMID: 24571482; PMCID: 4080974.

388. Ikeda H, Nishi S, Sakai M. Transcription factor Nrf2/MafK regulates rat placental glutathione S-transferase gene during hepatocarcinogenesis. The Biochemical journal. 2004;380(Pt 2):515-21. doi: 10.1042/BJ20031948. PubMed PMID: 14960151; PMCID: 1224169.

389. Ohta K, Ohigashi M, Naganawa A, Ikeda H, Sakai M, Nishikawa J, Imagawa M, Osada S, Nishihara T. Histone acetyltransferase MOZ acts as a co-activator of Nrf2-MafK and induces tumour marker gene expression during hepatocarcinogenesis. The Biochemical journal. 2007;402(3):559-66. doi: 10.1042/BJ20061194. PubMed PMID: 17083329; PMCID: 1863558.

390. Kalthoff S, Winkler A, Freiberg N, Manns MP, Strassburg CP. Gender matters: estrogen receptor alpha (ERalpha) and histone deacetylase (HDAC) 1 and 2 control the gender-specific transcriptional regulation of human uridine diphosphate glucuronosyltransferases genes (UGT1A). Journal of hepatology. 2013;59(4):797-804. doi: 10.1016/j.jhep.2013.05.028. PubMed PMID: 23714156.

391. Greer EL, Shi Y. Histone methylation: a dynamic mark in health, disease and inheritance. Nature reviews Genetics. 2012;13(5):343-57. doi: 10.1038/nrg3173. PubMed PMID: 22473383; PMCID: 4073795.

392. Chase A, Cross NC. Aberrations of EZH2 in cancer. Clinical cancer research : an official journal of the American Association for Cancer Research. 2011;17(9):2613-8. doi: 10.1158/1078-0432.CCR-10-2156. PubMed PMID: 21367748.

393. Ruthenburg AJ, Allis CD, Wysocka J. Methylation of lysine 4 on histone H3: intricacy of writing and reading a single epigenetic mark. Molecular cell. 2007;25(1):15-30. doi: 10.1016/j.molcel.2006.12.014. PubMed PMID: 17218268.

394. Balasubramanian S, Kanade S, Han B, Eckert RL. A proteasome inhibitor-stimulated Nrf1 protein-dependent compensatory increase in proteasome subunit gene expression reduces polycomb group protein level. The Journal of biological chemistry. 2012;287(43):36179-89. doi: 10.1074/jbc.M112.359281. PubMed PMID: 22932898; PMCID: 3476285.

395. Knutson SK, Kawano S, Minoshima Y, Warholic NM, Huang KC, Xiao Y, Kadowaki T, Uesugi M, Kuznetsov G, Kumar N, Wigle TJ, Klaus CR, Allain CJ, Raimondi A, Waters NJ, Smith JJ, Porter-Scott M, Chesworth R, Moyer MP, Copeland RA, Richon VM, Uenaka T, Pollock RM, Kuntz KW, Yokoi A, Keilhack H. Selective inhibition of EZH2 by EPZ-6438 leads to potent antitumor activity in EZH2-mutant non-Hodgkin lymphoma. Molecular cancer therapeutics. 2014;13(4):842-54. doi: 10.1158/1535-7163.MCT-13-0773. PubMed PMID: 24563539.

396. Crea F, Fornaro L, Bocci G, Sun L, Farrar WL, Falcone A, Danesi R. EZH2 inhibition: targeting the crossroad of tumor invasion and angiogenesis. Cancer metastasis reviews. 2012;31(3-4):753-61. doi: 10.1007/s10555-012-9387-3. PubMed PMID: 22711031.

397. Miranda M, Muriach M, Johnsen S, Bosch-Morell F, Araiz J, Roma J, Romero FJ. [Oxidative stress in a model for experimental diabetic retinopathy: treatment with antioxidants]. Archivos de la Sociedad Espanola de Oftalmologia. 2004;79(6):289-94. PubMed PMID: 15221675.

398. Sanchez R, Zhou MM. The role of human bromodomains in chromatin biology and gene transcription. Current opinion in drug discovery & development. 2009;12(5):659-65. PubMed PMID: 19736624; PMCID: 2921942.

399. Wu SY, Chiang CM. The double bromodomain-containing chromatin adaptor Brd4 and transcriptional regulation. The Journal of biological chemistry. 2007;282(18):13141-5. doi: 10.1074/jbc.R700001200. PubMed PMID: 17329240.

400. Michaeloudes C, Mercado N, Clarke C, Bhavsar PK, Adcock IM, Barnes PJ, Chung KF. Bromodomain and extraterminal proteins suppress NF-E2-related factor 2-mediated antioxidant gene expression. Journal of immunology. 2014;192(10):4913-20. doi: 10.4049/jimmunol.1301984. PubMed PMID: 24733848; PMCID: 4011694.

401. Hussong M, Borno ST, Kerick M, Wunderlich A, Franz A, Sultmann H, Timmermann B, Lehrach H, Hirsch-Kauffmann M, Schweiger MR. The bromodomain protein BRD4 regulates the KEAP1/NRF2-dependent oxidative stress response. Cell death & disease. 2014;5:e1195. doi: 10.1038/cddis.2014.157. PubMed PMID: 24763052; PMCID: 4001311.

402. Sangokoya C, Telen MJ, Chi JT. microRNA miR-144 modulates oxidative stress tolerance and associates with anemia severity in sickle cell disease. Blood. 2010;116(20):4338-48. doi: 10.1182/blood-2009-04-214817. PubMed PMID: 20709907; PMCID: 2993631.

403. Narasimhan M, Patel D, Vedpathak D, Rathinam M, Henderson G, Mahimainathan L. Identification of novel microRNAs in post-transcriptional control of Nrf2 expression and redox homeostasis in neuronal, SH-SY5Y cells. PloS one. 2012;7(12):e51111. doi: 10.1371/journal.pone.0051111. PubMed PMID: 23236440; PMCID: 3517581.

404. Yang M, Yao Y, Eades G, Zhang Y, Zhou Q. MiR-28 regulates Nrf2 expression through a Keap1-independent mechanism. Breast cancer research and treatment. 2011;129(3):983-91. doi: 10.1007/s10549-011-1604-1. PubMed PMID: 21638050; PMCID: 3752913.

405. Singh B, Ronghe AM, Chatterjee A, Bhat NK, Bhat HK. MicroRNA-93 regulates NRF2 expression and is associated with breast carcinogenesis. Carcinogenesis. 2013;34(5):1165-72. doi: 10.1093/carcin/bgt026. PubMed PMID: 23492819; PMCID: 3643421.

406. Eades G, Yang M, Yao Y, Zhang Y, Zhou Q. miR-200a regulates Nrf2 activation by targeting Keap1 mRNA in breast cancer cells. J Biol Chem. 2011;286(47):40725-33. doi: 10.1074/jbc.M111.275495. PubMed PMID: 21926171; PMCID: 3220489.

407. Kim JH, Lee KS, Lee DK, Kim J, Kwak SN, Ha KS, Choe J, Won MH, Cho BR, Jeoung D, Lee H, Kwon YG, Kim YM. Hypoxia-responsive microRNA-101 promotes angiogenesis via heme oxygenase-1/vascular endothelial growth factor axis by targeting cullin 3. Antioxidants & redox signaling. 2014;21(18):2469-82. doi: 10.1089/ars.2014.5856. PubMed PMID: 24844779; PMCID: 4245877.

408. Hou W, Tian Q, Steuerwald NM, Schrum LW, Bonkovsky HL. The let-7 microRNA enhances heme oxygenase-1 by suppressing Bach1 and attenuates oxidant injury in human hepatocytes. Biochimica et biophysica acta. 2012;1819(11-12):1113-22. doi: 10.1016/j.bbagrm.2012.06.001. PubMed PMID: 22698995; PMCID: 3480558.

409. Pulkkinen KH, Yla-Herttuala S, Levonen AL. Heme oxygenase 1 is induced by miR-155 via reduced BACH1 translation in endothelial cells. Free radical biology & medicine. 2011;51(11):2124-31. doi: 10.1016/j.freeradbiomed.2011.09.014. PubMed PMID: 21982894.

410. Esquela-Kerscher A, Slack FJ. Oncomirs - microRNAs with a role in cancer. Nature reviews Cancer. 2006;6(4):259-69. doi: 10.1038/nrc1840. PubMed PMID: 16557279.

411. Reichard JF, Motz GT, Puga A. Heme oxygenase-1 induction by NRF2 requires inactivation of the transcriptional repressor BACH1. Nucleic acids research. 2007;35(21):7074-86. doi: 10.1093/nar/gkm638. PubMed PMID: 17942419; PMCID: 2175339.

412. MacLeod AK, McMahon M, Plummer SM, Higgins LG, Penning TM, Igarashi K, Hayes JD. Characterization of the cancer chemopreventive NRF2-dependent gene battery in human keratinocytes: demonstration that the KEAP1-NRF2 pathway, and not the BACH1-NRF2 pathway, controls cytoprotection against electrophiles as well as redox-cycling compounds. Carcinogenesis. 2009;30(9):1571-80. doi: 10.1093/carcin/bgp176. PubMed PMID: 19608619; PMCID: 3656619.

413. Wagner AE, Boesch-Saadatmandi C, Dose J, Schultheiss G, Rimbach G. Anti-inflammatory potential of allyl-isothiocyanate--role of Nrf2, NF-(kappa) B and microRNA-155. Journal of cellular and molecular medicine. 2012;16(4):836-43. doi: 10.1111/j.1582-4934.2011.01367.x. PubMed PMID: 21692985.

414. Shah NM, Rushworth SA, Murray MY, Bowles KM, MacEwan DJ. Understanding the role of NRF2-regulated miRNAs in human malignancies. Oncotarget. 2013;4(8):1130-42. PubMed PMID: 24029073; PMCID: 3787145.

415. Papp D, Lenti K, Modos D, Fazekas D, Dul Z, Turei D, Foldvari-Nagy L, Nussinov R, Csermely P, Korcsmaros T. The NRF2-related interactome and regulome contain multifunctional proteins and fine-tuned autoregulatory loops. FEBS letters. 2012;586(13):1795-802. doi: 10.1016/j.febslet.2012.05.016. PubMed PMID: 22641035.

416. Vaissiere T, Sawan C, Herceg Z. Epigenetic interplay between histone modifications and DNA methylation in gene silencing. Mutation research. 2008;659(1-2):40-8. doi: 10.1016/j.mrrev.2008.02.004. PubMed PMID: 18407786.

417. Vrba L, Jensen TJ, Garbe JC, Heimark RL, Cress AE, Dickinson S, Stampfer MR, Futscher BW. Role for DNA methylation in the regulation of miR-200c and miR-141 expression in normal and cancer cells. PloS one. 2010;5(1):e8697. doi: 10.1371/journal.pone.0008697. PubMed PMID: 20084174; PMCID: 2805718.

418. Eades G, Yao Y, Yang M, Zhang Y, Chumsri S, Zhou Q. miR-200a regulates SIRT1 expression and epithelial to mesenchymal transition (EMT)-like transformation in mammary epithelial cells. The Journal of biological chemistry. 2011;286(29):25992-6002. doi: 10.1074/jbc.M111.229401. PubMed PMID: 21596753; PMCID: 3138315.

419. Murray-Stewart T, Hanigan CL, Woster PM, Marton LJ, Casero RA, Jr. Histone deacetylase inhibition overcomes drug resistance through a miRNA-dependent mechanism. Mol Cancer Ther. 2013;12(10):2088-99. doi: 10.1158/1535-7163.MCT-13-0418. PubMed PMID: 23943804; PMCID: 3808125.